

Synthesis of Phosphin-, Phosphon- and Phosphoramidates by Staudinger reactions

Dissertation zur Erlangung des akademischen Grades des
Doktors der Naturwissenschaften (Dr. rer. Nat.)

Eingereicht im Fachbereich Biologie, Chemie, Pharmazie
der Freien Universität Berlin

Vorgelegt von

INA WILKENING

Aus Bonn

2012

Die Arbeit wurde zwischen dem 15.01.2007 und 10.05.2012 unter der Leitung von Prof. Dr. Christian P. R. Hackenberger im Institut für Chemie und Biochemie angefertigt.

1. Gutachter: Prof. Dr. Christian P. R. Hackenberger

2. Gutachter: Prof. Dr. Rainer Haag

Disputation am 19.07.2012

Declaration

I herewith confirm that I have prepared this dissertation without the help of any impermissible resources. All citations are marked as such. The present thesis has neither been accepted in any previous doctorate degree procedure nor has it been evaluated as insufficient.

Berlin, 10th May 2012

Ina Wilkening

The work on this dissertation resulted so far in the following publications:

1) I. Wilkening, G. del Signore, C. P. R. Hackenberger, *Chem. Commun.* **2008**, 25, 2932-2934.
Synthesis of N,N-disubstituted phosphoramidates via a Lewis acid-catalyzed phosphorimidate rearrangement

2) I. Wilkening, G. del Signore, W. Ahlbrecht, C. P. R. Hackenberger, *Synthesis-Stuttgart* **2011**, 17, 2709-2720.
Lewis Acid or Alkyl Halide Promoted Rearrangements of Phosphor- and Phosphinimidates to N,N-Disubstituted Phosphor- and Phosphinamidates

3) I. Wilkening, G. del Signore, C. P. R. Hackenberger, *Chem. Commun.* **2011**, 47, 349-351.
Synthesis of phosphoramidate peptides by Staudinger reactions of silylated phosphinic acids and esters

4) R. Serwa, I. Wilkening, G. Del Signore, M. Mühlberg, I. Claussnitzer, C. Weise, M. Gerrits, C. P. R. Hackenberger, *Angew. Chem. Int. Ed.* **2009**, 48, 8234-8239.
Chemoselective Staudinger-phosphite reaction of azides for the phosphorylation of proteins

5) M. R. J. Vallée, P. Majkut, I. Wilkening, C. Weise, G. Müller, C. P. R. Hackenberger, *Org. Lett.* **2011**, 13, 5440-5443.
Staudinger-phosphonite reactions for the chemoselective transformation of azido-containing peptides and protein

Acknowledgments

I am very grateful to the following people who supported me scientifically and personally throughout the time of my doctoral studies at the Freie Universität Berlin:

Prof. Dr. Christian P. R. Hackenberger for giving me the opportunity to work in his group on this interesting subject, for the chance to participate in various national and international conferences, for helpful discussions and for the support that I was given and for the freedom in pursuing my ideas

Prof. Dr. Rainer Haag for being my second referee and for the support by him and his group during my doctoral studies,

Dr. Giuseppe del Signore for his previous work on the research projects and for helpful discussions,

Denise Homann, Silvia Teschner, Nico Rind, Maja Kandziora and all other students who worked with me on my project for their help, their enthusiasm for our research and the great time in the lab and outside,

All current and former members of the Hackenberger group for helpful discussions and support, for the nice working atmosphere and for turning the last years into great time,

Michaela Mühlberg and Verena Böhrsch for all the support, fruitful discussions in the lab and in the coffee room, for proofreading my thesis and for becoming good friends during my years in Berlin,

Dr. Andreas Schäfer and his team of the NMR service for all the NMR measurements and for their help in special measurements,

Dr. Andreas Springer and his team of the mass spectrometry for always helping me with the LC-MS and for the MS/MS measurements,

Katrin Wittig and Katharina Tebel for their support and their invaluable help in all administrative affairs,

The Deutsche Forschungsgemeinschaft (SFB 765-Multivalency as chemical organization and action principle), the Emmy Noether Programm and the Freie Universität Berlin for financial support,

All my friends and former fellow students, especially Frank, Johannes, Nina H. and Nina M.,
Timo, Vera and Martin for their support and the great time,

My friend and colleague Robert Vallee for all his support, patience and his faith in me,

My father and my brother for proofreading my complete thesis and my whole family for
supporting me during my entire studies, for giving me all their love and for their great faith in
me.

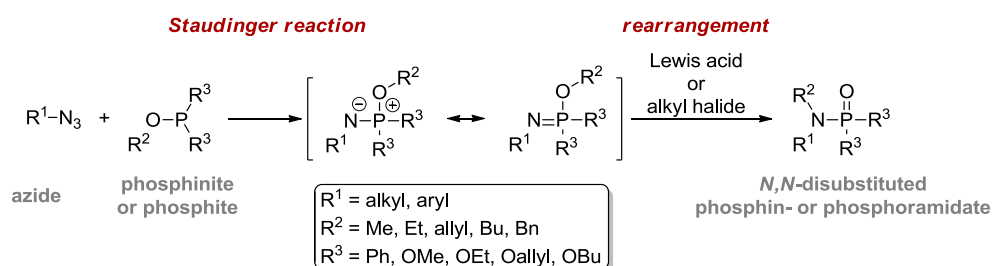
for my parents

Abstract

Phosphorus-nitrogen compounds play a decisive role in organic and medicinal research. Due to their unique properties and biological activity, they are applied as catalysts^[1] in organic transformations or as inhibitors^[2] for the treatment of diverse diseases. The **STAUDINGER REACTION** developed in 1919 by Herman Staudinger enables a straightforward entrance to various P-N compounds.^[3]

Within this thesis, different variants of the Staudinger reaction were investigated for the synthesis of phosphin-, phosphon- and phosphoramidates and their application for peptide and protein modifications.

In the first project, the Staudinger reaction and a following rearrangement was investigated.^[4] By performing the Staudinger reaction between phosphites and azides under anhydrous conditions, a rearrangement of the resulting phosphorimidates can be initiated by addition of alkyl halides or Lewis acids leading to *N,N*-disubstituted phosphoramidates (Scheme 1).^[5] Optimization of the reaction conditions and screening of different Lewis acids showed that heating in benzene at 80°C and 1 mol% of BF₃·Et₂O or TMSOTf are the most effective reaction conditions for the rearrangement. The Staudinger reaction and the subsequent rearrangement proceeded in high yields (63-99%) with a variety of different alkyl, aryl and allyl azides and with trimethyl, triethyl, tributyl and triallyl phosphite as trivalent phosphorus counterparts. The development of a one-pot procedure starting from alkyl bromides, mesylates or tosylates further facilitated the reaction by avoiding isolation of the potentially explosive azides. Moreover, the alkyl halide- and the Lewis acid-catalyzed rearrangement reaction could be transferred to phosphinimidates leading to *N,N*-disubstituted phosphinamidates in yields between 36% and 83%.



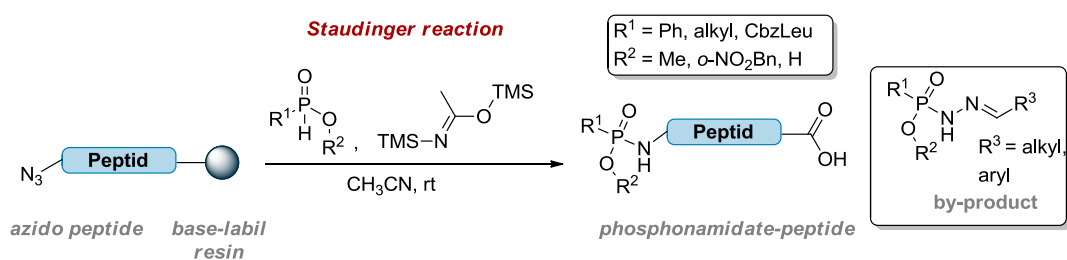
Scheme 1: Staudinger reaction and following Lewis acid- or alkyl halide-catalyzed rearrangement.

In the second project, the Staudinger reaction and following hydrolysis to phosphon- and phosphoramidates was probed as method for the bioorthogonal, site-selective and metal-free functionalization of peptides and proteins.^[6] Preliminary studies of the Staudinger reaction with

benzyl or phenyl azide and unprotected azido peptides with different phosphites and phosphonites could prove its applicability at room temperature in an aqueous environment as well as its bioorthogonality. All reactions led to high yields and a clean conversion of the azides to the desired phosphon- and phosphoramidates. Finally, the Staudinger-phosphite and the Staudinger-phosphonite reaction could be used for the functionalization of azido proteins, i.e. for PEGylation^[6b] or chemical phosphorylation.^[6a]

In the third project, the Staudinger reaction between silylated phosphinic acids and azides was applied to the synthesis of phosphoramidates and phosphoramidate peptides (Scheme 2).^[7] The treatment of phosphinic acids or their esters with a silylation reagent, like bis(trimethylsilyl)acetamide, under argon atmosphere generated silyl phosphonites, which could be reacted *in situ* with different aryl azides. Afterwards, desilylation was achieved with TBAF, HF-pyridine or sodium hydroxide solution. In all cases the desired phosphoramidates were obtained in moderate to excellent yields (30-95%). Furthermore, the described reaction procedure enabled the conversion of unprotected azido peptides containing a N-terminal *para*-azidobenzoic acid on solid support. The reaction on solid support allowed easy removal of reagents and simultaneous TMS-deprotection and cleavage from the resin under basic conditions (NaOH/1,4-dioxane). The phosphoramidate peptides were obtained in high conversions and purity. It has to be noted that the excess of silylation reagent leads to protection of the functional groups during the reaction.

When alkyl azides were used in the Staudinger reaction with silylated phosphinic acids, the reaction led to the formation of by-products. Especially if azido glycine peptides were employed in the reaction, the desired phosphoramidate was only formed in small amounts. Based on a more detailed exploration of the formed by-products, of the influence of different reaction conditions on the reaction and ¹⁵N-labeling experiments, a mechanism for the side reaction was proposed. The proposed mechanism of the side reaction is initiated by the decomposition of the phosphazide leading to the formation of methyl *P*-phenylphosphoramidate and a diazo compound. The diazo compound then further reacts with the silyl phosphonite under formation of the observed by-product with a P(O)-NH-N=C-moiety.



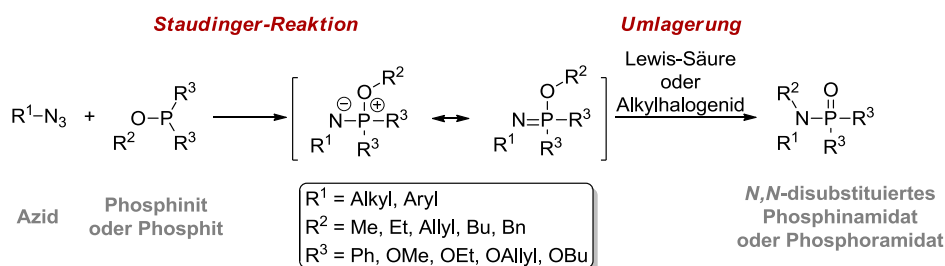
Scheme 2: Synthesis of phosphoramidate peptides by the Staudinger reaction.

Kurzzusammenfassung

Phosphor-Stickstoff-Verbindungen spielen in der organischen und medizinischen Chemie eine wichtige Rolle und finden beispielsweise Einsatz als Katalysatoren^[1] oder Inhibitoren^[2]. Die 1919 von Herman Staudinger entwickelte **STAUDINGER REAKTION**^[3] ermöglicht, einen Zugang zu P-N-Verbindungen und wurde im Rahmen dieser Arbeit näher untersucht.

Das erste Projekt dieser Arbeit bestand in der Untersuchung der Staudinger-Reaktion und einer nachfolgenden Lewis-Säure- oder Alkylhalogenid-katalysierten Umlagerung (Schema 1). Ausgehend von den über die Staudinger Reaktion hergestellten Phosphin- und Phosphorimidaten kann unter wasserfreien Bedingungen eine Umlagerung zu den entsprechenden *N,N*-disubstituierten Amidaten eingeleitet werden.^[5] Im Rahmen der Doktorarbeit wurden verschiedene Lewis-Säuren hinsichtlich ihrer Fähigkeit, eine solche Umlagerung von Phosphorimidaten zu initiieren, untersucht. $\text{BF}_3\cdot\text{EtO}$ und TMSOTf erwiesen sich als die geeignetsten Katalysatoren.^[4a] Um die Anwendungsbreite der Reaktion zu untersuchen, wurden unterschiedliche organische Azidverbindungen hergestellt und verwendet. Dabei lieferten sowohl primäre, sekundäre und tertiäre alkyliche als auch arylische Azide die entsprechenden Phosphoramidate in guten bis sehr guten Ausbeuten zwischen 63-99%.^[4] Außerdem war es möglich, auch die trivalenten Phosphorverbindungen zu variieren, und Methyl-, Ethyl-, Butyl- und Allylgruppen konnten erfolgreich umgelagert werden. Um die optimierte Umsetzung weiter zu vereinfachen und die Isolierung von potenziell explosiven Aziden zu vermeiden, wurde – ausgehend von Bromiden, Mesylaten oder Tosylaten – ein Eintopfverfahren entwickelt.

Neben den untersuchten Phosphoramidaten konnten auch *N,N*-disubstituierte Phosphinamidate durch die Lewis-Säure- oder Alkylhalogenid-katalysierte Umlagerung in Ausbeuten von 36% bis 83% gewonnen werden.^[4b]

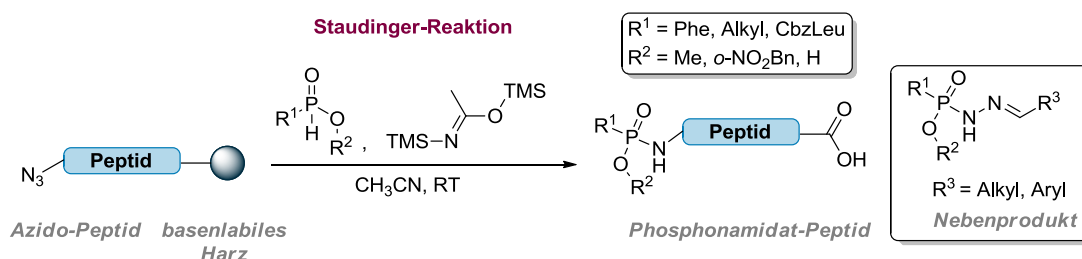


Schema 1: Staudinger-Reaktion und nachfolgende Lewis-Säure- oder Alkylhalogenid-katalysierte Umlagerung.

Wird die Reaktion von Phosphiten und Aziden unter wässrigen Bedingungen durchgeführt, erfolgt anstelle der Alkylierung des Stickstoffes die Protonierung zum Phosphoramidat. Erste Versuche zeigten, dass die Staudinger-Reaktion für die bioorthogonale Umsetzung von Azido-Peptiden erfolgreich genutzt werden kann und auch unter phys. pH-Wert durchführbar ist.^[6a] Basierend auf den anfänglichen Ergebnissen wurde die Staudinger-Reaktion für die metallfreie, ortsspezifische Funktionalisierung von Peptiden und Proteinen eingesetzt – beispielsweise zur PEGylierung^[6b] – und konnte zur chemischen Phosphorylierung^[6a] von Proteinen herangezogen werden.

Im letzten Teil der Arbeit wurde die Staudinger Reaktion verwendet, um den einfachen und direkten Zugang zu Phosphonamidat-haltigen Peptiden zu ermöglichen (Schema 2). Phosphinsäure-Derivate können durch Silylierung mit Bis(trimethylsilyl) acetamid unter wasser- und sauerstofffreien Bedingungen in die entsprechenden Phosphonite überführt und *in situ* mit den unterschiedlichen arylischen Aziden und Azido-Peptiden umgesetzt werden.^[7] Diese Methode erlaubt darüber hinaus die Durchführung der Synthese auch an der festen Phase, sodass nach Abspaltung vom Harz die gewünschten Phosphonamidat-haltigen Peptide mit hoher Reinheit erhalten werden können. Außerordentlich vorteilhaft ist die entwickelte Synthese zur Herstellung von Phosphonamidaten mit freier Hydroxylgruppe, die besonders instabil sind und aufwendige Entschützungs- und Reinigungsmethoden nicht zulassen.

Bei dem Einsatz von alkyischen Aziden kam es zu einer interessanten Nebenreaktion. Basierend auf umfangreiche Untersuchungen zu der Struktur der Nebenprodukte, Einfluss der Reaktionsbedingungen und ¹⁵N-Markierungsexperimenten, konnte ein Mechanismus für die Nebenreaktion vorgeschlagen werden. Erster Schritt ist dabei die Zersetzung des Phosphazids in Methyl *P*-Phenylphosphonamidat und eine Diazoverbindung. Letztere kann mit einem weiteren Äquivalent des Silylphosphonits zu dem dargestellten Nebenprodukt reagieren.



Schema 2: Synthese von Phosphonamidat-Peptiden mittels der Staudinger-Reaktion.

Abbreviations

AA	amino acid	LC-MS	liquid chromatography–mass spectrometry
Ac	acetyl	Me	methyl
Ar	aryl	MeCN	acetonitrile
AU	absorbance units	Melm	1-methylimidazole
BINAP	2,2'-bis(diphenylphosphino)-1,1'-binaphthyl	min.	minute
BINOL	1,1'-bi-2-naphthol	miRNA	micro ribonucleic acid
Bn	benzyl	mRNA	messenger ribonucleic acid
BSA	<i>N,O</i> -bis(trimethylsilyl)acetamide	MS	mass spectrometry
Bu	butyl	Ms	mesyl
Bz	benzoyl	MS/MS	tandem mass spectrometry
calcd.	calculated	MSNT	1-(mesitylene-2-sulfonyl)-3-nitro-1H-1,2,4-triazole
Cbz	carbobenzyloxy	MSTFA	<i>N</i> -methyl- <i>N</i> -(trimethylsilyl)trifluoroacetamide
config.	configuration	n. d.	not detected
d	day	NCL	native chemical ligation
dec	decyl	NMP	<i>N</i> -methyl pyrrolidone
DIEA	<i>N,N</i> -diisopropylethylamine	NMR	nuclear magnetic resonance
DMF	<i>N,N</i> -dimethylformamide	OEG	oligoethyleneglycole
DMS	dimethyl sulfide	OTf	triflate
DMSO	dimethyl sulfoxide	PEG	polyethylene glycol
DMTr	4,4'-dimethoxytrityl	PG	protective group
DNA	deoxyribonucleic acid	Ph	phenyl
DPPA	diphenylphosphoryl azide	pin	α -pinen
dr	diastereomeric ratio	pK _a	acid dissociation constant
ee	enantiomeric excess	PMB	<i>para</i> -methoxybenzyl
eq.	equivalent	Pr	propyl
ESI	electrospray ionization	prim.	primary
Et	ethyl	R	residue
Fmoc	fluorenylmethyloxycarbonyl	RNA	ribonucleic acid
h	hour	ROMP	ring-opening metathesis polymerization
hal	halogenid	rRNA	ribosomal ribonucleic acid
HBTU	2-(1H-benzotriazole-1-yl)-1,1,3,3-tetramethyluronium hexafluorophosphate	RT	room temperature
HMBA	4-hydroxymethylbenzoic acid	S	single strand
HMPA	hexamethylphosphoramide	sec.	secondary
HOBt	1-hydroxybenzotriazole	SPPS	solid-phase peptide synthesis
HPLC	high-performance liquid chromatography	TBAF	tetra- <i>n</i> -butylammonium fluoride
HRMS	high resolution mass spectrometry	TBDMS	<i>tert</i> -butyldimethylsilyl
Josiphos	1-[-2-(diphenylphosphino)-ferrocenyl]ethylbicyclohexylphosphine	TBDPS	<i>tert</i> -butyldiphenylsilyl
		TBSTFA	<i>N</i> -(<i>tert</i> -butyldimethylsilyl)- <i>N</i> -methyl-trifluoroacetamide
		TES	triethylsilyl

Tf	triflyl	TLC	thin layer chromatography
TFA	trifluoroacetic acid	TMS	trimethylsilyl
THF	tetrahydrofuran	TOF	time of flight
TIC	total ion current	TPP	triphenylphosphine
TIP	2,4,6-triisopropyl-phenyl	TPS	triphenylsilyl
TIPS	trisopropylsilyl	Ts	tosyl
TIS	triisopropylsilane	UV	ultraviolet

Table of contents

1	INTRODUCTION: PHOSPHORUS-NITROGEN COMPOUNDS AND THE STAUDINGER REACTION—A GENERAL SURVEY	1
1.1	The Staudinger reaction and its mechanism	3
1.2	Reactions of iminophosphoranes, phosphin-, phosphon- and phosphorimidates	5
1.2.1	Hydrolysis of iminophosphoranes, phosphin-, phosphon- and phosphorimidates	6
1.2.1.1	Hydrolysis of iminophosphoranes – the Staudinger reduction and its variants	6
1.2.1.2	Hydrolysis of phosphin-, phosphon- and phosphorimidates	11
1.2.2	Alkylation of iminophosphoranes, phosphin-, phosphon- and phosphorimidates	13
1.2.3	The aza-Wittig reaction	14
1.2.4	Rearrangement of phosphazenes	18
1.2.4.1	Thermal and electrophile catalyzed rearrangement	18
1.2.4.2	Phosphorimidate-amidate rearrangement catalyzed by Lewis acids	19
1.2.4.3	The 3-aza-2-phospha-1-oxa-Cope rearrangement	20
1.2.4.4	Synthesis of allenamides by the 3-aza-2-phospha-1-oxa-Cope rearrangement	28
1.2.5	Staudinger reaction with silylated phosphinic acid derivatives	30
1.3	Staudinger ligation & traceless Staudinger ligation	31
1.3.1	The Staudinger ligation	33
1.3.2	The traceless Staudinger ligation	34
1.3.3	Application of the Staudinger ligation & the traceless Staudinger ligation	36
1.3.3.1	Peptide ligation, peptide protein ligation and peptide cyclization by the traceless Staudinger ligation	36
1.3.3.2	The Staudinger ligation as method for bioconjugation	37
1.4	Phosphorus-nitrogen compounds in catalysis	39
1.4.1	Lewis base catalysis	39
1.4.2	Brønsted acid catalysis	43
1.5	Synthesis of phosphonamidates and phosphonamidate peptides via chloridates and chloridites	45
1.5.1	Synthesis of phosphonamidates from phosphonate mono- and diesters via phosphonochloridates	46
1.5.1.1	Synthesis of phosphonamidates from phosphonic acid diesters with phosphorus pentachloride	46
1.5.1.2	Synthesis of phosphonamidates from the phosphonic acid monoester	47

1.5.2	Synthesis of phosphoramidates from P(III)-precursors	48
1.5.3	Atherton-Todd reaction	49
1.6	Phosphoramidates as protease inhibitors	52
1.6.1	Proteases –function and classification	52
1.6.2	Protease inhibitors	53
1.6.3	Phosphoramidates as protease inhibitors	56
2	OBJECTIVE	61
3	DISCUSSION	65
3.1	Synthesis of <i>N,N</i>-disubstituted phosphin- and phosphoramidates via a Lewis acid- or alkyl halide-catalyzed rearrangement	65
3.1.1	Synthesis of <i>N,N</i> -disubstituted phosphoramidates via a Lewis acid-catalyzed phosphorimidate rearrangement	69
3.1.2	Lewis Acid or Alkyl Halide Promoted Rearrangements of Phosphor- and Phosphinimidates to <i>N,N</i> -Disubstituted Phosphor- and Phosphinamidates	83
3.2	Peptide and Protein Functionalization by the Staudinger-phosphite and the Staudinger-phosphonite reaction	123
3.2.1	Chemoselective Staudinger-Phosphite Reaction of Azides for the Phosphorylation of Proteins	127
3.2.2	Staudinger-Phosphonite Reactions for the Chemoselective Transformation of Azido-Containing Peptides and Proteins	149
3.3	Synthesis of phosphoramidates and phosphoramidate peptides from aryl azides by the Staudinger reaction	221
3.3.1	Synthesis of phosphoramidate peptides by Staudinger reactions of silylated phosphinic acids and esters	223
3.4	Staudinger reaction of silylated phosphinic acid esters with alkyl azides	255
3.4.1	Outline	255
3.4.2	Synthesis of alkyl azido compounds, methyl phenylphosphinate and monomethyl phenylphosphonate	257
3.4.2.1	Synthesis of alkyl azido substrates	257
3.4.2.2	Synthesis of azido peptides	257
3.4.2.3	Synthesis of methyl phenylphosphinate and monomethyl phenylphosphonate	259
3.4.3	Analysis of the product mixtures and products	260

3.4.4	Comparison of methyl (trimethylsilyl) phenylphosphonite and dimethyl phenylphosphonite in the Staudinger reaction with an azido glycine peptide	260
3.4.5	Staudinger reaction of methyl (trimethylsilyl) phenylphosphonite with small alkyl azides	262
3.4.5.1	More detailed examination of the Staudinger reaction with dodecyl azide	266
3.4.5.2	Isolation and structural analysis of products derived from the Staudinger reaction with 3-phenylpropyl azide	269
3.4.5.3	Mechanistic investigation by ¹⁵ N-labeling of 3-phenylpropyl azide	271
3.4.5.4	Solvent effects	280
3.4.5.5	Temperature effect	283
3.4.5.6	Influence of the silylation reagent on the Staudinger reaction	284
3.4.6	Staudinger reaction of azido glycine peptides with methyl phenylphosphinate and a silylation reagent	294
3.4.6.1	Temperature effect	295
3.4.6.2	Influence of the silylation reagent on the Staudinger reaction	296
3.4.6.3	Reaction of the azido glycine peptide with methyl phenylphosphinate and BSA in solution	299
3.4.6.4	MS/MS measurements of the isolated phosphoramidate peptide and the side product	299
3.4.7	Studies on the Staudinger reaction with 2-azido-2-methyl alanine peptides	300
3.5	Stability studies on phosphoramidates	302
3.5.1	Degradation of methyl <i>N,P</i> -diphenylphosphoramidate at different TFA-concentrations	303
3.5.2	Degradation of methyl <i>N</i> -benzyl- <i>P</i> -phenylphosphoramidate at different TFA-concentrations	306
4	CONCLUSION AND OUTLOOK	311
5	EXPERIMENTAL PART	319
5.1	Synthesis of azido compounds 7a,b,h,i	320
5.1.1	Synthesis of dodecyl azide (7a), 3-phenylpropyl azide (7b) and ¹⁵ N-labeled 3-phenylpropyl azide (¹⁵ N-7b)	320
5.1.2	Dodecyl azide (7a)	320
5.1.3	3-Phenylpropyl azide (7b)	321
5.1.4	¹⁵ N-3-Phenylpropyl azide (¹⁵ N-7b)	321
5.1.5	Synthesis of azido acetic acid (7h)	321
5.1.6	2-Azido-2-methylpropionic acid (7i)	322

5.2	Synthesis of methyl phenylphosphinate (182), monomethyl phenylphosphinate (187) and methyl <i>P</i>-phenylphosphonamidate (195)	323
5.2.1	Synthesis of methyl phenylphosphinate (182)	323
5.2.2	Synthesis of monomethyl phenylphosphinate (187)	323
5.2.3	Synthesis of methyl <i>P</i> -phenylphosphonamidate (195)	324
5.3	Staudinger reaction of silylated phosphinic acid esters with dodecyl and 3-phenylpropyl azide	325
5.3.1	General procedure for the Staudinger reaction with silylated phosphinic acid esters	325
5.3.2	Staudinger reaction with dodecyl azide (7a)	325
5.3.3	Synthesis of methyl <i>P</i> -phenyl-(3-phenylpropyl)phosphonamidate (183b)	326
5.3.4	Synthesis of methyl <i>P</i> -phenyl- ^{14/15} N-(3-phenylpropyl)phosphonamidate (¹⁵ N-183b) (1:1)	327
5.3.5	Synthesis of (<i>E/Z</i>)-methyl phenyl(2-(3-phenylpropylidene)hydrazinyl)phosphinate ((<i>E/Z</i>)-192b)	328
5.3.6	Synthesis of ^{14/15} N-(<i>E/Z</i>)-methyl phenyl(2-(3-phenylpropylidene)hydrazinyl)phosphinate (¹⁵ N-(<i>E/Z</i>)-192b) (1:1)	329
5.3.7	Dependence of the Staudinger reaction on the solvent, temperature and silylation reagent	330
5.3.7.2	Solvent effect	332
5.3.7.3	Temperature effect	335
5.3.7.4	Influence of the silylation reagent on the Staudinger reaction	336
5.3.8	Staudinger reaction with 1,3-dichloro-1,1,3,3-tetramethyldisiloxane	339
5.4	Peptides synthesis	339
5.4.1	Peptide synthesis on NovaSyn® TG HMBA resin – azido peptides 7c, d, f	339
5.4.1.1	Synthesis of azido glycine peptide 7c	341
5.4.1.2	Synthesis of azido glycine peptide 7d	341
5.4.1.3	Synthesis of 2-azido-2-methyl alanine peptide 7f	342
5.4.2	Peptide synthesis on a Gly-preloaded Wang resin – azido peptides 7e and g	343
5.4.2.1	Synthesis of azido glycine peptide 7e	343
5.4.2.2	Synthesis of 2-azido-2-methyl alanine peptide 7g	344
5.5	Staudinger reaction with azido peptides	345
5.5.1	Staudinger reaction on solid support – General procedure	345
5.5.2	Staudinger reaction in solution – General procedure	345
5.5.3	Staudinger reaction between azido glycine peptide 7c and dimethyl phenylphosphonite (188)	345
5.5.4	Staudinger reaction between azido glycine peptide 7c and methyl phenylphosphinate (182) with BSA	346

5.5.5	Staudinger reaction at 4 °C, rt and 30 °C	347
5.5.6	Staudinger reaction with different silylation reagents	349
5.5.6.1	Staudinger reaction with TBDPCL and methyl phenylphosphinate (182)	349
5.5.6.2	Staudinger reaction with TMSCl and methyl phenylphosphinate (182)	351
5.5.6.3	Staudinger reaction with MSTFA or TBDMSTFA and methyl phenylphosphinate (182)	352
5.5.7	Staudinger reaction in solution	355
5.5.8	Purification of 183e and (<i>E/Z</i>)- 192e for MS/MS analysis	356
5.5.9	Studies on the Staudinger reaction with 2-azido-2-methyl alanine peptides 7f and 7g	357
5.5.10	Stability studies	359
6	LITERATURE	363
7	CURRICULUM VITAE	373
8	APPENDIX	379
8.1	NMR spectra	379
8.1.1	NMR spectra of ¹⁵ N-3-phenylpropyl azide (¹⁵ N-7b)	379
8.1.2	NMR spectra to the Staudinger reaction between dodecyl azide (7a) and methyl phenylphosphinate (182) (6.eq.) with BSA (18 eq.)	380
8.1.3	NMR spectra of methyl <i>P</i> -phenyl-(3-phenylpropyl)phosphonamidate (183b)	383
8.1.4	NMR spectra of methyl <i>P</i> -phenyl- ^{14/15} N-(3-phenyl-propyl)phosphonamidate (¹⁵ N-183b)	386
8.1.5	NMR spectra of (<i>E/Z</i>)-methyl phenyl(2-(3-phenylpropylidene)hydrazinyl)phosphinate ((E/Z)-192b)	388
8.1.6	NMR spectra of ^{14/15} N-(<i>E/Z</i>)-methyl phenyl(2-(3-phenylpropylidene)hydrazinyl)-phosphinate (¹⁵ N-(E/Z)-192b)	391
8.2	Solvent effect – ³¹P-NMR and LC spectra (UV-trace)	393
8.3	Temperature effect – ³¹P-NMR and LC spectra (UV-trace)	397
8.4	Influence of the silylation reagent on the Staudinger reaction – ³¹P-NMR and LC spectra (UV-trace)	400
8.4.1	Silylation with BSA	400
8.4.2	Silylation with MSTFA	403
8.4.3	Silylation with TMSCl	406
8.4.4	Silylation with TESCI	408
8.4.5	Silylation with TBDMSCI	409
8.4.6	Silylation with MTBSTFA	409

8.4.7	Silylation with TBDSPCI	410
8.4.8	Silylation with TPSCI	412

1 Introduction: Phosphorus-nitrogen compounds and the Staudinger reaction—a general survey

Compounds containing a P(O)-N-motif play a decisive role in organic and medicinal research (Figure 1). In organic chemistry they are utilized as catalysts in stereoselective transformations based on the Lewis base or the Brønsted acid concept^[1], and they find application as inhibitors^[2] or as surrogates for naturally occurring phosphate groups^[2d, 6a, 8] in medicinal and biological chemistry.

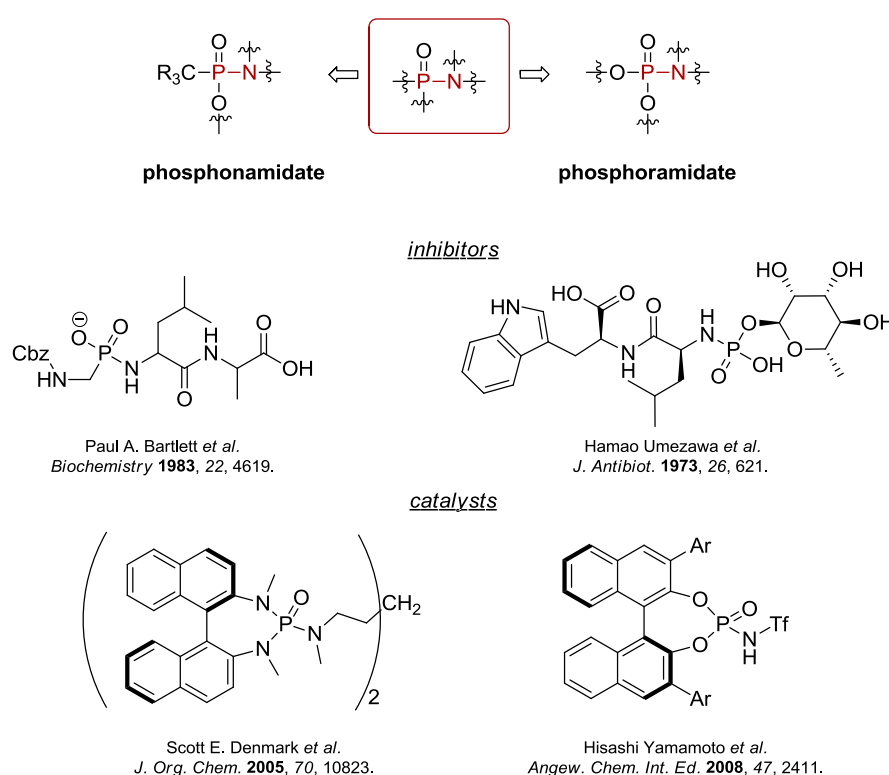


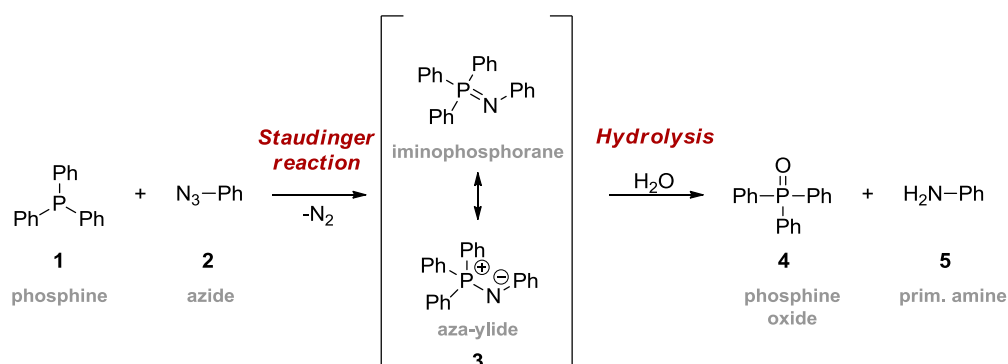
Figure 1: Phospon- and phosphoramidates in organic and medicinal research.^[1k, 1o, 2c, 2g]

In 1919 Hermann Staudinger and Jules Meyer invented the so-called Staudinger reaction, which comprises the conversion of azides with trivalent phosphorus species and enables a straightforward access to P-N compounds.^[3] The Staudinger reaction and the later established Staudinger ligation^[9] attracted the attention of many researchers over the last decade because of their exceptional reactivity and feasibility even in *in vivo* applications. Bertozzi and co-workers notably augmented this new interest in the Staudinger reaction by the development of the Staudinger ligation, which enables bioorthogonal formation of natural amide bonds and thereby functionalization as well as conjugation of biomolecules.^[9e]

receptors, and they feature structural diversity as well as the ability to form new structures and to alter their functions by posttranslational modifications.^[10] Moreover, their application as therapeutics is prevalent in the pharmaceutical industry. For this reason, the introduction of functional groups or incorporation of unnatural moieties into peptides and proteins is of great interest in bioorganic and biological chemistry and will allow the exploration of their role in biological processes and disease propagation in more detail.

1.1 The Staudinger reaction and its mechanism

The Staudinger reaction^[3] between trivalent phosphorous species and organic azides was first described by Staudinger and Meyer in 1919 inspired by the successful conversion of tertiary phosphines with aliphatic diazo compounds to phosphazines.^[11] They could show that the reaction of triphenylphosphine (**1**) with phenyl azide (**2**) accompanied by release of nitrogen leads to the formation of the iminophosphorane **3** via an intermediary formed phosphazide **9d** ($R^{1-4} = \text{Ph}$) (Scheme 3 and Scheme 4). Thereby, the iminophosphorane **3** is always in equilibrium with its aza-ylide form. Subsequent conversion of iminophosphorane **3** with different compounds like carbon dioxide, ketenes or isocyanates showed its unique reactivity.^[12] Up-to-date, the most famous consecutive reaction is the hydrolysis of iminophosphoranes like **3** towards phosphine oxide **4** and the primary amine **5**, commonly known as Staudinger reduction (Scheme 3).^[3]

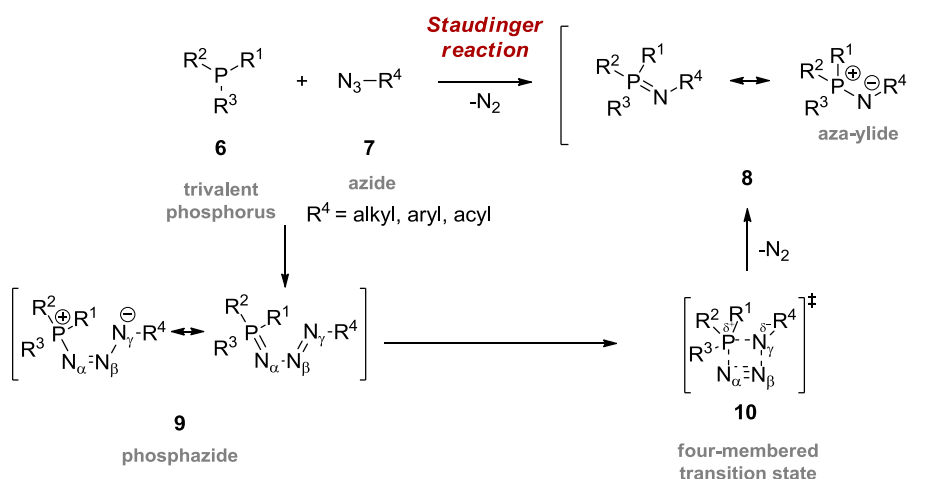


Scheme 3: Staudinger reaction between triphenylphosphine (**1**) and phenyl azide (**2**) and subsequent hydrolysis of the iminophosphorane **3**, known as Staudinger reduction.

During the first thirty years after the pioneering work of Staudinger and Meyer the Staudinger reaction received only little attention. Later on, in the 1950s, new interest arose in phosphazo compounds. Kabachnik *et al.*^[13] again addressed the Staudinger reaction and were able to make remarkable contributions to the further development of the Staudinger reaction and its

manifold opportunities and great scope of accessible products. By substituting the alkyl- or aryl-residue of a phosphine by alkoxy groups, hydrolysis of the intermediary formed imidates **8a-c** did not lead to complete P-N bond cleavage but to phosphin-, phosphon- or phosphoramidates, and, therefore, to new P-N-compounds which were difficult to prepare before (chapter 1.2.1.2).

For both reaction counterparts a multitude of reactants is accepted.^[12, 14] Nearly all kinds of symmetric and asymmetric trivalent phosphorus compounds can be applied in the Staudinger reaction, e.g. phosphines, halogenated phosphines, phosphorus acid esters, vinyl esters, amides and their bisphosphorus analogues, polymeric phosphines, and even cyclic derivatives. The same is true for the azido part. All types of alkyl and aryl azides can serve as substrates with also arenesulfonyl, acyl, phosphoryl or triorganyl azides being traditionally used as azido-components. This group has been considerably widened in the last years by azetidinyl azide, cyanazide, sulfonyl azides, phosphoryl azides, azidophosphonium salt, azidospirophosphoranes, tantalum tetrachloride azide, azidoborane, and nitroyl azides. Many more compounds for both reactants could be listed allowing a wide variety of accessible products.



- 6a** (phosphite), **8a** (phosphorimidate), **9a**, **10a**: R¹, R², R³ = Oalkyl, Oaryl
6b (phosphonite), **8b** (phosphonimidate), **9b**, **10b**: R¹ = alkyl, aryl; R², R³ = Oalkyl, Oaryl
6c (phosphinite), **8c** (phosphinimidate), **9c**, **10c**: R¹, R² = alkyl, aryl; R³ = Oalkyl, Oaryl
6d (phosphine), **8d** (iminophosphorane), **9d**, **10d**: R¹, R², R³ = alkyl, aryl

Scheme 4: Mechanism of the Staudinger reaction.

Mechanistically, the formation of the imidates **8a-c** and the iminophosphorane **8d** is a two-step process in which the overall kinetic process is determined by a second-order rate constant of the phosphazide formation and a first-order rate constant of its intramolecular decomposition (Scheme 4).^[12, 14b]

The Staudinger reaction is initiated by the nucleophilic attack of the trivalent phosphorus **6** at the terminal nitrogen of the azide **7** leading to the phosphazide **9** with retention of the phosphorus center. Here, electron-rich phosphorus compounds and electron-poor azides react most effectively, whereas sterical aspects do not show a major influence on the reaction rate.^[12, 14-15] Subsequently, the phosphazide **9** (the *Z*-isomer is displayed) stabilizes itself *via* a four-membered transition state **10**. Release of nitrogen then leads to the imidates **8a-c** or the iminophosphorane **8d**.

Although intermediary formed phosphazides **9** are relatively unstable, certain phosphazides **9** could be isolated and spectroscopically analyzed at low temperatures revealing new structural and electronic aspects.^[12, 14b, 16] Thus, branched and cyclic forms of the phosphazide **9** could be ruled out as X-ray crystallography proved a linear, acyclic structure with a nearly planar P-N₃-C chain. The N_α-N_β bond showed double-bond character increasing with the electron-withdrawing ability of the nitrogen substituent. Furthermore, X-ray crystallography confirmed almost exclusively *E*-configuration between the N_α-N_β-bond requiring a rotation before nitrogen can be released. In contrast to this observation, *ab initio* calculations in general identified the *Z*-configuration as the conformer of lower energy, which can be explained by the advantageous interaction of the partial charges.^[17] The phosphorus atom of the phosphazides **9** exhibits partial phosphonium character leading to a negative charge at the N_γ, which in case of aryl substituents can be delocalized to some extent. It is, thus, assumed that phosphazides **9** with *E*-configuration could be isolated because they possess a higher stability against loss of nitrogen, whereas *Z*-phosphazides **9** decomposed immediately. Except for one case, *Z*-phosphazides **9** could only be isolated if their decomposition was hampered by donor-acceptor interactions.^[18]

The following release of nitrogen was extensively studied proposing a four-membered transition state from which subsequently elemental nitrogen is formed by N_α and N_β. This hypothesis was proven by ¹⁵N-labeling of the phenyl azide **2** at the terminal position.^[12, 14b]

1.2 Reactions of iminophosphoranes, phosphin-, phosphon- and phosphorimidates

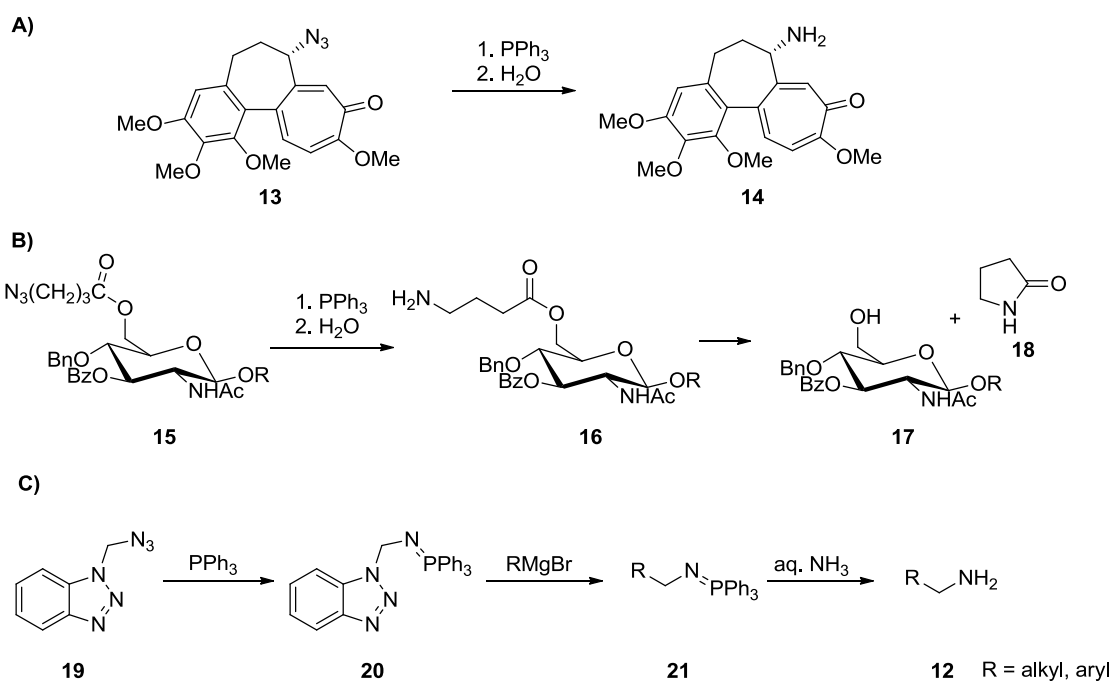
The nucleophilic nature of the nitrogen in aza-ylides **8** allows reactions with a variety of different electrophiles, and, depending on the nature of the electrophile used, different reaction pathways can be chosen. These range from simple protonation over aza-Wittig-type reactions to the synthesis of amides (Figure 3).

chemistry. The required azido group can easily be installed, commonly by nucleophilic substitutions, and it can serve as protective group during further transformations.

Triphenylphosphine (**1**) is generally used as trivalent phosphorus species since it is a cheap and manageable reagent and does not affect other functional groups. Trimethylphosphine is even more reactive than triphenylphosphine (**1**), P-N-bond cleavage proceeds under milder conditions and the formed oxide is water-soluble.^[23] It is, however, more expensive, has an intensive smell, and is more prone to oxidation due to the alkyl groups.

In addition to the standard reaction procedure supplementary protocols have been developed to ease and broaden the applicability of the Staudinger reduction in organic synthesis. Several one-pot procedures, starting from halides^[24], alcohols^[25] and acetates^[26], avoid azide isolation and primary amines **12** are obtained in good to excellent yields. Moreover, the Staudinger reduction was used to selectively remove protective groups of hydroxyl functions in carbohydrates or polyhydroxylated natural products (Scheme 6B).^[27]

To create a more general access to various amines **12**, a synthesis route was established in which the alkyl moiety of a Grignard reagent is homologized by one carbon atom with the assistance of an azido-benzotriazole derivative **19** (Scheme 6C).^[28]



Scheme 6: A) Synthesis of Colchicine (**14**) by use of the Staudinger reduction, B) Staudinger reduction as deprotection method in carbohydrate chemistry, C) Staudinger reduction as general entrance to prim. amines **12**.^{[20], [27],[28]}

One drawback of the Staudinger reduction is the equimolar amount of phosphine oxide formed and to further improve the Staudinger reduction, especially with respect to phosphine oxide removal, a ROMP gel-supported triphenyl phosphine was developed to yield the amine **12** as a pure product.^[29]

An interesting biological application of the Staudinger reduction is its use for template nucleic acid detection (Figure 4, Figure 5).^[30] Templated reactions, which either comprise the removal of an attached quencher^[30f, g] or the chemical conversion of profluorophore into a fluorophore^[30a-c, 30e, 30i, 30k], are very valuable, since they allow real-time visualization of oligonucleotides directly in living cells and since they exhibit high sequence specificity. These techniques rely on the hybridization of two oligonucleotide fragments with one fragment containing an azide and the second one a phosphine, to a complementary oligonucleotide template. Hybridization of both labeled fragments with the appropriate template shifts both reporters in spatial proximity and, thus, promotes the Staudinger reaction. Hydrolysis in an aqueous solution under the formation of an amine and triphenylphosphine oxide leads to the disconnection of both fragments and simultaneously to the dissociation from the oligonucleotide template. These methods have the potential to amplify the signal, since after release of the labeled fragments the free template can catalyze further reactions. Moreover, these methods have the advantage that the two fragments are not ligated after the Staudinger reduction, because fragment ligation is normally accompanied by undesired enhanced binding to the template.

Azido-rhodamine derivatives have successfully been utilized as profluorophores and, for example, have been applied in the investigation of miRNAs in living cells (Figure 4),^[30e] in the detection of natural DNA with a hybrid homo-DNA/DNA molecular beacon^[30k], and for the detection of the mRNA encoding O-6-methylguanine-DNA methyltransferase in intact cells^[30i]. As an alternative to the direct connection of the azide to the fluorophore, an α -azido ether can be used as reduction-triggered fluorescence probe. This method was applied for fluorophores, such as fluorescein^[30a] or coumarin^[30b], and resulted in the formation of the active fluorophore alcohol. This methodology was termed as reduction triggered fluorescence (RETF). In an application of an azido-fluorescein, the catalytic reaction of the probe offered a turnover number of 50 as fluorescence readout within 4 h and permitted introduction of the probes into human leukemia HL-60 cells by use of streptolysin O pore-forming peptide.^[30a] This procedure enabled the detection and quantification of a 28S rRNA and of a Actin mRNA signal above the

background by flow cytometry. In addition, the same RNA targets could also be imaged by fluorescence microscopy.

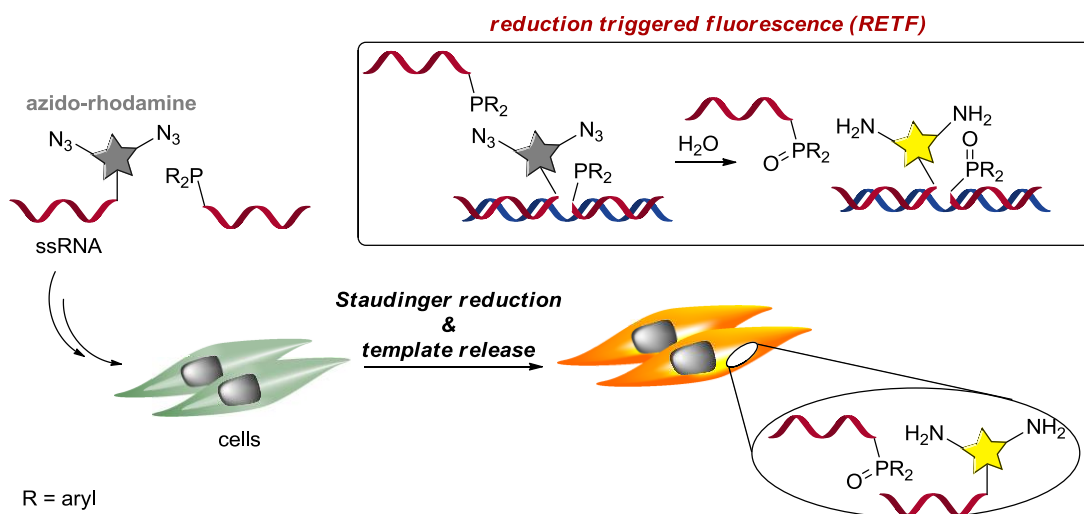


Figure 4: Rapid fluorescence imaging of miRNAs in human cells using the templated Staudinger reaction.^[30e]

Another approach results in linker cleavage after the Staudinger reaction and simultaneous release of a fluorescence quenching group in a Staudinger-triggered α -azido ether release (STAR) (Figure 5).^[31f, g]

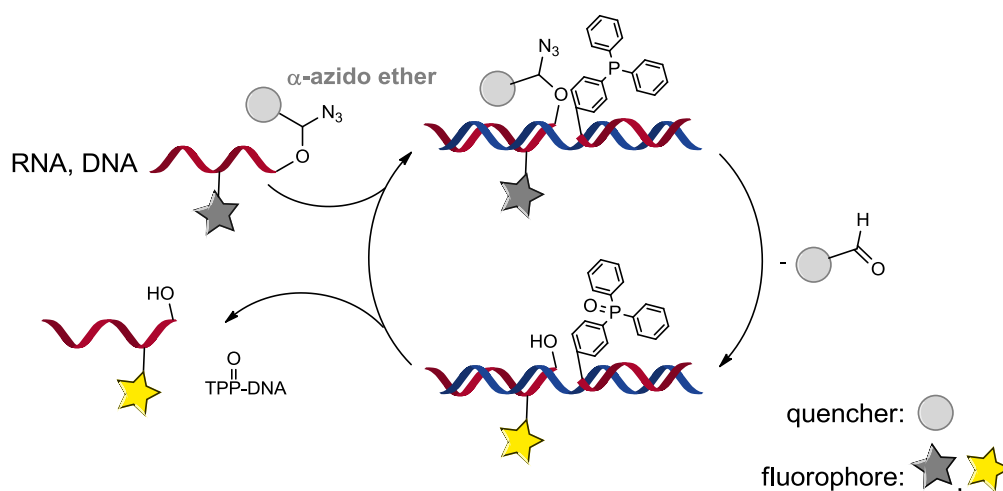
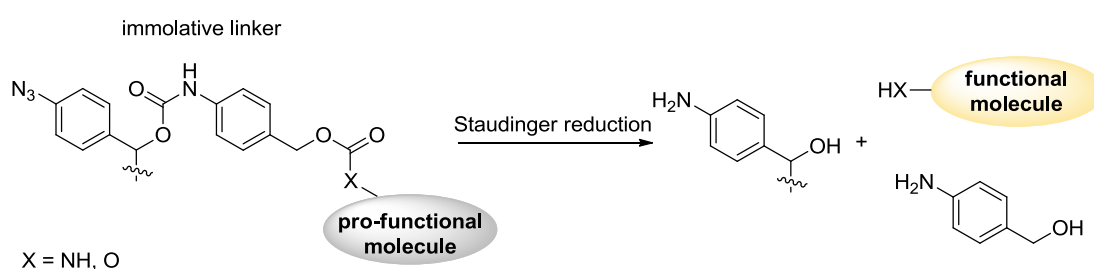


Figure 5: Application of the Staudinger reaction for templated reductive quencher release (Quenched Staudinger-triggered α -azido-ether release (Q-STAR)).^[30f]

In a first application, Franzini and Kool were able to yield a strong fluorescence turn-on signal in 20 min. with very low background and substantial amplification by turnover on the template.^[30f] A green/red pair of such probes allowed the discrimination of two bacterial species by a single nucleotide difference in their 16S rRNA. This methodology was further improved, and a 2-STAR

probe, containing two quencher groups tethered by separate reductively cleavable linkers, was established.^[30g] The background emission observed in this context, generated by off-template reactions or incomplete quenching, was among the lowest of any fluorogenic reactive probes for the detection of DNA or RNA.

Furthermore, the Staudinger reduction was used for the release of different functional molecules based on an azide-reduction triggered immolative linker (Scheme 7).^[30c] A *p*-azidobenzyl moiety was applied as an immolative linker, which can release a broad variety of molecules after the Staudinger reduction. These molecules are linked to the benzylic position via a carbonate or carbamate, which in turn can mask the function of the appended molecule.



Scheme 7: Azide-reduction triggered immolative linker for the release of functional molecules.^[30c]

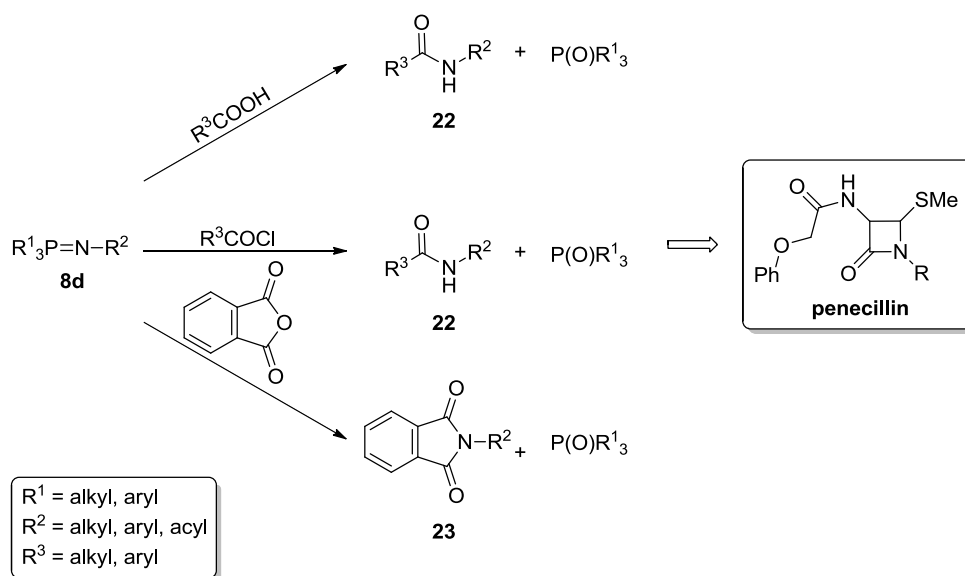
All the aforementioned biological applications profit from the Staudinger reaction with respect to its reaction kinetics and bioorthogonality. They enabled the reduction of unsighted activation and the analysis of localization, transcription or processing of RNA or DNA species in living eukaryotic cells.

1.2.1.1.2 Synthesis of amides

If an acid is used for hydrolysis instead of water after the Staudinger reaction, protonation of the nitrogen occurs, and the positively charged phosphorus can be attacked by the carboxylate (Scheme 8). Subsequent rearrangement of the formed intermediate accompanied by the elimination of triphenylphosphine oxide leads to the acylated secondary amine **22**. This method for amide bond formation has found application in the synthesis of small peptides^[31] and peptide lipids^[32] or acetamido-substituted glycopeptides^[33].

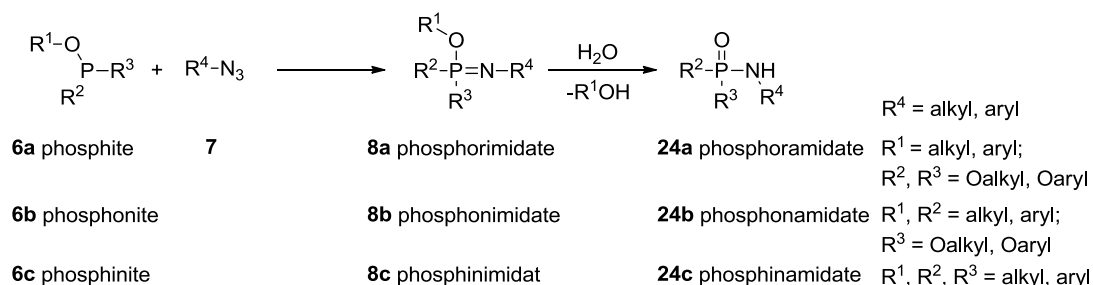
The presence of an anhydride entails the attack of the nitrogen at the carbonyl carbon, and a double acylation occurs promoting the synthesis of protected amines **23**. This method found particularly application in oligosaccharide synthesis (Scheme 8).^[34]

Besides acids and anhydrides acyl chlorides can also be used as shown in the synthesis of penicillin (Scheme 8).^[34b, 35]



Scheme 8: Reaction of iminophosphoranes **8d** with carboxylic acids, acyl chlorides and anhydrides.

1.2.1.2 Hydrolysis of phosphin-, phosphon- and phosphorimidates

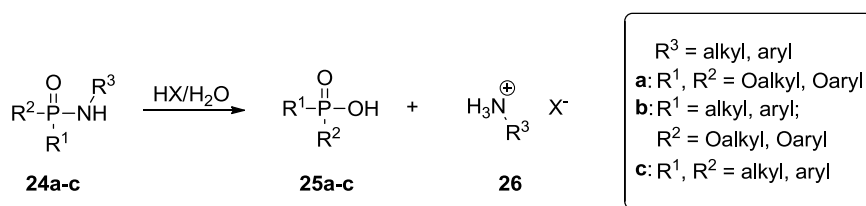


Scheme 9: Hydrolysis of phosphor-, phosphon- and phosphinimidates **8a-c** leading to the corresponding amidates **24a-c**.

If the trivalent phosphorus species contains at least one alkoxy substituent, under mild conditions hydrolysis does not lead to P-N bond cleavage but the formation of phosphor-, phosphon- or phosphinamidates **24a-c** (Scheme 9). During the process, the nucleophilic nitrogen is protonated and the alkoxy substituent is substituted by water under formation of a P-O double bond.

As already described for the Staudinger reduction, several one-pot procedures were developed from tertiary alcohols^[25b] and alkyl bromides^[36] in order to avoid azide isolation. The P-N-compounds obtained after hydrolysis can also be regarded as protected amines, and the

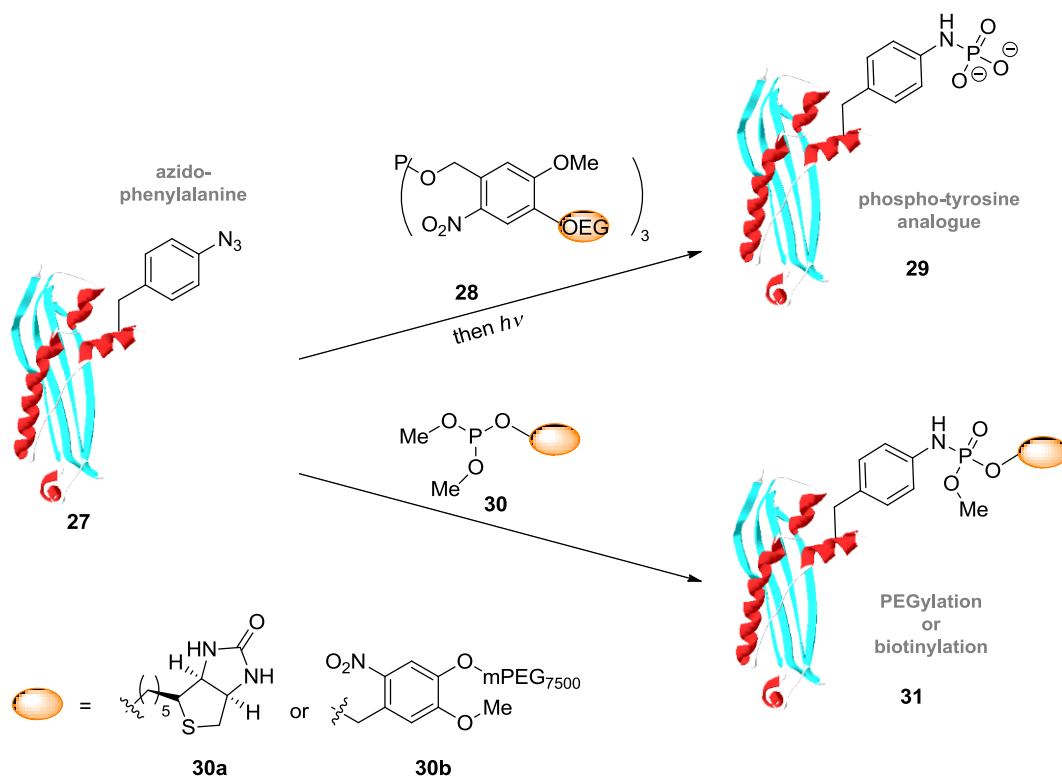
removal of the phosphorus moiety can be achieved by treatment with strong acids delivering the corresponding ammonium salt **26** (Scheme 10).^[12, 14b]



Scheme 10: Acidic cleavage of phosphor-, phosphon- and phosphinamidates **24a-c** delivers prim. amines **12** as their ammonium salts **26**.

The synthesis of phosphor- and phosphonamidates **24a** and **b** has just recently been identified as a method to bioorthogonally functionalize biomolecules or more precisely azido peptides and proteins **27** by treatment with phosphites **6a** and phosphonites **6b**.^[6, 37] By incorporating a light, cleavable ester group on the phosphite **28**, deprotection of the phosphoramidate to NH-P(O)(OH)₂ as surrogate for the natural phosphate group could be realized even on the protein level. Preliminary results and the development of the methodology as surrogate for protein phosphorylation is described more detailed in the discussion, but the results involved further investigations and strategies. As a result, the Staudinger reaction has been applied for the site-specific introduction of biotin into a protein^[37a] or as a PEGylation method^[37b] with phosphites **30a** and **30b** (Scheme 11).

As shown in the general reaction scheme (Scheme 9), hydrolysis always leads to the loss of one of the phosphorus substituents (-OR¹), and in case of unsymmetrical phosphites the alkoxy groups have to be carefully designed with respect to the chosen substituents. Generally, two different reaction mechanisms can be considered: either the water attacks at the alkyl group in an Arbusov-type reaction or a direct attack by water takes place at the phosphorus of the azaylide **8a-c**. Which reaction pathway is followed depends on the substituents, although the latter seems to be the more relevant pathway. If the water attacks at the phosphorus center, the amino substituent may also be expelled, but experiments suggested that this is rarely the case. To optimize the selectivity of hydrolysis, different unsymmetrical phosphites comprising two methyl-groups (R², R³ = OMe) and one other substituent (R¹ = Bn, Ph, Et, *i*Pr, dec) were synthesized and then used for the Staudinger reaction and hydrolysis.^[37a] The results indicated that benzyl- and phenyl-groups are more easily expelled than methyl groups and that longer or more branched substituents, like ethyl, *iso*-propyl or decyl, remained in the phosphoramidate to a greater extent.

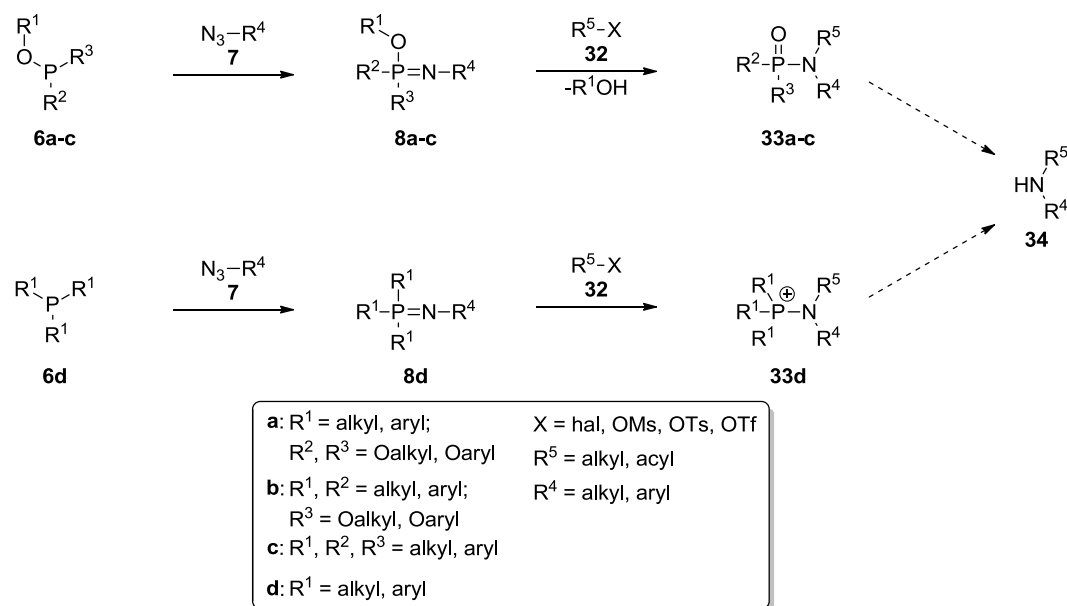


Scheme 11: Application of the Staudinger-phosphite reaction for the chemical phosphorylation and for biotinylation and PEGylation of azido proteins **27**.^[6, 37]

1.2.2 Alkylation of iminophosphoranes, phosphin-, phosphon- and phosphorimidates

The negatively charged nitrogen of iminophosphoranes **8d** and phosphor-, phosphon-, and phosphinamidates **8a-c** cannot only be protonated but also alkylated with appropriate electrophiles like **32** (Scheme 12).^[14b]

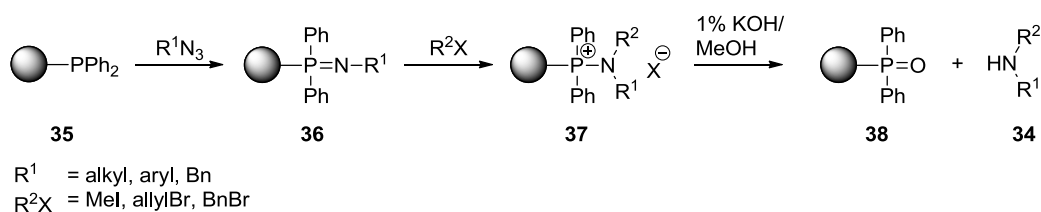
This occurs if for example simple alkyl halides or acyl halides like **32** are added to the reaction mixture. In case of iminophosphoranes **8d**, alkylation leads to phosphonium salts **33d**, which are afterwards hydrolyzed to the secondary amines **34** (Scheme 12, 2. equation), whereas compounds with an alkoxy group at the phosphorus generate *N,N*-disubstituted phosphor-, phosphon- or phosphinamidates **33a-c** by losing one alkyl-group under formation of a P-O double bond (Scheme 12, 1. equation). Here, the P-N bond can only be cleaved under strong acidic conditions.^[38]



Scheme 12: Alkylation of phosphor-, phosphon-, and phosphinamidates **8a-c** and iminophosphanes **8d**.

If the electrophilic carbon is present in the molecule itself, the reaction also works intramolecularly and results in cyclic derivatives. This strategy was strategically well placed in the synthesis of Tamiflu^[39] by installation of the leaving group at the nitrogen substituent leading to aziridines.

A polymer-bound, triphenylphosphine-supported reagent **35** allows a one-pot, two-step synthesis of secondary amines **34** from the corresponding azide and a reactive alkyl halide (Scheme 13).^[40] As described before, filtration of the polymer delivers the sec. amine **34** in high yields and purity. The only limitation of the procedure is that phenyl azides cannot be used and that the alkyl halide has to exhibit a certain reactivity.

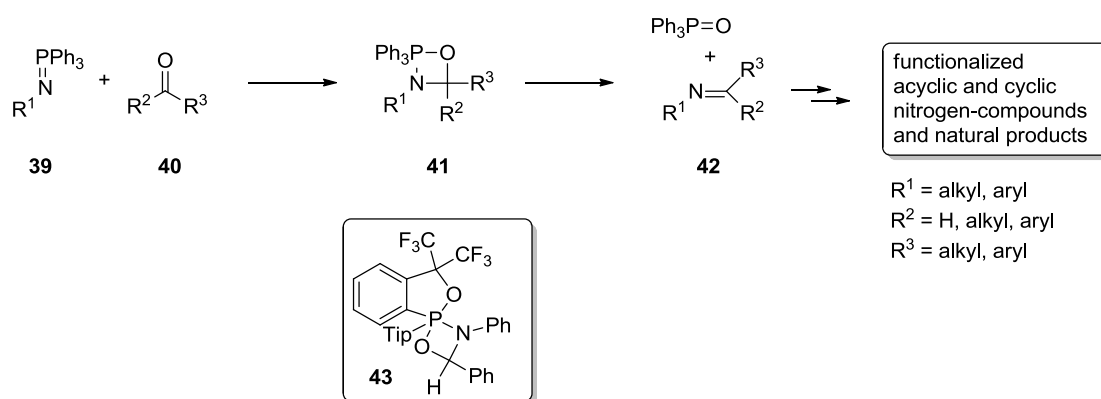


Scheme 13: Application of the Staudinger reaction and following alkylation on solid support for the preparation of sec. amines **34**.^[40]

1.2.3 The aza-Wittig reaction

In the previous sections, the scope of possible reactions based on the nucleophilic character of iminophosphanes **8d** and imidates **8a-c** was already attested. However, reactions in which the

phosphorus group is eliminated from the product in its oxidized form, like in the aza-Wittig reaction (Scheme 14), are even more attractive for organic chemists. With regard to its betainic structure the iminophosphorane **39** in its aza-ylide form is an analogue of the well-known Wittig reagent. About 30 years after the Staudinger reaction was discovered, iminophosphoranes were used in the so-called aza-Wittig reaction, which enables straightforward formation of C-N double bonds, and numerous publications describe their utility in organic chemistry.^[3, 12, 14b, 41]

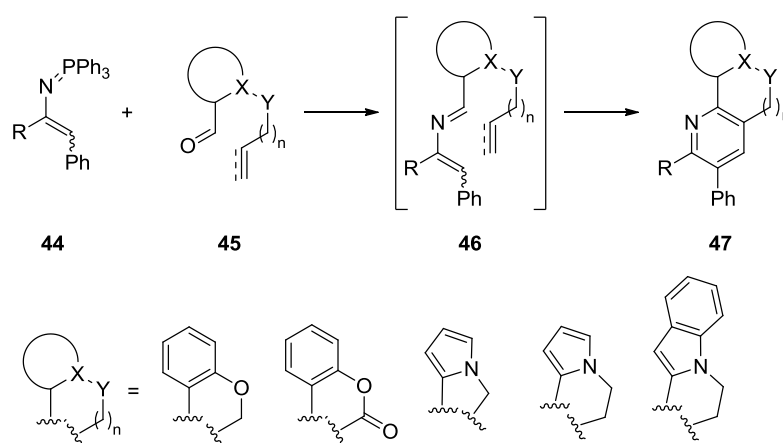


Scheme 14: The aza-Wittig reaction.

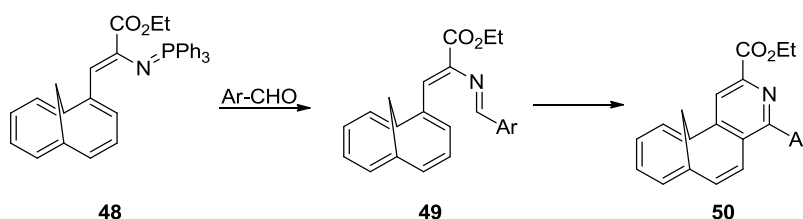
Mechanistically, the aza-Wittig reaction resembles the standard Wittig reaction, and a four-membered cyclic intermediate **43** could be isolated by using the very bulky Martin ligand for stabilization (Scheme 14).^[42] Subsequent thermolysis of the cyclic compound yielded phosphine oxide and the desired iminic compound **42** proving the course of an aza-Wittig reaction. Later, *ab initio* calculations further verified the experimental data and supported a tandem [2+2] cycloaddition–cycloreversion as mechanism with preferential or exclusive formation of the *E*-enantiomer of the imine.^[43] Comparison with the traditional Wittig reaction revealed the higher nucleophilicity of the ylide resulting in a higher reactivity in contrast to the aza-ylide, but still the aza-Wittig reaction proceeds smoothly and under mild reaction conditions.

The most common transformation is the reaction of iminophosphoranes **39** with aldehydes or ketones **40** yielding iminic compounds **42**. In this category the reaction of simple iminophosphoranes **39** yields imins or functionalized imines **42** in a first step but also amines, amides and enamides are accessible by simple subsequent transformations like reduction or acylation.^[41a] To overcome one of the biggest inconveniences of the aza-Wittig reaction – the formation of the phosphine oxide – Charetta *et al.* developed a solid-phase methodology that simplified very much the purification when the phosphine oxide stays at the solid support.^[44] This strategy was already described previously for the Staudinger reduction and the Staudinger

reaction with subsequent alkylation (chapter 1.2.1.1 and 1.2.2). The fact that makes the aza-Wittig reaction highly interesting for organic chemists, is the high reactivity of the formed imine **42**, which allows further transformation by a variety of different reactions. Especially, its applicability in tandem or domino reactions including different cyclization reactions characterizes its value as it gives direct access to heterocycles, which are frequently found in biologically active compounds and natural products. Hence, the synthesis of vinylic phosphazenes **44** is very valuable since they can serve as starting material for cycloaddition reactions. If the reaction is followed by an intramolecular cyclization, heterocyclic systems can be synthesized. This methodology has been applied to the synthesis of alkaloids like lavendamycin^[45] or, as shown in Scheme 15, of condensed pyridines **47**^[46]. Electrocyclic ring closures can also lead to heterocycle formation (Scheme 16).^[47]



Scheme 15: Synthesis of condensed pyridines **47** by the aza-Wittig reaction. Starting from a vinylic phosphazene **44** and an aldehyde **45**, the aza-Wittig reaction delivers intermediate **46**, which cyclizes to the pyridine **47**.^[46]

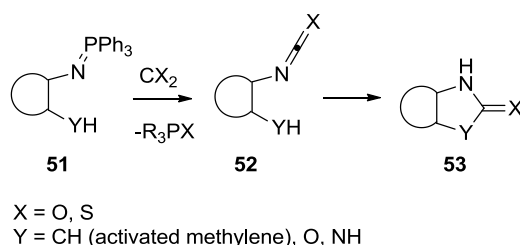


Scheme 16: Synthesis of 1,6-methano[methano[10]annuleno[3,2-c]pyridines **50** by the aza-Wittig reaction of **48** and aromatic aldehydes and following electrocyclization of the aza-Wittig product **49**.^[47]

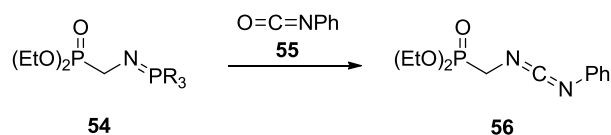
In Addition to aldehydes and ketones, carbon dioxide, carbon disulfide, isocyanates, isothiocyanates or even ketenes can serve as reaction partners leading to a wide variety of additional products. Reaction with carbon dioxide or carbon sulfide results in the formation of isocyanates or isothiocyanates, respectively. Again, following electrocyclic reactions or

intramolecular cyclizations are prospective for the synthesis of cyclic skeletons as displayed in the example for the five-membered polycycle **53** (Scheme 17).^[41a] If isocyanates **55** or isothiocyanates are used as reaction partners, carbodiimides like **56** are accessible (Scheme 18).^[48] This class of reactions takes place under neutral conditions and is compatible with all common hydroxyl protective groups and was, for example, used for the synthesis of mono- and disaccharides glycosyl carbodiimides.^[49] These are attractive intermediates since the carbodiimide group plays a pivotal role in the preparation of ureas, thioureas and guanidines through standard transformations. Carbodiimides are also noteworthy starting materials for different ring closure reactions like [4+2] or [2+2] cycloadditions, and they are used for heterocycle synthesis.^[41a] Ketenes are even more reactive than isocyanates and afford ketenimines. This was one of the first reactions with iminophosphoranes reported by Staudinger and Meyer.^[3]

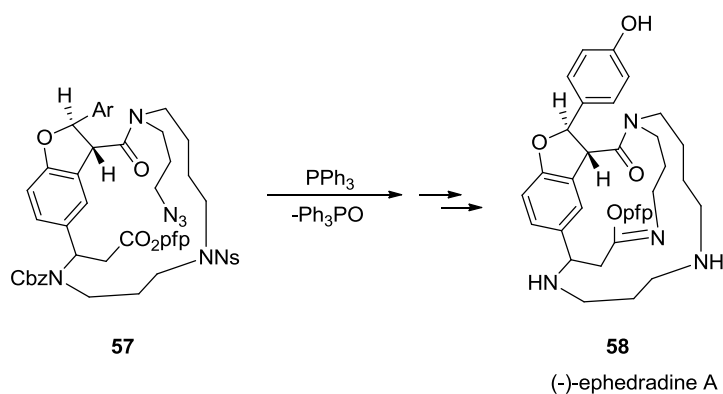
All the reactions discussed so far proceed intermolecularly, but intramolecular reactions are also possible and imply preparation of five- to higher-membered heterocyclic compounds under very mild reaction conditions. The structure formed is dependent on the carbonylic group. Aldehydes, ketones, esters, amides anhydrides and even heteroatom-oxygen double bonds like sulfoxides can react and were used for the synthesis of many natural products like (-)-stemospirone^[50], (-)-dendrobine^[51], (-)-benzomalvin^[52] or (-)-ephedradine A (**58**)^[53] (Scheme 19).



Scheme 17: Synthesis of polycyclic heterocycles **53** by an aza-Wittig reaction of **51** with carbon dioxide or carbon disulfide and following intramolecular cyclization of **52**.



Scheme 18: Synthesis of a functionalized carbodiimide **56**.^[48]



Scheme 19: Synthesis of (-)-ephedrine A (**58**) by the aza-Wittig reaction.^[53]

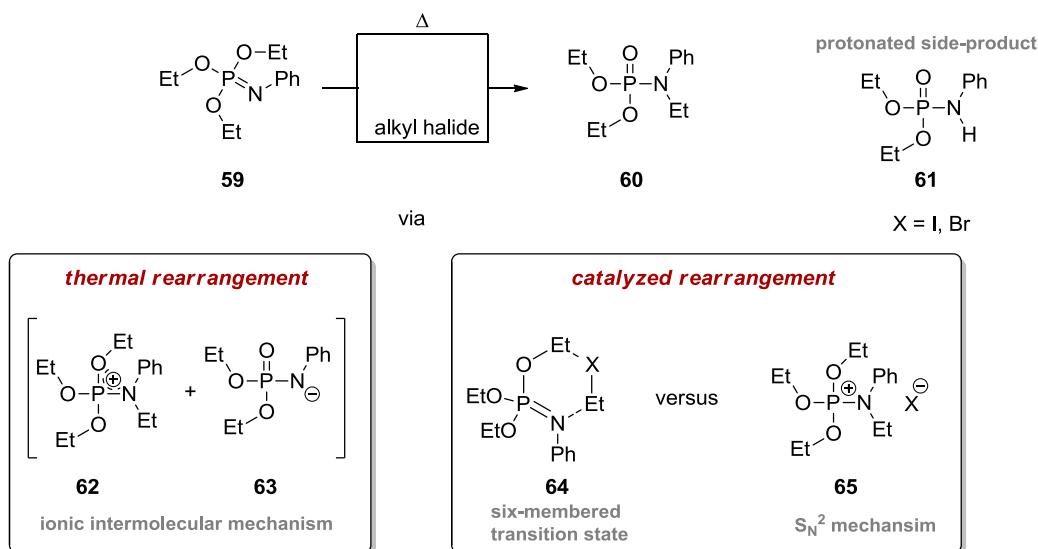
1.2.4 Rearrangement of phosphazenes

1.2.4.1 Thermal and electrophile catalyzed rearrangement

The rearrangement of phosphorimidates like **59** to the corresponding *N,N*-disubstituted phosphoramidates **60** was first presented by Kabachnik *et al.*^[5a] in 1970 who could show that the rearrangement can be initiated by alkyl iodides at elevated temperatures in acetonitrile (Scheme 20). Eight years later Challis *et al.*^[5b] performed further investigations on the kinetics, mechanism and reaction conditions using triethyl *N*-phenyl phosphorimidate **59** as the model substrate and various electrophilic agents as initiators of the rearrangement. In absence of any electrophilic additive, the rearrangement proceeded very slowly, and after 30 days at 100°C in nitrobenzene, only half of the phosphorimidate **59** was converted to the desired phosphoramidate **60**. Additionally, concurrent dealkylation leading to the phosphoramidate **61** was observed in about 9%. Studies on the reaction rates of this thermal rearrangement showed second-order kinetics supporting an intermolecular reaction mechanism. The thermal rearrangement is likely to proceed via an ionic intermolecular pathway in which one ethyl group of the phosphorimidate **59** is transferred to the nitrogen of another phosphorimidate molecule **59** leading to the ionic species **62** and **63**. Afterwards, intermediate **62** loses one ethyl group accompanied by formation of the P-O double bond, and the released ethyl group can further react with the phosphorimidate **59** or the anion **63**.

As already observed by Kabachnik *et al.*, the addition of alkyl halides facilitated the reaction and shortened the reaction time drastically.^[5a] Moreover, reaction rates showed dependence on the solvent polarity (MeCN > PhNO₂ > CCl₄) implying that ionic intermediates like **62** play a decisive role in the reaction mechanism.^[5b] These results supported the S_N² mechanism, in which the nitrogen of the phosphorimidate **59** attacks the alkyl halide leading to intermediate **65** and not

the formation of the six-membered transition state **64**. The halide afterwards attacks the ethyl group of the ethoxy group under formation of the P-O double bond and regeneration of the alkyl halide. The catalyzed reaction following is bimolecular, and the reaction rate is dependent of both the phosphorimide and the alkyl halide concentration.



Scheme 20: Thermal and electrophile catalyzed rearrangements of phosphorimidates **59**.

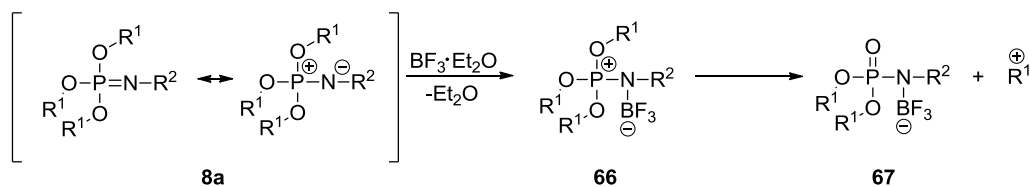
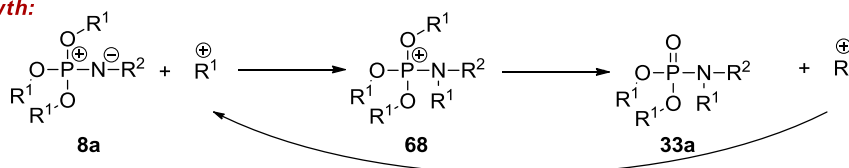
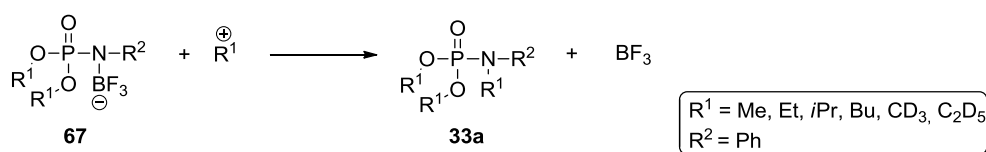
Testing of different electrophiles revealed that methyl iodide and ethyl iodide serve as effective additives, whereas EtNO_3 , EtI-AgNO_3 and isopropyl iodide were less active. Nonetheless, silver iodide, which precipitated from the reaction mixture when equimolar quantities of EtI-AgNO_3 were added, was able to catalyze the rearrangement heterogeneously to some extent. Coming from iodide to chloride, the catalytic ability decreases and addition of $i\text{PrCl}$ or EtCl had no relevance for the reaction. Product formation even with ineffective catalysts could be explained by presence of ethyl halide, which is formed during the reaction from the ethyl groups of the phosphorimide **59**.

Besides the alkyl halides, other additives were tested: ZnI_2 and I_2 showed a catalytic ability similar to EtI , while ZnBr_2 , MeCOBr and HBr were similar in activity to EtBr . Although 0.1 equivalent of HBr initiated the rearrangement, 1 equivalent only led to protonation of the phosphorimide.

1.2.4.2 Phosphorimide-amidate rearrangement catalyzed by Lewis acids

Kabachnik *et al.*^[5c-8] first investigated the Lewis acid-catalyzed rearrangement and observed that catalytic addition of $\text{BF}_3\text{-Et}_2\text{O}$ leads to the transfer of one alkyl group of the alkoxy substituent at

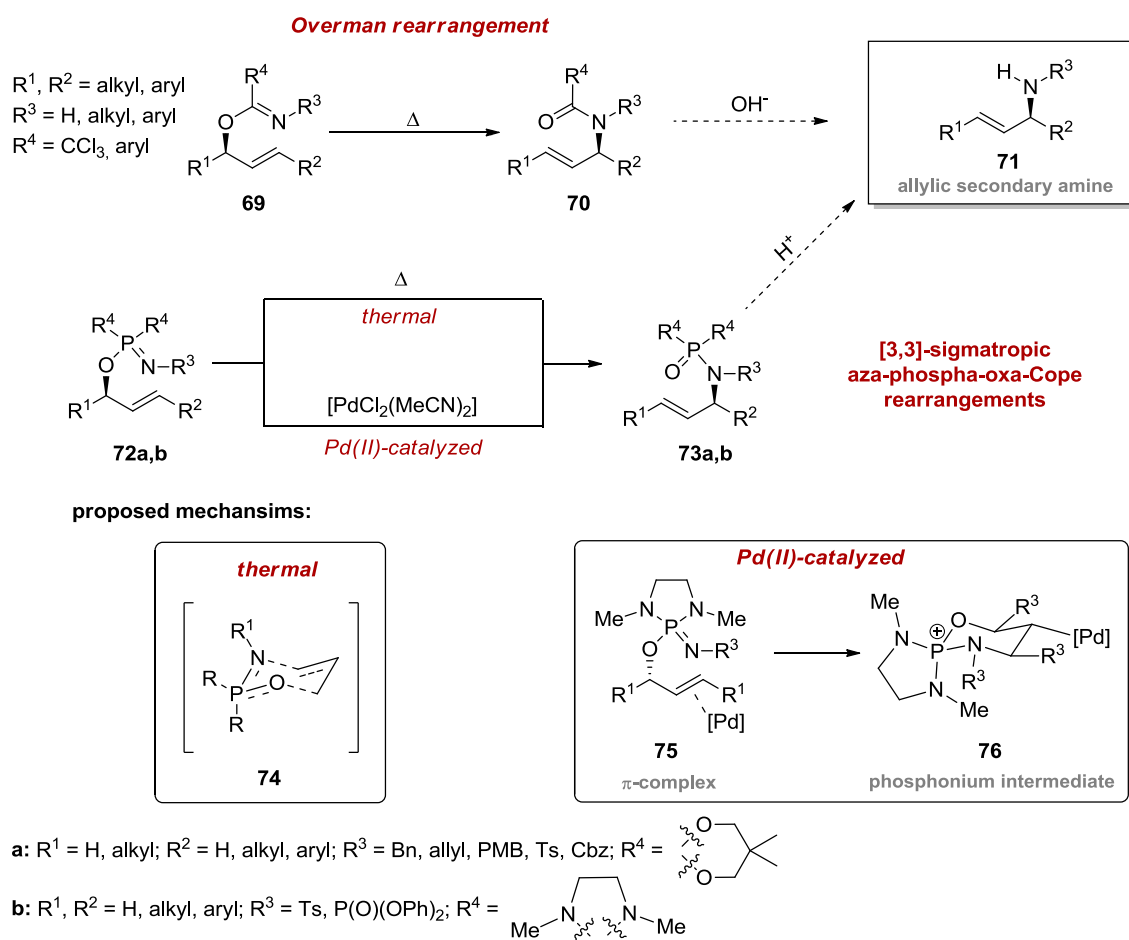
the phosphorus to the nitrogen of the phosphorimidate **8a** accompanied by formation of a P=O double bond (Scheme 21). The reaction was performed neatly by just adding a small amount of Lewis acid to the phosphorimidate **8a** at 0 °C and subsequent heating to 60-65°C for 6 h. Studies on the BF₃·Et₂O-complex of *N*-benzyl triphenyl phosphinimidate proved that coordination occurs at the nitrogen and leads mainly to a phosphonium compound. This observation gave rise to the assumption that also in the case of phosphorimidates **8a** a complex with a phosphonium structure **66** is formed, which alleviates the following rearrangement. It was confirmed by crossover experiments that a bimolecular mechanism is likely to take place, in which one of the alkyl groups of the ester is transferred to the nitrogen of another phosphorimidate molecule. The crossed product and two side products were observed in which one alkyl group of the ester was exchanged.

chain initiation:**chain growth:****chain termination:**

Scheme 21: Lewis acid-catalyzed rearrangement of phosphorimidates **8a**.^[5f]

1.2.4.3 The 3-aza-2-phospha-1-oxa-Cope rearrangement

Almost at the same time Mapp and Chen^[38b] as well as Batey and Lee^[38a] presented a rearrangement of allylic phosphorimidates **72a** or of (allyloxy) iminodiazaphospholidines **72b**, which are accessible by the Staudinger reaction, as a new entrance to allylic amines **71** (Scheme 22). Allylic amines **71** are essential building blocks for the synthesis of diverse biomolecules and natural products like α - and β -amino acids^[54], carbohydrate derivatives^[55] or alkaloids^[56]. Therefore, many efforts have been undertaken to enable their preparation.^[57]



Scheme 22: Overman rearrangement and 3-aza-2-phospha-1-oxa-Cope rearrangement towards allylic amines **71**.

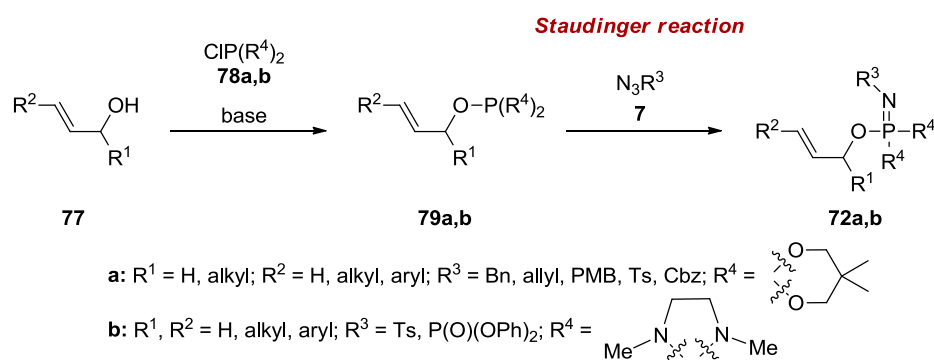
In contrast to the already known thermal or electrophile catalyzed rearrangement of other phosphorimidates **8a**^[5b, c], which is believed to occur in a bimolecular fashion, substitution of one alkoxy by an allyloxy group predominantly leads to an intramolecular [3,3]-sigmatropic rearrangement corroborated by crossover experiments.^[58] This aza-phospha-oxa-Cope rearrangement is an analogue of the famous and widely utilized Overman rearrangement^[59] that stands out due to its regiochemical control and the transfer of stereochemistry when starting from stereodefined allylic imidates **69**. [3,3]-sigmatropic rearrangements are popular for the controlled formation of C-C or C-N bonds because structurally complex target molecules are attained under simple reaction conditions and with very high selectivity resulting from the six-membered, chair-like transition state. The aza-phospha-oxa-Cope rearrangement delivers at first *N,N*-disubstituted phosphoramidates **73a** and phosphoramides **73b**, respectively, containing an allyl group at the nitrogen, which can be regarded as protected secondary allylic amines **71**. In contrast to the Overman rearrangement, where hydrolysis of the formed amides **70** delivering the free amine can be achieved under basic conditions, deprotection after the aza-phospha-oxa-

Cope rearrangement is possible by acidic treatment and thereby it accomplishes the synthetic repertoire for the synthesis of secondary allylic amines **71**.

The rearrangements described by Mapp *et al.*^[38b] and Batey *et al.*^[38a] differ in the starting materials but more importantly in the reaction conditions. While Mapp and Chen developed a procedure for a thermally induced rearrangement, Batey and Lee reported a Palladium-catalyzed alternative (Scheme 22). The thermally induced rearrangement proceeds analogue to the classical [3,3]-sigmatropic rearrangement in a concerted way via **74**, whereas a two-step mechanism is proposed for the Pd(II)-catalyzed variant. First a π -complex **75** of the palladium and the alkene is formed which initiates attack of the imidate nitrogen at the activated alkene in a *6-endo-trig* fashion. Subsequent deoxypalladation leads to the six-membered phosphonium intermediate **76**, which undergoes fast breakdown to the desired product **73b**.

In both cases the thermodynamic driving force of the occurring rearrangement is attained by interconversion of the $P^V=N-$ to the $P^V=O$ -compound, which is estimated at approximately 25 kcal mol⁻¹ based on the conversion of $(NH_2)_2(MeO)P=NH$ to $(NH_2)_2(MeNH)P=O$.^[5e, 38a, 60]

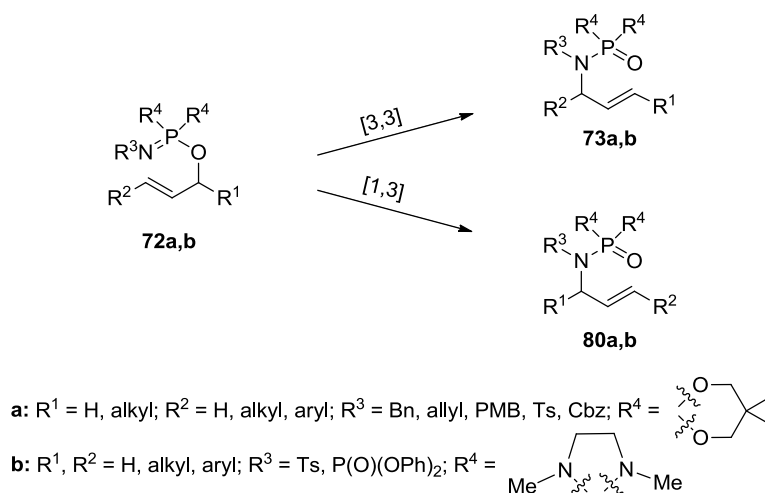
The synthesis of the starting material for the rearrangement is very similar. Dialkoxychlorophosphine **78a** or bis (dialkylamino) chlorophosphin **78b** is reacted with the allylic alcohol **77** in presence of base to the phosphite **79a** or the phosphoramidite **79b**, and afterwards the Staudinger reaction with the azide **7** is performed (Scheme 23). The rearrangement of the obtained phosphazenes **72a** and **72b** is then induced either in a one-pot reaction or after purification of the intermediates.



Scheme 23: Synthesis of P(III) reagents and following Staudinger reaction.

It is important to note that besides the desired [3,3]-rearrangement the formal [1,3]-sigmatropic shift can still occur leading to the undesired regioisomer **80** as described before. Reaction

conditions have to be optimized to favor the [3,3]-sigmatropic rearrangement and to simultaneously suppress the bimolecular pathway (Scheme 24).

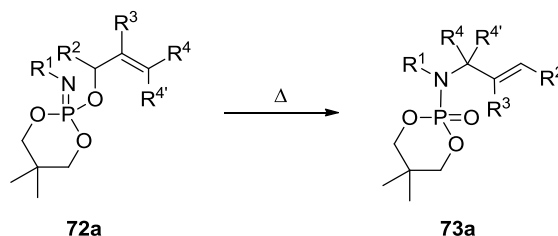


Scheme 24: [3,3] versus [1,3] rearrangement.

For the thermal rearrangement^[38b, 58], the choice of the trivalent phosphorus species, the type of solvent as well as the temperature plays a crucial role in optimizing yield. Polar solvents like acetonitrile promote the intermolecular pathway demonstrating the difference to the [3,3]-sigmatropic rearrangement. While the [3,3]-sigmatropic rearrangement proceeds via a concerted way, charged intermediates are formed in the stepwise intermolecular rearrangement (see chapter 1.2.4.1). Therefore, nonpolar solvents like benzene or toluene are more appropriate and lead exclusively to the formation of the desired product, albeit at low reaction rates. Finally, xylene turned out to provide the optimal combination of polarity and temperature resulting in high yields.

With respect to the trivalent phosphorus species, phosphites **79a** turned out to be more suitable than phosphinites. The diphenyl phosphinite-derived phosphinimidates only delivered the undesired [1,3]-product in acetonitrile at 80°C. Even in xylene and at higher temperature the ratio could only be improved approximately to a one-to-one mixture (50:50). Substitution of the diphenyl phosphinite, first by dioxyethyl and then diethoxy phosphite could prevent the formation of the [1,3]-product, but the yields were still unsatisfactory. Replacing the phosphorus substituents by the more bulky 2,2-dimethyl propyl group finally delivered the product in high yields and also prevented inadvertent cross reactivity of the two substituents. This observation can be explained by the electron donating effect of the alkoxy group which leads to the acceleration of the rearrangement and to increased yields, i.e. an effect already recognized in other [3,3]-sigmatropic rearrangements like the Claisen rearrangement.

It could further be demonstrated that the rearrangement works well for a variety of different substitution patterns of the allylic group. Hydrogen, alkyl, aryl and halogens were tolerated at the C2 or C3 position of the double bond. Even C3-disubstituted compounds like geraniol-derived phosphorimidates provided the product in high yield under formation of a quaternary center, which highlights the synthetic potential of the procedure. Moreover, the reaction was unaffected by the double bond geometry. Substitution in the C1 position even accelerated the reaction. The reaction time was reduced from 4 h to 1 h, and *E*-allylic amines could be prepared. *E*-allylic amines were formed with excellent stereochemical fidelity with a selectivity of >20:1 for the *E*-product, and the stereoinformation of the allylic alcohol was also conserved during the reaction. Variations are also possible in the nitrogen source, where benzyl, allyl and *p*-methoxybenzyl azide efficiently served as substrates (Scheme 25, Table I). Only electron-deficient azides like tosyl and Cbz-azide primarily led to the undesired regioisomer. This can be explained by the good leaving group ability of the phosphoramidate. To change the reactivity, an electron-withdrawing group was incorporated at the C2 position to facilitate the attack at the double bond in this position. Thus, reaction proceeded well with Cbz-azides, gave the product as pure *E*-olefin, and enabled access to β -amino acids after reduction of the double bond. The required allylic alcohols can easily be obtained by the Baylis-Hillman reaction.



Scheme 25: Reaction scope of the thermal rearrangement. ^[38b, 58]

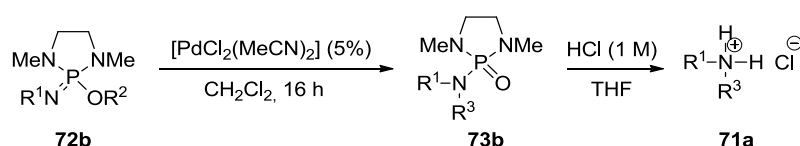
Table I: Selection of the reaction scope of the thermal rearrangement. ^[38b, 58]

R ¹	R ²	R ³	R ⁴ /R ^{4'}	Yield [%]
Bn	BnOCH ₂ -	H	H/H	65
Bn	H	-Cl	H/H	75
Bn	H	H	Et-/H	85
Bn	H	H	Me/	65
allyl	H	propyl	H	60
Cbz	Me	-CO ₂ Me	H	65
Ts	H	H	H	95

In the Pd-catalyzed version, established by Batey *et al.* ^[38a], (allyloxy) iminodiazaphospholidines **72b** received from a precedent Staudinger reaction serve as precursors for the rearrangement.

In contrast to the thermal rearrangement of iminodiazaphospholidines **72b** no [1,3]-products resulting from the competitive intermolecular mechanism based on ionization and recombination were observed with a Pd(II) catalyst.

As described before, iminodiazaphospholidines **72b** can easily be prepared by a one-pot procedure in toluene at room temperature starting from bis(dialkylamino) chlorophosphin **78b**^[61] and the allylic alcohol **77** to form a phosphoramidite **79b**^[62], which is subsequently reacted with the azido compound. Alternatively, phosphoramidites **79b** are accessible by sequentially adding the diamine and the allylic alcohol **77** to PCl₃. Screening of different Pd(II) catalysts to induce the rearrangement revealed [PdCl₂(MeCN)₂] as the only active catalyst, and the rearrangement proceeded smoothly at room temperature to the desired products **73b** in presence of 5% of the catalyst. In the preliminary studies two different azides, namely tosyl azide and diphenylphosphoryl azide (DPPA), were utilized and worked well, although a molecular sieve had to be added for the latter to ensure complete conversion and yields still were generally lower (Scheme 26, Table II). For this Pd-catalyzed rearrangement, different substitution patterns including substitutions α, β and γ to the oxygen of the alcohol **77** are accepted and showed high conversion rates. However, if sterically more demanding allylic alcohols **77** were used in the reaction, the conversion rate decreased or no product formation took place. This trend was demonstrated by 2-cyclohexenyl alcohol, which delivered a high yield of the rearranged product in the thermal rearrangement, but proved not to be an ideal substrate for the catalyzed variant. If starting from a γ,γ-disubstituted alcohol, no product was formed. Irrespective of this limitation, the catalyzed rearrangement features high *E*-selectivity and clean transfer of chirality, if enantioenriched alcohols are used. In presence of Pd(II)-catalysis the rearrangement proceeds at room temperature, i.e. under milder reaction conditions as compared to the thermal rearrangement, which makes this method more suitable for sensitive substrates. Following treatment of the obtained phosphoramides **73b** with hydrochloric acids leads to P-N-bond cleavage and delivers allylic tosylamides or HCl salts of allylic amines **71a**.



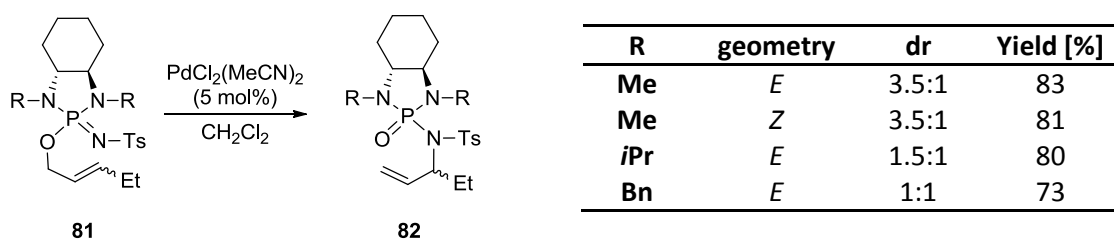
Scheme 26: Reaction procedure for the Pd-catalyzed rearrangement and subsequent release of the desired amine **71**.^[38a]

Table II: Exemplary reaction scope of the Pd-catalyzed rearrangement in dependence of the substitution pattern of the applied alcohol.^[38a]

R ¹	R ²	R ³	73b [%]	71 [%]
Ts			95	88
P(O)(OPh)			90	81
Ts			95	97
P(O)(OPh)			91	87
Ts			91	93
P(O)(OPh)			86	85
Ts			-	-
P(O)(OPh)			-	-
Ts			90	82
P(O)(OPh)			84	78

To further broaden the scope of the reaction Batey and coworkers strived towards the development of a diastereoselective and enantioselective variant of the rearrangement by incorporating a chiral auxiliary group in the phosphoramidite structure **79b** or by using a chiral Pd-ligand, a strategy already applied in enantioselective allylic imidate Overman rearrangements.^[59a, 59h, 63]

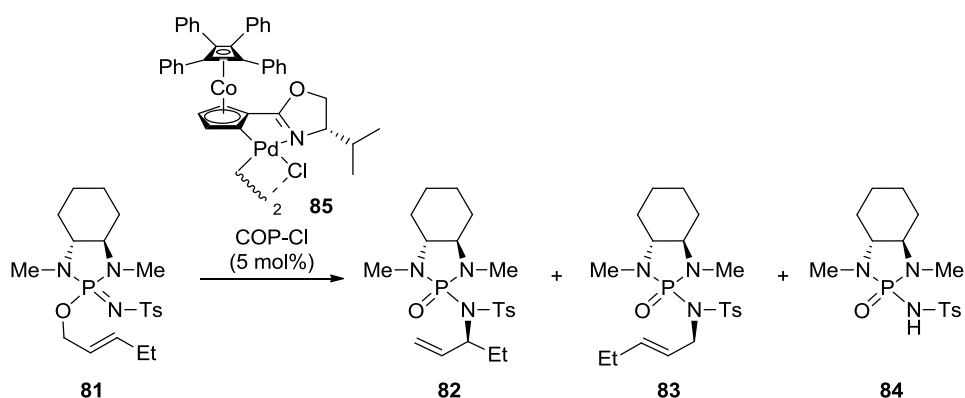
N,N'-dialkyl cyclohexanediamines were chosen as chiral auxiliaries because their C₂ symmetry prevents formation of diastereomeric mixtures at the phosphorus center and because preparation could be performed analogously to the previously published procedure (Scheme 27 and Table III).

**Scheme 27 and Table III:** Diastereoselective Pd-catalyzed rearrangement.^[63c]

Attempts to create tartrate-derived substituents turned out to be impossible due to their low temperature-resistance during the Staudinger reaction. When *Z*- and *E*-pent-2-en-1-ol were used as model allylic alcohol, diastereomeric ratios of up to 3.5 : 1 could be achieved, and after acidic cleavage the *S*-enantiomer was obtained in an ee of 56%. It is of interest, that both, the *Z*- and the *E*-alkene, favored formation of the same diastereomer. The analysis of the reaction intermediates provided a possible explanation: In case of the *trans* substrate two possible chair-like cationic intermediates can be passed through, yet one is disfavored due to the steric

interactions between the nitrogen substituent of the azide and the pseudo-axial methyl group at the nitrogen of the chiral diamine. A boat-like intermediate seems to be more likely in case of the *E*-substrates, as 1,3-diaxial interactions are facilitated leading also to the *S*-enantiomer.

Chiral ligands at the Pd(II) catalyst were also probed for an enantioselective variant of the rearrangement.^[63c] Initial investigations with phosphine-containing ligands like (*R*)-BINAP or (*R,S*)-Josiphos were unsuccessful in accordance to results obtained from the allylic imidate rearrangement.^[59f] Consequently, a chiral cobalt oxazoline palladacycles (COP-X), like **85**, which proved to be very effective in allylic imidate rearrangements^[59a, 59j, k, 64], was utilized for further studies (Scheme 28, Table IV). Surprisingly the COP-Cl ligand **85** seemed to be ineffective leading to more detailed examinations. Different reaction conditions including catalyst loading, reaction temperature and additives, such as molecular sieves and silver salts as catalyst counter ions, and different substrates were tested and revealed a strong dependence on the counter ion and the alkene geometry.



Scheme 28: Chiral cobalt oxazoline palladacycles (COP-Cl) **85** catalyzed rearrangement.^[63c]

Table IV: Yields and ee of the enantioselective Pd(II)-catalyzed rearrangement.^[63c]

81	additive	T (°C)	82 [%], ee		83 [%]	84 [%]
<i>E</i>	-	100	33	70	7	n.d.
<i>E</i>	MS	100	24	-	61	n.d.
<i>E</i>	-	120	47	69	8	20
<i>E</i>	AgOTs	50	31	81	7	12
<i>E</i>	AgNO ₃	50	31	82	4	n.d.
<i>E</i>	AgTFA	70	60	82	-	-
<i>E</i>	AgTFA	RT	16	86	-	-
<i>Z</i> ^{a,b}	AgTFA	50	97	92	-	-
<i>Z</i> ^{a,b}	AgTFA	RT	88	94	-	-

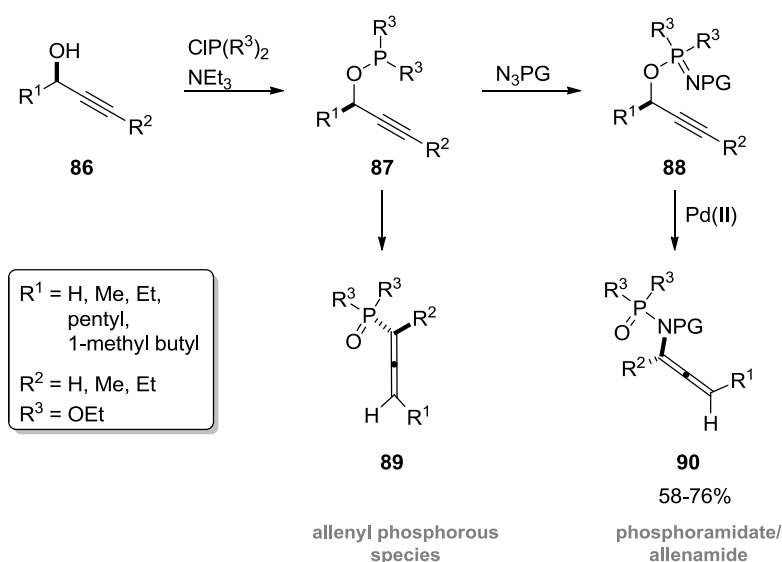
^a 0.8 M, ^b not displayed in the scheme

By replacing dichloromethane with toluene and increasing the reaction temperature to 120°C, COP-Cl **85** showed a moderate activity, and the desired product **82** was formed in a yield of 47% and with 69% ee. The presence of molecular sieve proved to be disadvantageous because it supports the formation of the undesired [1,3] product **83** and also promotes hydrolysis leading to a loss of the allylic substituent (compound **84**). Adding silver salts like AgNO₃, AgTFA and AgOTs further improved the ee to 82%, but yields at 50°C were still disappointing (30%) for the Z-substrate. The yield could nearly be doubled by increasing the substrate concentration to 0.8 M and by slightly increasing the temperature to 70°C. While higher ee values could be reached at lower temperature, this was accompanied by a decrease in yield. Unexpectedly, yields for the Z-substrate were by far higher (90%) with concurrent excellent ees of over 90% for the R enantiomer. Furthermore, the initial reaction rate for the E-substrates was estimated to be fourteen times faster than for the trans compound.

Mapp *et al.*^[58] adapted the Pd-catalyzed variant to the phosphorimidates **72a** derived from phosphites **79a** in order to increase the electrophilicity of the alkenes. In contrast to the thermal rearrangement, in which electron-withdrawing groups at the nitrogen like tosyl azide or Cbz azide gave only poor yields and conversion was only successful with electron-withdrawing groups in the C1-position, these substrates worked well in the catalyzed variant. Reactions with Cbz azide or tosyl azide with different substituted allyl groups gave moderate to excellent yields at room temperature and short reaction times (0.5 h) with 10 mol% catalyst and 2-12 h with 2 mol%, respectively. The diastereoselectivity was still high (*E/Z* > 20:1). Nevertheless, the electron-donating benzyl group at the nitrogen only led to the undesired regioisomer in the catalyzed variant.

1.2.4.4 Synthesis of allenamides by the 3-aza-2-phospha-1-oxa-Cope rearrangement

Having recognized the value of the rearrangement for organic synthesis, Mapp *et al.*^[65] extended the substrate scope to propargylic alcohols **86** as a starting material for a straightforward approach to allenamides **90**, which are versatile precursors for a variety of organic transformation (Scheme 29). Among the compounds accessible from allenamides are for example 1,2-aminoalcohols,^[66] cyclobutanes,^[67] dihydrofurans,^[68] pyranyl heterocycles^[69] or 2-amino-dienes.^[70] Therefore, many efforts have been made to develop a general entrance, but most methods need complex precursors, and especially enantiomerically enriched allenamides **90** are still hard to synthesize.^[71]



Scheme 29: Synthesis of propargylic phosphites **87** with following [2,3]-rearrangement or Staudinger reaction with following [3,3]rearrangement.^[65]

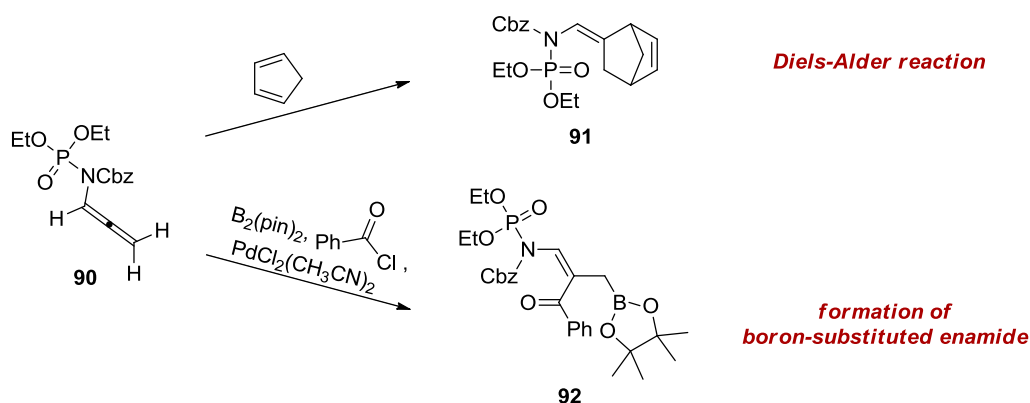
In contrast, the rearrangement allows preparation of allenamides **90** from readily available precursors (Scheme 29). Starting from propargylic alcohols **86**, which are commercially available or easily prepared even in an enantioenriched form,^[72] and a chlorophosphite, also a cheap starting material, an unsymmetrical phosphite **87** can be synthesized in one step in the presence of a mild base. This propargylic phosphite **87** can be converted to the desired phosphoramidate **88** by a Staudinger reaction and undergoes [3,3]-sigmatropic rearrangement in the presence of a Pd(II) catalyst. Although it is already known that propargylic P(III)-species are prone to undergo a [2,3]-rearrangement to form allenyl phosphorus species **89**, this could not be observed for the phosphite used. As shown previously by Mapp^[38b, 58] and Batey^[38a, 63c], regio- and stereochemistry is highly conserved during the rearrangement and the resulting allene is obtained fully protected and, hence, exists in a more stable form. Optimization of the reaction conditions revealed that in the case of these phosphites **87** the necessary phosphoramidates **88** could be obtained in good yields from electron deficient Cbz-azide, whereas phosphinites and phosphoramidites predominantly were transformed to the phosphinates **89**, derived from a [2,3]-rearrangement. As already demonstrated for allylic phosphoramidates **72a**, rearrangement of Cbz-protected phosphoramidates did not occur under thermal conditions and required a Pd(II) catalyst. It has to be noted that for these propargylic derivatives **88** bimolecular decomposition pathways play a more important role than for allylic phosphoramidates **72a** with an impact on yields of the desired allenes and catalyst loading. Substrate concentration as well as substrate structure had to be tuned carefully, and Mapp and coworker elucidated that low concentration

of the reactants and less constrained ethoxy groups at the phosphorus are more effective unlike the allylic rearrangement where the 2,2-dimethyl propyl group gave best results.

Testing the reaction scope revealed that 1-monosubstituted, 1,3- and 1,1-disubstituted and even 1,1,3-trisubstituted allenamides **90** are accessible in moderate to high yields. Only tertiary alcohols that would lead to 1,3,3-trisubstituted allenamides **90** underwent rapid [2,3]-rearrangement and did not give the desired allenamides **90**.

When enantioenriched propargylic alcohols **86** like (R)- and (S)-3-butyn-2-ol or (R)-(+)-1-octyn-3-ol served as starting material, products were obtained with 92% ee from each enantiomer or 80% ee, respectively .

Supplementary experiments showed that the fully protected phosphoramidates **90** could be stored at 0°C for more than two month with only slight decomposition, and they could successfully be used in further transformations like Diels-Alder reactions leading to **91** or for the synthesis of boron-substituted enamides **92** demonstrating the convenience of their preparation (Scheme 30).

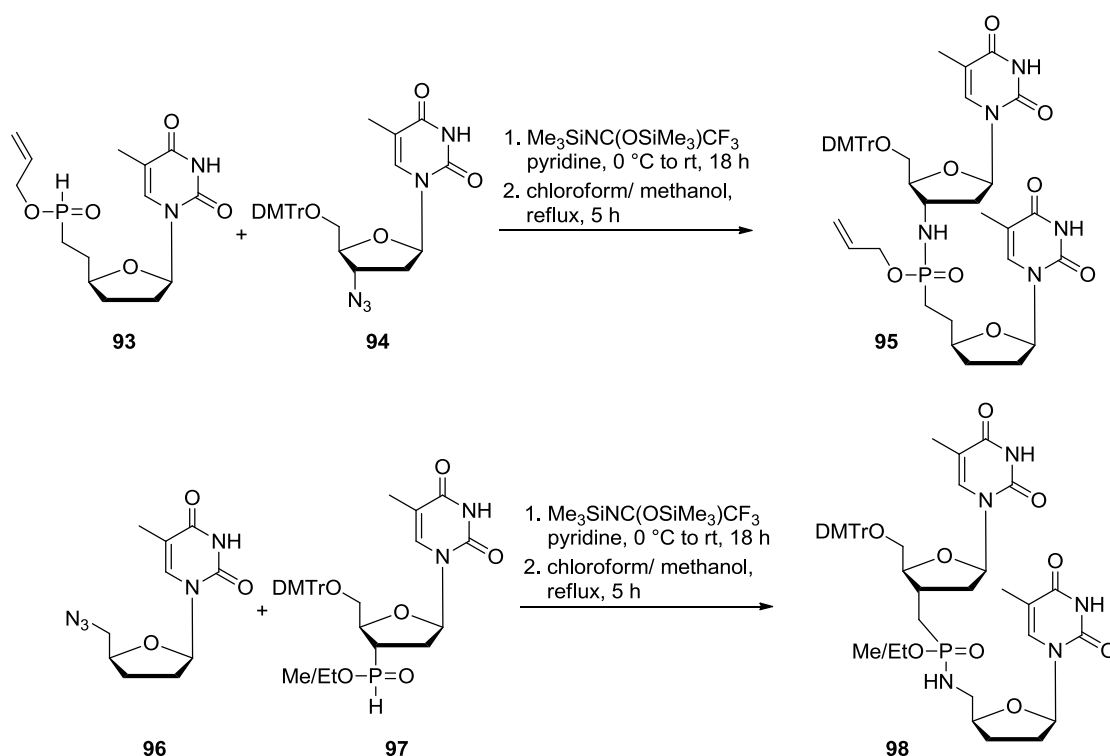


Scheme 30: Use of fully protected allenenes in a Diels-Alder reaction or for enamide synthesis.^[65]

1.2.5 Staudinger reaction with silylated phosphinic acid derivatives

The reaction of silylated trivalent phosphorus species with azides was first described in 2001 by Fairhurst *et al.*^[73] from Novartis Pharmaceuticals for the synthesis of phosphoramidate ester modified nucleic acids **95** and **98** (Scheme 31). Modified nucleic acids in which the labile phosphodiester linkage is replaced by more stable isosters such as phosphonates, phosphoramidates, phosphoramidates or phosphorothioate, are a remarkable area in medicinal

chemistry for the development of antisense agents with higher *in vivo* stability, better cell penetration and enhanced binding properties to the complementary RNA.^[73] Silylation of the nucleoside *H*-phosphinates **93** and **97** was achieved with bis(trimethylsilyl)trifluoroacetamide in pyridine and reaction with the appropriate azido-nucleoside **94** and **96** at room temperature delivered the silylated phosphonamidates **95** and **98**. Removal of the silyl groups by refluxing in chloroform/methanol yielded the desired products **95** and **98** after column chromatography as 1:1 mixtures of diastereomers in yields between 81-87%. The products were incorporated into oligonucleotides, and an enhanced binding could be observed with the 3'-C-P-N-5' isomer.



Scheme 31: Staudinger reaction of silylated phosphinic acid esters **93** and **97** with azides **94** and **96** for the synthesis of dinucleotides **95** and **98**.^[73]

This method was further optimized by separation of diastereomers on the phosphinate level. Assignment of the phosphorus stereochemistry was achieved by synthesizing a cyclic analogue which proved retention during the Staudinger reaction.

1.3 Staudinger ligation & traceless Staudinger ligation

Several bioconjugation methods based on covalently linked fluorescent markers, isotope tracing or affinity tags to biomolecules like proteins, DNA or glycans for labeling or immobilization were developed over the years and could effectively be used for *in vitro* applications like the thiol-

maleimide coupling or activated ester coupling.^[74] But methods for *in vivo* applications are rare, since the reactions have to meet specific requirements of the biological system including bioorthogonality, non-toxicity, and fast and quantitative conversion under physiological pH. Besides the very famous and commonly applied CuAAC “Click reaction”^[75] and its strain-promoted alternatives^[76], the Staudinger ligation based on the standard Staudinger reaction fulfills these requirements.

The Staudinger reaction is not only outstanding because of its scope of accessible products and reaction variants but also due to its unique reactivity, which makes the Staudinger reaction so universal for biological application. In 2000, Bertozzi and co-workers recognized this particular feature of the Staudinger reaction and developed a method that takes advantage of the specificity of the Staudinger reaction and makes the chemoselective formation of amide bonds possible even in *in vivo* application.^[9d,e]

As pointed out above with respect to the so-called “click”-reaction, azides show many desirable characteristics for the use in biological system as unnatural reporter group.^[77]

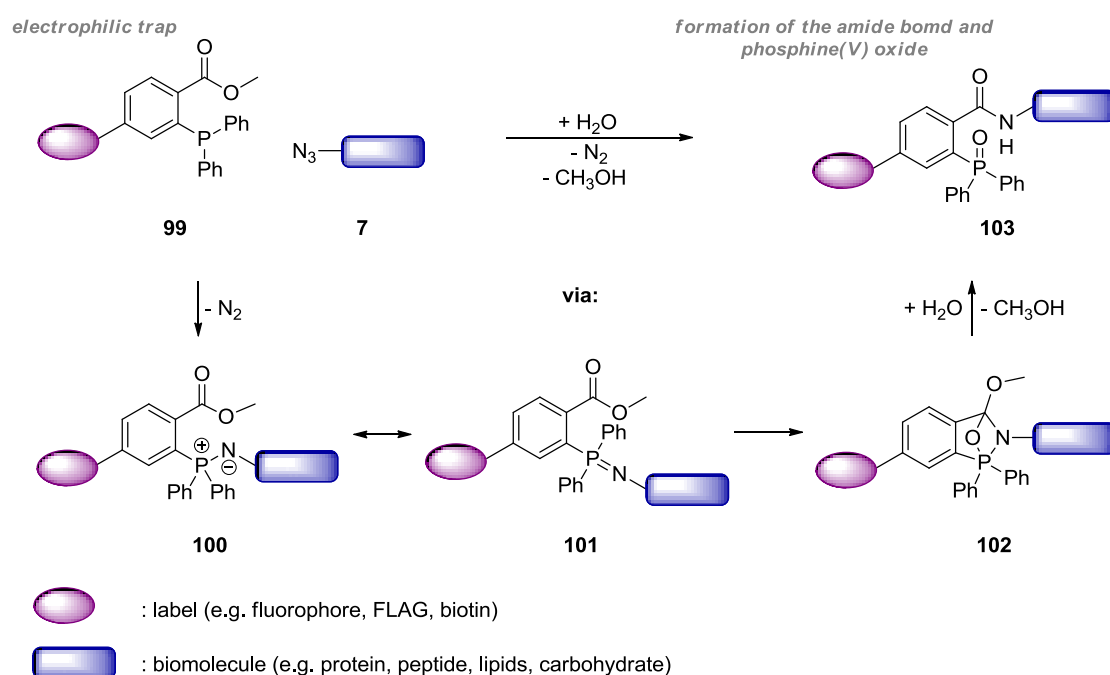
Azides are stable under most reaction conditions and only decompose and release nitrogen at high temperature, and only compounds with a very low molecular weight and electron donating substituents have an explosive nature at room temperature. Their electrophilicity is very low and for this reason, they do not react with nucleophiles present in biomolecules without the help of catalysts. As a quite small functional group incorporated in biomolecules like peptides, DNA or sugars they do not interfere with biological processes and do not significantly alter their chemical properties. Furthermore, the synthetic introduction of azido groups into various compounds can easily be achieved and has been described in numerous articles.^[77] Biochemical strategies for the site- and residue specific incorporation into biomolecules like proteins are developed and their application is state-of-the-art documenting that azides possess unique reactivity orthogonal to those of natural biomolecules and that they are predestined for *in vivo* applications.^[75b, 76a, b, 78]

The trivalent phosphorus counterpart shows higher reactivity that has to be taken into account for the design of possible applications. Depending on their structure, oxidation or hydrolysis can occur and the reaction conditions and molecule design have to be chosen accordingly. In addition, their nucleophilicity can cause problems as trivalent phosphorus can react with electrophiles like alkyl halides. This reaction is frequently used in the Arbusov reaction for the synthesis of phosphosponium salts, which are reagents for the Wittig reaction.^[79] Nevertheless,

Bertozzi and co-workers^[9d, e, 9k] and later also Hackenberger and co-workers^[80] could attest that the reaction proceeds without any interference with the biological system. Therefore, the Staudinger reaction can be considered as an innovative techniques for the investigation of biological processes, and it fits optimally into the concept of bioorthogonal reactions, a concept significantly coined by Caroline Bertozzi: “Key to these new techniques are bioorthogonal chemical reactions, whose components must react rapidly and selectively with each other under physiological conditions in the presence of the plethora of functionality necessary to sustain life”.^[78d]

1.3.1 The Staudinger ligation

In the Staudinger ligation, developed 2000 by Bertozzi and co-workers, an azide **7** reacts with a phosphine **99** to form an aza-ylide **100** as in the commonly used Staudinger reduction (Scheme 32).^[9d, e] The method was specifically devised for the metabolic engineering of cell surfaces. In the case of the Staudinger reduction this aza-ylide **100** is further hydrolyzed to give a primary amine and phosphine oxide. Because this reaction would lead to the disconnection of the created conjugation, Bertozzi and co-workers designed a system in which an electrophilic trap can be attacked by the nucleophilic nitrogen of the aza-ylide form **100**. The electrophilic trap is an activated ester so that an amide bond is formed, which represents a newly created stable connection.



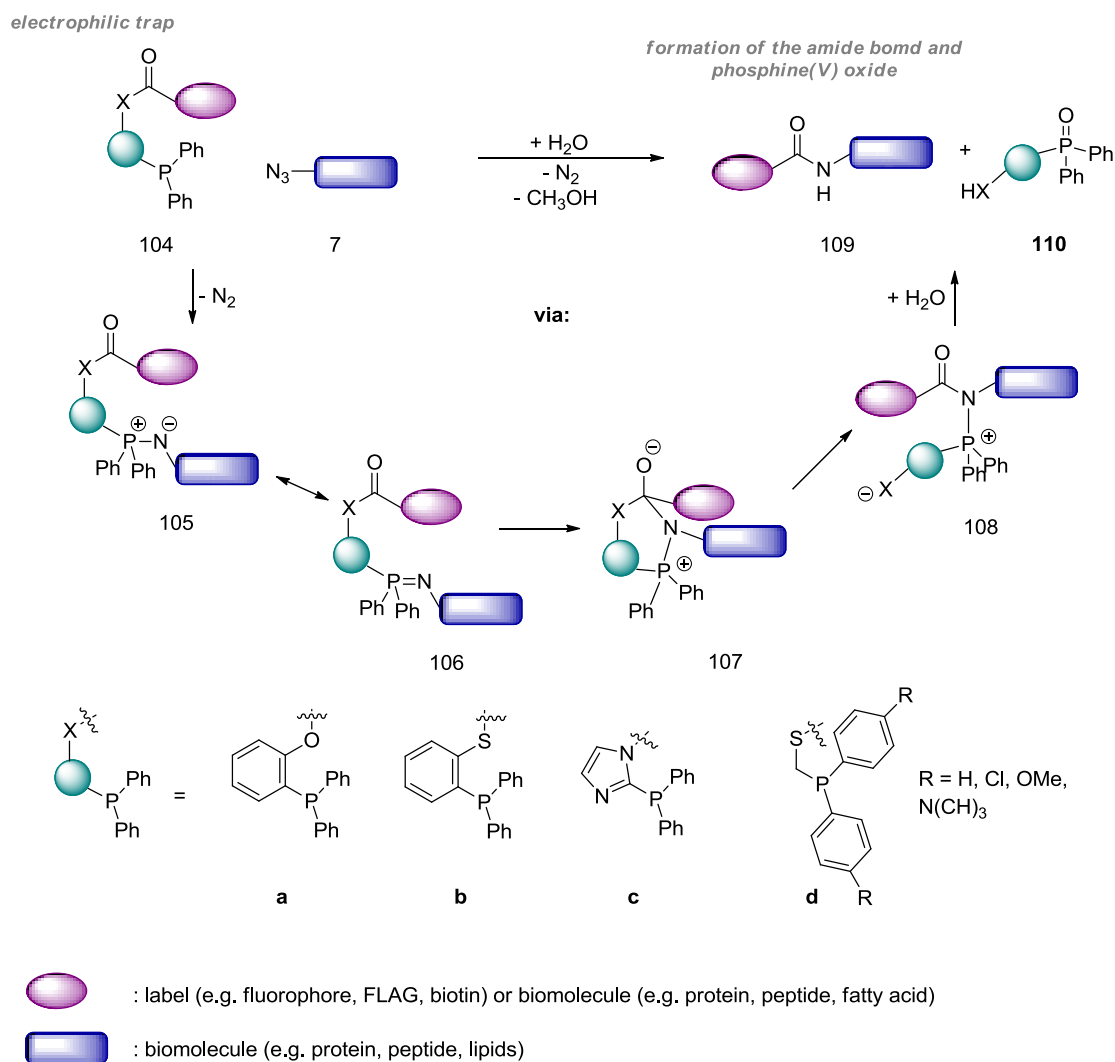
Scheme 32: Mechanism of the Staudinger ligation.

A terphthalic acid derivative was first used as phosphine component **99**. After release of nitrogen under the formation of iminophosphorane **101** that is in equilibrium with the aza-ylide **99**, the nucleophilic nitrogen attacks the carbonyl moiety leading to the oxaphosphetane **102**. In the subsequent hydrolysis the phosphine oxide **103** and the amide bond is formed and methanol is expelled.

1.3.2 The traceless Staudinger ligation

Later in the same year, Bertozzi^[9d] and Raines^[81] almost simultaneously published the so-called traceless Staudinger ligation, which obeys the same reaction principle but has a decisive advantage over the previously described Staudinger ligation for the synthesis of peptidic biomolecules (Scheme 33). In this methodology the phosphine species **110** is removed from the target molecule during hydrolysis and thereby allows the formation of a native amide bond without residual, unnatural moieties.^[9g] Loss of the phosphine species **110** was achieved by incorporating the phosphine into the ester group which is cleaved during the reaction leading to the amidophosphonium salt **108**. The P-N-bond of the resulting salt **108** can easily be hydrolyzed and the phosphineoxide species **110** with attached linker is eliminated.

To improve the conversion to the desired amide **109**, different linker systems were tested to find the optimal balance between reactivity and stability of the phosphine species **104**.^[82] In all the cases, the phosphorus bears at least two aromatic substituents. The aromatic substituents on the one hand, prevent fast oxidation of the trivalent phosphorus and, on the other hand, ascertain a conformational rigidity of the iminophosphorane **106** for stabilization. Thereby, 2-diphenylphosphanylphenol **104a**^[9d], readily prepared by a Pd-catalyzed reaction of 2-iodophenol with diphenylphosphane, and diphenylphosphanylmethanethiol **104d**^[82b] exhibited the best reactivity profiles. Further experiments showed that Gly-Gly ligation proceeds in high yields when using single amino acids, but changing one or both Gly-compounds to sterically more demanding amino acids may decrease the yield dramatically and frequently requires the re-optimization of the reaction conditions including the linker system.^[83] Ala-Ala ligation yielded, for example, with diphenylphosphanylmethanethiol **104d** the desired dipeptide by only 36 to 47%, but the yield could be increased to 82% by incorporating methoxy groups at the phenyl rings and by changing the solvent from DMF to 1,4-dioxane. The different derivatives of the phosphine thiols developed by Raines resulted, however, in good yields, especially in non Gly-Gly ligations. Due to the alkyl substituent handling of the now electron-rich phosphorus was eased by protection with a borane. Deprotection can be reached by both acidic and basic conditions.



Scheme 33: Mechanism of the traceless Staudinger ligation.

Raines and co-workers also investigated the mechanism of the traceless Staudinger ligation.^[82c] Based on the diphenylphosphanylmethanethiol linker **104d** mechanistic investigations with H₂O¹⁸ proved that the reaction proceeds via the amido phosphonium salt **108** and not *via* a possible aza-Wittig type reaction in case of the Gly-Gly ligation. Here, the diphenylphosphanylmethanethiol **104d** and (diphenylphosphino)methanol linker developed by Bertozzi^[9d] showed the highest reactivity while the Raines system featured a better chemoselectivity because the less electrophilic alkyl thiol is less prone to an attack by another nucleophile.

1.3.3 Application of the Staudinger ligation & the traceless Staudinger ligation

Staudinger ligation

1.3.3.1 Peptide ligation, peptide protein ligation and peptide cyclization by the traceless Staudinger ligation

Since the pioneering work of Merrifield^[84] in 1963, peptides can efficiently be attained by solid-phase peptide synthesis (SPPS) although this method still faces limitations. Coupling procedures are not productive for peptide lengths exceeding about 40-50 amino acids due to the formation of secondary structures, which cause inaccessibility of the terminal carboxylic acid and prohibit the next coupling step. This characteristic behavior of peptides is attended by low or no yields and an increasing amount of side and truncation products. To overcome this problem alternatives were developed headed by Kent *et al.*^[85] who established the Native Chemical Ligation (NCL) in 1994. The Native Chemical Ligation relies on the presence of an N-terminal cysteine^[85-86] which is rarely found in proteins, although nowadays conformational-assisted ligations and removable auxiliaries exist to overcome this limitation. The traceless Staudinger ligation offers an alternative pathway and permits bioorthogonal formation of natural amide bonds.

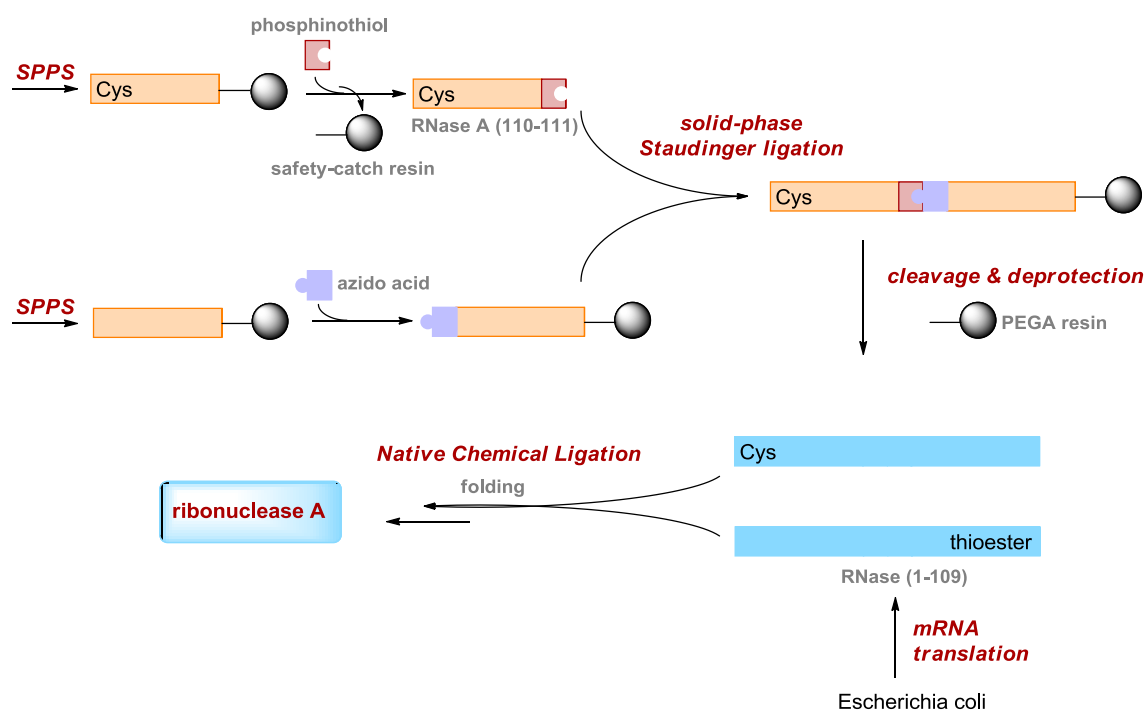


Figure 6: Protein assembly by orthogonal chemical ligation methods.^[87]

To prove the applicability of the traceless Staudinger ligation Raines *et al.*^[87] synthesized ribonuclease A by a three-segment approach (Figure 6). They combined the Staudinger ligation with the NCL and succeeded in getting the full-length protein. In this case they synthesized an azido peptide on resin using standard Fmoc protocols and then let the phosphinothiol peptide react with the on-resin azide under formation of the amide bond. The cleaved and deprotected peptide was converted with a thioester by NCL to get the whole protein. It is worth noting that although the Staudinger ligation should be a chemoselective process protected peptides or amino acids were employed.

Later on, Liskamp and coworkers used further the Staudinger reaction for the synthesis of different pentapeptides.^[88] They could again show that the reaction is not dependent on a glycine residue and that other side chains are tolerated. Despite the formation of the aza-ylide proceeding very fast, the shift to the amide bond occurred only slowly and in very low yields up to 36%. Due to the latter very slow process, side reactions like oxidation of the phosphine or ester hydrolysis occurred and basic side chains like lysine led to non-specific aminolysis. The reaction in non-aqueous solvents seemed to support the rearrangement.

Later Maarseveen and co-workers used the Staudinger ligation for the formation of small lactams by incorporating the azido group at the N-terminus and the thiol linker at the C-terminus.^[89] Since the phosphine was used in a borane-protected form, Staudinger ligation did not occur until deprotection with DABCO was performed.

The preceding idea was adopted by the group of Hackenberger^[80] who developed an acidic deprotection strategy for the borane group, which allows phosphine and side chain deprotection in one-step and directly delivers the unprotected peptide. By means of this system, they succeeded in synthesizing the cyclic peptide microcin.

1.3.3.2 The Staudinger ligation as method for bioconjugation

With regard to the investigation of biomolecules, site-selective labeling is an indispensable technique to detect and explore their function, mode of action as well as spatial and temporal distribution, particularly in *in vivo* experiments.^[75b, 78b, 90] By employing the Staudinger ligation, bioconjugation could be achieved with dyes, spin labels, affinity tags, and recognition motif including biotin, coumarin, FLAG-tag or ferrocene (Figure 7).^[9a, 9c, 90-91]

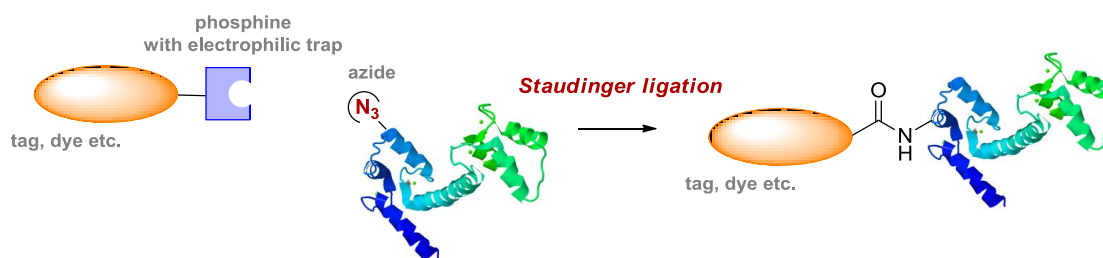


Figure 7: Site-selective labeling of biomolecules (here proteins) by the Staudinger ligation or traceless Staudinger ligation.

Biotinylation is a prevalent method for the tagging of biomolecules, since streptavidin as a ligand can be attached to fluorophores, resins or magnetic beads and is, therefore, very effective for immobilization or labeling.^[74h] An example where the Staudinger ligation could be applied for biotinylation represents cathepsin B.^[91b] Cathepsin B was treated with an azido-functionalized inhibitor that covalently binds to the enzyme by the reaction of a thiol functionality with the epoxide of the inhibitor. Following Staudinger ligation with the biotinylated phosphine and reaction with streptavidin allowed both fluorophore labeling *in vivo* as well as analysis by a streptavidin blot for further investigations. Also labeling of DNA is possible, as reported by Marx *et al.*^[92], who could show that polymerase-supported introduction of azide-modified triphosphates and reaction with a biotinylated phosphine led to labeled DNA.

Alternatively to the aforementioned method, in which attachment of the fluorophore requires a two-step process, a more direct method uses directly fluorophore-labeled phosphines.^[91a] A drawback of this method is the high amount of background fluorescent due to unreacted phosphine and oxidized phosphine species. First improvements were achieved by employing a coumarin-phosphine in which the fluorescent phosphine is photophysically inactive due to quenching by the electron lone pair of the phosphorus, whereas the oxidized Staudinger product is fluorescent.^[91f] But unwanted oxidation of the phosphorus still led to background signals. To further reduce this problem Bertozzi *et al.* designed a FRET-phosphine by incorporating fluorescein and an appropriate quencher in the phosphine compound.^[9f] In this case, reaction with the phosphine is accompanied by loss of the quencher resulting in a significant increase in emission intensity. Unreacted phosphine species still possess the quencher and do not give a background signal.

Besides biotin and fluorophores, also FLAG-phosphines were synthesized and used for *in vivo* investigations. For example, an azido modified glycosyl fluoride forms a covalently connected glycosyl-exo-glycosidase intermediate, and this activity based probe, after reaction with the FLAG-phosphine, could be isolated and separated from the enzyme mixture in the cell and

analyzed by SDS-PAGE and Western blot.^[91h] Furthermore, Bertozzi *et al.* investigated glycans on the cell surface by feeding with azido-GlcNaAc and following labeling with this FLAG-phosphine.^[91g, 93]

1.4 Phosphorus-nitrogen compounds in catalysis

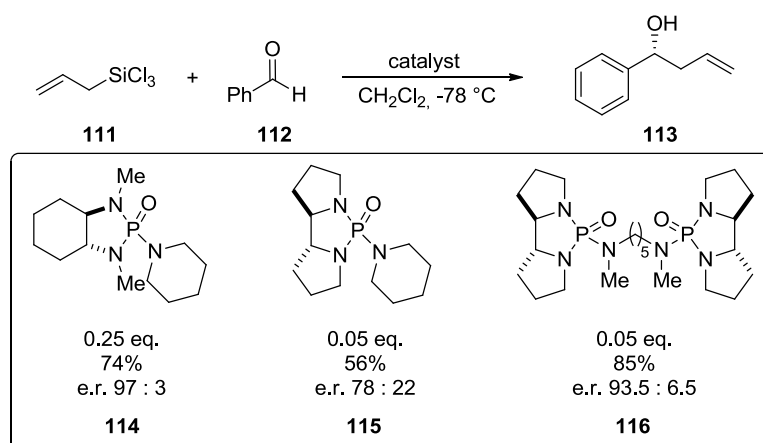
As a result of their structural appearance, phosphin-, phosphon- and phosphoramidates as well as phosphoramides can serve both as Lewis bases and Brønsted acids. As Lewis base, the double-bonded oxygen at the phosphorus is able to activate nucleophiles in organic transformations while the NH can serve as hydrogen donor to enhance the electrophilic nature of a molecule. These characteristic properties turn compounds containing a P(O)-N-motif that can also be described in a dipolar fashion into excellent catalysts for a variety of synthetic transformations.^[1] Additionally, incorporation of different substituents at the phosphorus as well as at the nitrogen allows not only a manifold diversity of molecular designs but also a precise tuning of their electronic properties and their three-dimensional structure. The possibility to introduce chiral components in the molecule makes them also suitable for asymmetric reactions. Research on their ability as catalyst was significantly expedited by the groups of Denmark^[1a-k], Yamamoto^[1l-o], Rueping^[1p-r], and List^[1s, t] who successfully used different P(O)-N-compounds as catalysts in organic reactions and put a lot of effort in testing their range of applications for asymmetric catalysis and their mode of action.

1.4.1 Lewis base catalysis

That phosphoramides are able to function as Lewis bases is well-known as HMPA is frequently used as coordinative reagent or solvent. It strongly coordinates Li-cations, breaks oligomers of Li-bases, is used for the acceleration of S_N^2 -reactions or serves as hydrogen-bond acceptor.^[94]

The first chiral phosphoramidate catalysts **114-116** were developed by Denmark *et al.* in 1994 for the first Lewis base-catalyzed Sakurai reaction with polyhalosilanes **111** (Scheme 34).^[1a] Analogous to the activation with fluoride ions, Lewis bases are able to promote the diastereodivergent allylation of aldehydes by a $n \rightarrow \sigma^*$ interaction whereupon the reaction proceeds via a cyclic, chair-like transition state. Preliminary results indicated that high catalyst loading entails high enantioselectivity, and kinetic studies revealed a non-integral order dependence of 1.77 on the phosphoramidate catalyst **114**.^[95] Both observations pointed towards a second catalysis pathway in which not only one but two phosphoramidate molecules are

coordinated to the silicon associated with the formation of a six-coordinated, hypervalent cationic siliconium ion. Based on these results a linked, dimeric phosphoramidate catalyst **116** was generated to support the two-phosphoramidate pathway and to diminish unfavorable entropic influences. Combination of a 2,2'-bispyrrolidine backbone and a pentane linker gave best results in respect to low catalyst loading, i.e. a high yield and very good enantioselectivity. Besides the simple allylsilane **111**, also γ -substituted and γ,γ -disubstituted derivatives could be employed, and quaternary centers were obtained in high selectivity. Nevertheless, reaction with an aliphatic aldehyde was not successful.

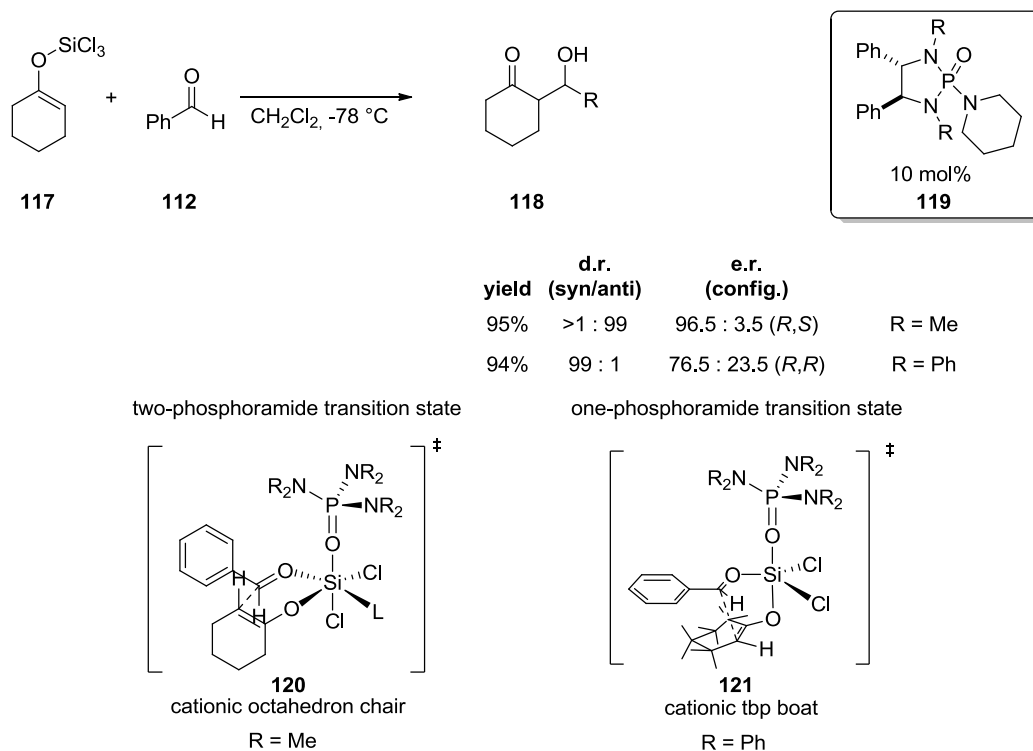


Scheme 34: First Lewis base-catalyzed Sakurai reaction.^[1a, 95]

After allylations could be successfully promoted by phosphoramidate catalysts, the structural similarity of allylic silanes to silyl enol ethers **117** encouraged Denmark *et al.*^[1b-f, 1j, 95-96] to investigate the ability of these catalysts in aldol reactions (Scheme 35).

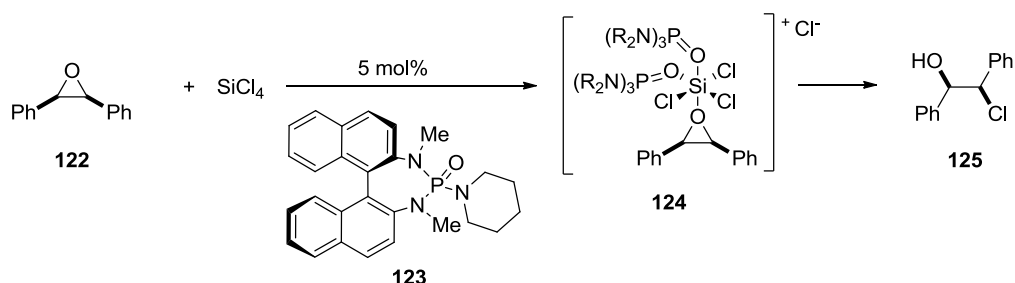
In a first attempt the very reactive acetate-derived trichlorosilylketene acetal was chosen as a model substrate with a binol-derived phosphoramidate as catalyst, but no synthetically useful levels of diastereoselectivity could be attained.^[1b] Changing the substrate to the less reactive ketone-derived trichlorosilyl ethers **117** gave better results.^[1c, 1e, f, 95, 96f, g] It is worth noting that anti- and syn-selectivity could be controlled by the choice of the catalyst and the catalysts should therefore participate in the reaction in a different manner. Based on the ion effect and reactivity studies, an ionized cationic silicate **121** was proposed for both cases as transition state, but determination of the order of dependence indicated that the order is one for the more sterically demanding catalyst whereas it is two for the smaller catalyst. It can be assumed that, as in the case of the allyl trichlorosilanes, a one- and a two-phosphoramidate pathway is possible.^[1j] To control the reaction pathway just by choosing the right catalyst and thereby the stereoselective

outcome of the reaction presents a very useful entrance to β -hydroxy ketones **118**. In addition, the reaction can be applied to the aldol reaction between two aldehydes which is difficult to achieve because polymerization has to be prevented.^[1g] In this case, the aldol product is protected as a chlorohydrine being inactive for further turnovers.



Scheme 35: Phosphoramidate-catalyzed aldol reactions (tbp = trigonal bipyramidal).^[97]

Even epoxides can be opened by means of SiCl_4 and a catalytic amount of phosphoramidate **123** (Scheme 36). The reaction is best described as a Lewis acid-mediated and Lewis base-catalyzed process.^[98]



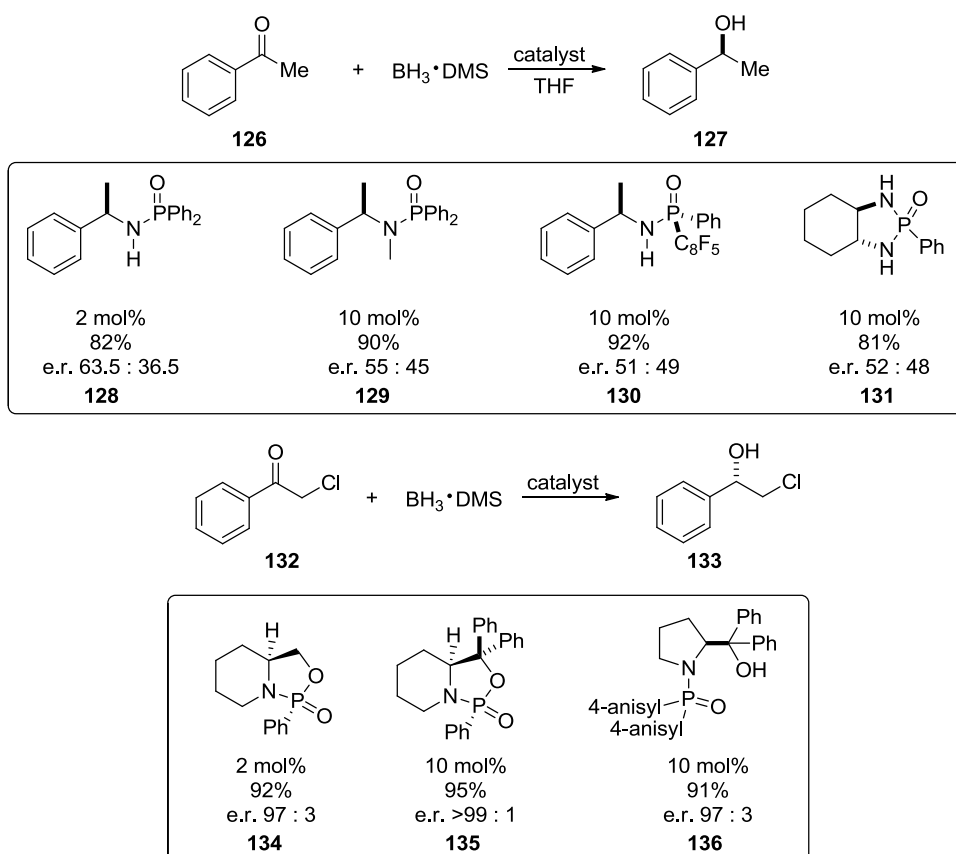
Scheme 36: Epoxide opening with a phosphoramidate catalyst **123**.^[98]

Trivalent boron species readily undergo formation of Lewis acid-Lewis base adducts with many different kinds of donors and are therefore predestined for Lewis base catalysis. In dependence

on the Lewis basicity, the reactivity of the boron species can be controlled and gives highly selective transformations.^[1u, 99]

Phosphin-, phosphon- and phosphoramides **128-131** effectively served as catalysts for the reduction of ketones **126** with a borane-dimethyl sulfide complex, a reaction that does not take place without activation (Scheme 37). First attempts featured high yields (80-92%) but only moderate selectivity (e.r. 63.5:36.5).^[1u, 99] Changing the structure of the applied catalyst to a cyclic form resulted in a much higher selectivity even with catalytic amounts of phosphinamides **134-135**.^[100]

Mechanistically, the oxygen of the catalyst is believed to coordinate the boron atom whereby the negative charge is enhanced and hydrogen transfer is assisted. Simultaneously, the now partially positive charged phosphorus atom can serve as a Lewis acid for the ketone activation. The presumed cyclic transition state explains both the rate of acceleration by double activation and the asymmetric induction, yet further mechanistic investigations are required.



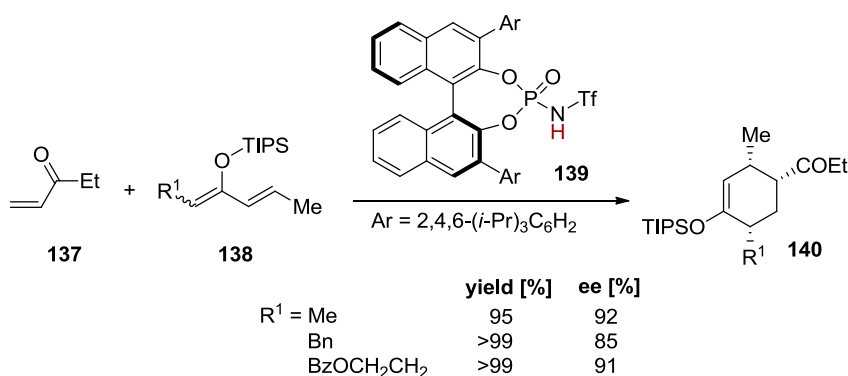
Scheme 37: Reduction of ketones **126** and **132** with different catalysts **128-131** and **134-136**.^[1u, 99]

1.4.2 Brønsted acid catalysis

In addition to the ability to serve as Lewis bases as described in the previous chapter, compounds containing a P(O)-N motif can also serve as Brønsted acids, if they carry a proton at the nitrogen. In 2006, Yamamoto *et al.*^[1m] identified chiral phosphoramidates as ideal candidates for Brønsted acid catalysis and synthesized the first BINOL-derived phosphoramidate catalyst **139** (Scheme 38) by the phosphorylation of optically active BINOL with POCl₃ and amidation of the resultant phosphoryl chloride with TfNH₂. It was already known that BINOL-derived phosphoric acids, first described by Terada and Akiyama, can act as Brønsted acid catalysts, but due to their estimated pK_a values between 1 and 2 their substrate scope is limited to rather basic nucleophiles.^[1r, 101] In contrast, pK_a values between 6 and 7 are estimated for BINOL-derived *N*-triflylphosphoramidate **139** allowing a broad applicability in organic transformations.^[1r]

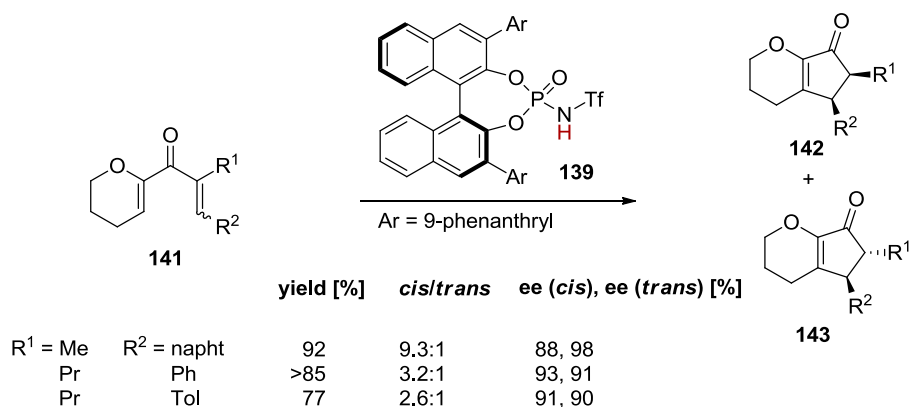
The first BINOL-derived phosphoramidate catalyst **139** was applied in an asymmetric Diels-Alder reaction with an α,β -unsaturated ketone **137** (Scheme 38).^[1m] Asymmetric Diels-Alder reactions with α,β -unsaturated ketones like **137** present a challenge for asymmetric synthesis since differentiation between the two oxygen lone pairs by a Lewis acid is difficult due to their similar steric and electronic environment. For this reason, the very promising application of the BINOL-derived *N*-triflylphosphoramidate **139** stimulated the development of metal-free alternatives.

Yamamoto *et al.* compared the phosphoramidate **139** with the analog phosphoric acid (OH instead of NH-Tf). They could demonstrate that the phosphoramidate **139** has a very high activity and the desired product **140** was obtained in a quantitative yield with high enantiomeric excess. In contrast, the phosphoric acid showed no catalytic activity.^[1m] Optimization of the reaction conditions finally led to the Diels-Alder product **140** of the ethyl vinyl ketone **137** and the siloxy diene **138** in yields between 34 and 99% and ee values of 82-92%.



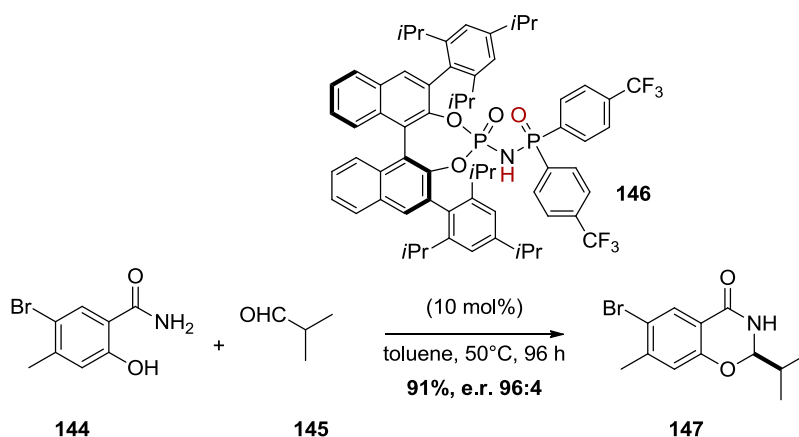
Scheme 38: Asymmetric Diels-Alder reaction and exemplary reaction scope.^[1m]

The same or similar catalysts also proved to be very effective in other reactions like the Nazarov reaction (Scheme 39) or 1,3-dipolar cycloadditions as observed by the groups of Rueping^[1p] and Yamamoto^[1o]. Thereby, application of the Nazarov reaction was broadened by the development Nazarov cyclization/ bromination cascade leading to enantioenriched α -halogenated ketones, which are versatile structural motifs in the synthesis of natural products and pharmaceuticals.^[1q]



Scheme 39: Nazarov reaction catalyzed by the phosphoramidate **139**.^[1p]

In 2010, List *et al.* introduced a the *N*-phosphinyl phosphoramidate **146** as a new motif for organocatalysis and successfully applied the catalyst for the direct asymmetric *N,O*-acetalization of aldehydes **145** (Scheme 40).^[1s] Mechanistically, it is proposed that the new catalyst **146** is able to not only serve as Brønsted acid for the activation of the imine but also activates the nucleophile by its Brønsted basic phosphinyl oxygen.

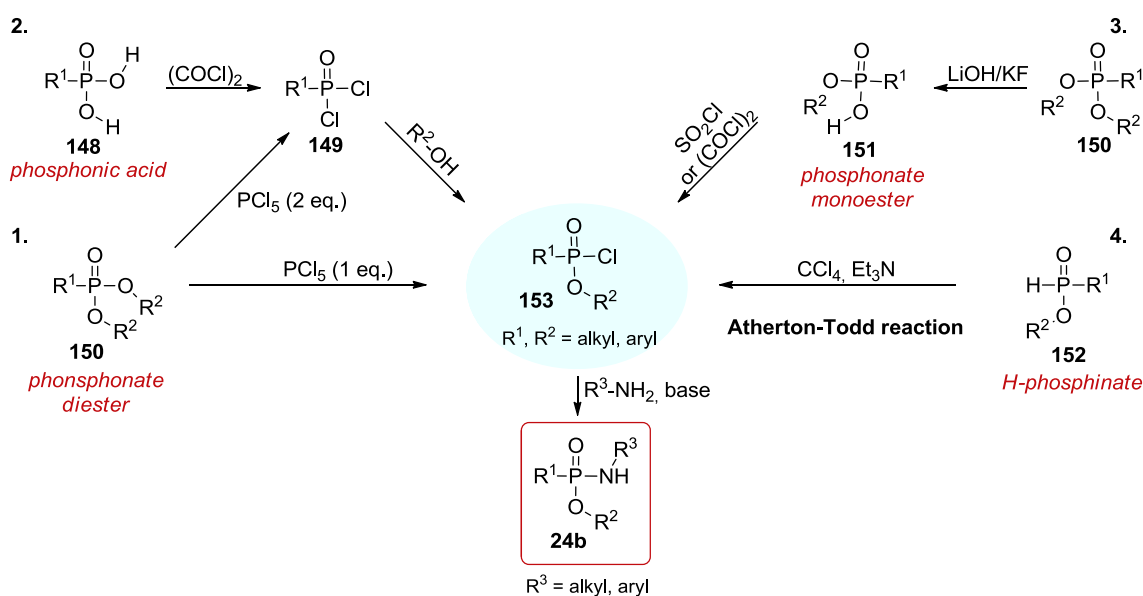


Scheme 40: *N*-Phosphinyl phosphoramidate **146** as a chiral Brønsted acid for the direct asymmetric *N,O*-acetalization of aldehydes **145**.^[1s]

1.5 Synthesis of phosphonamidates and phosphonamide peptides via chloridates and chloridites

The traditional synthesis of phosphonamidates **24b** is closely related to the synthesis of amides and can likewise be achieved by activation of the phosphorus in the form of a phosphonochloridate **153**, which is subsequently reacted with an amine in the presence of a base. Standard coupling procedures via an active ester also found application in certain cases but less frequently.^[102]

There are four commonly used accesses towards phosphonochloridates **153** (Scheme 41): 1. Reaction of a phosphonate diester **150** with one equivalent of phosphorus pentachloride, 2. Reaction of a phosphonic acid **148** with oxalyl chloride and following treatment of the dichloride **149** with an alcohol, 3. Treatment of the monoester **151** with thionyl chloride or oxalyl chloride, 4. Oxidative chlorination of phosphinite esters **152** with carbon tetrachloride in the presence of a strong base, well-known as Atherton-Todd reaction. In a similar approach substitution of the chloride occurs at the P(III) center prior to oxidation to P(V) (see 1.5.2).

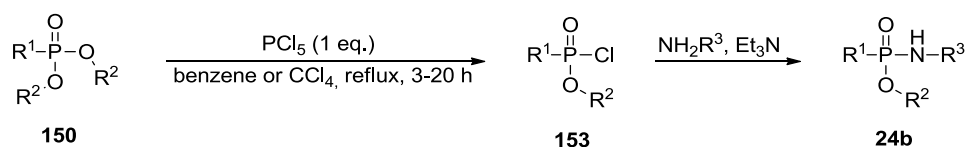


Scheme 41: Different accesses towards phosphonochloridates.

1.5.1 Synthesis of phosphoramidates from phosphonate mono- and diesters via phosphonochloridates

1.5.1.1 Synthesis of phosphoramidates from phosphonic acid diesters with phosphorus pentachloride

Phosphonochloridates **153** can readily be prepared by treatment of the phosphonate diester **150** with one equivalent of phosphorus pentachloride.^[2i, 103] Despite the fact that other chlorination reagents can be used for the conversion of one ester group by a chloride, such as oxalyl chloride,^[104] triphenylphosphine dichloride,^[105] thionyl chloride,^[106] phosgene^[107] or phosphoryl chloride,^[108] only phosphorus pentachloride has been employed to attain phosphoramidate peptides **24b** (Scheme 42). This method was first successfully applied for the synthesis of phthalyl protected phosphoramidate dipeptides from *O*-diethylphthalimidomethylphosphonate^[103e] or *O*-diisopropylphthalimido-methylphosphonate^[103b] and the glycine ethyl ester (Table V, entry 1). In the first case, also the ethyl esters of alanine and phenylalanine could be introduced in good yields. By application of the phthalyl protective group and the ethyl or benzyl ester at the phosphonate, tripeptides could be synthesized in yields between 47 and 75% (Table V, entry 2-4).^[2i] This signifies that the phthalyl groups as well as the carboxylic esters are well tolerated in the reaction. Nevertheless, several limitations of the reaction were recognized by further investigations.^[103c] The foregoing reaction works well for the isopropyl- and ethyl ester, but the reaction with benzyl esters in some cases is more intricate and involves long reaction times, incomplete conversion and generation of several by-products. Another disadvantage are the very harsh reaction conditions like refluxing of the reaction mixture at 80°C for several hours. For this reason, reactions with Cbz-protected compounds were not successful. As a result, the reaction found only application in the synthesis of small phosphoramidates **24b**, and seldom for the phosphoramidate peptide synthesis (Table V).^[2i, 103a-c]



Scheme 42: Chlorination of the phosphonate diester **150** with phosphorus pentachloride and subsequent reaction with amines to phosphoramidates **24b**.

Table V: Exemplary reaction scope of phosphonamidate peptides and similar compounds starting from the phosphonate diester and PCl_5 .^[2i, 103a-c]

R^1	R^2	R^3	yield [%]
PhtNCH ₂	<i>i</i> Pr	H-Gly-OEt	49
PhtNCH ₂	Bn	H-PheLeu-OBn	47
PhtNCH ₂	Et	H-PheMet-OMe	49
PhtNCH ₂	Et	H-PheLeu-OMe	75
PhtNCH ₂	Et	H ₂ N(CH ₂) ₄ NPht	53
PhtNCH ₂	Et	H-Ala-OMe	66
CH ₃ (CH ₂) ₂	<i>i</i> Pr	H-Ala-OEt	38
CH ₃ (CH ₂) ₂	<i>i</i> Pr	H-Asp-OEt	35
PhtNCH ₂	Et	H-ProPhe- <i>p</i> NA	48
PhtNCH ₂	Et	H-ProPheψ(CH ₂ -NH) <i>p</i> NA	37
PhtNCH ₂	Bn	H-ProPhe- <i>p</i> CMA	11

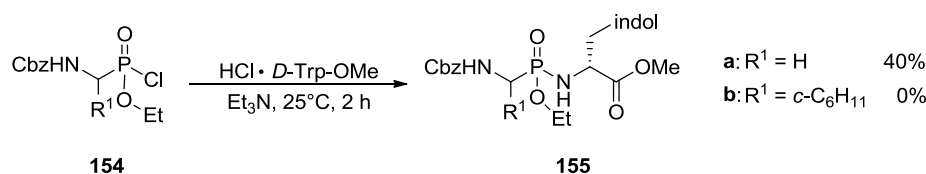
*p*CMA: 4-carboxymethylaniline; Pheψ(CH₂-NH)*p*NA: 1-(4-nitrophenyl) amino-(R)-2-benzyl-2-aminoethane; *p*NA: 4-nitroaniline

1.5.1.2 Synthesis of phosphonamidates from the phosphonic acid monoester

The most commonly used entry towards phosphonamidates **24b** is the reaction of the mono ester **151** with chlorination reagents, like thionyl chloride or oxalyl chloride, followed by the addition of an amine.^[2f, g, 103b, 104e, 106d, 109] The reaction sequence generally starts from the phosphonate diphenyl ester. Diphenyl esters are easily prepared by a three-component reaction published by Mastalerz *et al.*^[110] Heating of benzyl carbamate, the appropriate aldehyde and triphenyl phosphite in acetic acid for two hours leads directly to the desired phosphonates. Mechanistically, imin formation is followed by a nucleophilic attack of the phosphite and loss of one phenyl group. Transesterification with methanol, potassium fluoride and crown ether or sodium methanolate results in the dimethyl ester **150** that hydrolyzes to the monoester **151** under basic conditions.^[104e, 106d, 109g, 111] Treatment of this monoester **151** with the chlorination reagent affords the chloridate **153**, which is further reacted with the amine without previous purification owing to its instability against moisture.

This method was commonly used for the synthesis of phosphonamidate di- or tripeptides.^[2f, g, 103b, 104e, 106d, 109, 111b, 111e] In some cases good yields were obtained (60-80%) but were often they were much lower and unsatisfactory (0-50%) in dependence of the both the applied amine and the applied phosphonochloridate.

Hirschmann *et al.* studied the reaction sequence for the synthesis of phosphonamidate dipeptides **155**. They found that formation of the phosphonamidate bond is difficult to be realized depending on the applied amine, and therefore, they undertook further investigations concerning the chlorination reaction and the following substitution by an amine (Scheme 43).^[106b, 109f] As model substrate, they used Cbz-protected ethyl (aminomethyl)phosphonate or the Fmoc-protected phosphonate. Complete conversion to the chloridates **154** with oxalyl chloride could be observed within 30 min. showing two small additional signals in the ³¹P-NMR spectrum that could not be attributed to the active phosphorylating agents and proved to be pyrophosphonate anhydrides. These observed pyrophosphonate anhydrides are much less reactive towards nucleophiles. In contrast to carboxylic acids, the chlorinated phosphonates exhibited lesser reactivity (benzyl alcohol 89% and benzyl amine 64%). Coupling with the tryptophan methyl ester did only lead to 40% of the desired product **155a** and in the case of a cyclohexyl group at the α -carbon to the phosphonate no product could be identified (Scheme 43). By avoiding acidic conditions in the coupling procedure to prevent product decomposition a slightly better but still not satisfactory yield of 52% was obtained for the tryptophan derivative.



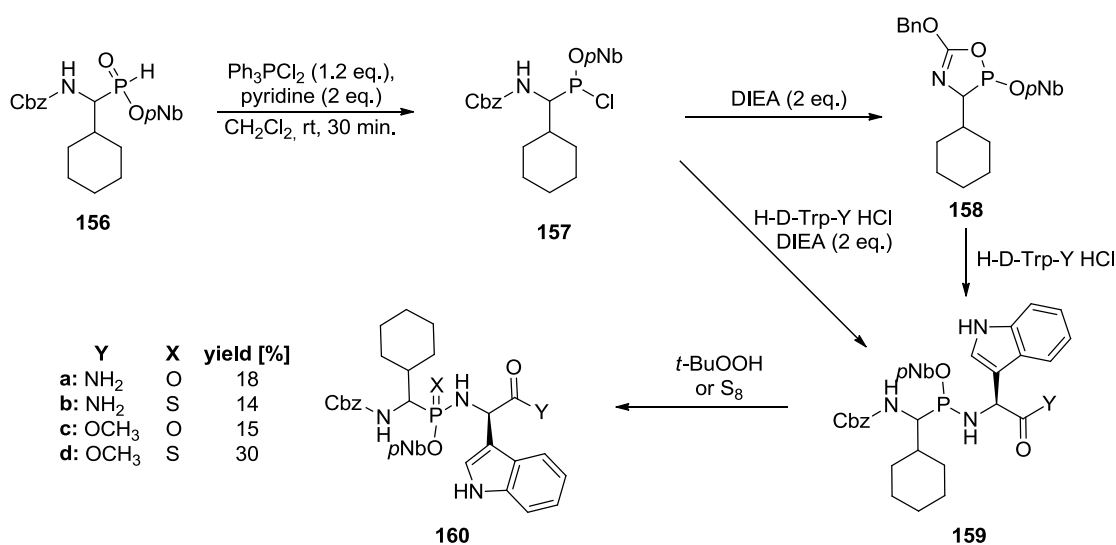
Scheme 43: Synthesis of phosphonamidate dipeptides.

1.5.2 Synthesis of phosphonamidates from P(III)-precursors

In 2001 Rushing and Hammer presented an alternative approach to the standard phosphorus(V) entry (Scheme 44).^[112] In analogy to the Atherton-Todd reaction, *H*-phosphinates **156** are used as starting material for this one-pot activation-coupling-oxidation procedure, but instead of phosphonochloridates the corresponding phosphonochloridites **157** are generated intermediately. This reaction sequence particularly gains in importance if the phosphorus(V) strategy fails, for example, in the case of amines with a high steric demand caused by bulky side chains of the amino acids.

Formation of the phosphorus(III) species was proven by ³¹P-NMR spectroscopy, and optimization of the reaction settings revealed 1.2 equivalents of Ph₃PCl₂ and two equivalents of pyridine in dichloromethane as best conditions for the chloridite formation. Subsequent addition of the amine, in this case *D*-tryptophan methyl ester hydrochloride or the corresponding amide, and a

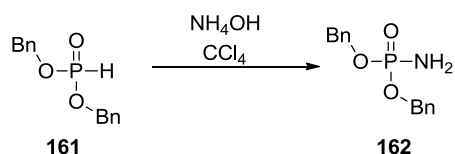
base led to the phosphonamidite **159**, which can afterwards be oxidized with *tert*-butyl hydroperoxide to the phosphonamidates **160a** or **c** or with S_8 to the thiophosphonamidate **160b** or **d**. In addition to the chloridite **157**, an oxazaphospholine **158** was identified as phosphitylating agent caused by *N,N*-diisopropylethylamine. The phosphonamidates **160a** and **c** and the thiophosphonamidate **160b** and **d** were obtained in yields between 14 and 30%. The low and moderate yields can be considered to be a success because these compounds were not accessible before by the standard phosphorus(V) procedures (compare 1.5.1.2). Since conversions observed by ^{31}P -NMR indicated a much better, nearly quantitative yield, the loss of compound was attributed to purification problems.



Scheme 44: Synthesis of phosphonamidates **160** via chloridites **157**.^[112] (*pNb* : *p*-nitrobenzyl)

1.5.3 Atherton-Todd reaction

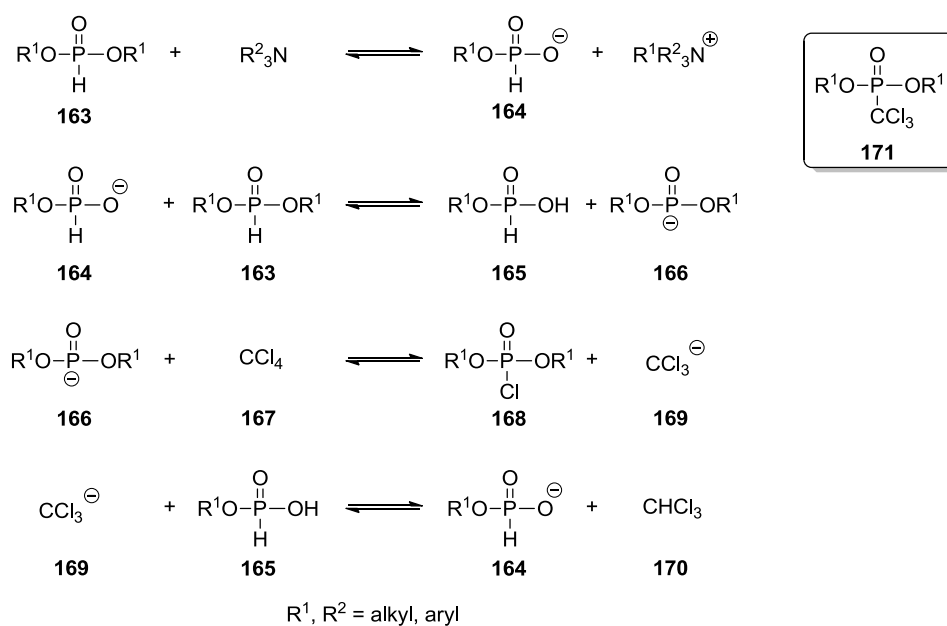
The Atherton-Todd reaction was first published in 1945 by Atherton, Openshaw and Todd who observed during the preparation of dibenzyl chlorophosphonate precipitation of a white solid which turned out to be dibenzyl aminophosphonate **162** (Scheme 45).^[113] Dibenzyl aminophosphonate **162** was formed when dibenzyl phosphite **161** dissolved in carbon tetrachloride was washed with diluted aqueous ammonia. The same reaction took place if, instead of ammonia, strong primary or secondary bases like cyclohexyl amine, benzyl amine, α -phenylethyl amine or morpholine were added leading to the formation of the corresponding amino phosphonates. In contrast, weak bases like aniline did not produce the desired product, but a conversion could be accomplished with moderate yields if strong tertiary bases in equimolar amounts were added to the reaction mixture.



Scheme 45: The first Atherton-Todd reaction.^[113]

Besides carbon tetrachloride also other polyhalogenated hydrocarbons and fully halogenated carbons were tried.^[114] Trichlorobromomethane turned out to be the most reactive species, and weak bases like aniline derivatives could be phosphorylated to phosphoramidates. Carbon tetrachloride is most commonly used. In the following years, the method became very useful for the preparation of phosphin-, phosphon- and phosphoramidates whereupon phosphoramidates were the most frequently synthesized target.

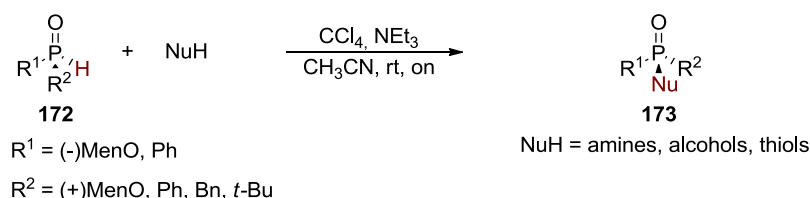
At first, a two-steps mechanism with intermediary formation of trichloromethyl phosphonate **171** as phosphorylating species was proposed (Scheme 46).^[113] Later on, this mechanism was revised and chloro phosphonate **168** was believed to be the reactive species based on their results with other polyhalogenated hydrocarbons and the reactivity towards alcohols.^[114] But the first reaction mechanism could not be fully excluded. 1993 Roundhill *et al.* further investigated the reaction mechanism and performed *ab initio* studies on the formation of the phosphorylating derivative which supported the mechanism based on a chloro phosphonate **168** as reactive species.^[115]



Scheme 46: Proposed mechanism of the Atherton-Todd reaction.^[115]

In the initial step, the amine reacts with the dialkyl phosphonate **163** to the corresponding monoalkylphosphonium salt **164**. In the next step, the anion **164** acts as a base and deprotonates another dialkyl phosphonate **163** from which ensues the very reactive dialkylphosphite anion **166**. Chlorination of the anion **166** generates the chlorophosphonate **168** and trichloromethanide **169**. The methanide **169** then reacts with the monoalkyl phosphonate **165** to yield chloroform **170** and the monoalkyl phosphonate anion **164** to close the catalytic cycle.

In 2010 Han *et al.*^[116] succeeded to show that, when starting from optically pure *H*-phosphinates or secondary phosphinoxides **172**, stereospecific coupling with amines and alcohols or thiols under mild Atherton-Todd conditions is possible (Scheme 47). The reaction proceeds with complete inversion of configuration at the phosphorus center and enables the synthesis of optically active organophosphorus derivatives **173**. The method works effectively for most amines although reaction with secondary amines is a bit slower under the used conditions. A wide variety of amines as well as of amino acid esters can be applied in the reaction, and even unprotected amino alcohols are tolerated as amines are much more reactive. Besides with bis(2-hydroxyethyl) amine (64% yield), all desired products are obtained in good to excellent yields between 74% and 95%. Conversion with alcohols and thiols proceeds equally smoothly, and only alkyl thiols did not result in a conversion.



Scheme 47: The Atherton Todd reaction starting from optically pure secondary phosphinoxides or *H*-phosphinates **172**.

Another method developed also by Han *et al.*^[117] is of great utility. Instead of carbon tetrachloride, Cu(II)Cl₂ is used as chlorinating reagent. CuCl₂ employed for chlorination was first described by Smith in 1962 who was able to convert (RO)₂P(O)H to the phosphonochloridate.^[118] By changing the reaction conditions to the less harsh conditions in THF at room temperature Han *et al.* could obtain the phosphonochloridate stereoselectively in quantitative yields from optically active phosphonates, and the chlorination took place with full retention of configuration at the phosphorus center. The phosphine and phosphonochloridates could be isolated and showed an unexpected high stability (five days at 70°C in benzene for a

phosphonochloridate) and they could be reacted with a variety of nucleophiles like Grignard reagents, Lithium organyles, thiols, alcohols and amines.

1.6 Phosphoramidates as protease inhibitors

1.6.1 Proteases –function and classification

Proteases represent one important enzyme class and belong like nucleases to the hydrolases. Proteases are responsible for the breakdown of peptides and proteins by the sequence-specific hydrolysis of amide bonds within a peptide or a polypeptide framework. Thereby, they control the synthesis, the turnover and the function of proteins. This regulatory function enables them to not only control many physiological processes such as digestion, fertilization, growth differentiation, cell signaling and migration, immunological defense, wound healing, and apoptosis but also to influence disease propagation.^[119]

There are eight types of proteases, namely aspartic (A), cysteine (C), glutamic (G), metallo (M), asparagin (N), serine (S), threonine (T) and unknown (U).^[120] Dependent on the catalytic center, different cleavage mechanisms can be noticed.^[121] Most phosphoramidate inhibitors have been synthesized for metalloproteases, and their cleavage mechanism is illustrated in Figure 8.

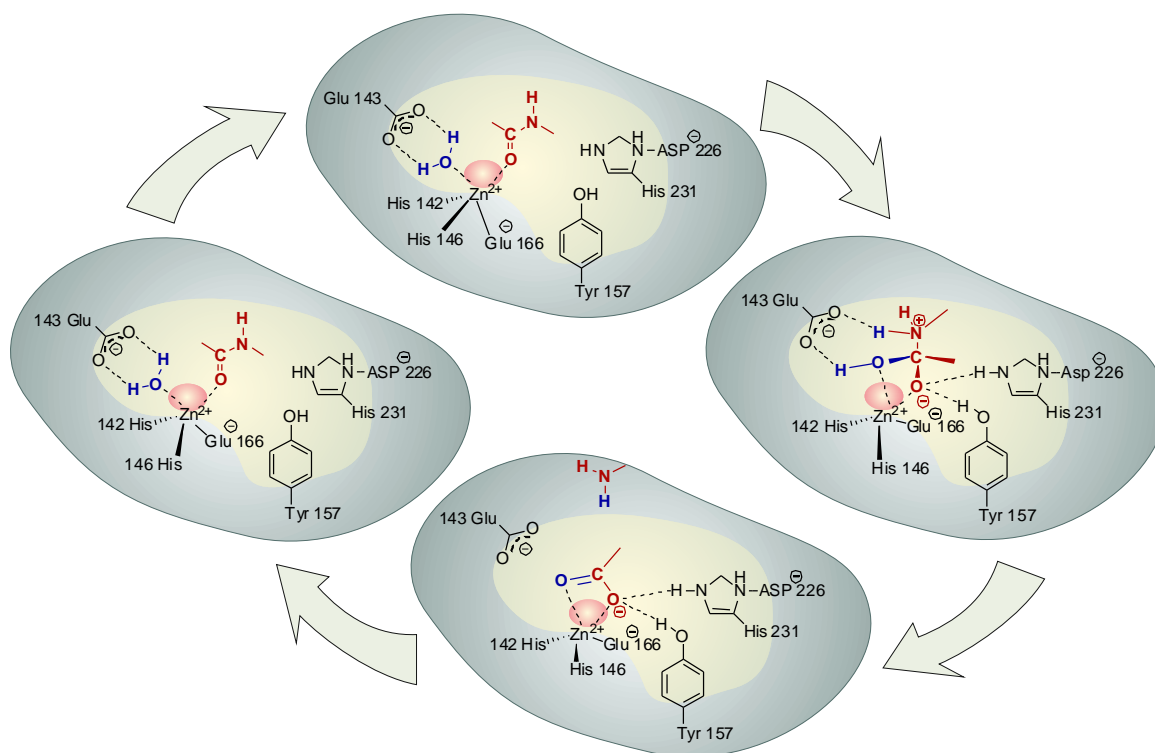


Figure 8: Cleavage mechanism of a zinc metalloprotease.^[121]

1.6.2 Protease inhibitors

Due to the variety of protease functions, their inhibitors exert a lot of potential as therapeutic tools for the treatment of diverse diseases including cancer, HIV, or Alzheimer, and many research groups have focused on their investigation.^[119, 122] As a result, many research efforts have been devoted to analyze the protein-substrate interactions or the synthesis and efficiency of potential inhibitors. In order to design successful protease inhibitors as biological tools there are many different pharmacokinetic and pharmacodynamic aspects to be considered. The inhibitors must have a high selectivity for a protease, a high stability against non-selective proteolytic degradation, good membrane permeability, a long lifetime in the bloodstream and the cells, low susceptibility to elimination, as well as good bioavailability.

A huge number of protease inhibitors have been designed for all major classes of proteases, especially with respect to their relevance in disease treatment. Some of them successfully passed the clinical trials and are applied for therapies (Table VI).^[123]

Table VI: Protease inhibitors approved in clinical use.^[123]

	Protease	Function	Disease	Inhibitor	Company
Aspartic protease	HIV-1 protease	HIV replication	AIDS	Saquinavir	Hoffmann-La Roche
				Indinavir	Merck
				Nelfinavir mesylate	Pfizer
				Amprenavir	Vertex Pharmaceuticals
				Ritonavir	GlaxoSmithKline
				Fosamprenavir	Abbott
				Atazanavir	GlaxoSmithKline
				Lopinavir	Bristol-myers Squibb, Abbott
	Renin	Generation of angiotensin I	Hypertension	Aliskiren	Novartis

Serine protease	Thrombin	Blood coagulation	Thrombosis Stroke, vascular clots, coronary infarction	Argatroban Lepirudin Desirudin	Mitsubishi Pharma Aventis (Hoechst Marion Roussel) Novartis
	Human neutrophil elastase	Cleavage of elastin	Respiratory disease	Sivelestat	Ono
	Broad spectrum	Anticoagulant	Pancreatitis, inflammation	Nafamostat mesilate	Japan Tobacco
Threonine protease	Proteasome		Myeloma cancer	Bortezomib	Millennium
MMP	ACE	Conversion of Angiotensin I to Angiotensin II	Hypertension, myocardial infarction	Captopril Trandolapril Enalapril Lisinopril Zofenopril Rarnipril Moexipril Imidapril Perindopril Qinapril Fosinopril Benazepril Cilazapril	Bristol-Myers Squibb Abbott Merck AstraZeneca Menarini group Aventis Boehringer Mannheim Trinity Pharmaceuticals Daiichi Pharmaceutical, Servier/Solvay Pfizer Bristol-Myers Squibb Novartis Roche
	MMP1, MMP2		Periodontitis	Periostat	CollaGenex

ACE: angiotension-converting enzyme; MMP: matrix metalloproteinase.

The employment of molecules, so-called peptidomimetics, bearing identifiable resemblance to the three-dimensional structure of peptides and proteins, is an elementary strategy for drug

design.^[124] Due to their structural and electronic similarity to the natural molecules, peptidomimetics can serve as ligands of a biological receptor and thereby imitate or inhibit the effect of a natural peptide. Therefore, many protease inhibitor structures and designs are based on the natural substrates in which the scissile bond is replaced by a non-cleavable isoster. The neighboring peptidic structure of the isoster can further be optimized with respect to specificity and binding energy. A strategy, which attracted considerable interest because of the high K_i values obtained, is the transition state concept in which the inhibitor does not just mimic the natural substrate, but its transition state, which is passed through during amide bond cleavage in case of proteases.^[2f-1, 125]

The general concept of transition state analogues is based on the observation that during the formation of these unstable intermediates additional, favorable binding interactions arise.^[126] These binding interactions diminish the activation energy for the following cleavage reaction and thereby induce an enhanced reaction rate. To take advantage of the stronger binding, motives are incorporated in the inhibitor design with the ability to mimic the structure of the transition state and to allow a stronger binding than the natural substrates. It has been described before that during the cleavage of the amide bond a tetrahedral transition state is passed through in a hydrate like structure (Figure 8). Over the last decades many different motives that mimic this charged tetrahedral structure have been designed such as reduced amides, carbinols, geminal diols, amino alcohols, ketones, and aldehydes or their hydrated forms (Figure 9).^[122q, 124b-e, 127] In addition to these carbon-based structures other non-carbon moieties were applied like silicon-, sulphur-, and phosphorus-based groups.^[2f, g, 122q, 124b-e, 125f, 127-128]

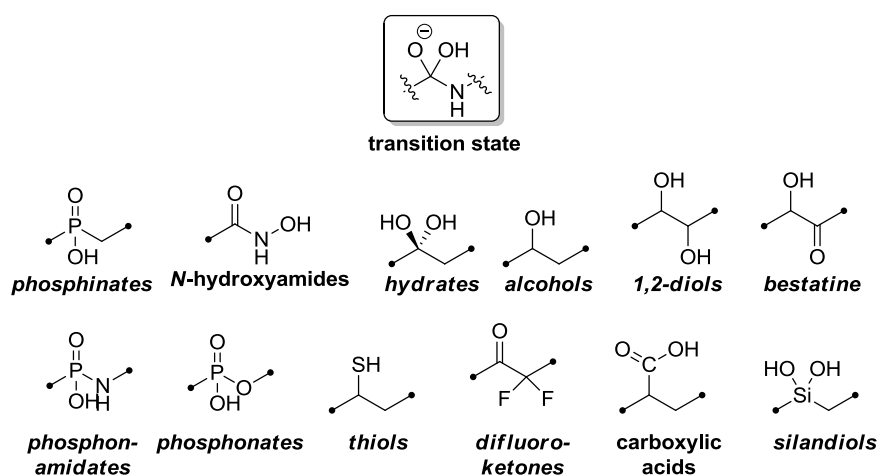


Figure 9: Transition state analogues of the tetrahedral intermediate passed through during amide bond hydrolysis.

1.6.3 Phosphoramidates as protease inhibitors

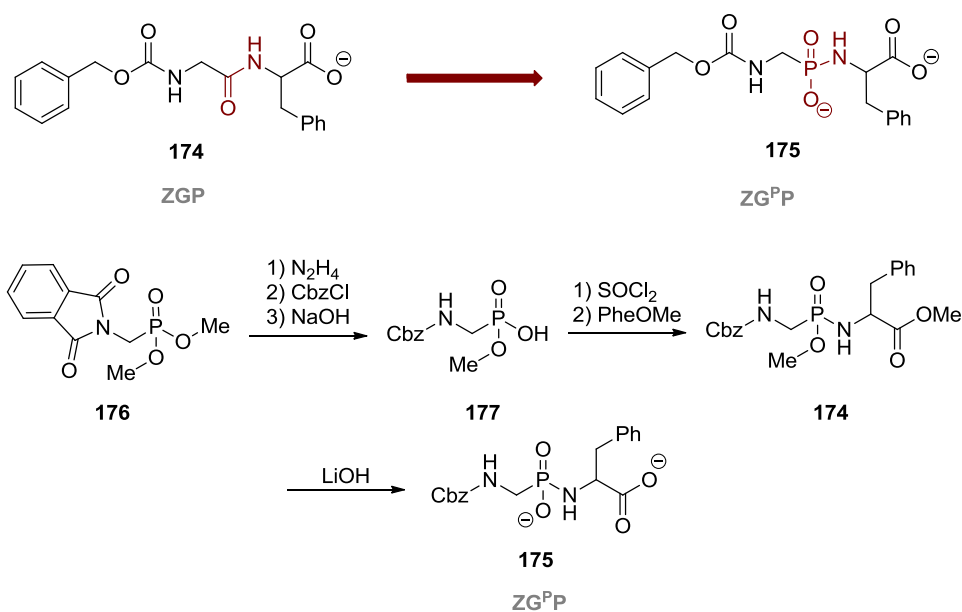
Among other organophosphorus compounds, phosphoramidates, which feature analogy to the hydrolysis transition state (Figure 9), are known to be suitable candidates as enzyme inhibitors, especially for different metalloproteases.^[2f-i]

During the process of the amide hydrolysis a high energy intermediate is formed that fits optimally into the active site of the enzyme. Phosphoramidates are able to mimic these unstable intermediates as they resemble the tetrahedral transition state of the peptide bond cleavage in both electronic and geometric features.^[125d] Therefore, they act as non-cleavable analogues with a high affinity to the enzyme-binding site and block the enzyme for further turnovers. Inhibition of various zinc metalloproteases, such as angiotensin-converting enzymes^[2i], enkephalinase^[2i], thermolysin^[2g, 129] or carboxypeptidase A^[2f, 109h], by phosphoramidate derivatives have already been established and feature K_i values in the micro- to nanomolecular range, and this work was significantly coined by the outstanding pioneering work by Bartlett *et al.* on the inhibition of carboxypeptidase A^[2f, 109h] and thermolysin^[2g, 129a-e].

In 1981 Bartlett and Jacobson^[2f] presented the first protease inhibitor based on a phosphoramidate peptide for carboxypeptidase A, the prime representative in the group of zinc peptidases (Scheme 48). Carboxypeptidase A specifically cleaves the C-terminal amino acid of oligopeptides, thereby favoring amino acids with aromatic side chains. In a first attempt to synthesize an effective inhibitor, *N*-[[[(benzyloxycarbonyl)amino] methyl] hydroxyphosphinyl]-*L*-phenylalanine dilithium salt (ZG^PP) (**175**) was prepared as analogue of the dipeptide carbobenzyoxyglycyl-*L*-phenylalanine (ZGP) (**174**), a natural substrate. The synthesis was performed starting from the diester **176** according to literature procedures^[130] followed by basic deprotection. By replacing the scissile bond of a natural substrate of carboxypeptidase A by a phosphoramidate moiety they obtained a potential protease inhibitor based on the transition state analogue concept.

As it was already shown for phosphoramidates like phosphoramidon^[128d], by crystallization with thermolysin the P(O)OHNH-moiety is apt to occupy the scissile bond position at the active side of the enzyme, and therefore, phosphoramidates are presumed to act as transition state analogues. Comparison of their structure with the newly synthesized phosphoramidate as well as with the active sites of carboxypeptidase A and thermolysin led to the assumption that phosphoramidates **175** can also be regarded as transition state analogues. The fact that phosphoramidates exist as zwitterions at a pH of 7.5 whilst phosphoramidates are believed to

be a simple monoanion makes out the main difference in addition to the substitution of the oxygen by the NH-group.



Scheme 48: Design and synthesis of the first phosphoramidate inhibitor for carboxypeptidase A.^[2f, 130]

One drawback of phosphoramidates **175** as inhibitors is their intrinsic instability in their deprotected form. At pH values below 2.3, P-N bond cleavage occurs within minutes as shown for ZGPP **175**.^[2f] But above a pH of 5 their stability is sufficient to conduct protease inhibitor assays without any decomposition. Additionally, it could be proven that carboxypeptidase A did not catalyze P-N bond cleavage and that the phosphonic acid derivatives derived from eventual acidic cleavage do not show any inhibitory activity. The investigations of Bartlett and Jacobsen further verified that this phosphoramidate **175** is a potent, competitive inhibitor and the second tightest binder of this enzyme with a K_i value of 90 nM at pH 7.5. The special affinity of ZGP **174** to the active site of carboxypeptidase A resides in the ((carbobenzyloxy)amino)methyl moiety, which presumably occupies the S1 and S2 binding sites. The ability to incorporate such residues in the phosphoramidate structure is a significant advantage of this approach over the use of simple *N*-phosphoryl amino acids. By decreasing the pH from 7.5 to 6, a 15-fold increase in binding strength was observed, and a favorable hydrogen bond between the now protonated glutamic acid in the active site with the phosphoryl oxygen served as explanation, but more detailed experiments are needed for clarification. These preliminary results initiated further investigations by the group of Bartlett, and many other groups picked up this idea as can be seen from the variety of publications.^[2j-l, 129f, 131]

Additional investigations on phosphoramidates as transition state analogues on the protease thermolysin provided further evidence that the compounds are real transition state analogues and not merely multisubstrate ground-state analogues.^[129b] Phosphoramidate tripeptides were synthesized and exhibited K_i values between 1.7 μM to 9.1 nM, the best values ever reported for thermolysin.^[129b] It is suggested that these excellent inhibition values of phosphoramidate derivatives arise partly from the interaction of the phosphoryl oxygen with the active site zinc ion during the cleavage process and partly through interactions of amino acid side chains with binding sites of the enzyme.

In order to compare the binding efficiency of different phosphor(V) derivatives, Bartlett and Marlowe demonstrated that the binding of the dipeptide phosphoramidate derivatives are 1000-fold tighter than the binding of the phosphonate analogues to the enzyme thermolysin.^[129b] These analogues were prepared by replacing the Gly-Leu of a small substrate peptide bond by either a phosphonate ester or a phosphoramidate. The results indicate that the stronger binding can be explained by the additional hydrogen bond donor of the NH-group that does not exist in the phosphonate ester.

The above observation was investigated more extensively by Grobelny *et al.* on thermolysin.^[129f] They prepared analogues of the natural substrate in which the amide bond was replaced by P(O)-NH, P(O)-CH₂ or P(O)-O. Determination of the pK_a values proved that in the first two compounds the basicity of the oxygen anion, which ligands the zinc ion, is significantly higher than in the P(O)-O compound and that these compounds are also better ligands. The free energy of solvation of the aforementioned three compounds is very similar so that this aspect does not explain the better inhibitory function of the phosphoramidates. These observations supported the theory that the better binding efficiency of the phosphoramidate compared to the phosphinate originates from the better ability of NH to form hydrogen bonds and to serve as ligand. Although, the value of the hydrogen bond had to be corrected from the proposed of 4.1 kcal/mol to 1.5 kcal/mol.

Moreover, careful studies of inhibitors of the human neutrophil collagenase implied that extending the peptide portion of the phosphoramidate peptides in both *N*- and *C*-terminal directions could noticeably improve the binding strength (Figure 10).^[132] The human neutrophil collagenase is a metalloprotease which catalyzes the hydrolysis of native, triple-helical interstitial collagens into characteristic $\frac{3}{4}$ and $\frac{1}{4}$ fragments. Cleavage takes place between a glycine and a isoleucine bond of the $\alpha 1$ (I) chains in type I collagen. The sequence of the natural substrate is Pro-Gln-Gly-Ile-Ala-Gly. The simple phosphoramidate dipeptide showed a K_i value of

only 2.1. Elongation in the N-terminal direction improved the K_i value to 0.15 but elongation in the C-terminal direction was even more effective (K_i 0.071). The best K_i value (K_i 0.014) was achieved by extension of the peptide in both directions. Along those lines, the incorporation of functional amino acids into phosphonopeptides and phosphoramidate peptides, which resemble the natural protease substrate, are supposed to increase binding affinity and the data show that this concept is very promising for the inhibitor design. However, due to the limitations in the phosphoramidate synthesis routes (see 1.5), these assumptions could only partially be validated, yet. In the applied phosphoramidate glutamine was not incorporated in the sequence and isoleucine was substituted for leucine.

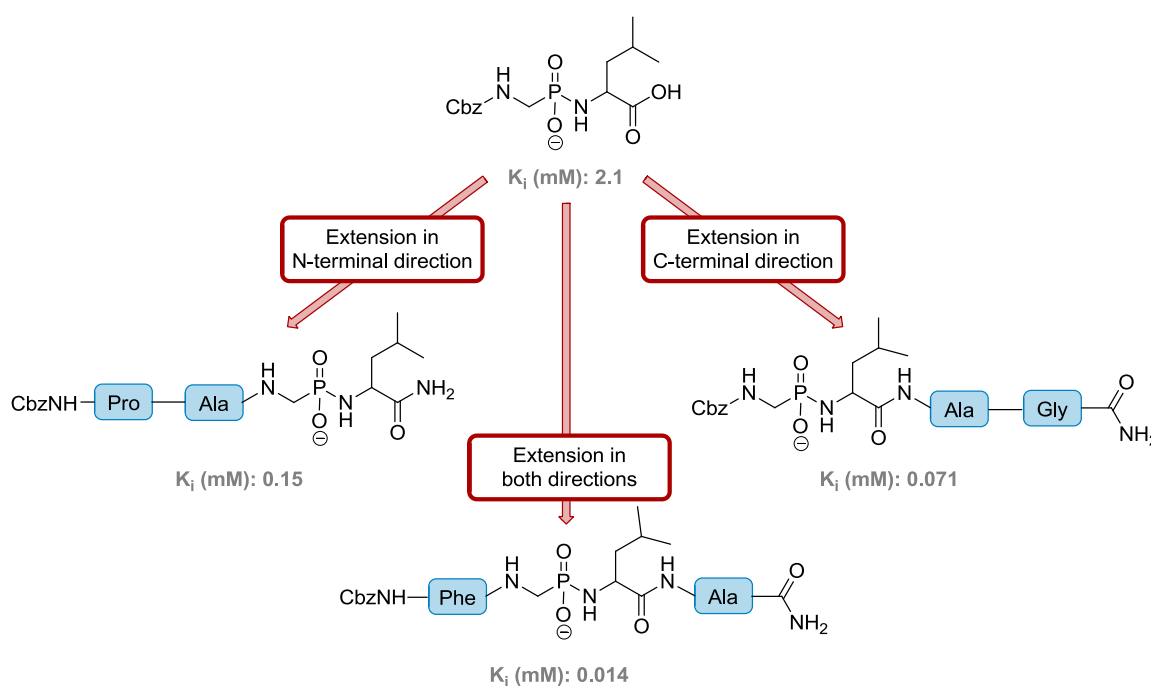


Figure 10: Elongation of the peptide sequence and its influence on the K_i values.^[132]

It is worthwhile to note that not only peptidases are potential target molecules for these classes of compounds. In a similar way, class C β -lactamase^[133], HMG-CoA reductase^[134], and D-alanyl-D-alanine ligase^[135] are effectively inhibited by P(V)-based transition state analogues. The transition state concept was also applied to hapten designs, which subsequently generate antibodies catalyzing diverse reactions like the formation of dipeptides and larger peptides or possessing peptide ligase activity.^[136] Likewise, several phosphonopeptides have shown potent antibacterial activity.^[111j, 137]

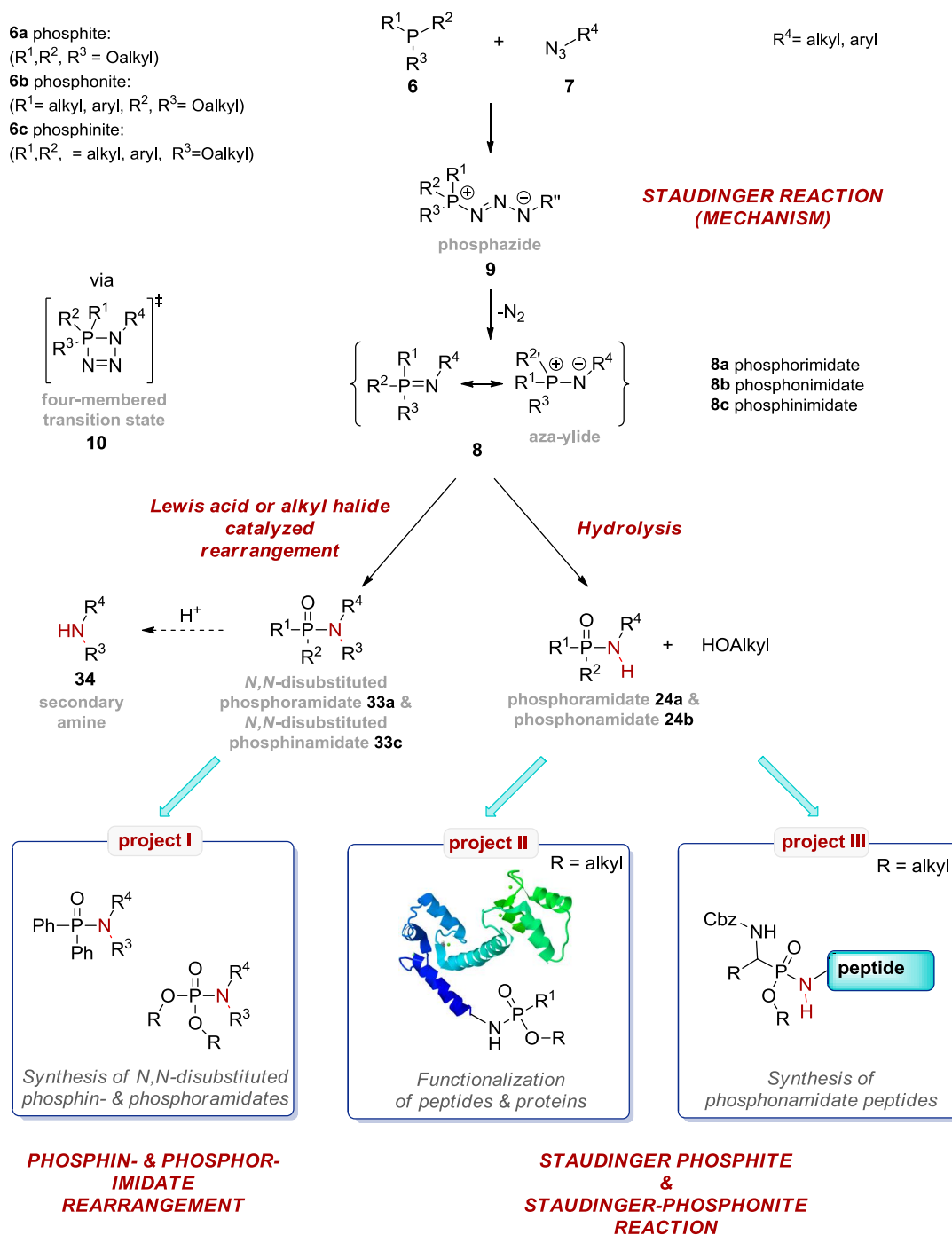
2 Objective

As outlined in the introduction, phosphin-, phosphon- and phosphoramidates possess interesting properties, which are very valuable for their application in organic transformations but also for therapeutic use.^[1, 2] Therefore, synthetic methods that facilitate their synthesis and broaden the accessible product spectrum are highly desirable. The Staudinger reaction^[3] between azides and trivalent phosphorus species represents a straightforward strategy to create P-N-bonds and permits a variety of different substitution patterns. Moreover, the reaction proceeds in a bioorthogonal manner and does not interfere with functional groups found in the natural products kingdom and, additionally, stands out due to its mild reaction conditions and absence of any further reagents or additives.^[9a-e] For this reason, the Staudinger reaction is predestined for the application in complex products or even biomolecules due to its unique selectivity. Within this thesis, synthetic pathways of the Staudinger reaction are intensively studied, optimized and extended, on the one hand, to find an easier entrance to various phosphin-, phosphon- and phosphoramidates and on the other hand, to probe their practicability for peptidic and proteinogenic systems. The key aspects of this thesis can be divided up into three major projects as displayed on the next page (Scheme 49).

Project I: Synthesis of *N,N*-disubstituted phosphin- and phosphoramidates by the Staudinger reaction & subsequent rearrangement

The aim of the first project was the synthesis of different *N,N*-disubstituted phosphon- and phosphinamidates **33a** and **c** by means of the Staudinger reaction and a subsequent rearrangement (Scheme 49). Besides the fact that the synthesis of these P-N compounds itself is worthwhile, the phosphorus moiety at the nitrogen can be regarded as a protective group. In contrast to iminophosphoranes derived from azides and trialkyl phosphines, the P-N bond of phosphin- and phosphoramidates is not easily hydrolysable and can only be cleaved under strong acidic conditions.^[38] Furthermore, if the nitrogen bears two other substituents in addition to the phosphorus moiety, secondary amines **34** can be obtained after acidic treatment.

It has already been shown by Challis *et al.*^[5b] and Kabachnik *et al.*^[5a, 5c-g], that, by performing the Staudinger reaction under anhydrous conditions, a rearrangement of the imidates **8a** can be initiated either by extensive heating or by addition of alkyl halides or Lewis acids delivering *N,N*-disubstituted derivatives **33a**. Although several methods for the synthesis of secondary amines **34** are presently available, being able to prevent overalkylation, in many cases several synthetic steps and complex precursor molecules are required.^[138]



Scheme 49: Illustration of the three main projects of this thesis and the applied reaction pathways.

In contrast, alkyl as well as aryl azides **7** needed for the Staudinger reaction can be installed fairly easily in one step and the azido group can be carried through many reaction steps without being affected. Concerning the trivalent phosphorus species, many derivatives are commercially available or can be synthesized from commercially available precursors by simple transformations.

With regard to the first project, the Staudinger reaction and the subsequent rearrangement between azides **7** and phosphites **6a** should be more intensively studied and optimized with respect to the Lewis acid catalysis, reaction conditions and the scope of products. Furthermore, the reaction procedure should be transferred to phosphinimidates **8c** not being rearranged before. Finally, a one-pot procedure should be developed in order to avoid isolation of the potentially explosive azides **7** and to facilitate the procedure.

Project II: Functionalization of peptides and proteins by the Staudinger reaction

The site-selective functionalization of peptides and especially of proteins is a challenging and very desirable target in bioorganic and biological chemistry. The installation of for instance affinity tags, fluorophores or posttranslational modifications and their surrogates permits to study, analyze and isolate biomolecules and provides access to a more profound knowledge of complex biological processes. A common method to achieve the site-selective attachment of functional molecules represents the famous “click”-reaction between azides and alkynes.^[75] Although alternatives have been established to the use of toxic copper, the preparation of the required “special” alkyne derivatives is often complicated. As demonstrated by Bertozzi *et al.*^[9d, e], the Staudinger reaction constitutes a striking method even for *in vivo* applications. Nevertheless, by extending the reaction margin, also in this case limitations were revealed with respect to the reactivity versus the stability of the phosphines and the reaction rate of the intramolecular rearrangement.^[83]

Within this work, first results should be gained about the Staudinger-phosphite and the Staudinger-phosphonite reaction regarding their applicability for the functionalization of unprotected peptides (Scheme 49). Based on these preliminary results, the reaction should later on be transferred to the protein level within the scope of new projects and syntheses.

Project III: Synthesis of phosphoramidates and phosphoramidate peptides by the Staudinger reaction starting from silylated phosphinic acids

The target of the second project was the application of the Staudinger reaction for the synthesis of phosphoramidates **24b** and phosphoramidate peptides (Scheme 49). Phosphoramidates **24b** aroused, especially as transition state analogues of peptide bonds during their hydrolysis, a remarkable interest during the last decades elicited from the seminal investigations of Bartlett and coworkers.^[2f-h, 109h, 129a-e, 139]

Despite the fact that inhibitory abilities and K_i values of phosphoramidates for different proteases like thermolysine^[2g, 129] or carboxypeptidase A^[2f, 109h] look promising and targets like HIV proteases or secretases, involved in Alzheimer disease, demand specific inhibitors and

systematic investigations, only a few phosphoramidates were tested so far. Up to now, almost all phosphoramidates are of low molecular weight and predominantly very small, protected phosphoramidate peptides have been synthesized due to the limitation of methods existing for their preparation.^[2]-1, 131a, 132, 140] Common strategies, as described in the introduction, are based on a nucleophilic substitution at the phosphorus(V) center and require elaborate protection strategies. The Staudinger reaction would allow a straightforward access to phosphoramidates and phosphoramidate peptides. The incorporation of phosphoramidate groups into whole peptides with the natural substrate sequence of the protease could thus permit the synthesis of inhibitors with a much higher specificity and binding strength.^[132]

Because substitution of the carboxylic group of amino acids by phosphonite groups is rather difficult and the obtained phosphonites are very prone to hydrolysis and oxidation, an alternative strategy should be probed. It is possible to convert phosphinic acid or their esters to their trivalent form by treatment with a silylation reagent.^[73, 141] The obtained trivalent silyl phosphonites can then be reacted with azides to form phosphoramidates **24b**. This strategy has two main advantages: first, phosphinic acids and their esters are fairly stable, and secondly, the synthesis of phosphinic acids and aminophosphinic acids is readily established and aminophosphinic acids with aliphatic side chains are accessible.^[142] The same refers to some aminophosphinic acids with functionalized side chains, although their synthesis is more challenging.^[142] The azido-functionalized counterparts from small molecules up to azido peptides can be prepared by common procedures in high yields.

Within this project, the described methodology should be applied for the direct synthesis of phosphoramidates **24b** and phosphoramidate peptides starting from unprotected azido peptides and silylated phosphinic acids. The accomplished investigation include optimization of the reaction conditions and probing of different azido and phosphinic acid derivatives as well as silylation reagents. In this context, special attention should be paid to the synthesis of phosphoramidates **24b** containing a free OH-group at the phosphorus and the employment of unprotected peptides to circumvent deprotection of the acid-sensitive phosphoramidates **24b**. Moreover, the Staudinger reaction should be carried out on the solid support to alleviate separation from phosphorus-containing reagents and side products as well as silyl species, which are added in excess to the reaction mixture.

3 Discussion

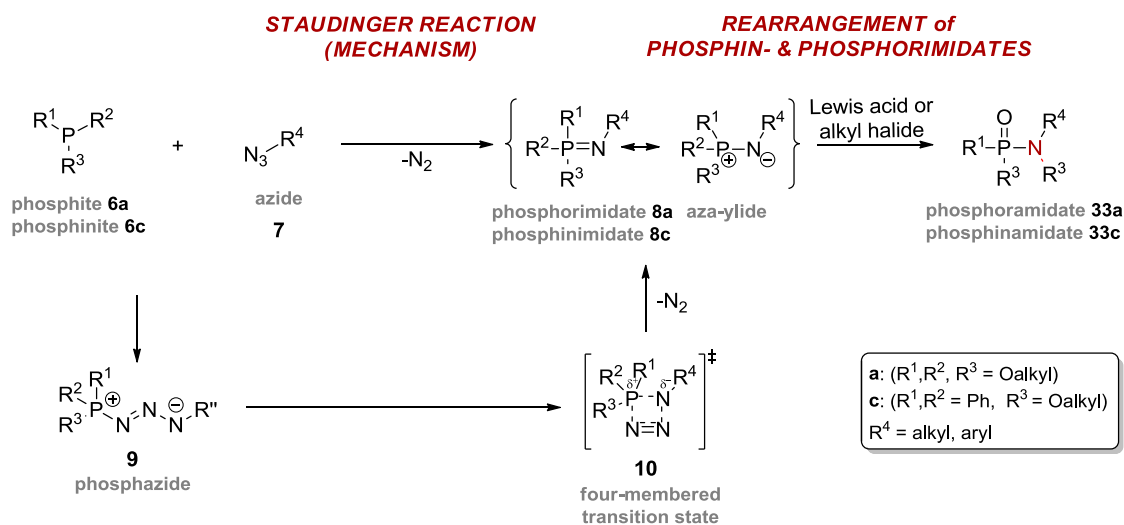
3.1 Synthesis of *N,N*-disubstituted phosphin- and phosphoramidates via a Lewis acid- or alkyl halide-catalyzed rearrangement

P–N bond-containing molecules have emerged as an important class of compounds in modern organic chemistry with numerous applications in catalytic synthetic transformations.^[1a-j, 1l-u] Amongst these, phosphoramidates have attracted considerable interest as they have been applied in high-yielding, enantioselective Lewis base-activated catalytic processes, including aldol additions^[1b-g, 1i, j] and allylation reactions^[1a, 1h].

Apart from their significance for catalysis, *N,N*-disubstituted phosphin- and phosphoramidate derivatives can be regarded as protected secondary amines, and, hence, can be transformed into this important class of compounds, which are commonly present in the pharmacological and natural product kingdoms, by simple deprotection under acidic conditions.^[38]

The Staudinger reaction and the subsequent rearrangement allows direct access to *N,N*-disubstituted phosphoramidates **33a** from organic azides **7** and phosphites **6a** via a two-step/one-pot process (Scheme 50). The reaction sequence firstly includes the reaction of azides **7** with phosphites **6a** to give phosphorimidates **8a**, which are analogous to the iminophosphoranes, formed during the Staudinger reaction of azides with phosphines. In the following reaction step, the crude phosphorimidates **8a** undergo a rearrangement to their corresponding *N,N*-disubstituted phosphoramidates **33a**. Thereby, the rearrangement can be induced either thermally or by addition of Lewis acids or alkyl halides.^[5] Within the scope of the presented investigations, different additives were probed as catalysts to promote the rearrangement of phosphorimidates **8a** derived from benzyl azide and trimethyl phosphite.^[4a] BF₃·Et₂O and TMSOTf turned out to be most effective yielding the *N,N*-disubstituted phosphoramidate in yields of 99% and 98%. Optimization of the reaction procedure revealed heating of the azide **7** and the phosphite **6a** in benzene for 2 h at 80°C for the phosphorimide formation and additional 2 h after adding the catalyst for the rearrangement as optimal conditions. Besides benzyl azide, a variety of alkyl azides, including primary, secondary, tertiary azides and even protected azido-GlucNAc, was employed in the Staudinger reaction and the subsequent rearrangement with trimethyl phosphite. In all cases, the desired phosphoramidates **33a** were obtained in good to high yields (67-89%). Moreover, phenyl azide as well as aryl azides

containing a nitro- or methoxy- substituent were converted to the desired phosphoramidates **33a** in high yields (85-88%).^[4]



Scheme 50: Staudinger reaction and following rearrangement.

Instead of trimethyl phosphite, triethyl, tributyl and triallyl phosphite could also be employed in the Staudinger reaction with following rearrangement and the phosphoramidates **33a** were generated in yields between 63% and 93%.

In order to further facilitate the reaction sequence and avoid isolation of the potentially explosive azides **7**, a one-pot procedure for the formation of *N,N*-disubstituted phosphoramidates **33a** was developed. The reaction sequence starts from alkyl halides, mesylates or tosylates, which are converted to the azido compound with sodium azide. The phosphite can directly be added to the reaction mixture followed by BF₃·Et₂O after complete formation of the phosphorimidate **8a**. The *N,N*-disubstituted phosphoramidates **33a** were obtained in yields between 32% and 92%.

Later on, the rearrangement of phosphinimidates **8c** was probed. The alkyl halide-catalyzed process was transferred to phosphinimidates **8c**, and methyl, ethyl and benzyl groups could successfully be rearranged delivering the corresponding *N,N*-disubstituted phosphinamidates **33c** in yields between 60% and 83%. Next, the rearrangement of phosphinimidates **8c** was probed with BF₃·Et₂O as catalyst. In case of phosphinimidates **8c** derived from methyl diphenylphosphinite and benzyl or phenyl azide, the rearrangement with BF₃·Et₂O led to comparable yields of 87% and 75%. In contrast, the rearrangement of an ethyl or a benzyl group was significantly lower (36-51%).

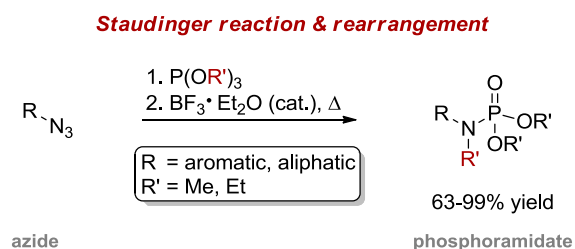
In conclusion, a new protocol for the preparation of secondary phosphin- and phosphoramidates **33c** and **a** from azides **7** and phosphites **6a** or phosphinites **6c** via a one-pot procedure, including

the formation of phosphin- or phosphoramidates **8c** and **a** and their subsequent Lewis acid-catalyzed rearrangement, was developed. This reaction sequence tolerates a wide range of substrates and offers the possibility of synthesizing phosphin- and phosphoramidates **33c** and **a** in good yields and in high purity. Considering the importance of these compounds in catalysis and in organic synthesis as precursors to secondary amines, this transformation is of high utility and complements the Staudinger reduction pathway, which directly converts azides into primary amines.

Responsibility assignment: The concept of research was provided by Professor C. P. R. Hackenberger. Dr. Guisepppe del Signore, a postdoctoral researcher, performed initial experiments to probe the feasibility of the reaction and the prospect of success of the project; moreover, he performed the rearrangements with alkyl halides. Diploma student Wiebke Ahlbrecht worked on the rearrangement of benzyl diphenylphosphinimidates. Some of these experiments were repeated and verified by the author. All other experiments described in this thesis were planned and performed by the author. Furthermore, the corresponding publications were also planned and written by the author under supervision of Professor C. P. R. Hackenberger.

3.1.1 Synthesis of *N,N*-disubstituted phosphoramidates via a Lewis acid-catalyzed phosphorimidate rearrangement

Ina Wilkening, Giuseppe del Signore and Christian P. R. Hackenberger



Scheme 51: Reaction scheme.

Abstract: A Lewis acid-catalyzed rearrangement of phosphorimidates allows a direct, high-yielding transformation of azides with commercially available phosphites into secondary phosphoramidates.

This chapter was published in the following journal:

Ina Wilkening, Giuseppe del Signore and Christian P. R. Hackenberger
Chemical Communication **2008**, 25, 2932-2934.

DOI: 10.1039/B802030B

Received: 5 February 2008, Accepted: 27 March 2008

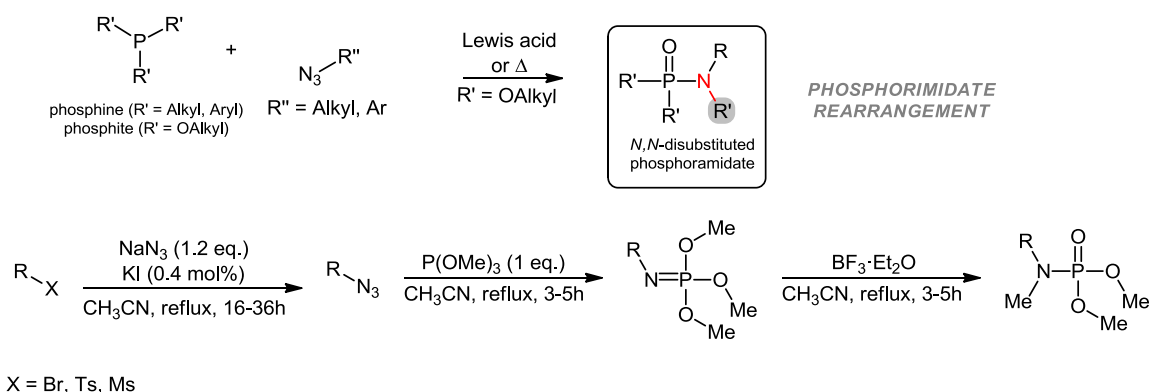
First published on the web: 18 April 2008

The original article is available at:

<http://dx.doi.org/10.1039/B802030B>

3.1.2 Lewis Acid or Alkyl Halide Promoted Rearrangements of Phosphor- and Phosphinimidates to *N,N*-Disubstituted Phosphor- and Phosphinamidates

*Ina Wilkening, Giuseppe del Signore, Wiebke Ahlbrecht, Christian P. R. Hackenberger**



Scheme 52: Reaction scheme.

Abstract: In this paper, we describe the synthesis of *N,N*-disubstituted phosphor- and phosphinamidates via alkyl halide- or Lewis acid-catalyzed rearrangements of phosphor- or phosphinimidates. Furthermore, we introduce a novel one-pot procedure for the synthesis of *N,N*-disubstituted phosphoramidates which prevents the isolation of potentially explosive alkyl azide derivatives. In this reaction sequence, several alkyl halides are converted in situ into the corresponding azides and reacted with phosphites to generate phosphorimidates. Final addition of a catalytic amount of Lewis acid to the mixture affords the *N,N*-disubstituted phosphoramidates in good to excellent overall yields.

This chapter was published in the following journal:

*Ina Wilkening, Giuseppe del Signore, Wiebke Ahlbrecht, Christian P. R. Hackenberger**

Synthesis **2011**, *17*, 2709-2720.

DOI: 10.1055/s-0030-1260141

Received: 4. May 2011

The original article is available at:

<http://dx.doi.org/10.1055/s-0030-1260141>

3.2 Peptide and Protein Functionalization by the Staudinger-phosphite and the Staudinger-phosphonite reaction

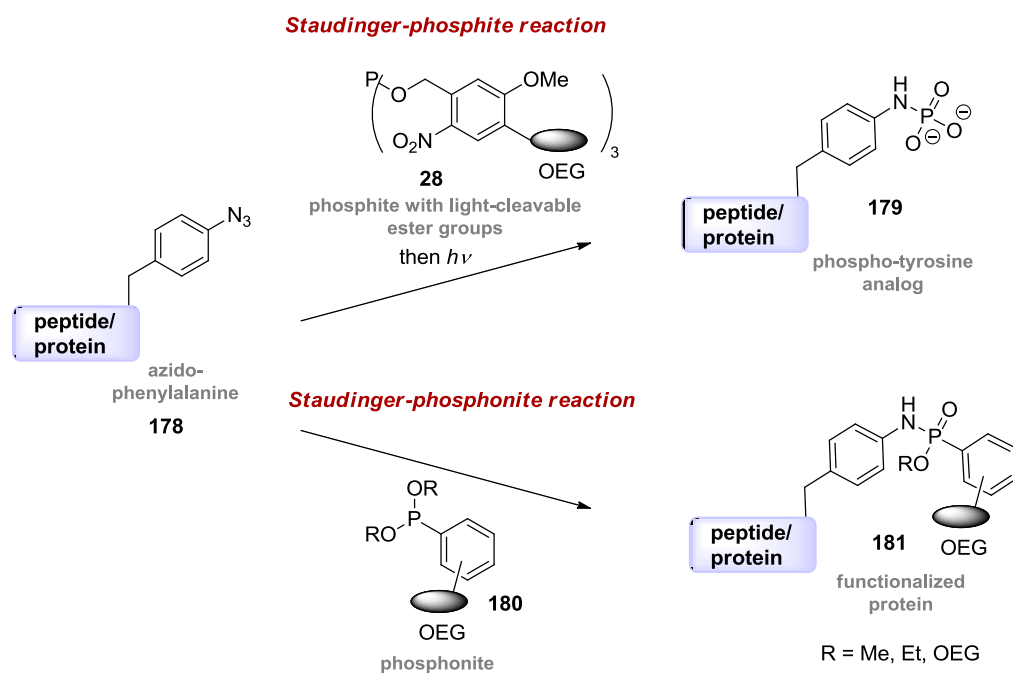
The selective transformation of a particular functional group in the presence of additional chemical functionalities by chemoselective reactions is an important tool in organic synthesis as well as chemical biology.^[78d, 143] In addition to simplifying synthetic routes for the synthesis of natural products, these reactions allow the site-specific modification of proteins by selectively conjugating functional modules to proteins, which carry bioorthogonal reporters.^[143c, d] In combination with the many advances for the introduction of bioorthogonal functionalities into biopolymers, this concept has proven to be especially useful in the area of proteomic research, in particular for elucidating the role of posttranslational modifications in key biological processes such as cellular recognition and signal transduction.^[144]

For biological applications, a chemoselective reaction must transform a single chemical functionality within a complex biomolecule under mild aqueous conditions at ambient temperature. Furthermore, for full spatial control of the location of the desired modification unit within the target biopolymer, reactions are particularly useful, in which both reaction partners are non-natural, since they can address a unique chemical functionality within a complex biopolymer.

The presented investigations on the Staudinger reaction prove that the Staudinger-phosphite reaction between azides and phosphites meets these requirements and is suitable for the metal-free, chemoselective transformation of azides in peptides and proteins (Scheme 53).^[6a]

First, the scope and applicability of this transformation under mild reaction conditions for peptide modifications was determined. The Staudinger reaction was probed with phenyl azide and symmetrical phosphites, and it could be shown that the reaction occurs in high yields (78%–90%) at room temperature in various solvents including CH₂Cl₂, *N,N*-dimethylformamide, dimethylsulfoxide, and even pure water. Moreover, the reaction between unprotected azido peptides **178** and phosphites in aqueous buffers at pH 7.4–8.2 at room temperature proceeded with almost quantitative conversion to the phosphoramidate peptide in less than 8 hours. Finally, the Staudinger-phosphite reaction was successfully applied for the modification of azido proteins **178**. Upon combination with a light-sensitive phosphite **28**, the phosphoramidate esters can be hydrolyzed to yield an analogue **179** of a phosphorylated tyrosine residue in proteins, which can be recognized by phosphotyrosine-specific antibodies. In conclusion, chemoselective

transformations by the Staudinger-phosphite reaction proceed in various solvents and buffers at room temperature, conditions suitable for quantitative modification reactions in proteins. Furthermore, this Staudinger reaction is very easy to perform as it utilizes phosphites, which can be prepared by standard organic synthesis protocols and which are stable against oxidation upon exposure to air.



Scheme 53: Site-selective functionalization of peptides and proteins by the Staudinger-phosphite or Staudinger-phosphonite reaction.

As alternative P(III)-reagents for the chemoselective functionalization of azido biopolymers, phosphonites like **180** were probed in the Staudinger reaction (Scheme 53).^[6b] Phosphonites possess a high intrinsic reactivity in Staudinger reactions and have the potential to transfer a single functional module or label that is attached to the carbon chain at phosphorus to an azido-containing biopolymer. The reaction was first probed with dimethyl phenylphosphonite and benzyl azide as well as unprotected azido peptides and the corresponding phosphoramidates and phosphoramidate peptides were obtained in high yields. Afterwards several water-soluble phosphonites **180** were synthesized and probed with respect to their stability and performance in this bioorthogonal transformation of azido peptides **178** in aqueous systems. Thereby, phosphonites **180** with OEG-chains at all substituents proved to be most efficient as conversion rates between 65% and 95% could be achieved with a 50 mM concentration. Finally, the Staudinger-phosphonite reaction was transferred to the protein level, and calmodulin containing

p-azido phenylalanine could be converted to the functionalized phosphoramidate protein by approximately 70%.

Responsibility assignment:

1) Staudinger-phosphite reaction

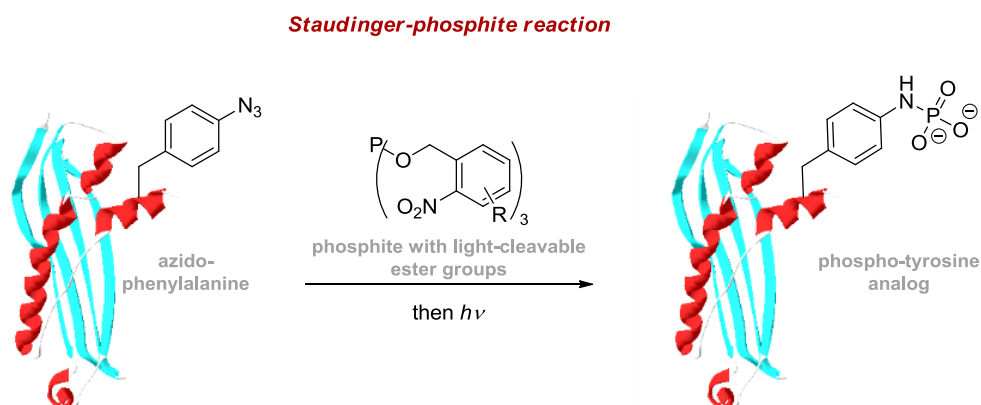
The concept of research for the Staudinger-phosphite reaction was provided by Professor C. P. R. Hackenberger. Initial experiments of the Staudinger-phosphite reaction with phenyl azide and azido-peptides in organic solvents and water were performed by the bachelor students Denise Homann and Silvia Muth under supervision of the author. The project was overtaken by Dr. Remigiusz Serwa, a postdoctoral researcher, who performed further studies of the Staudinger-phosphite reaction between phosphites and azido peptides and the azido protein and synthesized the 2-nitrobenzyl phosphite. Master student Michaela Mühlberg performed first reactions between the azido protein and trimethyl phosphite. Iris Claußnitzer and Dr. Michael Gerrits provided the azido protein obtained by non-natural protein translation using the amber-suppression based orthogonal system. Dr. Christoph Weise was responsible for the MALDI measurements.

2) Staudinger-phosphonite reaction

The concept of research for the Staudinger-phosphonite reaction was provided by Professor C. P. R. Hackenberger. Initial experiments of the Staudinger-phosphonite reaction with benzyl azide and azido-peptides in organic solvents were performed by the author. The project was overtaken M. Robert J. Vallée, who synthesized all not commercially available phosphonites and performed further studies of the Staudinger-phosphonite reaction between phosphonites and azido peptides as well as the azido protein. In the synthesis of different phosphonites he was supported by his master student Gregor Müller. Paul Majkut provided the azido calmodulin obtained by non-natural protein translation using the amber-suppression based system and performed the analysis of the phosphoramidate calmodulin by Westernblot. Christoph Weise was responsible for the MALDI measurements. The paper was written by Robert Vallée under supervision of Professor C. P. R. Hackenberger and support of the author.

3.2.1 Chemoselective Staudinger-Phosphite Reaction of Azides for the Phosphorylation of Proteins

Remigiusz Serwa Dr., *Ina Wilkening*, Giuseppe Del Signore Dr., Michaela Mühlberg, Iris Claußnitzer, Christoph Weise Dr., Michael Gerrits Dr., Christian P. R. Hackenberger Dr.



Scheme 54: Staudinger-phosphite reaction of an azido protein for the preparation of phospho-tyrosine analogs.

Abstract

Extending the toolbox: The title reaction was identified as a chemoselective means to modify azides in peptides and proteins in high yields at room temperature in various solvents including aqueous buffers at physiological pH. In combination with nonnatural protein translation the Staudinger-phosphite reaction allows the site-specific incorporation of phosphorylated Tyr analogues in proteins.

This chapter was published in the following journal:

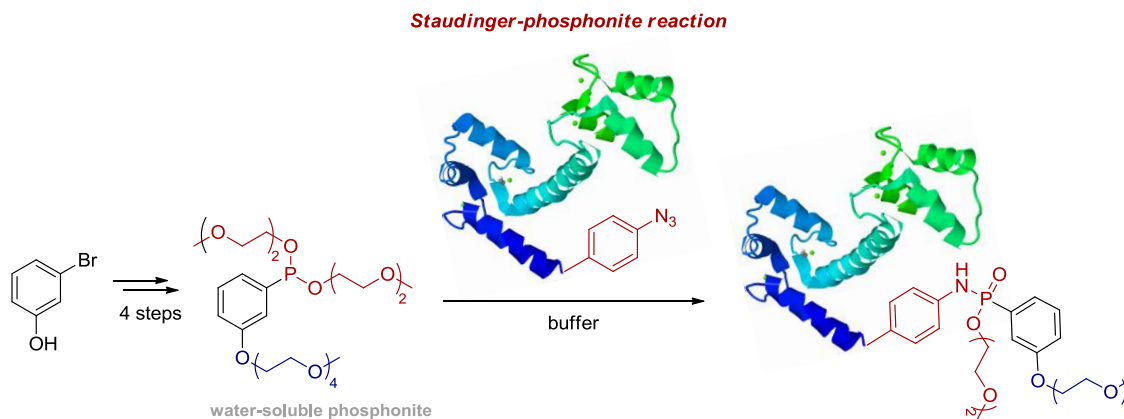
Remigiusz Serwa Dr., Ina Wilkening, Giuseppe Del Signore Dr., Michaela Mühlberg, Iris Claußnitzer, Christoph Weise Dr., Michael Gerrits Dr., Christian P. R. Hackenberger Dr.
Angewandte Chemie International Edition **2009**, *48*, 8234–8239,
 DOI: 10.1002/anie.200902118
 Article first published online: 27 July 2009

The original article is available at:

<http://dx.doi.org/10.1002/anie.200902118>

3.2.2 Staudinger-Phosphonite Reactions for the Chemoselective Transformation of Azido-Containing Peptides and Proteins

M. Robert J. Vallée, Paul Majkut, *Ina Wilkening*, Christoph Weise, Gregor Müller, and Christian P. R. Hackenberger



Scheme 55: Functionalization of calmodulin by the Staudinger-phosphonite reaction.

Abstract

Site-specific functionalization of proteins by bioorthogonal modification offers a convenient pathway to create, modify, and study biologically active biopolymers. In this paper the Staudinger reaction of aryl-phosphonites for the chemoselective functionalization of azido-peptides and proteins was probed. Different water-soluble phosphonites with oligoethylene-substituents were synthesized and reacted with unprotected azido-containing peptides in aqueous systems at room temperature in high conversions. Finally, the Staudinger-phosphonite reaction was successfully applied to the site-specific modification of the protein calmodulin.

This chapter was published in the following journal:

M. Robert J. Vallée, Paul Majkut, *Ina Wilkening*, Christoph Weise, Gregor Müller, and Christian P. R. Hackenberger

Organic Letters **2011**, *13*, 5440–5443.

DOI: 10.1021/ol2020175

Publication Date (Web): 29 September 2011

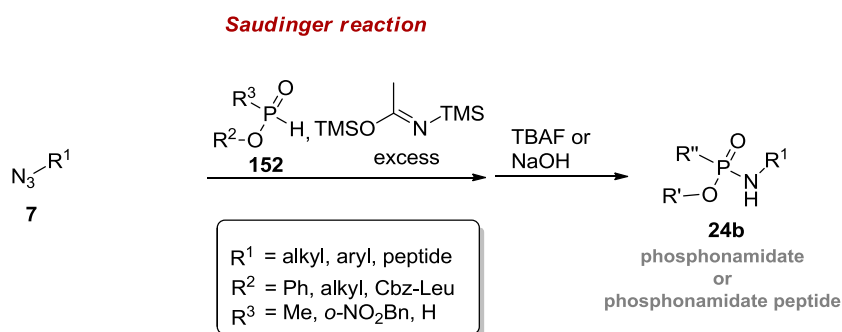
The original article is available at:

<http://dx.doi.org/10.1021/ol2020175>

3.3 Synthesis of phosphoramidates and phosphoramidate peptides from aryl azides by the Staudinger reaction

Phospon- and phosphoramidates are of great interest in various areas of modern organic chemistry, including applications in asymmetric catalysis^[1a-j, 1l-u] as well as bioorganic and pharmaceutical research^[2]. In contrast to the rather stable phosphoramidates, phosphoramidates are known to be more prone to P(O)–NH bond cleavage under acidic conditions, in particular if a free OH group is present at the phosphorous atom.^[2f] Nevertheless, phosphoramidate peptides, in which an amide bond is replaced by P(O)–OR,NH- or P(O)–OH,NH-group, have found considerable attention as promising protease inhibitors.^[2f-l] Upon incorporation into a peptide backbone phosphoramidates can be regarded as analogues of the transition state during peptide bond cleavage by proteases and thereby mimic the natural substrate. This potency makes phosphoramidate peptides interesting synthetic targets for the development of protocols to probe different proteases in the elucidation of a variety of biological processes and as targets for drug discovery for the treatment of diseases like HIV^[2j, k] and others.

The objective of the presented investigation was the development of a synthetic strategy, which enables a straightforward and acid-free access to phosphoramidates and phosphoramidate peptides by the Staudinger reaction (Scheme 56).^[7] Phosphinic acids or their esters **152** can be converted by silylation into the trivalent silylated phosphonite species *in situ*, which can be used directly in the subsequent Staudinger reaction with azides **7** to deliver phosphoramidates **24b**.^[73]



Scheme 56: Synthesis of phosphoramidates and phosphoramidate peptides **24b** by the Staudinger reaction.

Within this project it could be demonstrated that the Staudinger reaction of silyl phosphonites with different aryl azides in solution delivers the desired phosphoramidates **24b** in good to high yields (30-95%). Furthermore, the synthetic route could be transferred to solid-supported aryl azido peptides **7**. The advantages of such a solid-supported process include the easy removal of reagents and additives and the possibility to combine this route with standard Fmoc-based solid-phase peptide synthesis (SPPS). For this purpose, a base-labile HMBA resin was chosen as solid support, which after SPPS enables a side chain deprotection by TFA to deliver an immobilized, unprotected azido peptide. The Staudinger reaction between the unprotected azido peptides and silyl phosphonites led to good or high conversions into the corresponding phosphoramidate peptides (52-86%) as determined by UV without the need of acidic protective group manipulations.

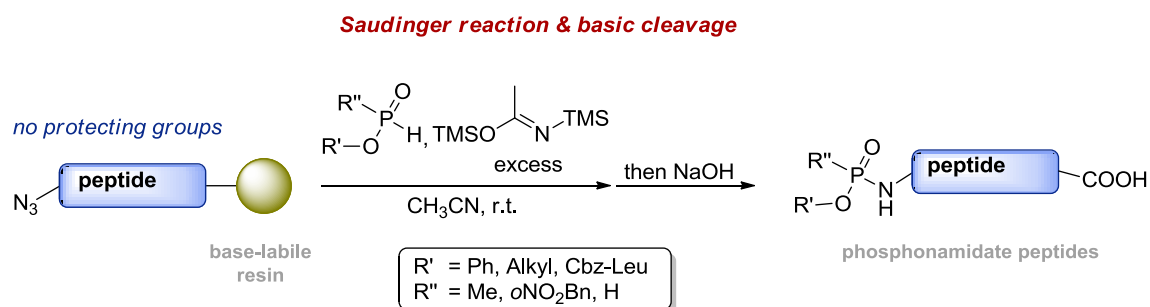
After the successful synthesis of peptide esters, the strategy was probed for the synthesis of the very labile phosphoramidate peptides containing a free OH-group at the phosphorus. The phosphoramidate peptides were generated as major products (64-87%), and only small amounts (7–25%) of the corresponding amino peptides appeared in the LC-MS traces, which are presumably formed by P(O)–NH bond cleavage. Finally, a phosphinic acid *ortho*-nitrobenzyl ester was applied in the Staudinger reaction allowing the synthesis of a relatively stable phosphoramidate peptide, which can be converted to the more labile phosphoramidate peptide with a free OH-group by UV irradiation.

Responsibility assignment:

The concept of research was provided by Professor C. P. R. Hackenberger and Dr. Guiseppe del Signore, a postdoctoral researcher, performed initial experiments. All experiments and mechanistic investigations described in this thesis and the corresponding journal article were planned and performed by the author. Furthermore, the corresponding publication was also planned and written by the author under supervision of Professor C. P. R. Hackenberger.

3.3.1 Synthesis of phosphoramidate peptides by Staudinger reactions of silylated phosphinic acids and esters

Ina Wilkening, Giuseppe del Signore and Christian P. R. Hackenberger



Abstract:

The Staudinger reaction of unprotected azido peptides with silylated phosphinic acids and esters on the solid support offers a straightforward acid-free entry to different phosphoramidate peptide esters or acids under mild conditions in high purity and yield.

This chapter was published in the following journal:

Ina Wilkening, Giuseppe del Signore and Christian P. R. Hackenberger
Chemical Communication, 2011, 47, 349-351.

DOI: 10.1039/C0CC02472D

Received: 9. July 2010, Accepted: 6 August 2010

First published on the web: 7 September 2010

The original article is available at:

<http://dx.doi.org/10.1039/C0CC02472D>

3.4 Staudinger reaction of silylated phosphinic acid esters with alkyl azides

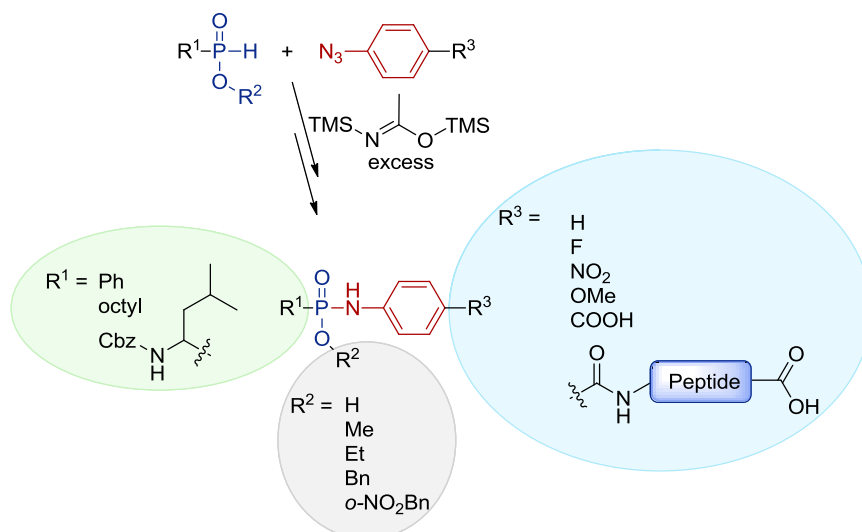
3.4.1 Outline

The synthesis of phosphoramidates and phosphoramidate peptides is a challenging target in organic and bioorganic research. Particularly with regard to surrogates for naturally occurring amide bonds, phosphoramidates attracted the attention of many researchers.^[2f-1] Through their steric and their electronic features, phosphoramidates are able to mimic the transition state that is passed through during the hydrolysis of amide bonds catalyzed by proteases, and they are, therefore, regarded as very effective transition state analogues.^[125d] Because of these properties, they have found various applications in medicinal research especially as inhibitors for metallo proteases.^[2f-1] Since versatile methods for their preparation are lacking (see chapter 1.5.1.2), only a rather small number of phosphoramidates is available, most of which are small molecules with a limited number of functional groups. While phosphoramidates that contain a free OH-group at the phosphorus have interesting features for the use as inhibitors due to their higher similarity to the transitionally existing hydrates during amide bond cleavage, their preparation causes problems as they are unstable under acidic conditions,^[2f] which makes the removal of protective groups, chemical transformations in general and their purification difficult.

Contrary to the synthetic accessibility of phosphoramidates is the desire for more complex phosphoramidates with a higher selectivity or specificity. By studying the ability of phosphoramidate peptides to inhibit the human neutrophil collagenase, Bartlett and coworkers found that elongation of the dipeptide in both N- and C-terminal direction could enhance the binding strength and the effectiveness as an inhibitor.^[132] Furthermore, by employing the natural substrate sequence the specificity can be increased, which could reduce side effects in biological and medicinal application.

We could already show in our previous communication^[7] described in chapter 3.3 that the Staudinger reaction can be applied for the synthesis of small phosphoramidates containing different functional groups as well as for fully unprotected phosphoramidate peptides (Scheme 58). Treating the phosphinic acids and their esters with a silylation reagent, like BSA, generates the required trivalent phosphorus species, and they react excellently with aryl azides by the Staudinger reaction to form the desired phosphoramidates and phosphoramidate peptides.

Thereby, the temporary global protection with the trimethylsilyl group impeded possible side reactions. This synthetic strategy stands out due to its facile and straightforward procedure but also due to the mild reaction conditions and clean conversion resulting in high yields, which makes the reaction very efficient and purification easy.

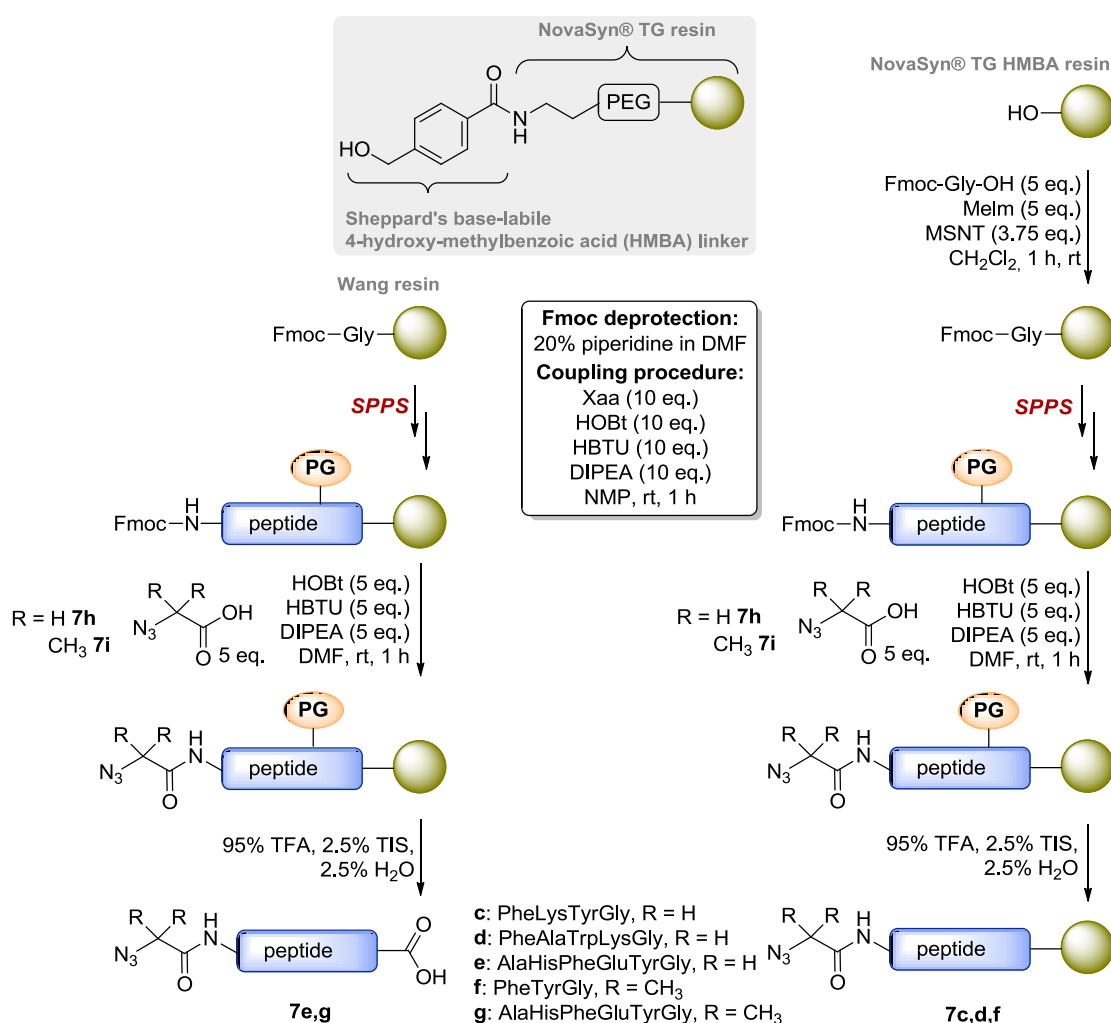


Scheme 58: Schematic overview of introducible substituents to phosphonamides by the Staudinger reaction.^[7]

Aryl azides serve as ideal compounds for the Staudinger reaction because of their high reactivity towards trivalent phosphorus species due to the $-I$ -effect of the aromatic ring. Additionally, aryl azides, such as *para*-azidobenzoic acid, can be easily attached to peptides by standard protocols. Nevertheless, the aromatic system has only minor resemblance to a natural peptidic structure and a broader scope of applicable azides is in general desirable. Consequently, different alkyl azides should be probed and with respect to phosphonamide peptides *para*-azidobenzoic acid should be substituted by azido glycine (**7h**) or similar derivatives to get closer to a natural substrate (Scheme 59). However, when the Staudinger reaction was performed under the same conditions as described for aryl azides, unexpected by-products occurred, which initiated a series of investigations concerning structural aspects and the mechanistic origin of the by-products. Two alkyl azides, namely dodecyl azide (**7a**) and 3-phenylpropyl azide (**7b**), as well as azido peptides **7c-g** with different amino acid sequences containing either azido glycine (**7h**) or α -azidoisobutyric acid (**7i**) at the N-terminus were used in the Staudinger reaction with methyl phenylphosphinate (**182**) as a model substrate. The influence of different reaction conditions on the reaction outcome was studied by variation of the solvent, the temperature and the silylation reagent. The results will be discussed in the chapter 3.4.5.

using HOBt (10 eq.), HBTU (10 eq.) and DIPEA (10 eq.) in NMP for coupling of the single amino acids at the peptide synthesizer (Scheme 61). For manual coupling only 5 equivalents of the reagents were used. Thereby, Fmoc deprotection was achieved with piperidine (20% in DMF (v/v)).

For the Staudinger reaction in solution, azido peptides **7e** and **g** were synthesized on a preloaded Wang resin, and cleavage and deprotection was achieved simultaneously using a TFA cleavage cocktail (95% TFA, 2.5% TIS, 2.5% H₂O) (Scheme 61, left). Azido glycine (**7h**) or α -azidoisobutyric acid (**7i**) were coupled manually using 5 equivalents of the acid and the coupling reagents. The obtained azido peptides **7e** and **g** were purified by HPLC prior to the Staudinger reaction.

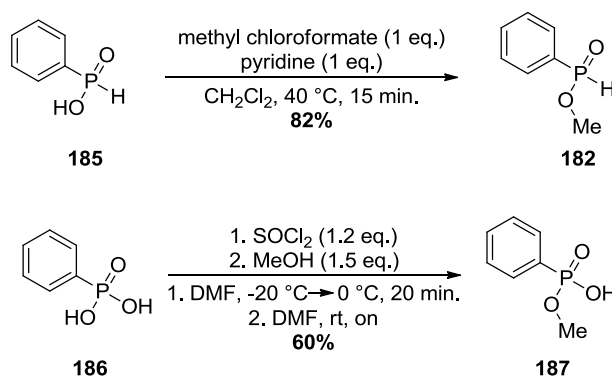


Scheme 61: Solid-phase peptide synthesis of azido peptides **7c-g** for the Staudinger reaction on solid support and in solution.

Since phosphoramidates **183**, especially if they are derived from alkyl azides, are not stable under strong acidic conditions (see chapter 3.5), resins that require treatment with

trifluoroacetic acid for peptide cleavage from the linker are not suitable for the envisioned synthesis on solid support. Therefore, a NovaSyn® TG resin derivatized with Sheppard's base-labile 4-hydroxy-methylbenzoic acid linker was used (Scheme 61, right). This enables global deprotection of the side chains prior to the Staudinger reaction without cleaving the peptide from the resin. The standard TFA cleavage cocktail was used for the on-resin deprotection (95% TFA, 2.5% TIS, 2.5% H₂O). The solid-supported, unprotected azido peptides **7c**, **d** and **f** could then be reacted with the silyl phosphonite. The final phosphoramidate peptides **183c**, **d** and **f** could afterwards be cleaved from the resin with a sodium hydroxide solution (1 M in H₂O/1,4-dioxane, 1:3).

3.4.2.3 Synthesis of methyl phenylphosphinate and monomethyl phenylphosphonate



Scheme 62: Synthesis of methyl phenylphosphinate (**182**) and monomethyl phenylphosphonate (**187**).

The methyl phenylphosphinate (**182**) was synthesized from phenylphosphinic acid (**185**) by the Hewitt reaction developed by D. G. Hewitt in 1979 (Scheme 62).^[146] Methyl chloroformate and pyridine as a base were added successively to a solution of the phosphinic acid **185** in dichloromethane. The reaction proceeded fast and delivered the desired phosphinate **182** in high yield and high purity. For these reasons, the Hewitt reaction is preferable to alternative esterification reactions. Mechanistically, first a mixed anhydride is formed which then decomposes and forms the desired ester under release of carbon dioxide.

Monomethyl phenylphosphonate (**187**), a standard for the stability studies, could be obtained by a typical procedure from phenylphosphonate (**186**) (Scheme 62). The phosphonate **186** was transferred to the chloridate by addition of thionyl chloride. Substitution with methanol delivered the monoester **187** in a moderate yield.^[147]

3.4.3 Analysis of the product mixtures and products

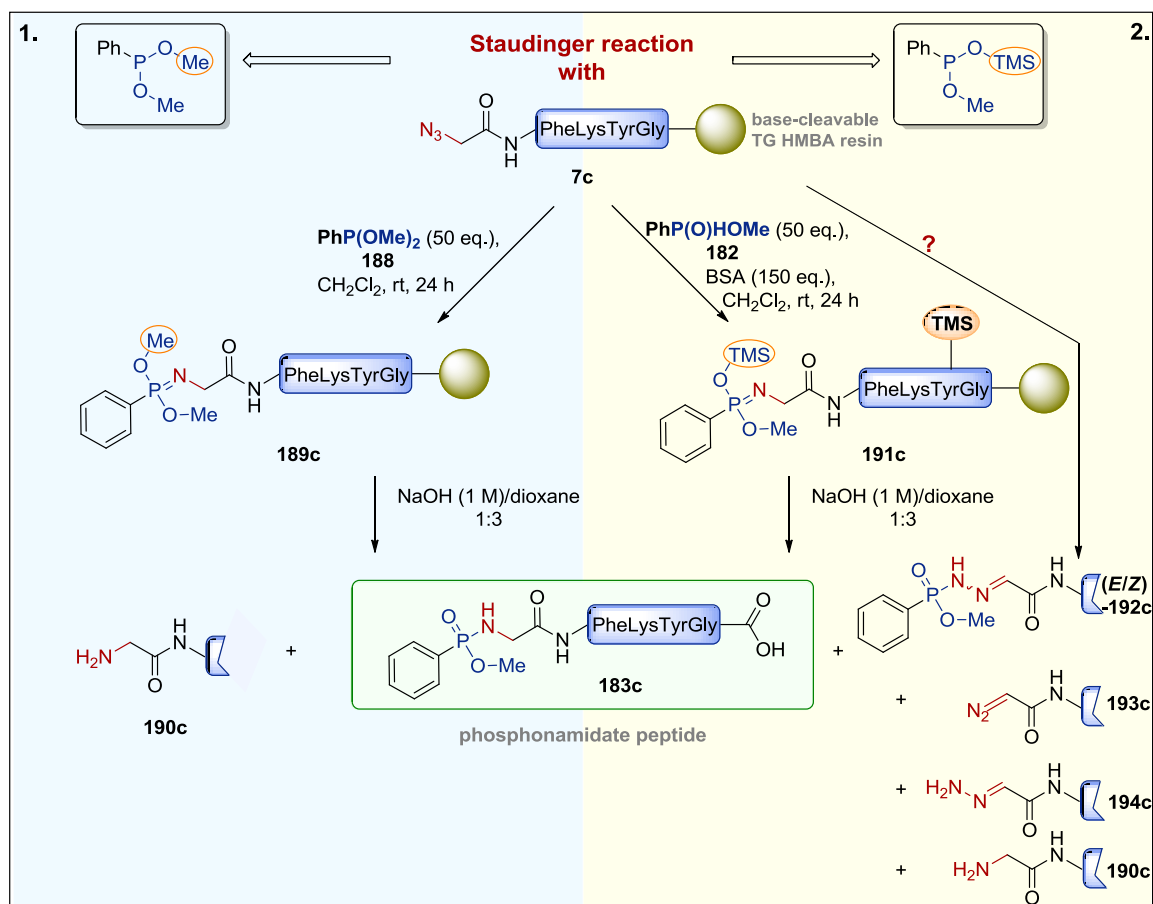
All compounds were analyzed by LC-MS and HRMS. In case of the small molecules the UV-signals of the phosphoramidates **183a** and **b** and the by-products **192a** and **b** in the UV-trace at 226 nm of the LC-MS spectra were integrated, and ratios were calculated based on a measured calibration curve. The ratios of the peptidic systems were determined by integration of the UV-trace at 280 nm. As reported in the previous communication,^[7] integrals at 280 nm are not significantly influenced by the N-terminal phosphoramidate moiety, which justifies the results.

Small molecules were additionally analyzed by one- and two-dimensional NMR spectroscopy i.e. ¹H-NMR, ¹³C-NMR, ³¹P-NMR, ¹⁵N-NMR, H,H-COSY, HMQC and HMBC. Some of the by-products e.g. **195** could not be quantified by LC-MS, and TBAF-containing reaction mixtures could not directly be injected to the HPLC. Thus, ³¹P-NMR spectra of the crude reaction mixtures were used to support and complete the obtained results. It has to be noted that integration of the ³¹P-NMR signals is not as precise as integration of the ¹H-NMR signals due to the relaxations times of the compounds and decoupling of the signals. However, the phosphorus in the compounds compared within this study is chemically and magnetically very similar making the results significant. Only in case of different silylation reagents all signals were integrated to determine the conversion of the starting material. Ratios obtained were in good agreement with the data received by integration of the UV-trace of the measured LC-MS spectra.

3.4.4 Comparison of methyl (trimethylsilyl) phenylphosphonite and dimethyl phenylphosphonite in the Staudinger reaction with an azido glycine peptide

Encouraged by the previously obtained results with peptides containing *para*-azidobenzoic acid at the N-terminus,^[7] the azido glycine peptide **7c** was transformed with methyl phenylphosphinate (**182**) and BSA on solid support to get the corresponding phosphoramidate peptide **183c** (Scheme 63). But when the peptide **7c**, containing azido-glycine **7h** at the N-terminus, was applied in the Staudinger reaction, besides the expected phosphoramidate peptide **183c**, a significant or even dominating amount of a side product with a mass of +13 m/z appeared with a very similar retention time during HPLC measurement (Figure 11). The ratio will be further discussed in chapter 3.4.6. The detected mass of +13 m/z could be explained by the structure (*E/Z*)-**192c** (Scheme 63, 2.). Peptides with a diazo- and a hydrazone-moiety at the N-terminus were also found (compounds **193c** and **194c**), and they accounted for 22% in

comparison to compounds **183c** and (*E/Z*)-**192c**. The compounds **193c** and **194c** could result from the decomposition of (*E/Z*)-**192c** by P-N bond cleavage or from the phosphazide, the first intermediate of the Staudinger reaction arising from the nucleophilic attack of the trivalent phosphorus at the azide. The by-products (*E/Z*)-**192c**, **193c** and **194c** containing two nitrogen atoms show that elimination of molecular nitrogen seems to be hampered in the reaction with silylated phosphinic acids and that an alternative reaction pathway exists. The amino peptide **190c**, which was always observed as a side product in the reaction with aryl azides and which emanates from unspecific hydrolysis of the imidate, could only be detected in traces.



Scheme 63: Staudinger reaction of an azido glycine peptide **7c** with 1. dimethyl phenylphosphonite (**188**) and 2. methyl phenylphosphinate (**182**) and BSA and detected products (**183c**, **190c**, (*E/Z*)-**192c**, **193c** and **194c**). In case of dimethyl phenylphosphonite (**188**) the phosphonamidate peptide **183c** was the major product, and only small amounts of the corresponding amino peptide **190c** were generated resulting from unselective hydrolysis. In contrast, for methyl phenylphosphinate (**182**) and BSA compounds (*E/Z*)-**192c**, **193c** and **194c** were predominantly formed, and only tiny quantities of the desired phosphonamidate peptide **183c** could be found.

In contrast, when dimethyl phenylphosphonite (**188**) was used in the Staudinger reaction, primarily the desired phosphonamidate peptide **183c** (86%) was generated together with minor amounts of the amino peptide **190c** (Scheme 63, 1.; Figure 11).^[6b] The by-product **192c** was not

found. This observation led to the assumption that the silyl group may have a major impact on the reaction mechanism and is responsible for the formation of the observed by-products. This unexpected reaction process requested a more extensive investigation. Preliminary results on the reaction mechanism and by-product formation are summarized in chapters 3.4.5 and 3.4.6.

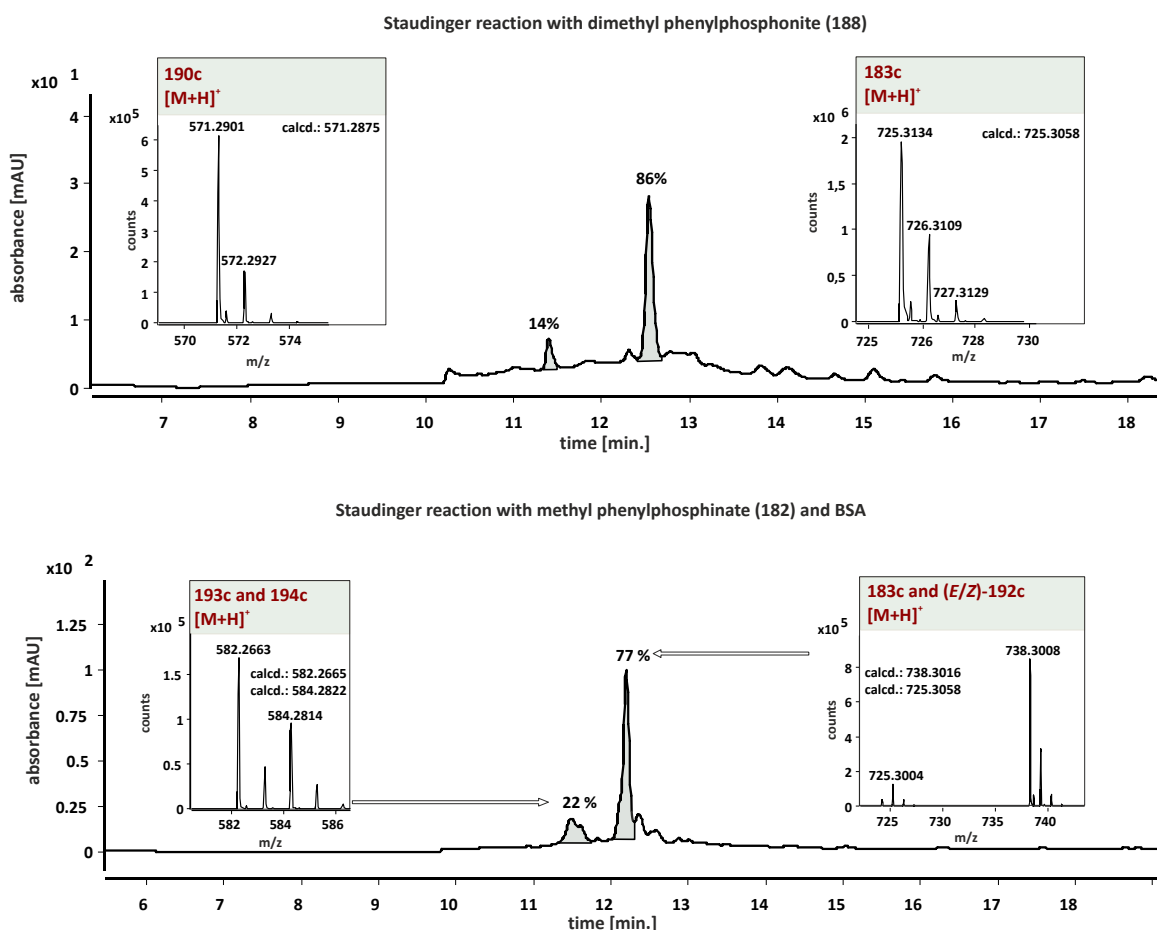


Figure 11: LC-MS spectra of both reactions illustrated in Scheme 63: Comparison of the Staudinger reaction of azido glycine peptide **7c** with dimethyl phenylphosphonite (**188**) and methyl phenylphosphinate (**182**) with BSA.

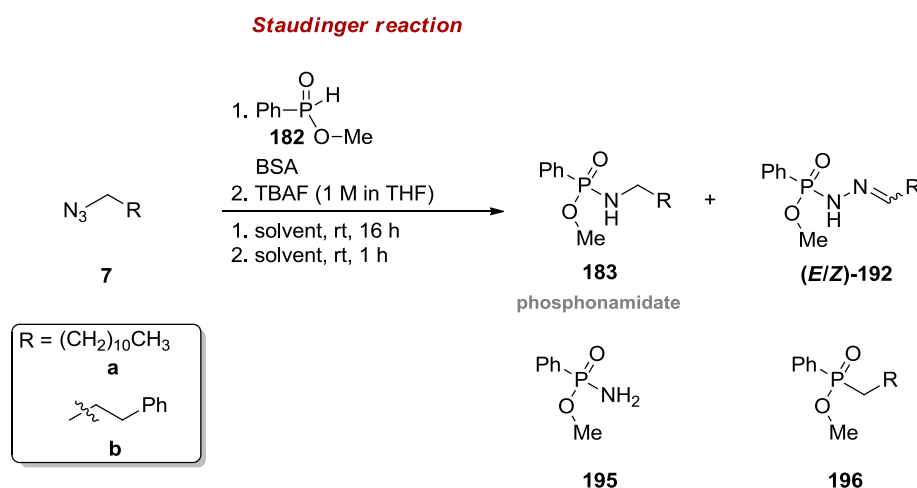
3.4.5 Staudinger reaction of methyl (trimethylsilyl) phenylphosphonite with small alkyl azides

The peptidic products of the Staudinger reaction described in chapter 3.4.4 could only be analyzed by HRMS and HPLC, which validates their molecular formulae, yet more spectroscopic data were necessary to prove their exact structure. For this reason, two alkyl azides were chosen to gain additional information by NMR spectroscopy and labeling experiments. Dodecyl azide (**7a**) and 3-phenylpropyl azide (**7b**) were selected as model substrates in the first instance. Neither azides contain any functional groups or electronic specifics that can influence the

reaction and its mechanism. Moreover, both azides and their expected products after the Staudinger reaction can be easily analyzed by NMR and LC-MS.

In addition to the structural and mechanistic information, the influence of the following reaction conditions was investigated: silylation reagents, solvents, temperature and equivalents of the reagents.

In all performed experiments, methyl phenylphosphinate (**182**) was added to a solution of the azide **7a** or **b** in the appropriate solvent followed by the silylation reagent (Scheme 64). Due to the susceptibility of the formed silyl phosphonite to oxygen and water, all reactions were performed under argon atmosphere and in anhydrous solvents. The reaction mixtures were stirred overnight, and TBAF (1 M in THF) was added to remove the silyl group. ³¹P-NMR spectra were measured of the crude reaction mixtures to get a first idea of the formed products and their ratios. Afterwards TBAF was removed by filtration over silica gel, and the product mixtures were further analyzed by LC-MS. Pure products were obtained by HPLC purification.



Scheme 64: Staudinger reaction of dodecyl azide (**7a**) or 3-phenylpropyl azide (**7b**) with methyl phenylphosphinate (**182**) and BSA.

Comparison of the ³¹P-NMR spectra of the crude reaction mixtures revealed always the same four signals after the Staudinger reaction and treatment of the reaction mixtures with TBAF (Figure 12-17). Only an excess of methyl phenylphosphinate (**182**) gave additional signals between 35.00 and 46.00 ppm. Exemplary five different ³¹P-NMR spectra and applied reaction conditions are shown below (Table VII):

Table VII: Ratios of compounds **183**, (**E/Z**)-**192**, **195** and **196** determined by integration of the ³¹P-NMR spectra after the Staudinger reaction and treatment with TBAF.

reaction conditions	azide	182 (eq.)	BSA (eq.)	solvent	products				
					196	195	183	(Z)-192	(E)-192
a)	7b	1	3	CH ₂ Cl ₂	-	23%	58%	3%	16%
b)	7b	1	3	CH ₃ CN	-	32%	43%	5%	20%
c)	7b	6	18	CH ₃ CN	9%	27%	38%	5%	21%
d)	7a	1	3	CH ₃ CN	1%	40%	29%	5%	25%
e)	7a	6	18	CH ₃ CN	2%	31%	26%	6%	22%

Reaction conditions: 1. **7a** or **7b**, PhP(O)HOMe (**182**), BSA, rt, 16 h; 2. TBAF (1 M in THF), rt, 1 h. The signals were assigned based on the results discussed in chapters 3.4.5.1 and 3.4.5.2. The signal of compounds **195** and **196** were assigned by comparison with literature data and synthesized standards.^[116,148]

The NMR spectra illustrate that in contrast to the reactions with aryl azides the use of alkyl azides leads to several by-products in considerable amounts (42-74%), which cannot be explained by the known mechanism of the Staudinger reaction. The proposed structures are displayed in Scheme 64 (compounds (**E/Z**)-**192**, **195** and **196**). The by-product (**E/Z**)-**192** was already observed with the azido peptide **7c** in the LC-MS spectrum and accounts for 19-30% of the phosphorus compounds in the reactions with azides **7a** and **b**. Due to the double bond, the by-product (**E/Z**)-**192** exists as an *E*- and a *Z*-isomer, and the ratio of the *E*-isomer (**E**)-**192** and the *Z*-isomer (**Z**)-**192** was always approximately 4:1. The data show that the conversion to the desired phosphoramidate **183** was in all cases higher when 3-phenylpropyl azide (**7b**) was applied in the reaction (38-58%) whereas with dodecyl azide (**7a**) the corresponding phosphoramidate **183a** was only formed in less than 30%. Moreover, the solvent seems to have a considerable influence on the reaction as the conversion towards **183b** declined by 26% if dichloromethane was exchanged for acetonitrile (Table VII: conditions a and b). The amount of **195** and (**E/Z**)-**192**, however, rose to nearly the same extent when the solvent polarity was increased. The ratio between the phosphoramidate **195** with a signal at 25-26 ppm and the by-product (**E/Z**)-**192** remained almost constant. The impact of the solvent polarity will be discussed in more detail in chapter 3.4.5.4. Another important factor is the ratio of the azide **7** to the phosphinate **182**. If the methyl phenylphosphinate (**182**) was added to the reaction mixture in excess (Table VII: c and e) an additional by-product **196** was formed in 9% and 2%, respectively, which was not formed or only to a very low amount (<1%) if just one equivalent of phosphinate **182** was used. The signal at 35.19 ppm (reaction conditions e) could not be clarified so far. The origin of compounds **192**, **195** and **196** will be explained later in chapter 3.4.5.3.

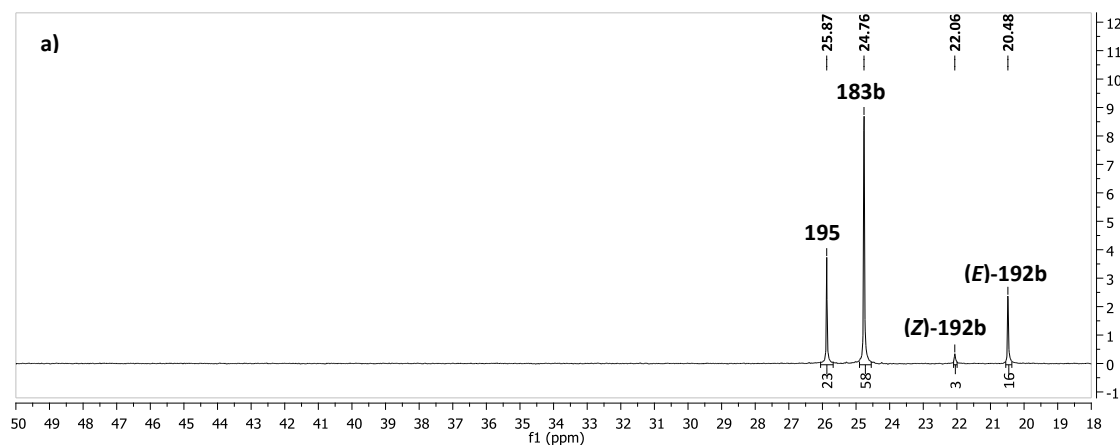


Figure 12: ^{31}P -NMR spectrum (162 MHz) of the crude reaction mixture of the Staudinger reaction between 3-phenylpropyl azide (**7b**) and methyl phenylphosphinate (**182**). Reaction conditions a): 1. **7b** (1 eq.), PhP(O)HOMe (**182**) (1 eq.), BSA (3 eq.), CH_2Cl_2 , rt, 16 h; 2. TBAF (1 M in THF, 3 eq.), CH_2Cl_2 , rt, 1 h.

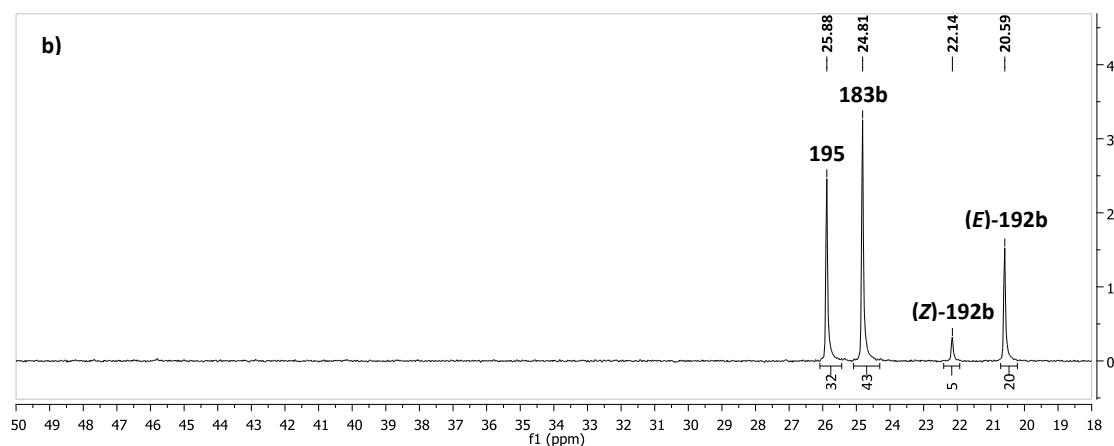


Figure 13: ^{31}P -NMR spectrum (162 MHz) of the crude reaction mixture of the Staudinger reaction between 3-phenylpropyl azide (**7b**) and methyl phenylphosphinate (**182**). Reaction conditions b): 1. **7b** (1 eq.), PhP(O)HOMe (**182**) (1 eq.), BSA (3 eq.), CH_3CN , rt, 16 h; 2. TBAF (1 M in THF, 3 eq.), CH_3CN , rt, 1 h.

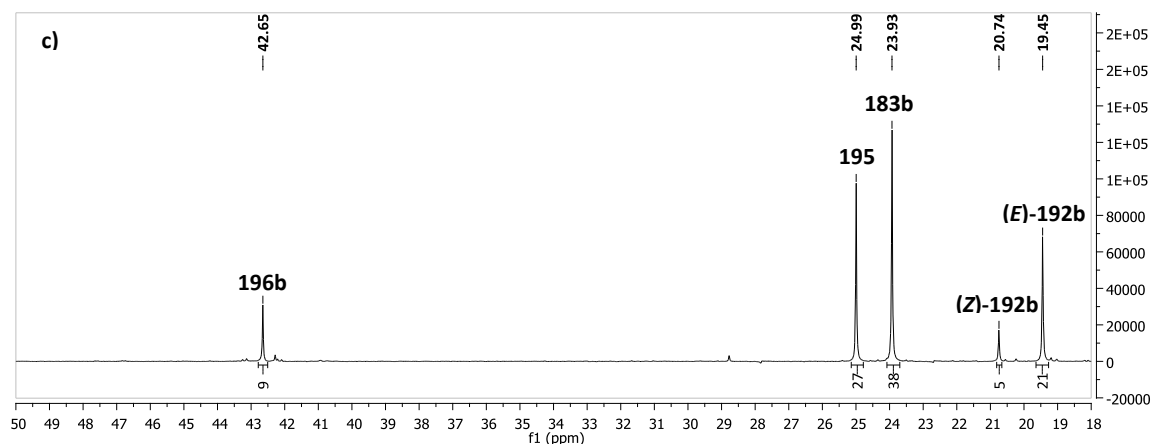


Figure 14: ^{31}P -NMR spectrum (162 MHz) of the crude reaction mixture of the Staudinger reaction between 3-phenylpropyl azide (**7b**) and methyl phenylphosphinate (**182**). Reaction conditions c): 1. **7b** (1 eq.), PhP(O)HOMe (**182**) (6 eq.), BSA (18 eq.), CH_3CN , rt, 16 h; 2. TBAF (1 M in THF, 18 eq.), CH_3CN , rt, 1 h.

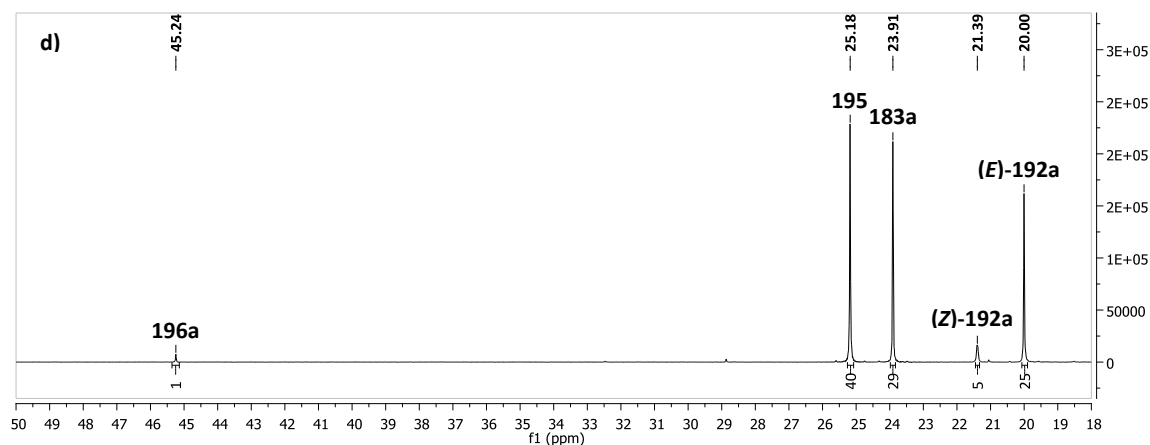


Figure 15: ^{31}P -NMR spectrum (162 MHz) of the crude reaction mixture of the Staudinger reaction between dodecyl azide (**7a**) and methyl phenylphosphinate (**182**). Reaction conditions d): 1. **7a** (1 eq.), $\text{PhP}(\text{O})\text{HOME}$ (**182**) (1 eq.), BSA (3 eq.), CH_3CN , rt, 16 h; 2. TBAF (1 M in THF, 3 eq.), CH_3CN , rt, 1 h.

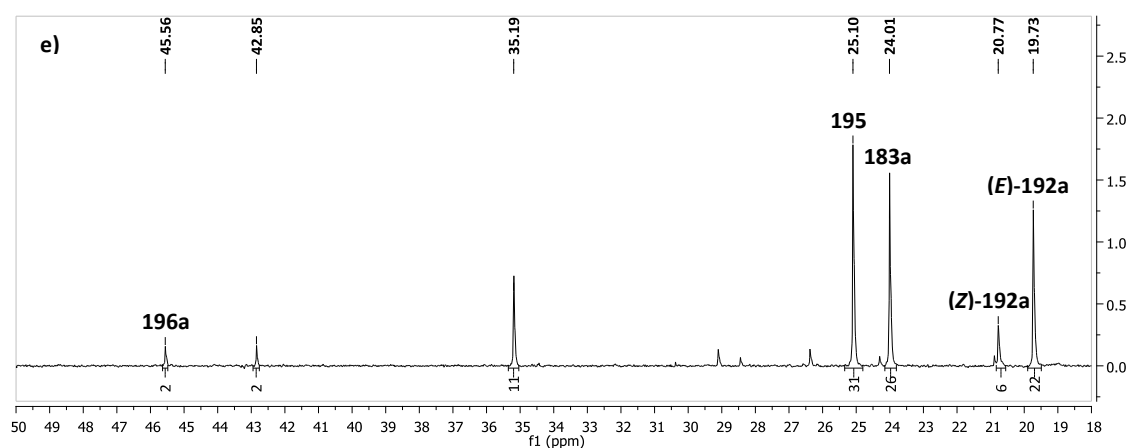
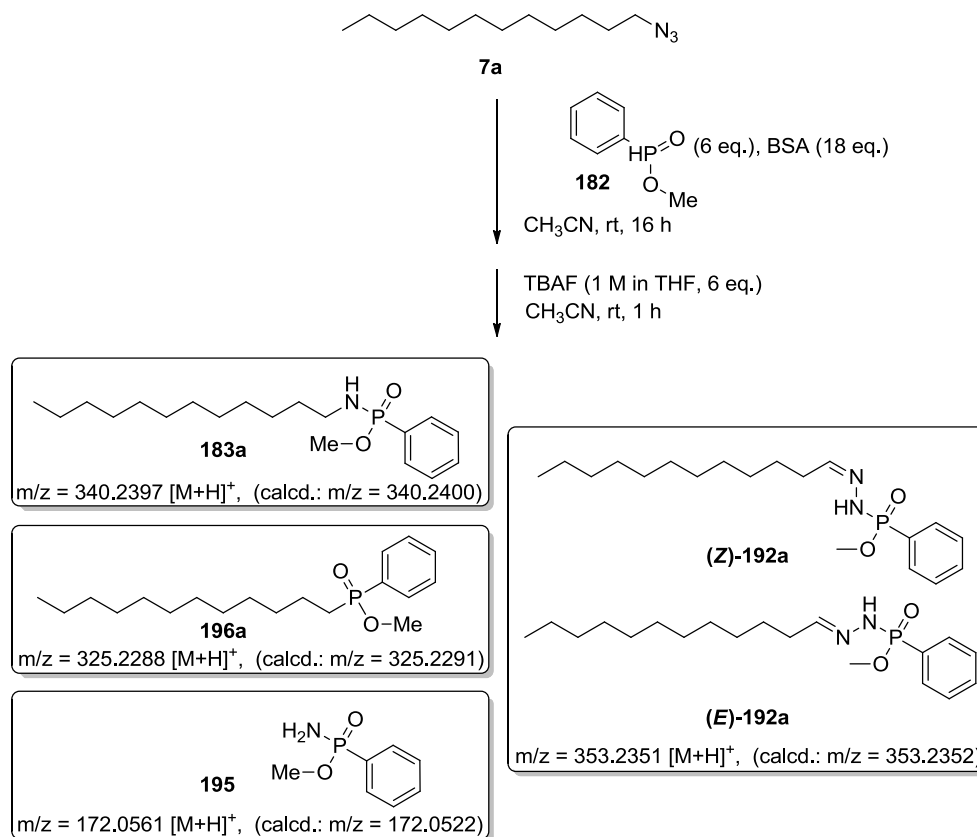


Figure 16: ^{31}P -NMR spectrum (162 MHz) of the crude reaction mixture of the Staudinger reaction between dodecyl azide (**7a**) and methyl phenylphosphinate (**182**). Reaction conditions e): 1. **7a** (1 eq.), $\text{PhP}(\text{O})\text{HOME}$ (**182**) (6 eq.), BSA (18 eq.), CH_3CN , rt, 16 h; 2. TBAF (1 M in THF, 18 eq.), CH_3CN , rt, 1 h.

3.4.5.1 More detailed examination of the Staudinger reaction with dodecyl azide

To gain more information about the structure and origin of the observed side product (**E/Z**)-**192a**, the test reaction with dodecyl azide (**7a**), 6 equivalents methyl phenylphosphinate (**182**) and 18 equivalents BSA in acetonitrile (conditions e) was further analyzed by NMR spectroscopy and HRMS (Scheme 65). Apart from the desired phosphoramidate **183a**, the side products (**E**)-**192a** and (**Z**)-**192a** with a mass of 353.2351 m/z could be detected in the HRMS spectra but to a much lower extent than with the azido glycine peptide **7c**. Moreover, the compound **196a** with a mass of 325.2288 m/z appeared as well as a compound with a mass of 172.0561 m/z, which argues for the formation of methyl *P*-phenylphosphoramidate (**195**). The structures and high resolution masses of the obtained compounds are given in Scheme 65. The four detected

products in the HRMS spectrum were assigned to the four signals in the ^{31}P -NMR spectra (Figure 16) based on our own (chapter 3.4.5.2) as well as reported interpretations.^[116, 148]



Scheme 65: Test reaction with dodecyl azide (**7a**) and detected products.

The four by-products could not be separated effectively from the phosphoramidate **183a** by column chromatography, but initial NMR spectra of a fraction enriched with the side products **(E)-192a** and **(Z)-192a** supported the structures presented in Figure 17.

The ^1H -NMR spectrum shows two triplets at 6.54 ppm and 7.16 ppm at a ratio of 1:4. The signals can be explained by the proposed structures for the side products **(E)-192a** and **(Z)-192a** depicted in Figure 17, because the chemical shifts and multiplet structures match a CH-group in the compound next to the nitrogen. The two signals with a ratio of 1:4 can be attributed to the Z- and a E-isomer of the double bond, whereby the thermodynamically more stable E-isomer is formed in higher amounts. This matches the two signals in the ^{31}P -NMR spectrum at 20.77 ppm and 19.73 ppm at a ratio of ~1:4.

Two-dimensional NMR experiments further proved that the protons with the shifts of 7.16 and 6.54 ppm are connected to carbon atoms with shifts of 148.5 and 147.8 ppm that are typical for a $-\text{CH}=\text{N}$ -group. Moreover, the HMBC and the H,H-COSY spectra ascertained their location next

to the methylene-group of the alkyl chain with a shift of 32.1 ppm (*E*-isomer) and 25.8 ppm (*Z*-isomer) for the carbons and 2.18 ppm (*E*-isomer) and 2.10 ppm (*Z*-isomer) for the protons.

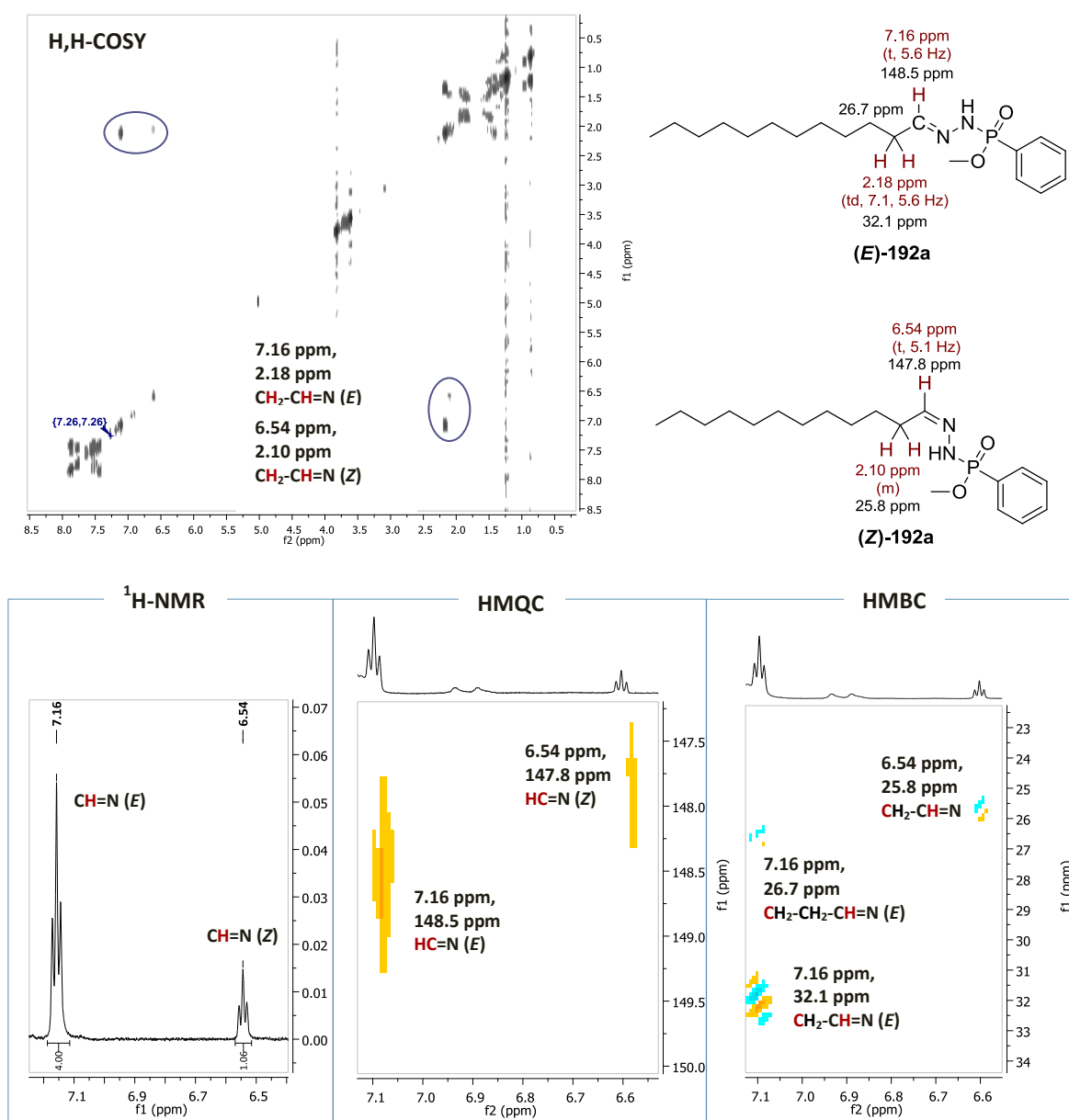
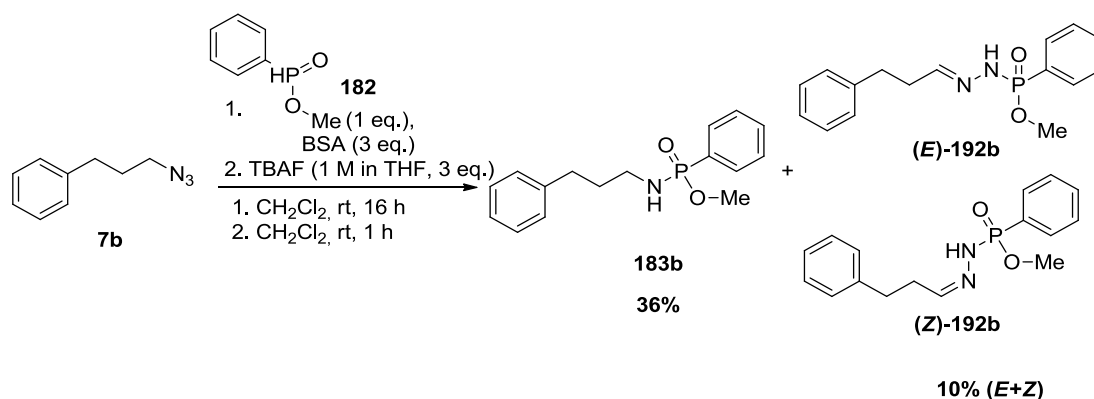


Figure 17: $^1\text{H-NMR}$, H,H-COSY , HMQC and HMBC spectra details of (*E/Z*)-192a.

All three compounds **183a**, (*E*)-192a and (*Z*)-192a could be detected in the LC-MS spectrum with a similar retention time. Since the dodecyl derivatives could not be separated by column chromatography and did not give sufficient signals in the UV-trace, separation was not possible. Therefore, 3-phenylpropyl azide (**7b**) was employed in the continuation of the investigation. The products of this reaction can be separated by HPLC and have only three methylene groups, which make substance assignment and integration by NMR spectra much easier and more precise.

3.4.5.2 Isolation and structural analysis of products derived from the Staudinger reaction with 3-phenylpropyl azide

The Staudinger reaction was performed with 3-phenylpropyl azide (**7b**) and one equivalent of methyl phenylphosphinate (**182**) as a starting point because the previous results confirmed that in the reaction with an excess of phosphinate **182** additional by-products are formed (Scheme 66). The obtained products were pre-purified by column chromatography to remove the TBAF. The pre-purified product mixture was separated by HPLC to yield the pure compounds **183b** and (*E/Z*)-**192b** for NMR analysis. After HPLC purification the phosphonamidate **183b** was only obtained in a yield of 36%, the side products (*E/Z*)-**192b** in a yield of 10%. These results reflect their ratio of occurrence determined by the ³¹P-NMR (ratio 4:1, Figure 12) of the crude reaction mixture after addition of TBAF but also indicate that substantial quantities were probably lost during the purification process.



Scheme 66: Reaction of 3-phenylpropyl azide (**7b**) with methyl phenylphosphinate (**182**) and BSA.

The ¹H-NMR spectrum of (*E/Z*)-**192b** confirmed that the signal for the third CH₂-group at 1.70 ppm is missing and that the aromatic protons integrate to six instead of five protons (Figure 18). This is in agreement with results from chapter 3.4.5.1 where the proton signal of the –CH= group of (*E*)-**192a** is located at 7.16 ppm. Additionally, although the bigger triplet of the –CH= group of (*E*)-**192b** seems to lie in the region of the phenylic protons, the triplet of the *Z*-isomer (*Z*)-**192b** could be identified at 6.55 ppm. This signal was not observed in the ¹H-NMR spectrum of the phosphonamidate **183b**.

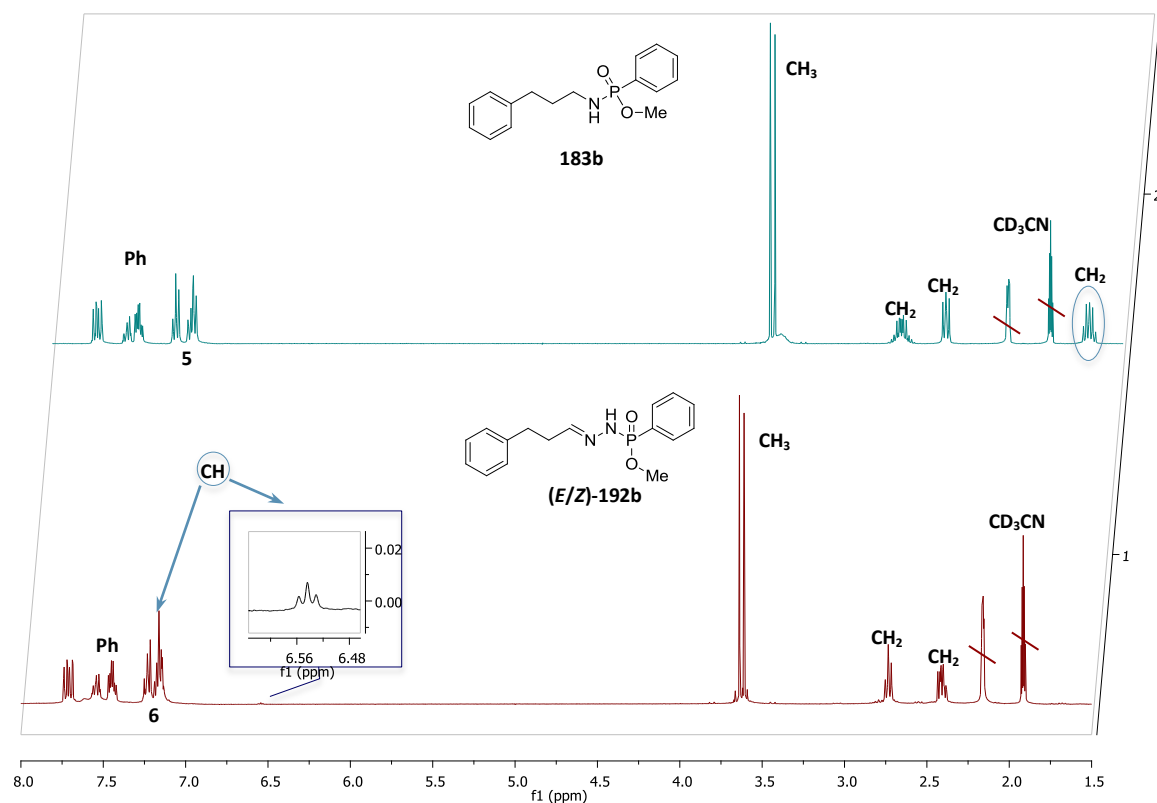


Figure 18: ¹H-NMR spectra of (*E/Z*)-methyl phenyl(2-(3-phenylpropylidene)hydrazinyl)phosphinate (**(E/Z)-192b**) and of the phosphoramidate **183b** (400 MHz, CD₃CN).

More information was obtained by two-dimensional NMR spectroscopy (Figure 19). H,H-COSY and HMBC spectra of (*E/Z*)-methyl phenyl(2-(3-phenylpropylidene)hydrazinyl)phosphinate (**(E/Z)-192b**) provided evidence that the protons of the CH-groups at 7.21 ppm (*E*-isomer) and 6.55 ppm (*Z*-isomer) couple with the neighboring methylene groups at 2.43 ppm (*E*-isomer) and 2.49 ppm (*Z*-isomer) for the protons and 33.2 ppm (*E*-isomer) for the carbon (signal for the *Z*-isomer was too weak). Furthermore, the proton with a shift of 7.21 ppm is located at a carbon with chemical shift of 148.5 ppm (signal for the *Z*-isomer was too weak). These signals again are not present in the NMR spectra of the phosphoramidate **183b**. In conclusion, analysis and comparison of the NMR spectra of the compounds **(E/Z)-192b** with **183b** reveal the absence of the third methylene group as a basic difference whereas the signals of aryl protons and of the methoxy group nearly stay unchanged. Instead of signals representing the third methylene group, other signals appear arguing for a –CH=–group that is located between the alkyl chain and a nitrogen supporting the presented structure of the side product **(E/Z)-192b**. Presence of the additional nitrogen in the molecule is also supported by the ESI-TOF HRMS.

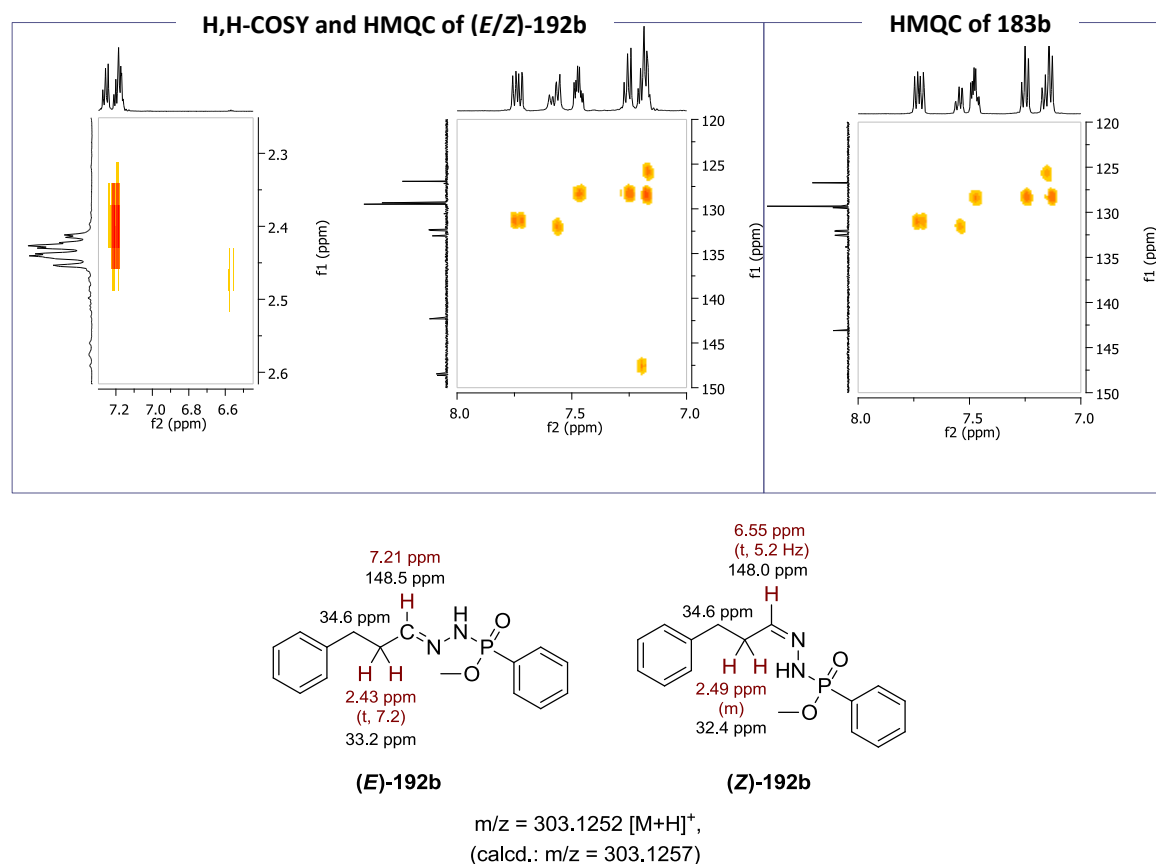
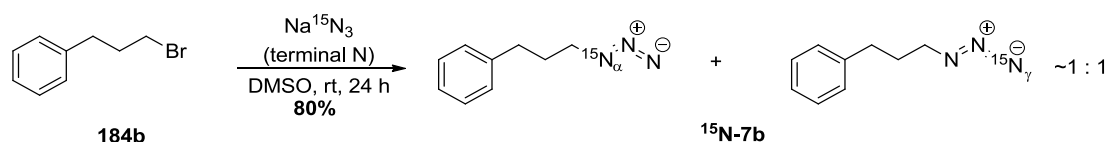


Figure 19: *H,H-COSY and HMQC spectra of (E/Z)-methyl phenyl(2-(3-phenylpropylidene)hydrazinyl)phosphinate ((E/Z)-192b). The spectra show the coupling of the –CH= with the neighboring methylene group and the additional cross signal at 148.5 ppm (left). In contrast, the HMQC spectrum of the phosphonamidate 183b does not show the signal at 148.5 ppm (right).*

3.4.5.3 Mechanistic investigation by ^{15}N -labeling of 3-phenylpropyl azide

In order to gain additional information about the reaction mechanism related to the observed (E/Z)-methyl phenyl(2-(3-phenylpropylidene)hydrazinyl)phosphinate ((E/Z)-192b), ^{15}N -labeling experiments were performed. Introduction of nitrogen-15 (^{15}N) into the azido-moiety in the α - and γ -position was achieved by nucleophilic substitution with ^{15}N -labeled sodium azide starting from the alkyl bromide **184b** (Scheme 67).



Scheme 67: *Synthesis of ^{15}N -labeled 3-phenylpropyl azide (^{15}N -7b).*

The reaction delivered the desired azide ^{15}N -7b as a mixture of regioisomers in a statistical ratio of approximately 1:1 as both terminal nitrogen of the azide can attack the bromide **184b**.

Incorporation of ^{15}N into the azide $^{15}\text{N-7b}$ was confirmed by ^{15}N -NMR showing a singlet at -173.67 ppm for the terminal nitrogen and a multiplet at -312.51 ppm for the nitrogen directly connected to the alkyl chain.

The labeled azide $^{15}\text{N-7b}$ was employed in the Staudinger reaction with methyl phenylphosphinate (**182**) and three equivalents of BSA as silylation reagent (in analogy to Scheme 66). The position of ^{15}N in the products should shed light on mechanistic details with respect to (*E/Z*)-methyl phenyl(2-(3-phenylpropylidene)hydrazinyl)phosphinate (**(*E/Z*)-192b**) formation and should indicate which nitrogen is expelled and which stays in the molecule (Scheme 68). Due to the labeling in two positions (N_α and N_γ) always a mixture of labeled and unlabeled products was expected based on the reaction mechanism.

At first, the reaction was performed in dichloromethane as before and the products were analyzed by LC-MS. Both compounds – the phosphoramidate **183b** and **(*E/Z*)-192b** – showed incorporation of ^{15}N in the isotope pattern (Figure 20). Besides the phosphoramidates $^{15}\text{N-183b}$ and **183b** and the expected side products **(*E/Z*)-192b** and $^{15}\text{N-192b}$, methyl *P*-phenylphosphoramidate (**195** and $^{15}\text{N-195}$) was found, probably arising from the decomposition of the phosphazide. Methyl *P*-phenylphosphoramidate (**195** and $^{15}\text{N-195}$) elutes already after 3-6 min. due to its high polarity and does not give a clear signal in the UV-trace.

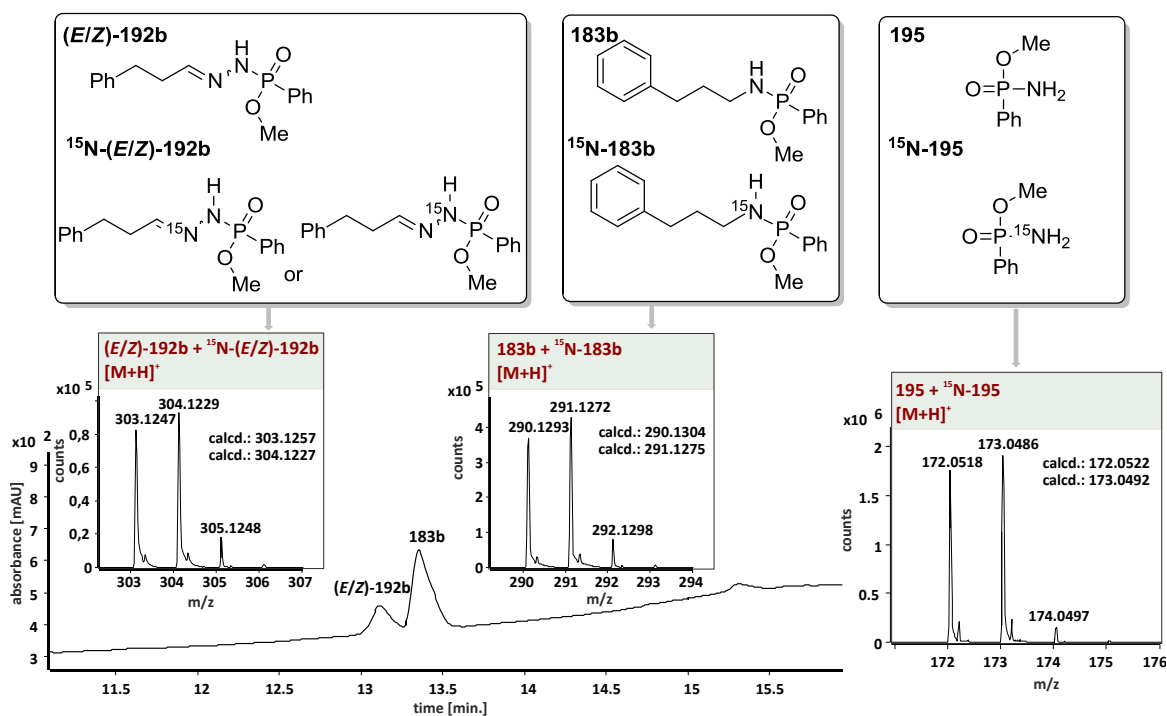


Figure 20: LC-MS spectrum of the Staudinger reaction with ^{15}N -labeled azide $^{15}\text{N-7b}$ and observed labeled products. Reaction conditions: 1. $^{15}\text{N-7b}$ (1 eq.), PhP(O)HOMe (**182**) (1 eq.), BSA (3 eq.), CH_2Cl_2 , rt, 16 h; 2. TBAF (1 M in THF, 3 eq.), CH_2Cl_2 , rt, 1 h.

phosphorus side products without the label. In the ^{15}N -NMR spectrum three main signals were observed. The signals were assigned to the identified masses mentioned above based on the results from the previous chapters and signals in the ^{15}N -NMR spectrum could be attributed to the signals in the ^{31}P -NMR spectrum by analysis of the ^{31}P - ^{15}N coupling constants. Since only 50% of the phosphoramidate **183b** and the (*E/Z*)-methyl phenyl(2-(3-phenylpropylidene)-hydrazinyl)phosphinate (**(E/Z)-192b**) were labeled with ^{15}N , the ^{31}P -NMR gave two signals for each compound: one singlet for the unlabeled compound and one doublet for the labeled one due to the ^{31}P - ^{15}N -coupling. The signals at 24.81 ppm (s) and 24.80 ppm (d, $^1J_{\text{N-P}} = 16.3$ Hz) in the ^{31}P -NMR spectrum and -342.81 ppm (d, $^1J_{\text{N-P}} = 16.3$ Hz) in the ^{15}N -NMR spectrum were attributed to methyl *P*-phenylphosphoramidate (**195** and ^{15}N -**195**); the signals at 23.89 ppm (s) and 23.88 ppm (d, $^1J_{\text{N-P}} = 17.9$ Hz) in the ^{31}P -NMR spectrum and -335.13 ppm (d, $^1J_{\text{N-P}} = 17.9$ Hz) in the ^{15}N -NMR spectrum to the phosphoramidates **183b** and ^{15}N -**183b**. The signals at 19.69 ppm and 19.68 ppm ($^2J_{\text{N-P}} = 14.4$ Hz) and -60.19 ppm (d, $^2J_{\text{N-P}} = 14.3$ Hz) in the ^{15}N -NMR spectrum were assumed to belong to (*E*)-**192b** and ^{15}N -(*E*)-**192b**. Additionally, in the ^{31}P -NMR a weak signals at 20.83 ppm (s) and 20.83 ppm (d, $^2J_{\text{N-P}} = 16.3$ Hz) represents the *Z*-isomers (*Z*)-**192b** and ^{15}N -(*Z*)-**192b**, but the quantity was too low to be observed in the ^{15}N -NMR spectrum despite extended measuring time. The isomers were obtained in a one to four ratio (*Z*:*E*) as before. Furthermore, the phosphoramidates **183b** and ^{15}N -**183b** and $^{14/15}\text{N}$ -(*E/Z*)-methyl phenyl(2-(3-phenylpropylidene)hydrazinyl)phosphinate (**(E/Z)-192b** and ^{15}N -(*E/Z*)-**192b**) were separated by HPLC and again analyzed by NMR spectroscopy confirming assignment of the signals and allowing analysis of the $^1J_{\text{N-H}}$ -coupling constants (see Figure 22, Figure 23 and Table VIII).

Table VIII: NMR signals for all detected ^{15}N -labeled compounds after the Staudinger reaction. Reaction conditions: 1. ^{15}N -**7b** (1 eq.), PhP(O)HOMe (**182**) (1 eq.), BSA (3 eq.), CH_3CN , rt, 16 h, 2. TBAF (1 M in THF, 3 eq.), CH_3CN , rt, 1 h.

compound	^{31}P -NMR	^{15}N -NMR
^{15}N - 183b ^a	23.88 ppm ($^1J_{\text{N-P}} = 18.0$ Hz)	-334.64 ppm ($^1J_{\text{N-P}}$, 18.1 Hz, $^1J_{\text{N-H}}$ 83.4 Hz)
^{15}N -(<i>E/Z</i>)- 192b ^a	20.22 ($^2J_{\text{N-P}} = 15.6$ Hz) (<i>Z</i> -isomer), 19.15 ($^2J_{\text{N-P}} = 13.1$ Hz) (<i>E</i> -isomer)	– -64.22 (d, $^2J_{\text{N-P}} = 13.1$ Hz) (<i>E</i> -isomer)
^{15}N - 195 ^b	24.80 ppm ($^1J_{\text{N-P}} = 16.3$ Hz)	-342.81 ($^1J_{\text{N-P}} = 16.4$ Hz)

^a NMR data of the purified compounds (^{31}P -NMR, 162 MHz, CD_3CN ; ^{15}N -NMR, 41 MHz, CD_3CN). ^b data obtained from the reaction mixture (^{31}P -NMR, 202 MHz, CD_3CN ; ^{15}N -NMR, 51 MHz, CD_3CN).

In the Staudinger reaction, when nitrogen is released from the four-membered transition state **198b**, a mixture of the labeled product ^{15}N -**183b** – coming from the azide $^{15}\text{N}_\alpha$ -**7b** – and the unlabeled product **183b** – coming from azide $^{15}\text{N}_\gamma$ -**7b** – is expected as can be seen in Scheme 68. Consequently, only one signal was observed for the phosphoramidate in the ^{15}N -NMR spectrum

showing a $^1J_{N,H}$ -coupling to the directly bound hydrogen at -334.64 ppm with a large N-H-coupling constant of 83.4 Hz (Figure 22).

With regard to the (*E*)-methyl phenyl(2-(3-phenylpropylidene)hydrazinyl)phosphinate (^{15}N -(*E*)-**192b**) two possible positions of the ^{15}N were supposed – either next to the alkyl chain or bound to the phosphorus – but only one compound could be detected in the ^{15}N -NMR spectrum (Figure 23). The signal does not show a direct N-H-coupling supporting position N_α (next to alkyl chain) for the ^{15}N leading to the assumption that the nitrogen bound to the phosphorus in the phosphazide is expelled. This assumption is in agreement with the detection of labeled methyl *P*-phenylphosphonamidate ^{15}N -**195** by HRMS, and it gave a first hint that during the reaction mechanism the whole methyl *P*-phenyl-phosphonamidate-moiety is lost prior to formation of the four-membered transition state **198b** that would lead to the release of N_2 .

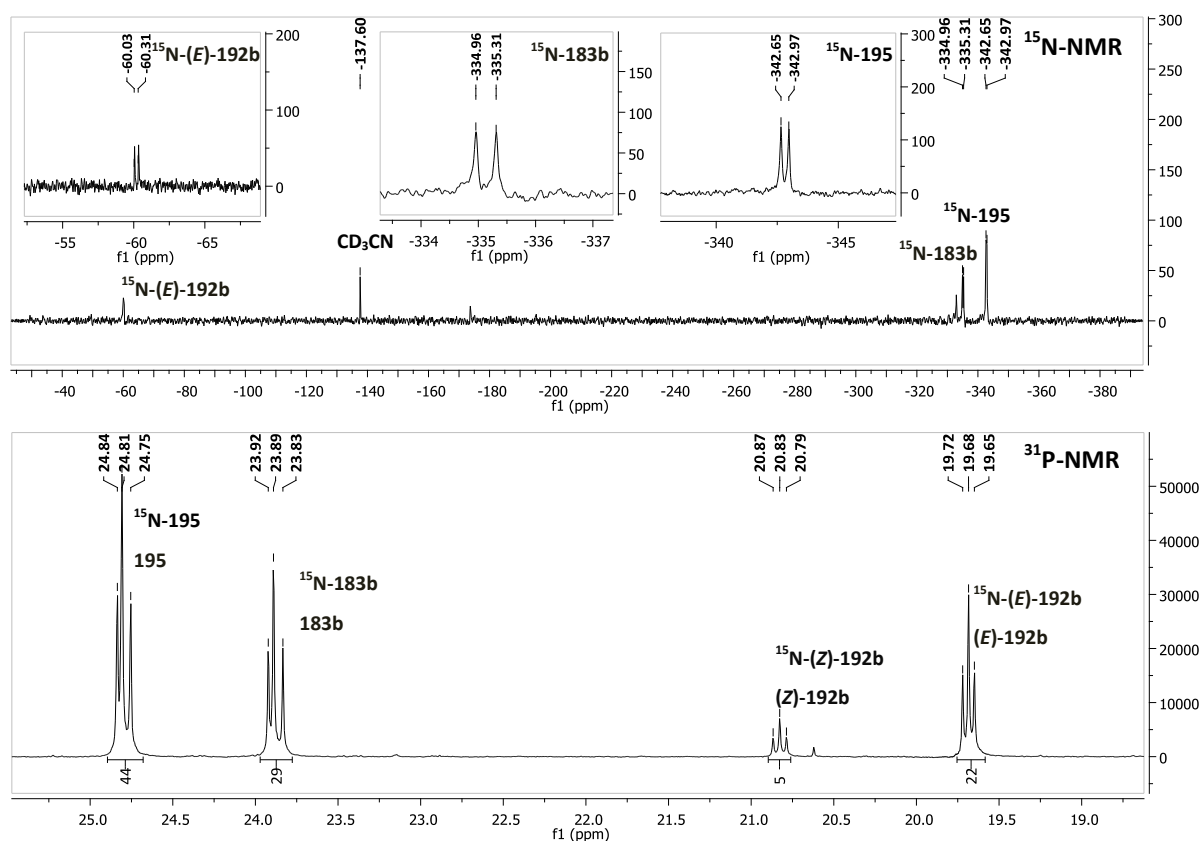


Figure 21: ^{15}N -NMR spectrum (51 MHz, CD_3CN , proton-decoupled) of the crude reaction mixture showing three main signals (above) and corresponding ^{31}P -NMR spectrum (202 MHz, CD_3CN) with the four products after removal of TBAF. Reaction condition: 1. ^{15}N -**7b** (1 eq.), $\text{PhP}(\text{O})\text{HOMe}$ (**182**) (1 eq.), BSA (3 eq.), CH_3CN , rt, 16 h; 2. TBAF (1 M in THF, 3 eq.), CH_3CN , rt, 1 h.

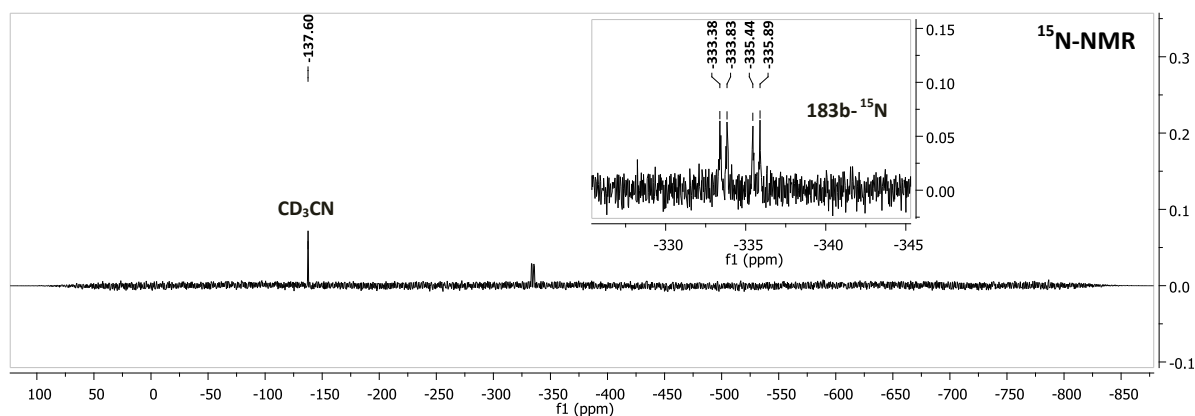


Figure 22: ^{15}N -NMR spectrum (41 MHz, CD_3CN) of the isolated phosphoramidate ^{15}N -**183b**. Reaction condition: 1. ^{15}N -**7b** (1 eq.), PhP(O)HOMe (**182**) (1 eq.), BSA (3 eq.), CH_3CN , rt, 16 h; 2. TBAF (1 M in THF, 3 eq.), CH_3CN , rt, 1 h.

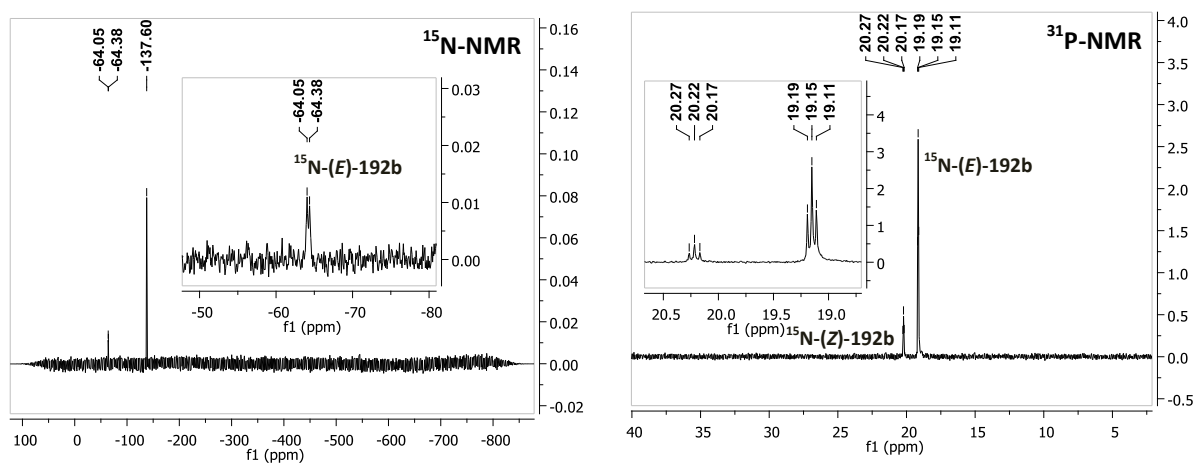
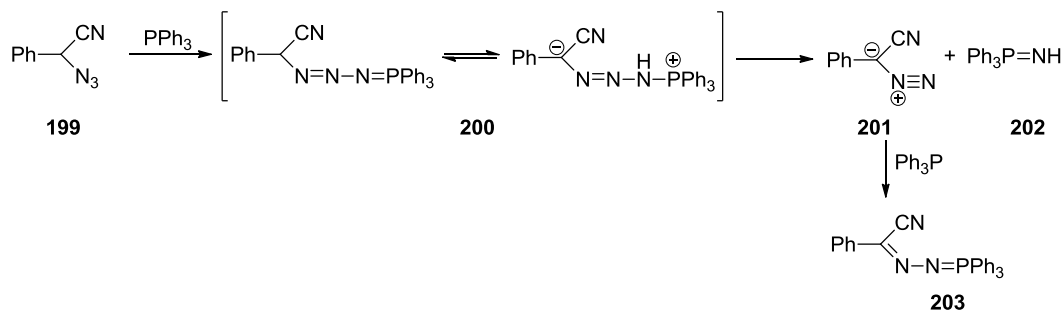


Figure 23: ^{15}N -NMR (41 MHz, CD_3CN) and ^{31}P -NMR (162 MHz, CD_3CN) spectra of the isolated methyl phenyl(2-(3-phenylpropylidene)hydrazinyl)phosphinate ^{15}N -**(E/Z)-192b**. Reaction condition: 1. ^{15}N -**7b** (1 eq.), PhP(O)HOMe (**182**) (1 eq.), BSA (3 eq.), CH_3CN , rt, 16 h; 2. TBAF (1 M in THF, 3 eq.), CH_3CN , rt, 1 h.

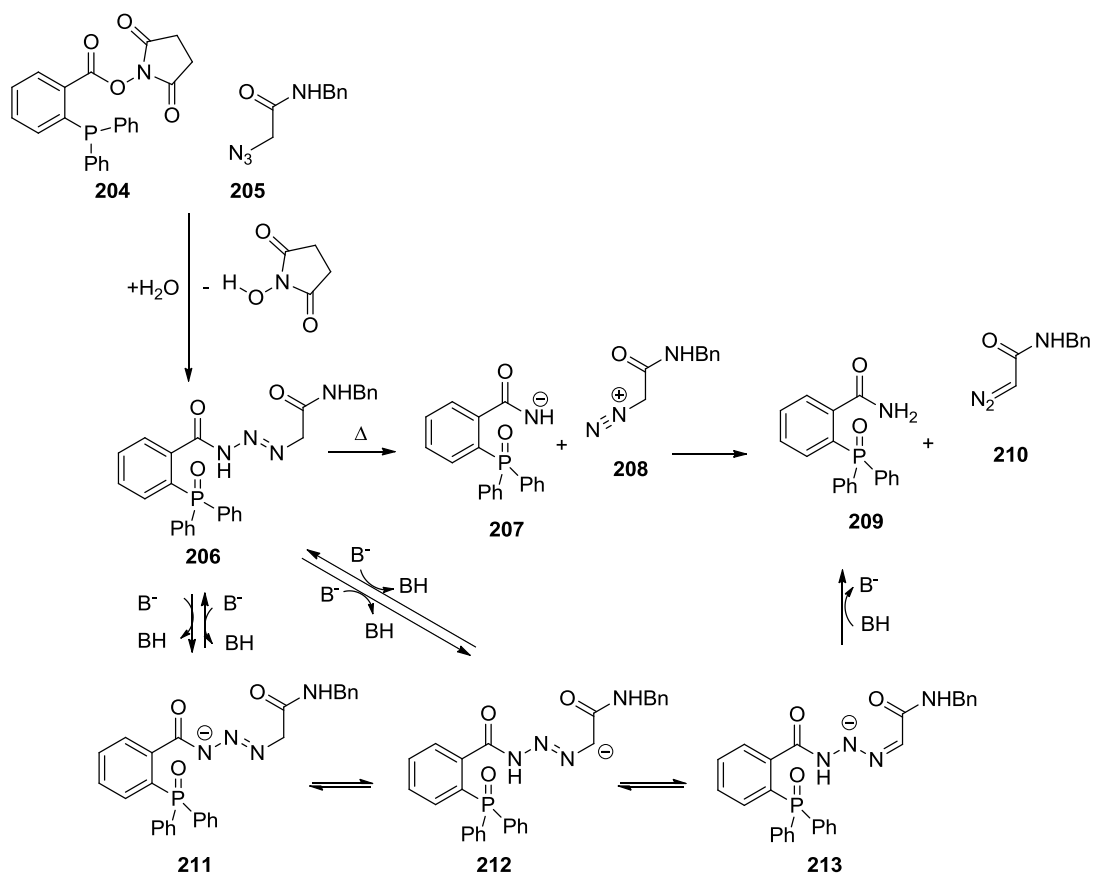
A comparable reaction, starting from a triphenylphosphine and an electron-deficient azide **199**, was previously observed by Molina *et al.* (Scheme 69).^[149]



Scheme 69: Staudinger reaction between azide **199** and triphenylphosphine and proposed mechanism by Molina *et al.*^[149]

In this reaction, the phosphazide **200** is in equilibrium with an ionic structure due to the electron-withdrawing nature of the nitrile. Because of this ionic structure, the phosphazide **200** decomposes to the phosphinimine **202** and the diazo compound **201**. The diazo species **201** then reacts with an excess of phosphine and forms compound **203**, which is very similar to our observed side product (**E/Z**)-**192b**.

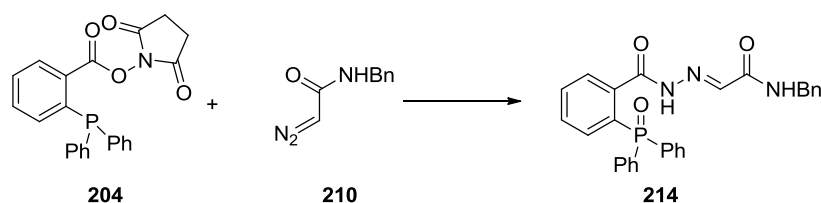
Just recently Raines *et al.*^[150] also reported the synthesis of diazo compounds **210** by a modification of the Staudinger ligation (Scheme 70).



Scheme 70: Synthesis of the diazo compound **210** by a modified Staudinger ligation published by Raines *et al.*^[150]

In this case, the phosphazide is trapped in the same way as the iminophosphorane in the normal Staudinger ligation. The resulting acyl triazine **206** – like the phosphazide **200** in the reaction of Molina explained before – decomposes to the amide **209** and the diazo compound **210**. The above authors also observed that the formed diazo compound **210** can in turn react with the phosphine **204** under the formation of an analog **214** of the methyl phenyl(2-(3-phenylpropylidene)hydrazinyl)phosphinate (**E/Z**)-**192b** detected by us (Scheme 71). In contrast

to our reaction, a phosphine is applied that cannot form a P-O double bond, and the negatively charged nitrogen is again trapped by the activated carboxylic acid leading to **214**.



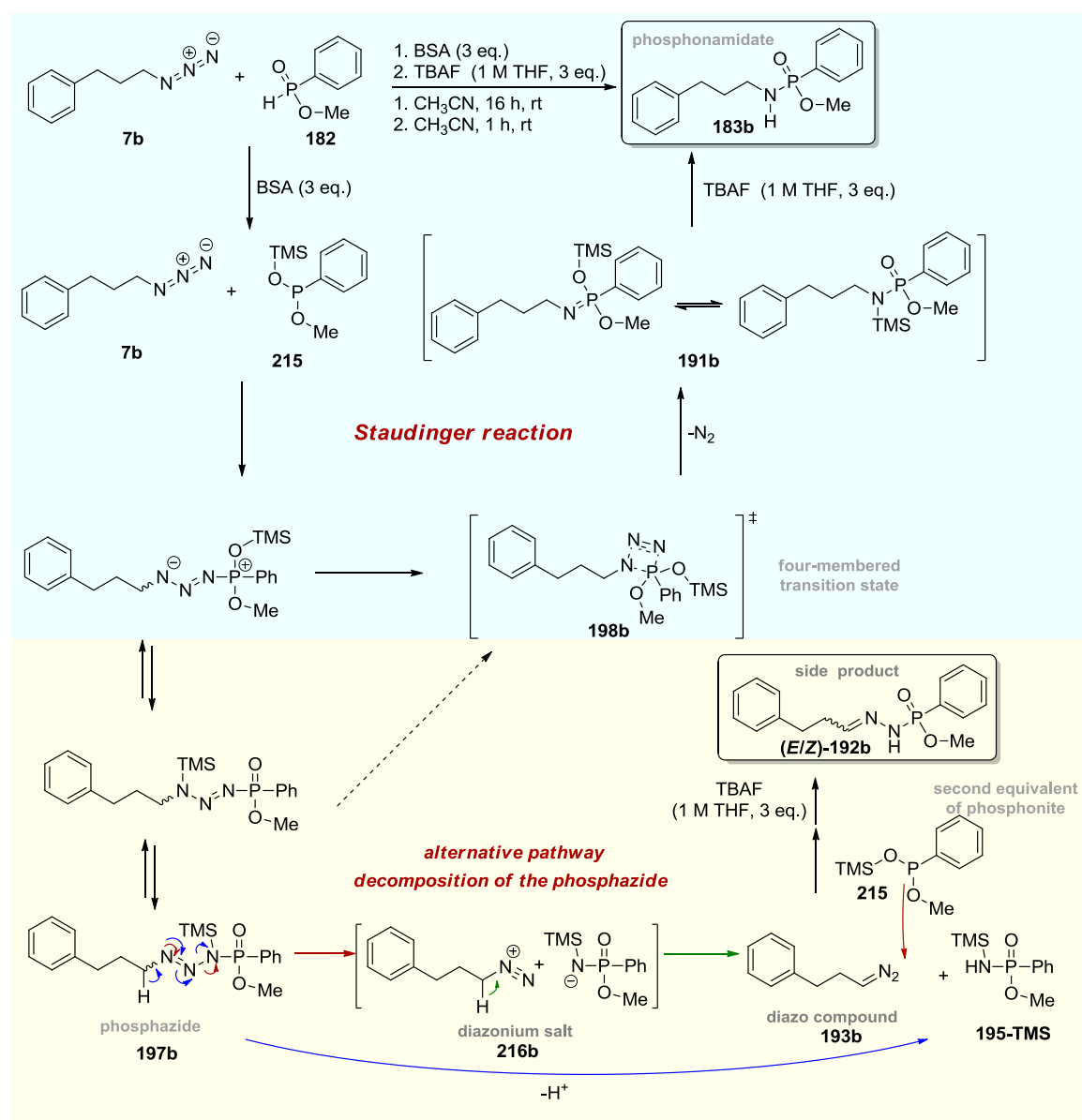
Scheme 71: Reaction of the diazo compound **210** with phosphine **204** by Raines.^[150]

In the reaction described by Raines *et al.*^[150], heating of the acyl triazine **206** leads directly to its decomposition into the diazonium species **208** and the deprotonated amide **207**. Alternatively, if a base is present, deprotonation of the acyl triazine **206** can also lead to formation of the anions **211**, which exists in three tautomeric forms, and reprotonation of the tautomeric structure **213** yields directly the diazo compounds **210** without intermediate generation of the diazonium salt. The deprotonation of **206** is eased by the position of the hydrogen α to the amide in the glycine derivative.

A similar reaction pathway might be responsible for the high amount of by-product formed with our azido peptides **7c-e** containing a N-terminal azido glycine **7h**.

Taking into account these similar observations by the groups of Raines^[150] and Molina^[149] together with our own results, the following mechanism is proposed (Scheme 72). In the Staudinger reaction, the phosphazide **197b** stabilizes itself by the formation of the four-membered transition state **198b**, which enables the release of nitrogen. However, if a silyl group is used instead of an alkyl group, this silyl group can migrate to the negatively charged nitrogen of the phosphazide **197b** leading to the displayed tautomeric structures. This has the effect that a P-O double bond is formed, which abolishes the positive charge of the phosphorus and likewise the negative one of the nitrogen otherwise facilitating bond formation between the two of them. Therefore, this migration can prevent the formation of the four-membered, cyclic transition state **198b**, normally occurring in the Staudinger reaction, by both steric and electronic effects. The steric demand of the silyl group may shift the *E/Z*-ratio of the phosphazide **197b** making the formation of the cyclic transition state evolving from the *Z*-isomer more difficult. Hence, the phosphazide **197b**, which is quite unstable, may disintegrate under formation of phosphoramidate **195** and a diazo compound **193b**. This reaction is analogue to the decomposition of the acyl triazine **206** in the reaction published by Raines *et al.*^[150] (Scheme

70) and the phosphazide **200** described by Molina *et al.*^[149] (Scheme 69). Hence, it is not clear if our reaction proceeds *via* the diazonium species **216b** (red pathway) or directly via the blue pathway as in the base-catalyzed variant by Raines *et al.*^[150] The latter is more likely in case of the azido peptides due to the C-H-acidity of azido glycine. Apart from its formation, the diazo compound **193b** can as proposed by Raines react with a silyl phosphonite **215** to form the observed (*E/Z*)-methyl phenyl(2-(3-phenylpropylidene)hydrazinyl)phosphinate ((*E/Z*)-**192b**) (Scheme 72).



Scheme 72: Proposed mechanism of the Staudinger reaction between silyl phosphonite **215** and alkyl azide **7b**.

This mechanism ought to be in accordance with the results mentioned before. The ^{15}N next to the methylene group stays in the molecule whereas the ^{15}N next to the phosphorus becomes

part of the formed methyl *P*-phenyl phosphonamidate ¹⁵**N-195**, which could also be detected by HRMS. Moreover, the appearance of the phosphinate **196b** (Scheme 65), which was also detected by HRMS, can be explained by nucleophilic substitution of the diazonium cation **216b** with the silyl phosphonite **215** under release of nitrogen. The dependence of phosphazide formation and disintegration on the solvent polarity and other silylation reagents are discussed in the chapters 3.4.5.4-3.4.6.

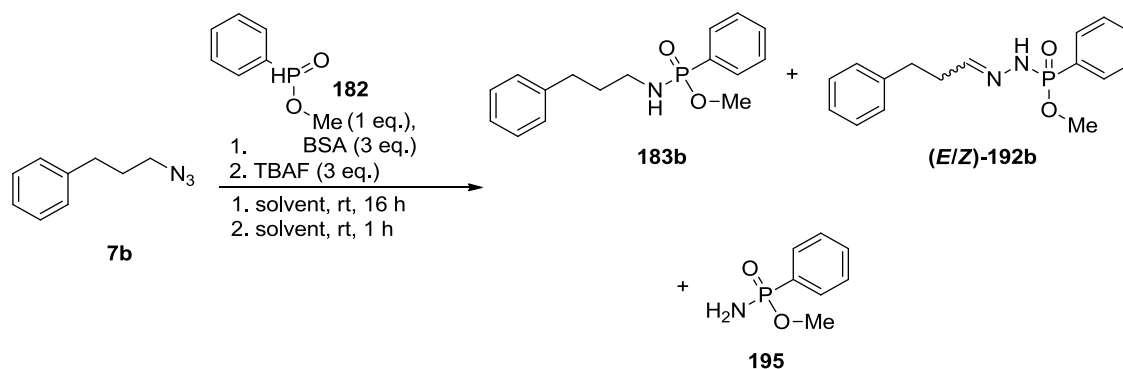
3.4.5.4 Solvent effects

In the first reactions described at the beginning of chapter 3.4.5 between 3-phenylpropyl azide (**7b**) and methyl phenylphosphinate (**182**) with three equivalent of BSA, an influence of the solvent on the product formation was observed. In these reactions the conversion to the desired phosphonamidate **183b** was significantly higher in CH₂Cl₂ than in the by far more polar solvent acetonitrile. Furthermore, the reaction mechanism proposed for the by-product formation, especially via the diazonium species, does forebode a dependence on the solvent applied. For this reason the standard reaction between the azide **7b** and methyl phenylphosphinate (**182**) was performed in eight different aprotic solvents (*n*-hexane, benzene, tetrahydrofuran, dichloromethane, pyridine, acetonitrile, *N,N*-dimethylformamide and dimethyl sulfoxide) in order to investigate the influence of the solvent polarity on the side product formation.

The reaction was performed as displayed in Scheme 73. ³¹P-NMR spectra were measured after addition of TBAF. For the measurement of the LC-MS spectra, TBAF was removed by filtration over silica. Ratios between **183b**, (*E/Z*)-**192b** were determined by integration of the ³¹P-NMR signals and by integration of the UV-trace of the LC-MS spectra. The ratios together with the corresponding relative permittivity of the applied solvents are displayed in Diagram 1 and Table IX. To insure the validity of the results obtained by integration of the UV-trace, a calibration curve was measured previously.

By performing the reaction in solvents of different polarity, it could be shown that increase in the polarity of the solvent entails an increase of (*E/Z*)-methyl phenyl(2-(3-phenylpropylidene)hydrazinyl)phosphinate (*E/Z*)-**192b**. Results of the ³¹P-NMR and HPLC differ slightly by not more than 5%. The fraction of methyl phenyl(2-(3-phenylpropylidene)hydrazinyl)phosphinate (*E/Z*)-**192b** in the solvent *n*-hexane was only 15% (UV) and amounts to up to 68% (UV) in DMSO. In very unpolar solvents like *n*-hexane, benzene and THF, the amount of (*E/Z*)-**192b** remained under 20%. With dichloromethane and pyridine as solvents, the formation of **183b** was still satisfactory with 70% to 77%. Thereby,

dichloromethane, which has a relative permittivity of only 8.93, gave an unexpected high amount of **(E/Z)-192b**, even higher than pyridine with a relative permittivity of 12.91.



Scheme 73: Model reaction to study the influence of the solvent polarity.

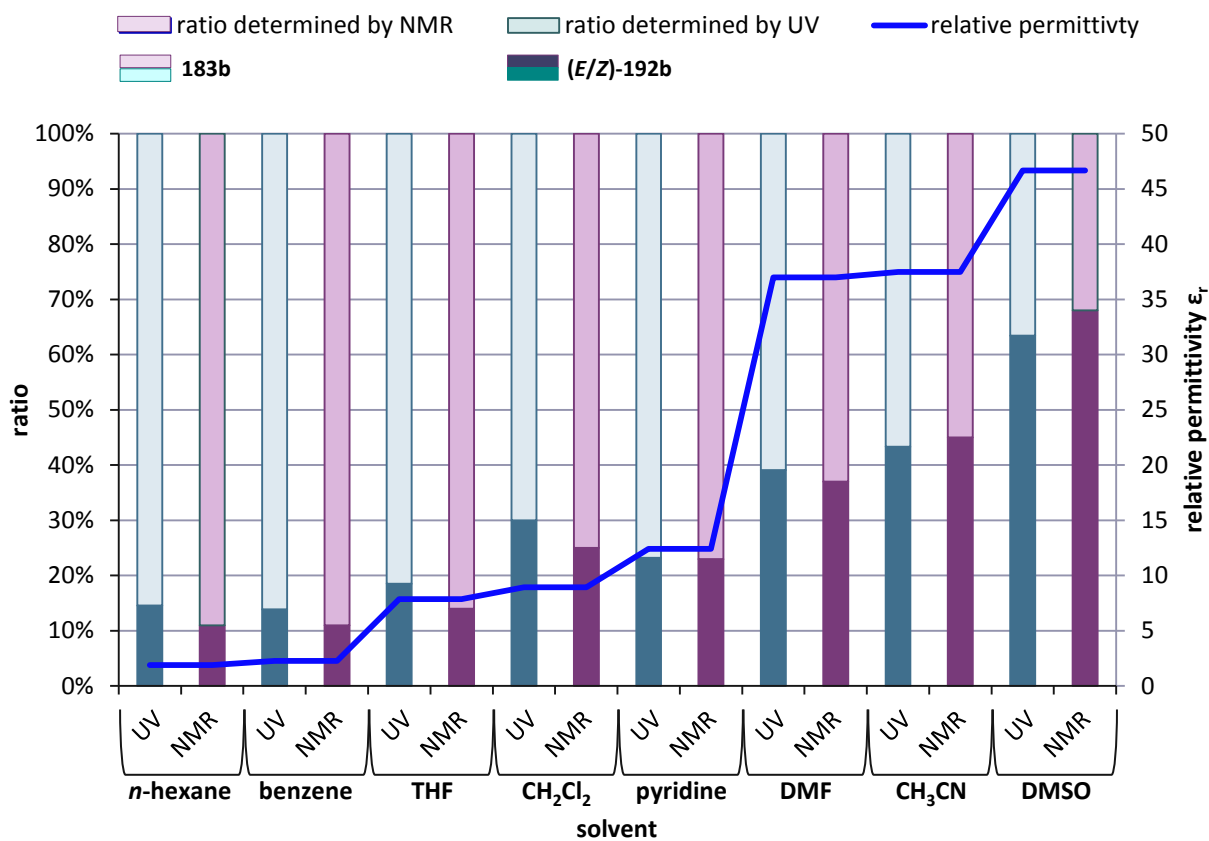


Diagram 1: Solvent effect on the formation of **(E/Z)-192b**: Ratios of **(E/Z)-192b** and **183b** determined by ³¹P-NMR and by integration of the corresponding signals of the UV-trace (226 nm) of the LC-MS spectra after Staudinger reaction with BSA and addition of TBAF. For the LC-MS spectra TBAF was removed prior to injection (left axis). Relative permittivity of the applied solvents (right axis).

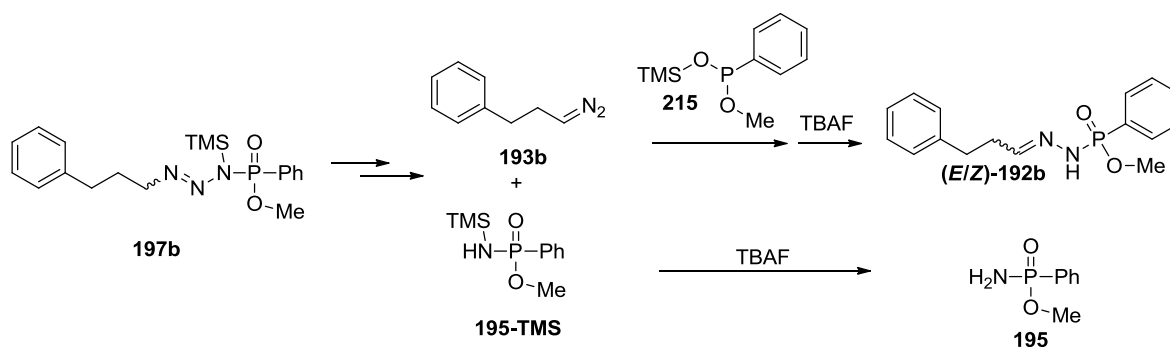
Table IX: Data to Diagrams 1. Reaction conditions: 1. ^{15}N -**7b** (1 eq.), PhP(O)HOMe (**182**) (1 eq.), BSA (3 eq.), rt, 16 h, 2. TBAF (1 M in THF, 3 eq.), rt, 1 h.

solvent	<i>(E/Z)</i> - 192b		183b		relative permittivity ^{[151]a}
	UV (226 nm)	NMR	UV (226 nm)	NMR	
<i>n</i> -hexane	15%	11%	85%	89%	1.88
benzene	14%	11%	86%	89%	2.27 ^b
THF	19%	14%	81%	86%	7.58
CH ₂ Cl ₂	30%	25%	70%	75%	8.93
pyridine	23%	23%	77%	77%	12.91
CH ₃ CN	39%	37%	61%	63%	35.94
DMF	43%	45%	57%	55%	36.71
DMSO	63%	68%	37%	32%	46.45

^a relative permittivity of the pure liquid at 25 °C, ^b at 20 °C

A significant increase in the polarity for acetonitrile and DMF also led to much higher amounts of *(E/Z)*-**192b** from 37 to 45%. In DMSO the amount of *(E/Z)*-**192b** was even higher than the amount of **183b**. Moreover, in case of DMSO signals in the ³¹P-NMR spectrum between 0 ppm and 15 ppm integrated for nearly 40% of the whole product mixture.

The obtained results are in accordance with the proposed mechanism as the methyl phenyl(2-(3-phenylpropylidene)hydrazinyl)phosphinate *(E/Z)*-**192b** formation is accompanied by ionic species (Scheme 72). More polar solvents supported the heterologous dissociation of the phosphazide **197b** leading to the diazo compound **193b** and methyl *P*-phenyl phosphonamidate **195**. The diazo compound **193b** can then react with the silyl phosphonite **215** to form *(E/Z)*-**192b**. For this reason, the amount of *(E/Z)*-**192b** can only be equal or lower than the amount of methyl-*P*-phenyl phosphonamidate (**195**) resulting from the dissociation of the phosphazide **197b** (Scheme 74).



Scheme 74: Formation of *(E/Z)*-**192b** and **195** from the phosphazide **197b**.

It was observed that the NMR signal at ~26 ppm, which was attributed to methyl *P*-phenyl phosphonamidate (**195**), increased to the same extent as the signal of methyl phenyl(2-(3-

phenylpropylidene)hydrazinyl)phosphinate (**(E/Z)-192b**) (Diagram 2). Phosphinate (**(E/Z)-192b**) and methyl *P*-phenyl phosphonamidate (**195**) were formed in a ratio of approximately one to one determined by ^{31}P -NMR whereby the amount of methyl *P*-phenyl phosphonamidate (**195**) was slightly higher in most cases. These findings again support the proposed mechanism.

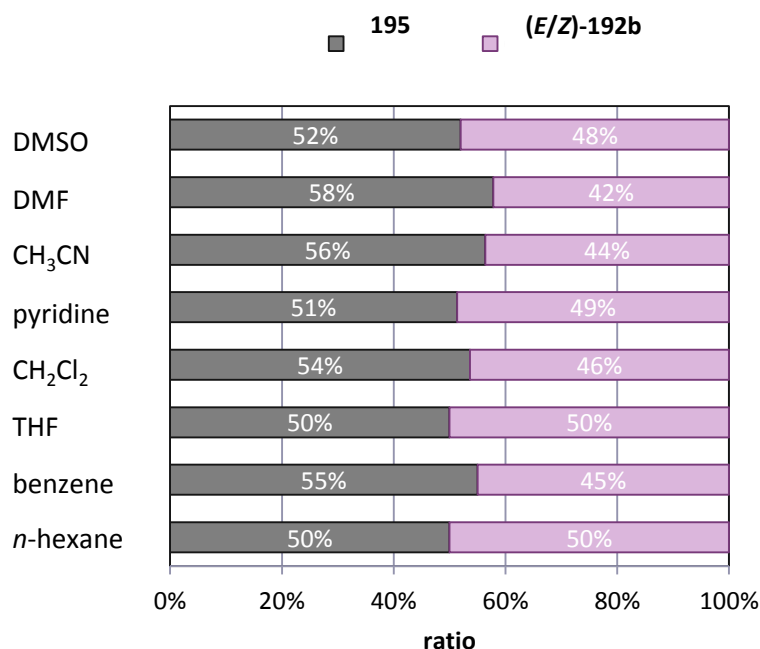
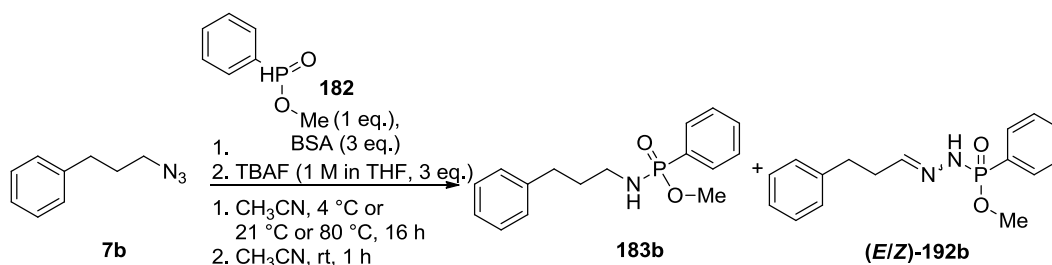


Diagram 2: Ratio of compounds (**(E/Z)-192b**) and phosphonamidate **195** in different solvents determined by ^{31}P -NMR. Reaction conditions: 1. ^{15}N -**7b** (1 eq.), $\text{PhP}(\text{O})\text{HOMe}$ (**182**) (1 eq.), BSA (3 eq.), rt, 16 h, 2. TBAF (1 M in THF, 3 eq.), rt, 1 h.

3.4.5.5 Temperature effect

Performing the reaction at three different temperatures (4°C, rt, 80°C) in acetonitrile had no significant effect on the methyl phenyl(2-(3-phenylpropylidene)hydrazinyl)phosphinate (**(E/Z)-192b**) formation (Scheme 75, Diagram 3, Table X).



Scheme 75: Model reaction to study the influence of different temperatures.

At 0°C slightly more (*E/Z*)-**192b** was formed (35-42%) than at 80 °C (26-31%). This might be explained by the higher stability of the phosphazide **197b** promoting migration of the silyl group before nitrogen can be released and perhaps isomerization of the phosphazide **197b**. In conclusion, an increase of the reaction temperature by 76°C led to about 10% more phosphonamidate **183b**.

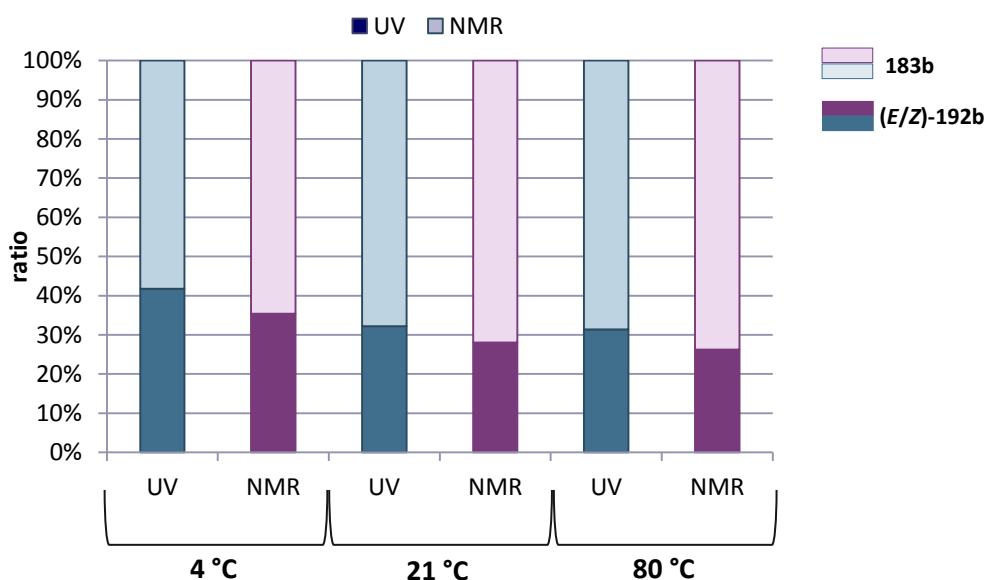


Diagram 3: Temperature dependence of (*E/Z*)-**192b** formation based on ^{31}P -NMR and integration of the UV trace (226 nm) of the corresponding LC-MS spectra.

Table X: Data to Diagram 3: Ratios of (*E/Z*)-**192b** and **183b** at 0 °C, 21 °C and 80 °C. Reaction conditions: 1. ^{15}N -**7b** (1 eq.), PhP(O)HOMe (**182**) (1 eq.), BSA (3 eq.), CH_3CN , 16 h, 2. TBAF (1 M in THF, 3 eq.), CH_3CN , 1 h.

temperature (°C)	<i>(E/Z)</i> - 192b		183b	
	UV (226 nm)	NMR	UV (226 nm)	NMR
0°C	42%	35%	58%	65%
21°C	32%	28%	68%	72%
80°C	31%	26%	69%	73%

3.4.5.6 Influence of the silylation reagent on the Staudinger reaction

To investigate the dependence of the applied silyl group on the formation of the by-products (*E/Z*)-**192b** and **195**, different silylation reagents were used to assist the Staudinger reaction of 3-phenylpropyl azide (**7b**) and methyl phenylphosphinate (**182**) (Figure 24 and Scheme 76).

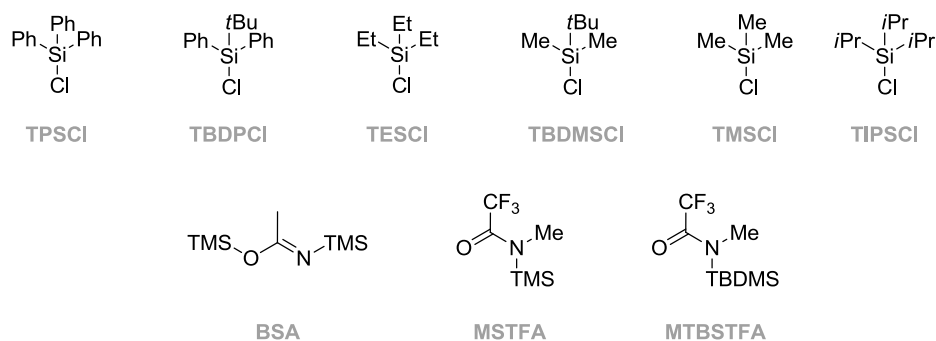
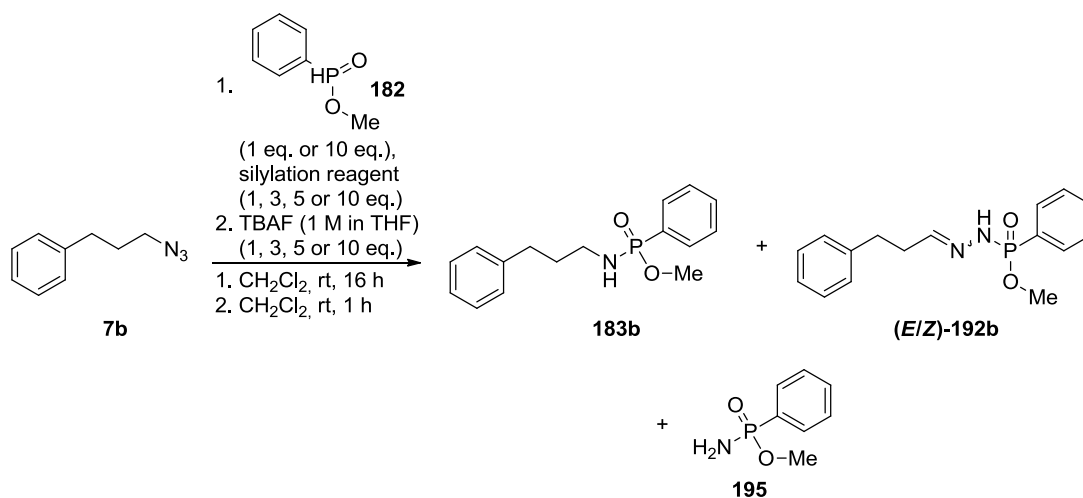


Figure 24: Different silylation reagents applied in the following studies.



Scheme 76: Staudinger reaction with different silylation reagents.

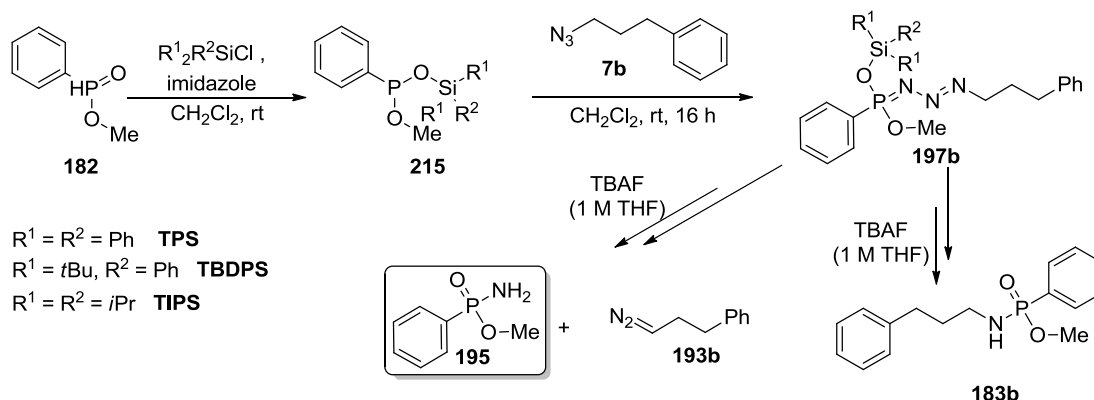
To capture the formed hydrogen chloride and promote silylation, a base was applied with each silyl chloride. In the case of TPSCI, TBDPSCI, TBDMSCI and TIPSCI, one equivalent of imidazole was added, whereas triethylamine was used for TMSCI and TESCO. In all reactions one equivalent of **182** was used unless otherwise noted. Silylation of phosphinates with silyl chlorides is described to proceed well in dichloromethane and the Staudinger reaction in dichloromethane led to full conversion of the azide **7b** and phosphinate **182** (chapter 3.4.5.4), therefore, it was chosen as solvent for the following studies.^[141a, b]

3.4.5.6.1 Silylation with TPSCI, TBDPSCI and TIPSCI

The Staudinger reaction with TPSCI, TBDPSCI and TIPSCI was not successful, and the phosphonamidate **183b** was not formed or only in very small amounts.

With TPSCI as silylation reagent, no product formation was observed at all, and the ³¹P-NMR spectrum only showed phosphinic acid **185**. The methyl ester seems to hydrolyze due to the treatment with TBAF-solution. The analogue reaction with TBDPSCI gave similar results. The

Staudinger reaction was conducted with one, three and five equivalents of TBDPSCI in dichloromethane (Scheme 77). With one equivalent of TBDPSCI, mainly unreacted phosphinic acid **185** (~73%) was determined by ^{31}P -NMR, and the additional signal at 24.91 ppm was attributed to methyl *P*-phenylphosphonamidate (**195**), which was also detected in the MS spectrum. No phosphonamidate **183b** or methyl phenyl(2-(3-phenylpropylidene)hydrazinyl)-phosphinate ((*E/Z*)-**192b**) was detected, neither by NMR spectroscopy nor by HRMS. When the equivalents of the silylation reagent were increased to three and five, it seemed that the phosphinate **182** fully reacted with TBDPSCI, and signs of small amounts of phosphonamidate **183b** appeared in the NMR and HRMS spectra, but no signal of methyl phenyl(2-(3-phenylpropylidene)hydrazinyl)phosphinate ((*E/Z*)-**192b**) was visible. When introducing five equivalents, the ratio between methyl *P*-phenylphosphonamidate (**195**) and the desired phosphonamidate **183b** was 97:3, and many signals in the range of phosphonic acid derivatives between 0 to 15 ppm appeared in the ^{31}P -NMR spectrum (~79%). Furthermore, an LC-MS spectrum was measured before adding TBAF to the reaction mixture, and in that case, monosilylated methyl *P*-phenylphosphonamidate **195-TBDPS** was detected as the major product besides the phosphonic acid derivatives, which was in agreement with the ^{31}P -NMR spectrum. The results supported the assumption that electronic and steric aspects of the TBDPS-group did not support the Staudinger reaction, and although the (*E/Z*)-**192b** could not be detected in all the cases, the conversion to the desired phosphonamidate **183b** was very low as well. Even if the phosphazide was formed, it mainly decomposed to methyl *P*-phenylphosphonamidate (**195**), and the silyl phosphonite **215-TBDPS** seemed not to be very reactive towards both, the azide **7b** and the diazo compound **193b** (Scheme 77). The results were not promising for further investigations, and the TBDPS-group was not deemed very suitable for the Staudinger reaction.

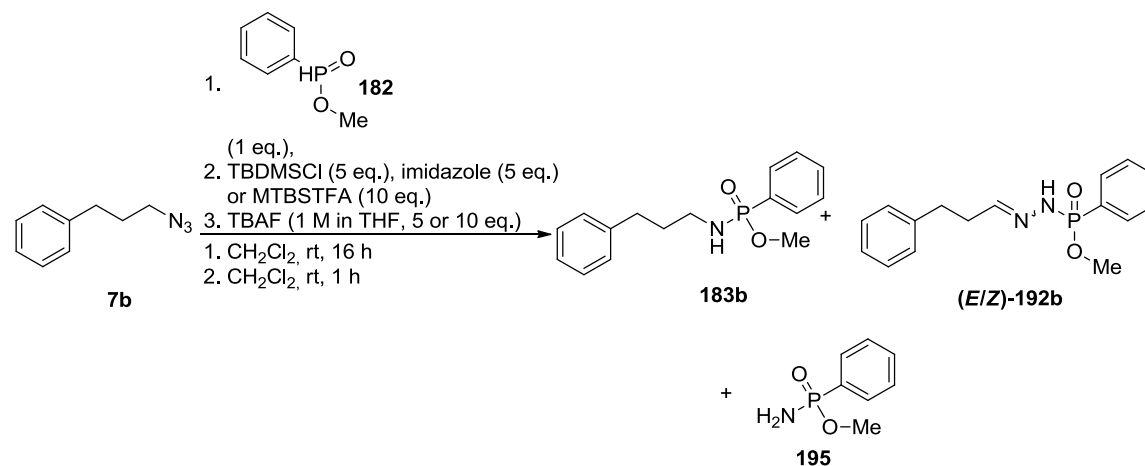


Scheme 77: Staudinger reaction with TPSCI, TBDPSCI and TIPSCI as silylation reagents. The reaction scheme describes the mechanistic course of events. Besides compound **195** (21-27%) mainly *P(V)*-compounds resulting from oxidation and hydrolysis of **182** were observed (70-100%).

With three equivalents of TIPSCl, the methyl *P*-phenylphosphonamidate (**195**) prevailed in the LC-MS spectrum, measured after addition of TBAF, and only negligible amounts of phosphonamidate **183b** were detectable. Methyl phenyl(2-(3-phenylpropylidene)-hydrazinyl)phosphinate ((*E/Z*)-**192b**) was not observed at all.

3.4.5.6.2 Silylation with TBDMSCl

When TBDMSCl (5 equivalents) was used as silylation reagent almost no conversion to the phosphonamidate **183b** could be noticed (Table XI, Scheme 78). The ³¹P-NMR spectrum indicated 32% methyl *P*-phenyl-phosphonamidate (**195**) and only 2% phosphonamidate **183b**, but still **183b** and **195** sum up to only 34% of the whole mixture. This agrees with the LC-MS spectrum where just small amounts of phosphonamidate **183b** were detected. (*E/Z*)-**192b** was detected in less than 1%. When the silylation reagent was changed to MTBSTFA, methyl *P*-phenyl-phosphonamidate (**195**) could be identified in an amount of 27%, but the desired phosphonamidate **183b** was formed in 17% as determined by NMR. This is in accordance with the isolated yield of 14% of the phosphonamidate **183b**. (*E/Z*)-**192b** was again detected in less than 1%. Nevertheless, also in this case the methyl phenylphosphinate (**182**) was not fully converted.



Scheme 78: Staudinger reaction with TBDMSCl or MTBSTFA as silylation reagents.

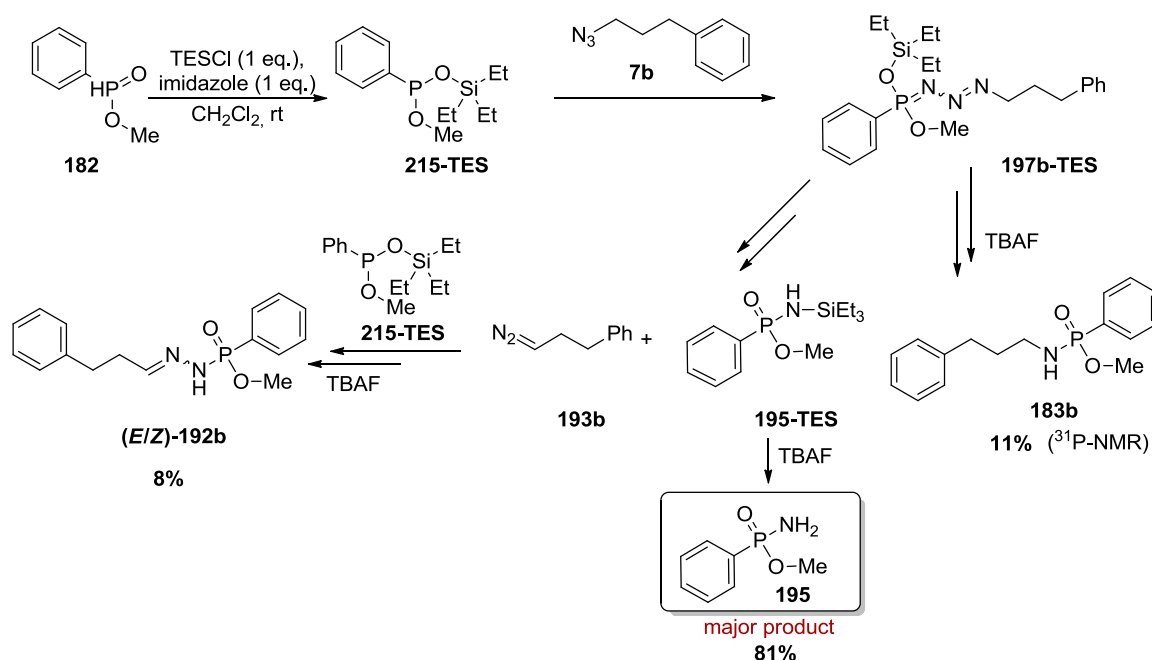
Table XI: Ratios of the observed compounds after the Staudinger reaction with TBDMSCl and MTBSTFA based on the integration of ³¹P-NMR signals.

silylation reagent	equivalents	195	183b	(<i>E/Z</i>)- 192b	other
TBDMSCl	5	32%	2%	<1%	66%
MTBSTFA	10	27%	17%	1%	55%

3.4.5.6.3 Silylation with TESCl

The reaction was carried out with one and three equivalents of TESCl, and in either case mainly methyl *P*-phenylphosphonamidate (**195**) was observed (Scheme 79).

With one equivalent of TESCl, integration of the UV-trace proved that methyl phenyl(2-(3-phenylpropylidene)hydrazinyl)phosphinate ((*E/Z*)-**192b**) was formed at a ratio of 46 to 54 in relation to the phosphonamidate **183b**. However, an amazing 82% of methyl *P*-phenylphosphonamidate (**195**) were formed compared to both products **183b** and (*E/Z*)-**192b**, and the measurement of a LC-MS spectrum prior to the addition of TBAF with three equivalents of TESCl, again, predominantly showed the silylated methyl *P*-phenyl phosphonamidate (**195-TES**). This observation showed one more time that formation of the cyclic transition state of the Staudinger reaction is impeded and that the silyl phosphonite **215-TES** does not merge with the diazo compound **193b**. It could also be concluded from the ^{31}P -NMR spectrum that phosphinic acid **185** was still present in significant amounts after the reaction (21%).

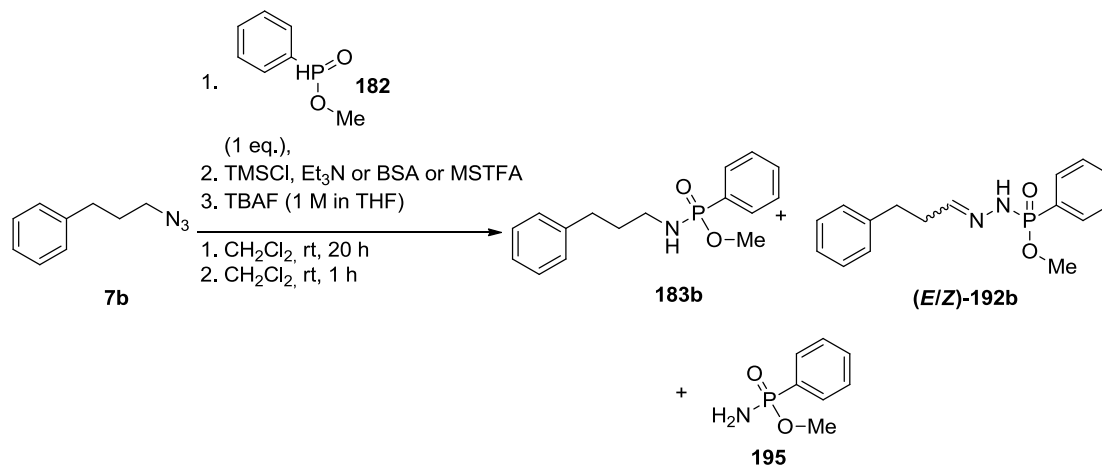


Scheme 79: Staudinger reaction with TESCl as silylation reagent. The reaction scheme describes the mechanistic course of events. Given ratios of observed products were determined by ^{31}P -NMR.

3.4.5.6.4 Silylation with TMSCl, BSA and MSTFA

In comparison to TBDMSCl and TESCl, the results with one and five equivalents of TMSCl were slightly better, but decomposition to the methyl *P*-phenylphosphonamidate (**195**) was again the prevailing phenomenon (53-70%) (Table XII, Scheme 80). But it is noteworthy that only

proportionally small amounts (15-17%) of other signals than for **195**, **183b** and (*E/Z*)-**192b** appeared supporting high conversion to the phosphazide **197b**. Moreover, an increasing excess of TMSCl led to a higher amount of **195**. **183b** and (*E/Z*)-**192b** were formed in the same ratio (88:12) with one and five equivalents of TMSCl.



Scheme 80: Staudinger reaction with TMSCl, BSA or MSTFA as silylation reagents.

Table XII: Ratios of the observed compounds based on the integration of ³¹P-NMR signals and ratios of **183b** : (*E/Z*)-**192b** determined by ³¹P-NMR and integration of the UV-trace.

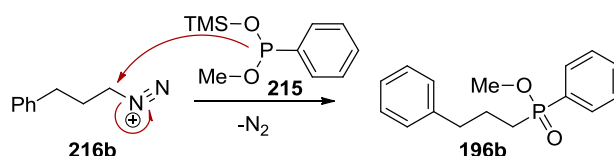
TMSCl	195	183b	(<i>E/Z</i>)- 192b	other	183b : (<i>E/Z</i>)- 192b (³¹ P-NMR)	183b : (<i>E/Z</i>)- 192b (UV)
1 eq.	53%	30%	2%	15%	94 : 6	88 : 12
5 eq.	70%	12%	1%	17%	92 : 8	88 : 12

BSA and MSTFA silylated the phosphinate **182** very effectively but compared to MSTFA, BSA gave much better results regarding the amount of the desired phosphonamidate **183b** (3-10 eq., 58-70%) and the ratio between **183b** and (*E/Z*)-**192b** (Table XIII). Comparison of the data also show that an excess of BSA is needed for the reaction as with 1 equivalent of BSA conversion of the methyl phenylphosphinate (**182**) to the phosphazide **197b** was incomplete leading to small amounts of products (**195**, **183b**, (*E/Z*)-**192b** = 46%) whereas with 1 equivalent of MSTFA these products summed up to 97%. With an increasing amount of BSA the amount of **183b** improved from 33% to 70%, whereas by increasing the equivalents of MSTFA from 1 to 10 the amount of **183b** decreased by 40% and the ratio of **183b** to (*E/Z*)-**192b** switched. As described before, if more (*E/Z*)-**192b** is generated, also more phosphonamidate **195** is formed. Between 9 and 23% of methyl *P*-phenyl-phosphonamidate (**195**) were detected with 1, 3 and 5 equivalents of BSA, which was not reached with ten equivalents.

Table XIII: Ratios of the observed compounds based on the integration of ^{31}P -NMR signals and ratios of **183b** : (*E/Z*)-**192b** determined by ^{31}P -NMR and integration of the UV-trace (226 nm) of the LC-MS spectra.

reagent	195	183b	(<i>E/Z</i>)- 192b	other	183b : (<i>E/Z</i>)- 192b (^{31}P -NMR)	183b : (<i>E/Z</i>)- 192b (UV)
1 eq. BSA	9	33	4	54	89 : 11	90 : 10
3 eq. BSA	23	58	19	0	75 : 25	75 : 25
5 eq. BSA	15	63	9	13	88 : 12	88 : 12
10 eq. BSA	0	70	5	25	97 : 2	97 : 3
1 eq. MSTFA	35	35	27	3	56 : 44	61 : 39
10 eq. MSTFA	59	16	23	2	41 : 59	37 : 63

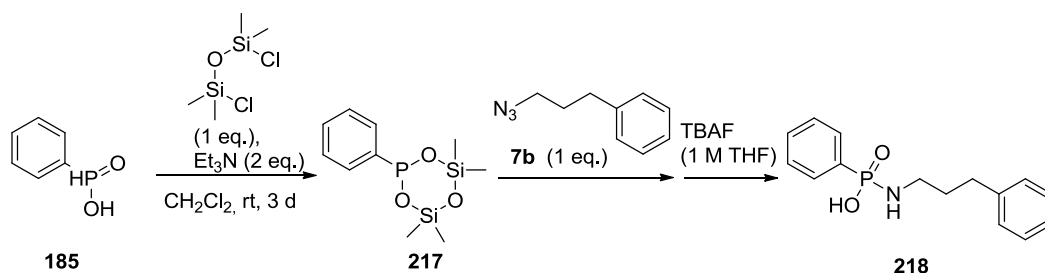
When the reaction was conducted with one equivalent MSTFA, but ten equivalents of methyl phenylphosphinate (**182**), the ratio between the phosphonamidate **183b** and methyl phenyl(2-(3-phenylpropylidene)hydrazinyl)phosphinate (*E/Z*)-**192b** changed from 37:63 to 26:74. Additionally, the compound **196b** with the direct P-C connection was formed. Similar results were obtained with 6 equivalents of methyl phenylphosphinate (**182**) and 18 equivalents of BSA. In this case the ratio changed from 75:25 to 59:41 and **196b** was detected in 9%. This shows that an excess of methyl phenylphosphinate (**182**) is accompanied by a higher amount of the side-product (*E/Z*)-**192b**. This agrees with the proposed mechanism. The formed diazo compound **193b** can react with the excess of the trivalent phosphorus species to the known side product (*E/Z*)-**192b**. **196** can be formed by direct substitution of the diazonium cation (Scheme 81) or by attack of the trivalent phosphorus species at the phosphazide **197b**.



Scheme 81: Possible mechanism of the phosphinate formation.

3.4.5.6.5 Staudinger reaction with a cyclic silyl phosphonite

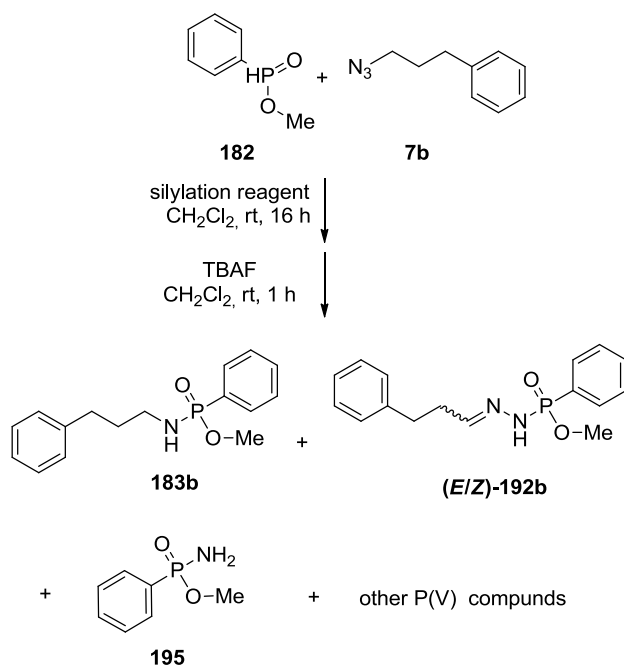
It was attempted to produce a cyclic silyl phosphonite **217** to perhaps facilitate formation of the four-membered transition state and to also avoid migration of the silyl group (Scheme 82). Unfortunately, no formation of the product **218** could be stated even with elongated reaction time. Obviously reaction conditions have to be further optimized to get the Staudinger reaction working.



Scheme 82: Staudinger reaction with a cyclic silyl phosphonite **217**.

3.4.5.6.6 Summary

The Diagram 4 summarizes the most important effects of all different silylation reagents in CH_2Cl_2 by comparison of the obtained ratios determined by ^{31}P -NMR spectroscopy and LC-MS (Scheme 83). In the ^{31}P -NMR spectra the sum of all integrals was set to 100%. In the LC-MS measurement only the phosphonamide **183b** and the by-product (*E/Z*)-**192b** were detected, and for this reason the sum of **183b** plus (*E/Z*)-**192b** in the ^{31}P -NMR spectra was set to 100% for a better comparability.



Scheme 83: Detected products of the Staudinger reaction between 3-phenylpropyl azide (**7b**) and methyl phenylphosphinate (**182**) with different silylation reagents in CH_2Cl_2 .

As described in chapter 3.4.5, besides the expected phosphonamide **183b**, the side products (*E/Z*)-**192b** and **195** occurred in the ^{31}P -NMR spectrum if one equivalent of methyl phenylphosphinate (**182**) was used. However, if the methyl phenylphosphinate (**182**) was either not fully converted to the silyl phosphonite **215** or the silyl phosphonite **215** was not reactive

enough for the Staudinger reaction, hydrolyzed and oxidized phosphorus species appeared in the ^{31}P -NMR spectrum between 0 and 15 ppm (grey column). The diagram shows that only in case of BSA reasonable amounts of **183b** (33-70%) were produced and only comparatively small quantities of the by-product (**E/Z**)-**192b** (2-20%). Nevertheless, an excess of BSA should be added to assure complete conversion of the phosphinate **182** to its silylated form **215**. In contrast, MSTFA, which possesses a TMS-donor strength comparable or even higher than BSA, delivered **183b** only in up to 40%, and a larger excess even led to less **183b**-formation (16%). The ^{31}P -NMR spectrum proved that >95% of the detected products emerge from the phosphazide **197b** so that the reactivity of the reagent was not responsible for the low yield of the phosphonamidate **183b**, but MSTFA seems to facilitate the side reactions as high amount of (**E/Z**)-**192b** (22-27%) and **195** (35-59%) were found. With TMSCl more than 80% of **182** was converted to the phosphazide **197b**, but the amount of **195** (54-70%) was even higher than with MSTFA. Nevertheless, the amount of (**E/Z**)-**192b** was very low (1-3%), a tendency that was observed for all silyl chlorides but also MTBSTFA. This could be explained by either a low concentration or a low reactivity of the silyl phosphonite **215**. Alternatively, decomposition of the phosphazide occurs mainly not until TBAF is added, which would also exclude formation of (**E/Z**)-**192b**.

From TMSCl to TPSCl conversion of the silyl phosphonite **215** to the phosphazide **197b** and subsequent reaction to both **183b** and (**E/Z**)-**192b** decreased rapidly illustrating that more stable and sterically more demanding silyl groups are not advantageous for the Staudinger reaction. Moreover, silylation of the phosphinate **182** gets less efficient. But it has to be noted that TBDMSCl led to worse results in comparison to MTBSTFA.

In conclusion, the higher the steric demand and stability of the silyl groups, the stronger is the disintegration of the phosphazide **197b** and the less is its formation. Moreover, if silylation reagents were used, which caused the formation of ammonium salts and produced a very polar environment, also facilitated the decomposition of **197b**, whereas the acetamide derivatives BSA and MTBSTFA provided in excess gave better results. Summarizing the results with different silylation reagents and with different solvents, one equivalent of methyl phenylphosphinate, unpolar solvents like *n*-hexane or benzene and an excess of BSA gave the highest amount of the desired phosphonamidate **183b**.

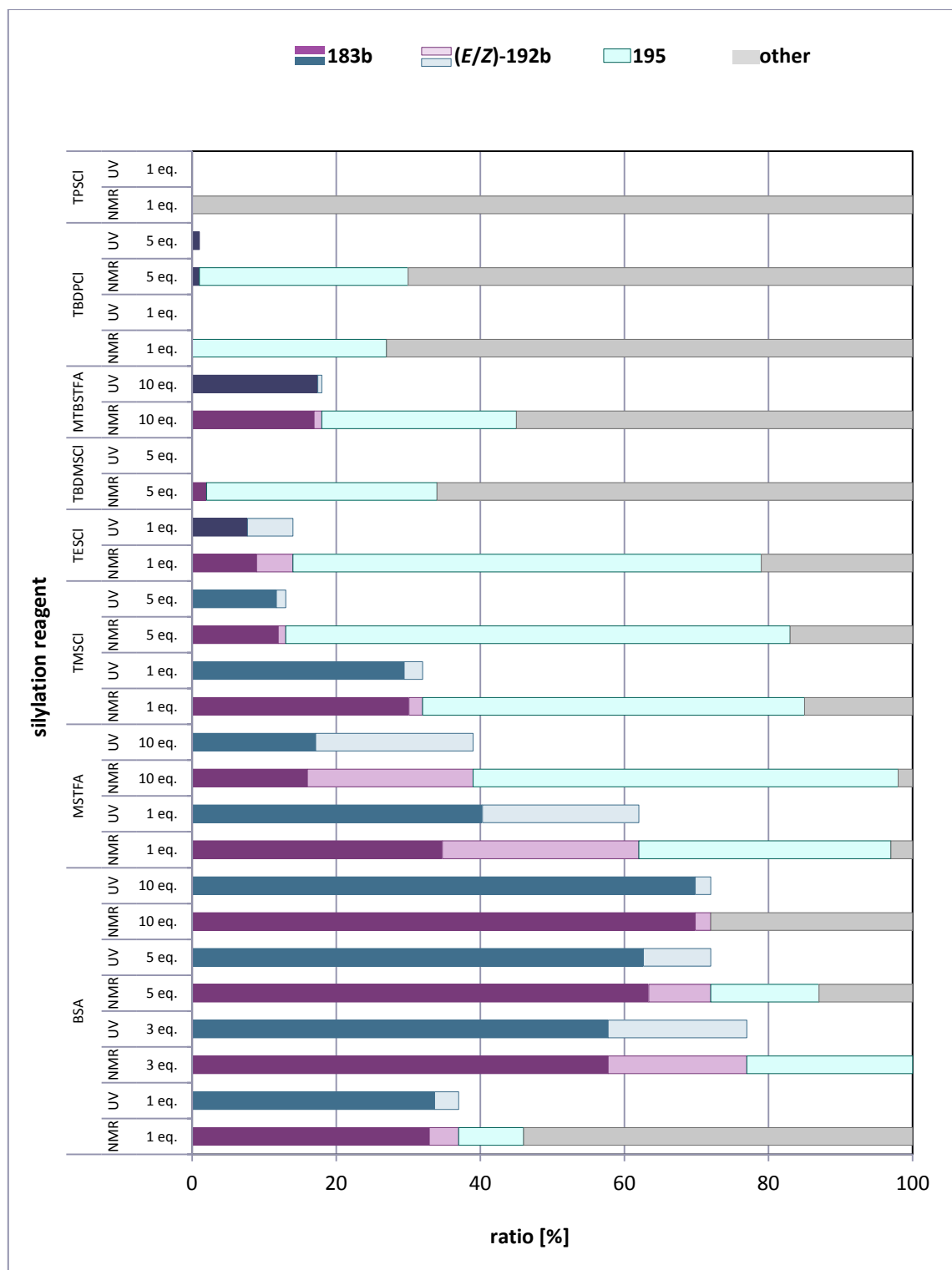
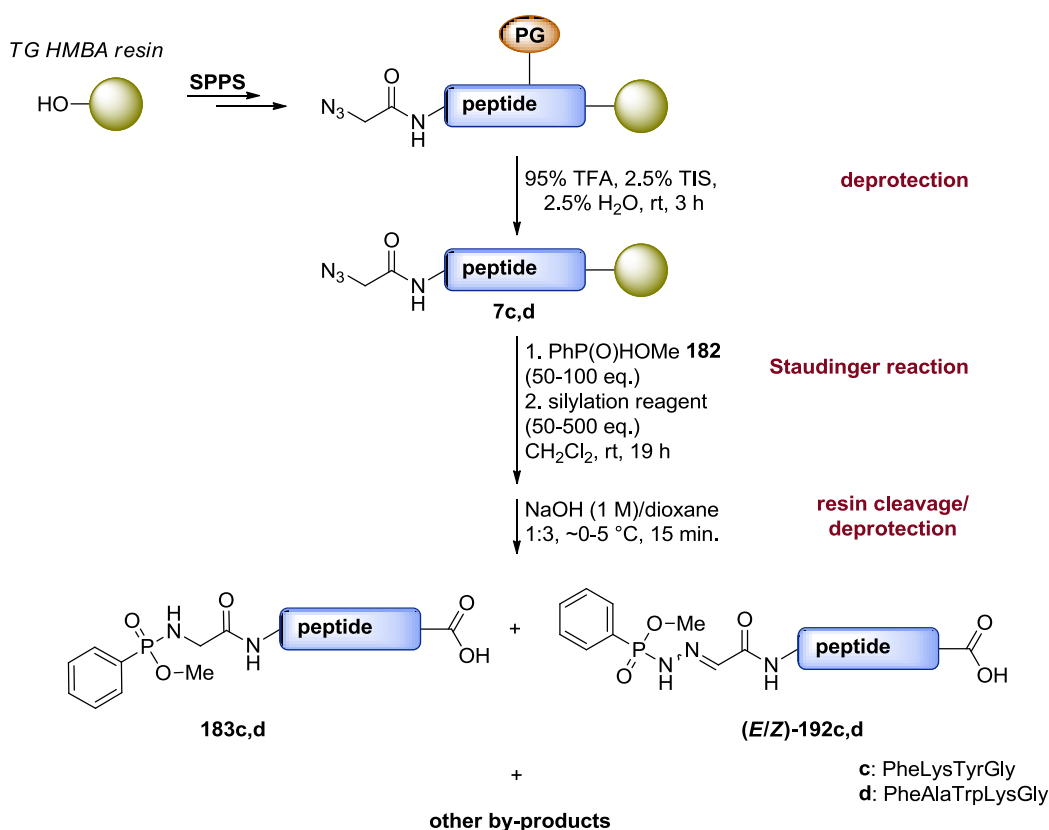


Diagram 4: The diagram shows the ratios of the observed products of the Staudinger reaction between 3-phenylpropyl azide (**7b**) and methyl phenylphosphinate (**182**) with different silylation reagents in CH_2Cl_2 determined by integration of ^{31}P -NMR spectra and integration of the UV trace (226 nm) of the LC-MS measurements. The ^{31}P -NMR spectra were measured after addition of TBAF. TBAF was removed before taking LC-MS measurements. For a better comparability the amount of **183b** plus (**E/Z**)-**192b** in the ^{31}P -NMR spectra was set to 100% in the UV measurement.

3.4.6 Staudinger reaction of azido glycine peptides with methyl phenylphosphinate and a silylation reagent

Aiming at the synthesis of peptides containing the phosphoramidate-motif as surrogate of the natural amide bond on solid support, the Staudinger reaction was performed with different azido peptides. In contrast to chapter 3.3, azido glycine **7h** instead of *p*-azidobenzoic acid^[7] was incorporated at the N-terminus of the peptide to get closer to the natural protease substrate. As described before (chapter 3.4.4 and 3.4.5), the reaction with azido glycine peptides or alkyl azides in general leads to the formation of several by-products which will be further investigated within this chapter.

The solid-supported azido peptides were obtained by standard Fmoc solid-phase peptide synthesis (SPPS) on a base-labile NovaSyn TG HMBA resin to allow on-resin deprotection and cleavage under basic conditions preventing decomposition of the phosphoramidate **183** as described in chapter 3.4.2.2. The resulting peptides were deprotected with a TFA cleavage cocktail (95% TFA, 2.5% TIS, 2.5% H₂O), and a test cleavage with aqueous NaOH-solution (1 M)/1,4-dioxane (1:3) proved the success of the peptide synthesis. Afterwards the Staudinger reaction was accomplished on-resin by adding the methyl phenylphosphinate **182** followed by the silylation reagent to the unprotected solid-supported azido peptide in dichloromethane. Since the silyl phosphonite **215** is very sensitive to oxygen and water, the resin was dried under high vacuum, and the reaction was performed under argon atmosphere in anhydrous solvents. The reaction was allowed to proceed under gentle agitation. After 19-24 h the solution of the reacting matter was removed and the resin was washed with dichloromethane. Cleavage from the resin was achieved with a one to three mixture of 1 M sodium hydroxide solution and 1,4-dioxane, and the obtained solution was brought to neutral pH before LC-MS measurement was executed for reaction control (Scheme 84). As mentioned before, the described by-product (*E/Z*)-**192c** as well as other by-products **190c**, **193c** and **194c** were observed beside the desired phosphoramidate **183c** as outlined in Scheme 63. This observation demanded further investigations.

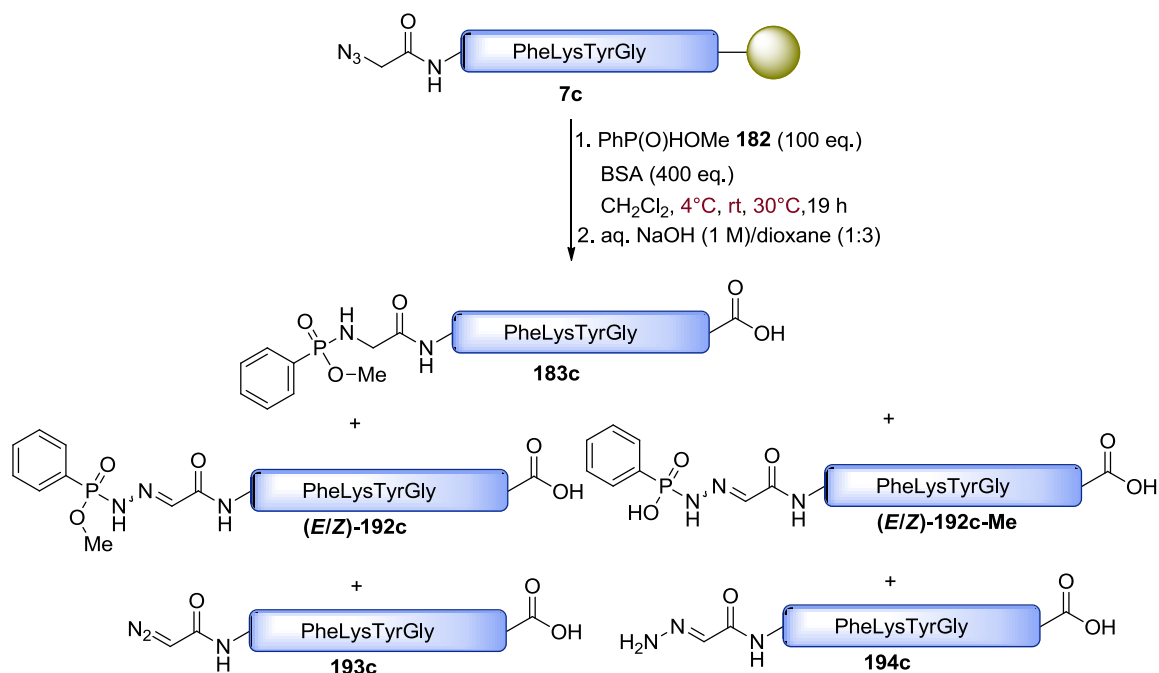


Scheme 84: Standard procedure for the Staudinger reaction on solid support with azido glycine peptides **7c-d**.

3.4.6.1 Temperature effect

The Staudinger reaction was first studied at three different temperatures (4°C, rt and 30°C) (Scheme 85). Therefore, azido peptide **7c** was reacted with methyl phenylphosphinate (**182**) and an excess of BSA in CH₂Cl₂ for 19 h on resin. When the reaction was carried out at 4°C, no phosphonamidate **183c** could be identified at all and also at room temperature and 30 °C only very small quantities of the phosphonamidate **183c** were observed in the UV trace of the LC-MS spectra (2-5%). At 4 °C the side product **(E/Z)-192c** as well as **(E/Z)-192c-Me**, resulting from the cleavage of the methyl ester were the only detectable molecules. At room temperature and 30 °C these two compounds sum up to 47% and 57%. If ester cleavage occurred before or after Staudinger reaction still has to be clarified. Moreover, at room temperature and 30 °C compounds **193c** and **194c** were additionally observed and account for 43% and 30%.

In conclusion, a change in the reaction temperatures did not lead to much higher amounts of the desired phosphonamidate peptide **183c** and compounds arising from decomposition of the phosphazide **197c** account for 90-100% of all detected compounds. Decreasing the temperature was even disadvantageous for the phosphonamidate formation (compare 3.4.5.5, Staudinger reaction at 4 °C with azide **7b**) but presents a possibility to exclusively obtain **(E/Z)-192c**.

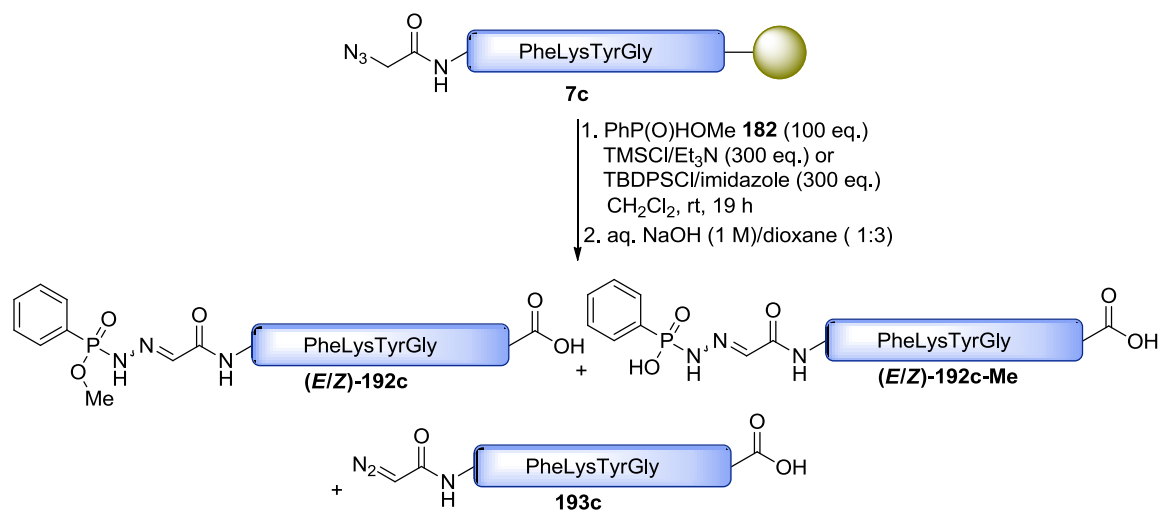


Scheme 85: Staudinger reaction with an azido glycine peptide **7c** at 4°C, rt and 30°C.

3.4.6.2 Influence of the silylation reagent on the Staudinger reaction

On the peptide level, silylation reagents other than BSA were also probed. When using TMSCl and methyl phenylphosphinate (**182**) at room temperature, the side product **(E/Z)-192c** as well as the diazo compound **193c** were predominantly produced at a ratio of >1:3 (Scheme 86). When changing to the larger and more stable TBDPS-group, again only the side product **(E/Z)-192c** and the diazo-compound **193c** were generated. Integration of the UV-trace at 280 nm showed 53% of the side product **(E/Z)-192c** and 27% of the diazo-compound **193c**. Due to the lower reactivity of the TBDPS-group, 20% of the azido-peptide **7c** were not converted. All compounds were obtained with a single TBDPS-group still present on the azido-peptide **7c**.

Similar to the observations with 3-phenylpropyl azide (**7b**), application of the silyl chlorides led mainly or in case of the azido peptides exclusively to the disintegration of the phosphazide **197**. With the azido peptides the phosphonamidate **183c** was not formed at all but the by-product **(E/Z)-192d** was observed in much higher amounts than with **7b**, possibly due to the high excess of silyl phosphonites **215-TMS** or **215-TBDPS** (chapter 3.4.5.6.1 and 3.4.5.6.3).



Scheme 86: Staudinger reaction between an azido glycine peptide **7c** and **182** with TMSCl/Et₃N and TBDPSCI/imidazole as silylation reagents.

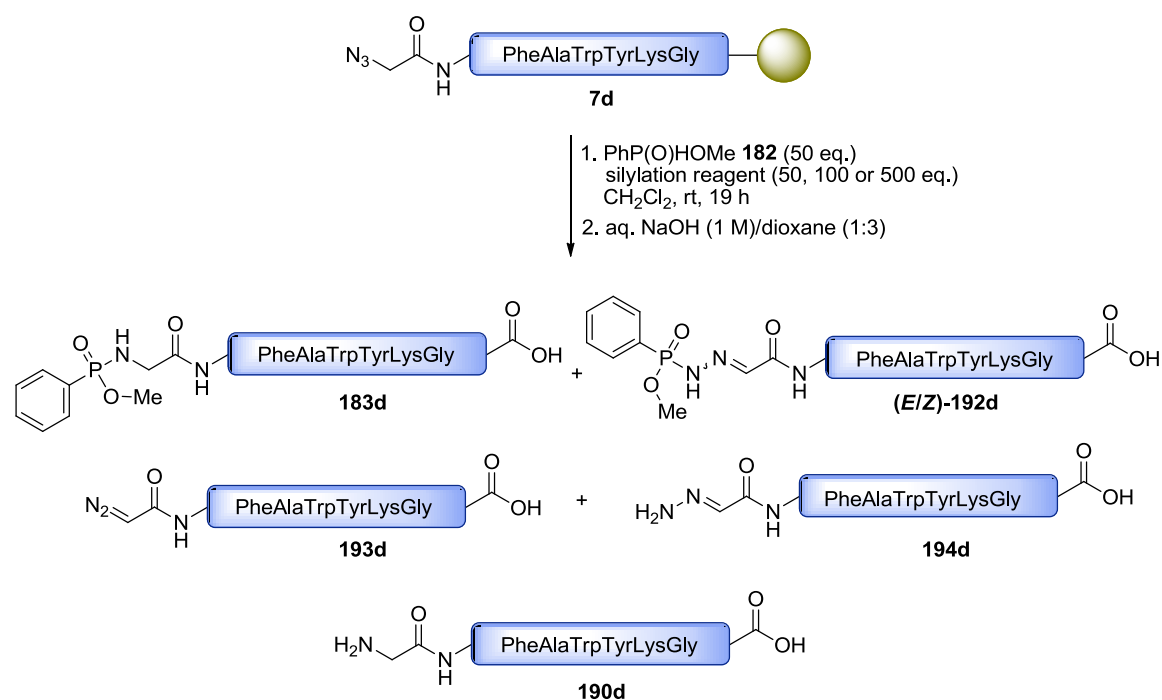
To gather more information on the products, reactions with different equivalents of MSTFA and TBDMSTFA were executed and the products were analyzed by LC-MS (Scheme 87, Table XIV). For these studies model peptide **7d** was chosen with incorporated tryptophan to gain a higher UV activity at 280 nm, an area where the phosphonamide moiety as well as the side product do not absorb so that integration and comparison of the different peptidic signals yield accurate results. With the azido peptides no difference between MSTFA and BSA was observed and MSTFA was applied for a better comparability to MTBSTFA.

Five different compounds could be detected in the spectra. In addition to the desired product **183d** and the side product **(E/Z)-192d**, the diazo compound **193d** resulting from the decomposition of the phosphazide **197d**, a hydrazone derivative **194d** and the amine **190d** were identified. The latter two compounds could arise from the hydrolysis of the phosphonamide **183d**, the phosphonimide **191d** or the corresponding side product **(E/Z)-192d**.

The results reflect again the higher reactivity of MSTFA as compared to MTBSTFA (compare chapter 3.4.5.6). While 50 equivalents of MSTFA were sufficient to completely convert the azido peptide, at least 100 equivalents of MTBSTFA were needed, and the conversion showed some irregularities. However, with regard to the amount of phosphonamide **183d**, MTBSTFA gave much better results. With MTBSTFA as silylation reagent, the phosphonamide **183d** was formed in 16-21%, which presents a significant improvement over the 2-5% detected with MSTFA and BSA. These results are in accordance with the findings obtained with 3-phenylpropyl azide (**7b**), where the conversion to the phosphonamide **183b** was also low but **(E/Z)-192b** was only formed in 1%. Moreover, products arising from the disintegration of the phosphazide **197b**

summed up to only 12-17%, a much lower amount compared to the 80-82% observed with MSTFA. A disadvantage of MTBSTFA are the high amounts of the amino peptide **190d** formed in the reaction resulting from unspecific hydrolysis of the imidate **191d** or decomposition of the product **183d**, which has to be further investigated.

In conclusion, the synthesis of phosphoramidate peptides by the Staudinger reaction with silyl phosphonites **215** on solid support turned out to be rather difficult. The analysis showed that in case of peptides, more phosphoramidate **183d** is formed with the TBDMS-group than with the TMS-group. Nevertheless, the conversion to the phosphoramidate **183d** was unsatisfactory in all cases, and reaction conditions have to be further optimized. However, the described reaction enables the synthesis of (*E/Z*)-**192** (64% with 50 eq. MSTFA) and the diazo peptides **193d** (43% with 500 eq. MSTFA).



Scheme 87: Observed products of the Staudinger reaction with azido glycine peptide **7d** and MSTFA or MTBSTFA as silylation reagent.

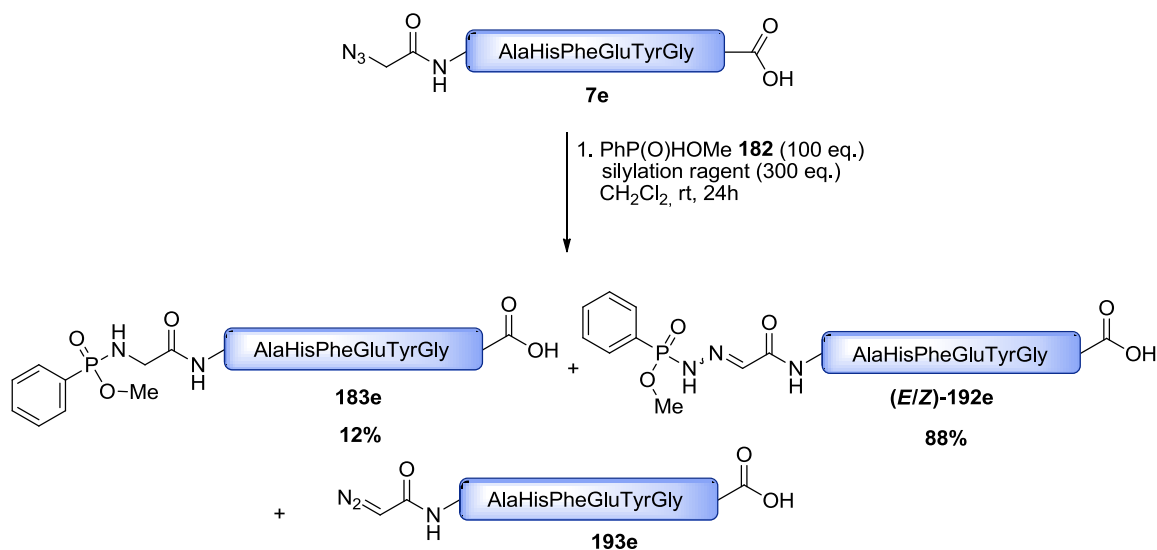
Table XIV: Ratios of the observed products determined by integration of the UV-trace of the LC-MS spectra at 280 nm.

compound	MSTFA (50 eq.)	MSTFA (500 eq.)	MTBSTFA (50 eq.)	MTBSTFA (100 eq.)	MTBSTFA (500 eq.)
183d	2%	3%	5%	12+19 ^a %	10%+6 ^a %
(E/Z)-192d	64%	32%	3%	8%	4%
193d	9%	43%	13%	4%	7%
194d	9%	5%	1%	1%	1%
190d	13%	17%	5%	55%	34%
7d	3%	0%	72%	<1%	38%

^a Second value represents the phosphoramidate peptide with one silyl group on the peptide.

3.4.6.3 Reaction of the azido glycine peptide with methyl phenylphosphinate and BSA in solution

The reaction with an azido glycine peptide **7e** was additionally performed in solution at room temperature and gave similar results with respect to the phosphoramidate formation (Scheme 88). The reaction of the fully unprotected azido glycine peptide **7e** in solution resulted mainly in the side product (*E/Z*)-**192e** (90% based on UV 280 nm) and yielded only 10% of the product **183e**, which was slightly more than before. The diazo compound **193e** could only be detected in traces and the amounts were too low to give a signal in the UV trace. In comparison to the reaction on solid support, the reaction in solution seems to facilitate the conversion of the diazo compound **193e** with the excess of silyl phosphonite **215** to (*E/Z*)-**192e**. When MTBSTFA was used as silylation reagent, product **183e** and the side products (*E/Z*)-**192e** and **196e** were formed. Their separation was not possible so far as one TBDMS group remained on the peptide and further experiments are needed to determine the ratios.



Scheme 88: Staudinger reaction with an azido glycine peptide **7e** in solution.

3.4.6.4 MS/MS measurements of the isolated phosphoramidate peptide and the side product

To further specify the peptide modification at the N-terminus after the Staudinger reaction, the product mixture was separated by HPLC to obtain small quantities of pure products **183e** and (*E/Z*)-**192e** for MS/MS measurement (Figure 25). For both peptides **183e** and (*E/Z*)-**192e**, significant fragments could be detected as listed in Table XV. It could be elucidated by the comparative assessment of the fragments that addition of $m/z = 13$ to the phosphoramidate

183e fragments leads to the corresponding fragments detected for the side product (**(E/Z)-192e**). These results support the assumption that an additional nitrogen is incorporated in the N-terminal part of the peptide (Figure 25).

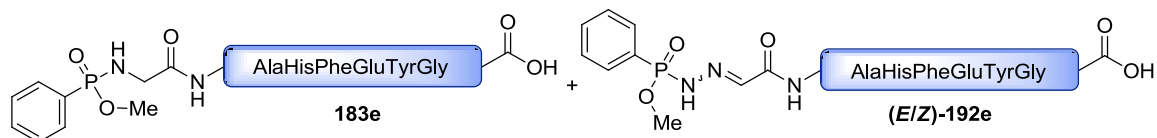


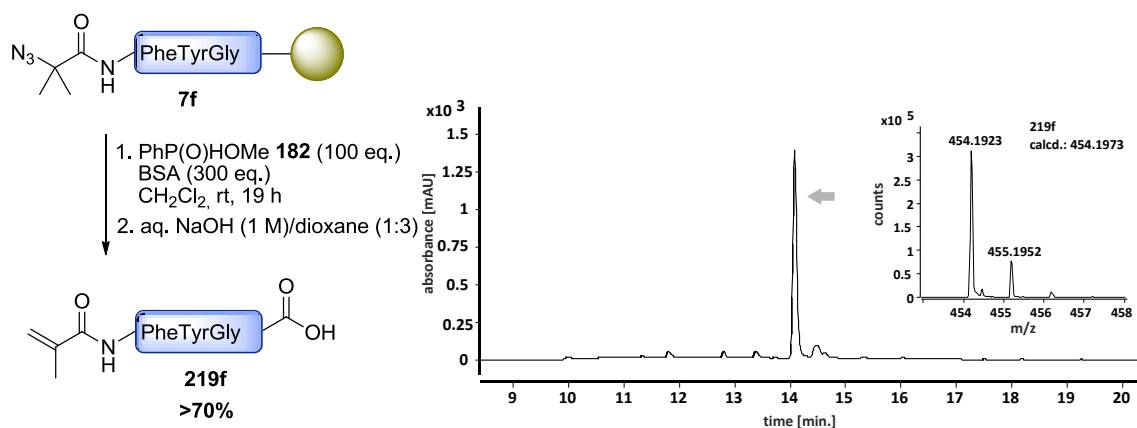
Figure 25: Phosphoramidate peptides **183e** and **(E/Z)-192e** for MS/MS analysis.

Table XV: MS/MS results: detected fragments in comparison.

183e			(E/Z)-192e		
mass (obs.)	mass (calc.)	fragment	mass (obs.)	mass (calc.)	fragment
285.1347	285.1346	HisPhe			
392.1486	392.1482	a4	405.1449	405.1435	a4
420.1450	420.1431	b4	433.1391	433.1384	b4
539.2196	539.2166	a5	552.2131	552.2119	a5
567.2146	567.2115	b5	580.2082	580.2068	b5
652.2759	652.2726	y5			
678.2483	678.2436	b6-H₂O	691.2412	691.2388	b6-H₂O
696.2590	696.2541	b6	709.2526	709.2494	b6
841.3084	841.3069	b7-H₂O			
			844.3245	844.3178	a7
859.3250	859.3175	b7	872.3172	872.3127	b7
876.3464	876.344	c7	889.3412	889.3393	c7
934.3531	934.3495	[M+H]⁺	947.3478	947.3447	[M+H]⁺
956.3358	956.3314	[M+Na]⁺	969.3304	969.3267	[M+Na]⁺

3.4.7 Studies on the Staudinger reaction with 2-azido-2-methyl alanine peptides

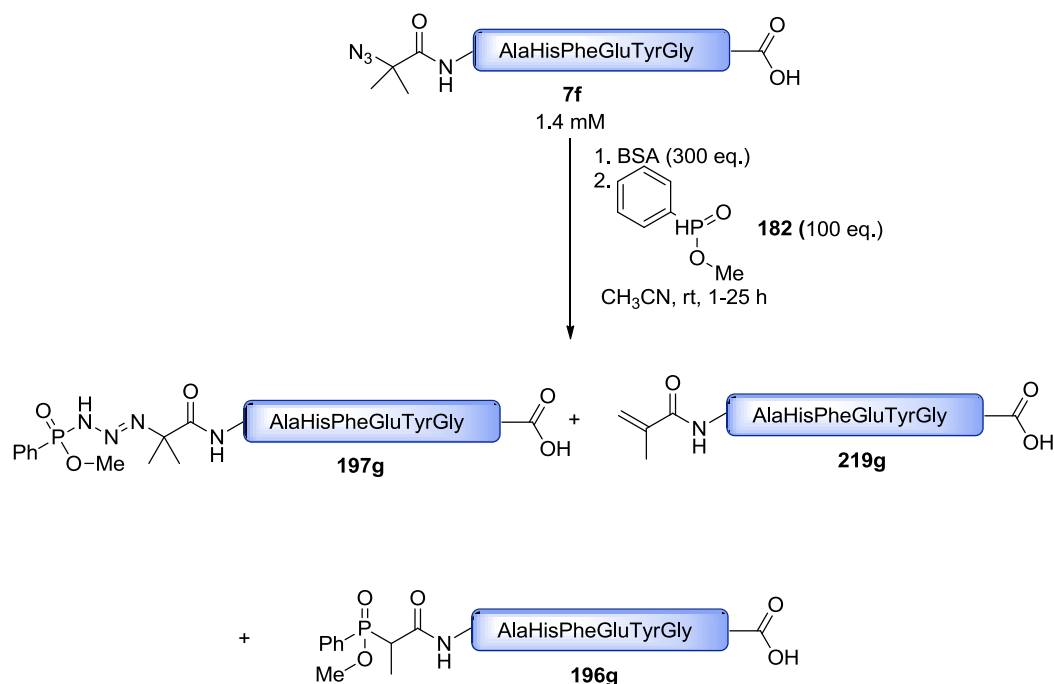
In order to determine whether the methylene group next to the azide and its possible deprotonation is responsible for the decomposition of the phosphazide **197** and formation of **(E/Z)-192**, an unnatural amino acid **7i** with a quaternary carbon next to the azide was employed. The reaction was carried out on resin as well as in solution. First, the azido peptide **7f** was reacted with methyl phenylphosphinate (**182**) and BSA in dichloromethane on resin. After 19 h, the peptidic products were cleaved from the resin under basic conditions and a LC-MS measurement revealed an α,β -unsaturated carbonyl compound **219f** as major product (>70% based on the integration of all peptidic compounds at 280 nm) (Scheme 89 and Figure 26).



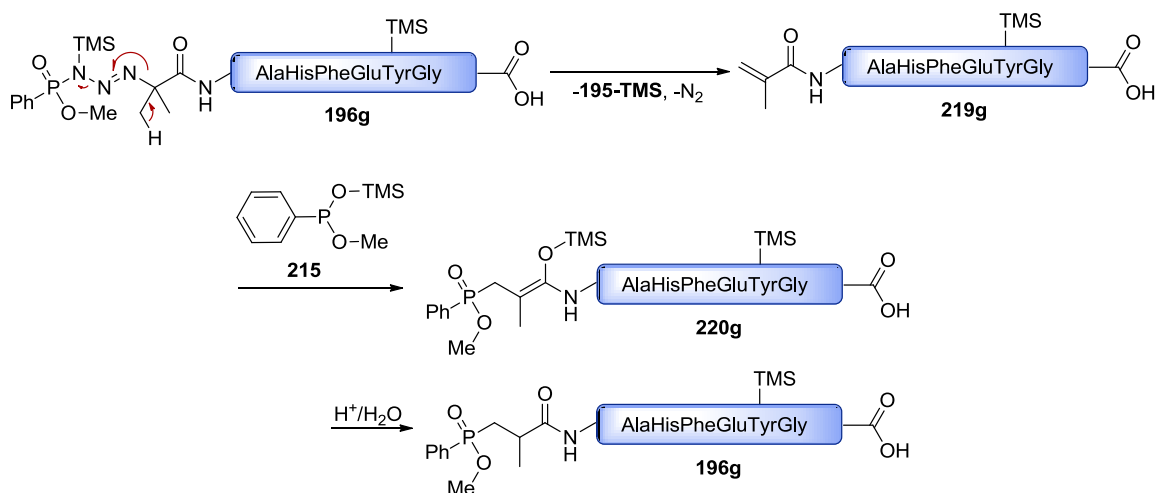
Scheme 89 and Figure 26: Staudinger reaction with azido peptide **7f** on solid support (left) and corresponding LC-MS spectrum (UV trace at 280 nm) (right).

An α,β -unsaturated carbonyl compound as by-product of the Staudinger reaction was never observed before and the most likely explanation for its formation is the elimination of the phosphazide-moiety in form of the phosphonamidate **195** and elemental nitrogen. To investigate the reaction without the influence of strong basic conditions required for the cleavage from the resin, which facilitate the elimination reaction, the reaction was performed in solution in acetonitrile (Scheme 90). After a reaction time of one hour, only two compounds could be found by evaluation of the HRMS spectrum as recorded below (Scheme 90). The azide **7g** had fully reacted with the silyl phosphonite **215** to the phosphazide **197g**. The second signal was identified as the elimination product **219g** with complete loss of the phosphazide moiety to yield the α,β -unsaturated carbonyl **219g**, but no phosphonamidate **183g** could be detected. To prove that elimination does not only occur in the MS, an LC-MS spectrum was recorded. The phosphazide **197g** and a small amount of elimination product were detected in the LC-MS spectrum at different retention times. It is important to note that no side product (*E/Z*)-**192g** was observed, what gave rise to the assumption that deprotonation next to the nitrogen is a major cause for the side product formation and again supports the thesis that the side product (*E/Z*)-**192** is formed from the diazo compound **193**. This hypothesis is also in agreement with the results obtained with alkyl azides (chapter 3.3) and can explain that steric and electronic effects are very important for the formation of the four-membered transition state **198g** if a silyl group is taking part in the reaction. After 25 h the phosphazide **197g** was completely decomposed and only the elimination product **219g** and the phosphinate **196g** could be detected.

It is known from literature that silyl phosphonites **215** can react with α,β -unsaturated carbonyl compounds like **219g** under formation of the silyl enolate **220g**.^[152] The enolate **220g** hydrolysis during HPLC measurement to the phosphinate **196g**.



Scheme 90: Staudinger reaction with a tertiary azide **7g**.

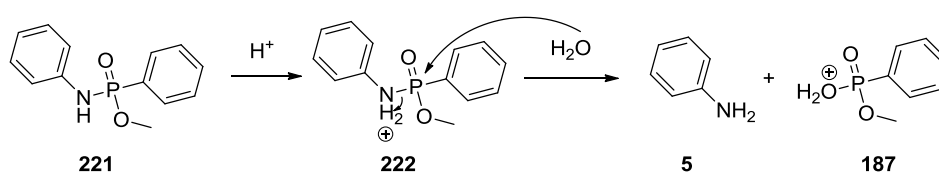


Scheme 91: Formation of the elimination product **219g** and subsequent reaction of the α,β -unsaturated amide **219g** with the phosphonite **215** to the phosphinate **196g**.^[152]

3.5 Stability studies on phosphoramidates

As mentioned before in chapter 3.4.2.2 the Fmoc solid-phase peptide synthesis requires acidic conditions for side chain deprotection (50-100% TFA, 2-3 h). Furthermore, most of the commonly used resins are cleaved under acidic conditions. The P-N-bond of phosphoramidates is susceptible to acidic cleavage, which leads to the formation of phosphonic acid derivatives and primary amines (Scheme 92).^[38b] Substituents at the phosphorus center and the amine have

thereby an influence on the stability of the P-N-bond. For instance, electron-withdrawing groups on the nitrogen decrease the capability for protonation and increase their stability on that expense. To probe the stability of benzyl and aryl phosphoramidates **223** and **221** under common cleavage conditions for peptide synthesis, four different TFA solutions (1%, 25%, 50% and 95% TFA in CH₂Cl₂) were used for stability tests. An equal amount of each of the two compounds was dissolved in 0.5 mL of each TFA-solution, and degradation of the compounds was controlled by ³¹P-NMR spectroscopy between 0 and 26 h. Since the NMR spectra exhibited many signals resulting from protonated intermediates and their interpretation turned out to be rather difficult, HRMS spectra were measured to get a better idea of the formed derivatives.



Scheme 92: P-N-bond cleavage under acidic conditions.

3.5.1 Degradation of methyl *N,P*-diphenylphosphoramidate at different TFA-concentrations

In Table XVI all compounds detected by ESI-TOF MS in TFA-solutions of different concentrations within three hours are compiled. It can be concluded from the measurement that methyl *N,P*-diphenylphosphoramidate (**221**) is stable for more than two hours if the TFA concentration is not higher than 25%, and even with 50% TFA the phosphoramidate **221** can be detected in high proportion compared to the phosphonic acid ester **187** after 2 h 32 min. In 95% TFA the phosphoramidate **221** was completely degraded after 2 h 30 min. Hydrolysis of the monomethyl ester **187** does not occur under all applied conditions.

*Table XVI: Stability study of methyl *N,P*-diphenylphosphoramidate (**221**) in four different TFA solutions. Compounds detected by HRMS ESI-TOF are shown in dependence on the time and TFA concentration.*

TFA concentration	time		
		221	187
95% TFA	30 sec. 2 h 27 min.	major peak no	small major peak

50% TFA	30 sec.	major peak	very small
	14 min.	major peak	small
	2 h 32 min.	large	large
25% TFA	30 sec.	major peak	very small
	22 min.	major peak	very small
	2 h 32 min.	major peak	small
1% TFA	30 sec.	major peak	no
	12 min.	major peak	no
	2 h 42 min.	major peak	no

For the NMR study, methyl *N,P*-diphenylphosphonamidate (**221**) was dissolved in four different trifluoroacetic acid (TFA) solutions in dichloromethane (1%, 25%, 50%, 95%), and ³¹P-NMR spectra of the four samples were measured as a function of time with increasing time-lag. In order to obtain the ability to assign a signal to one of the expected compounds, **187** was measured as standard in the four TFA-solutions. Because phenyl phosphonic acid is commercially available, the monomethyl ester **187** was synthesized from the acid according to a procedure described in chapter 3.4.2.3 (Scheme 62).

Table XVII: Observed signals of the monomethyl ester **187** in different TFA-solutions.

TFA concentration	1%	25%	50%	95%
³¹ P-NMR (ppm)	21.27	26.83	27.12	27.44

In case of 1% TFA the ³¹P-NMR spectrum of methyl *N,P*-diphenylphosphonamidate (**221**) showed only one signal at 21.9 ppm of the phosphonamidate **221** even after 26 h which is in accordance with the HRMS results where no degradation could be observed. Results of the other TFA-solutions can be seen in the diagrams below (Diagram 5-Diagram 7). With reference to the case of 1% TFA, the signal at 25.87 ppm should correspond to the methyl *N,P*-diphenylphosphonamidate (**221**) or its protonated form **222** whereas the signal at 26.96 ppm should be caused by the monomethyl phenylphosphinate **187** in agreement with Table XVII (Diagram 5). The diagram shows that after about three hours in 25% TFA, half of the phosphonamidate **221** is cleaved (Diagram 5). The doubling of the TFA concentration to 50% shortens this time to about one hour (Diagram 6). Finally, in the case of 95% TFA, a value of 0% phosphonamidate **221** is already reached after one and a half hours (Diagram 7). These findings also match with the HRMS measurements where the phosphonamidate **221** could not be detected anymore after 2 h 30 min. Note that increasing the TFA concentration is accompanied by a slight downfield shift of the NMR signals. Additional signals observed in the NMR spectrum could not be assigned to known compounds but the signal between 19 ppm and 20 ppm (red

line, Diagram 5-Diagram 7) seems to be a cleavage intermediate, which increases at the beginning when the decomposition starts and declines when most of the phosphoramidate **221** is disintegrated.

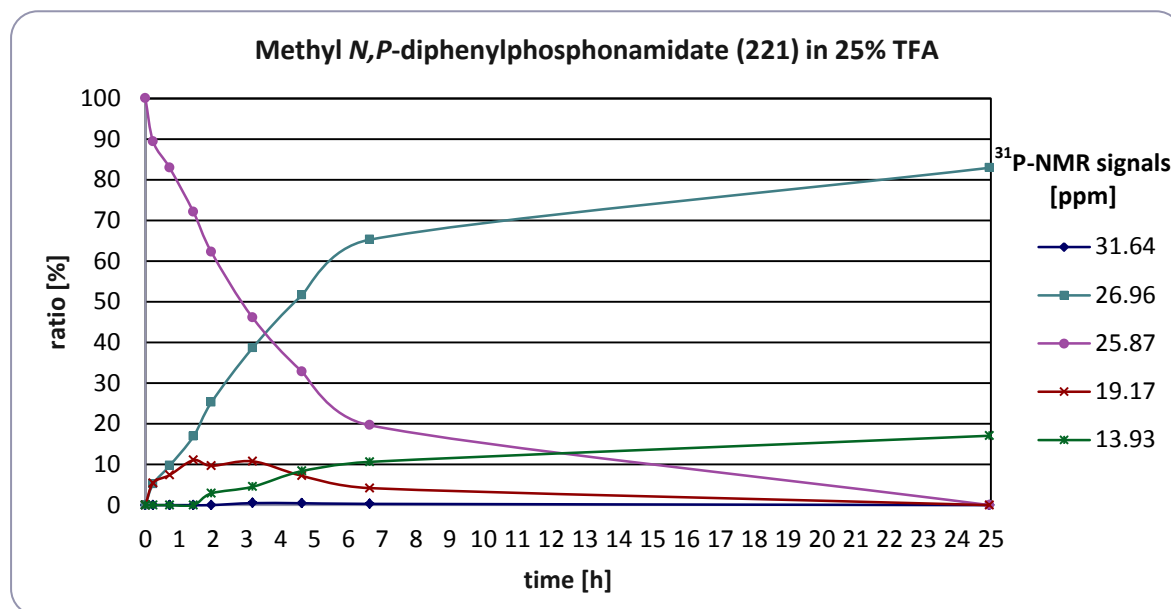


Diagram 5: Decomposition of methyl *N,P*-diphenylphosphoramidate (**221**) in 25% TFA.

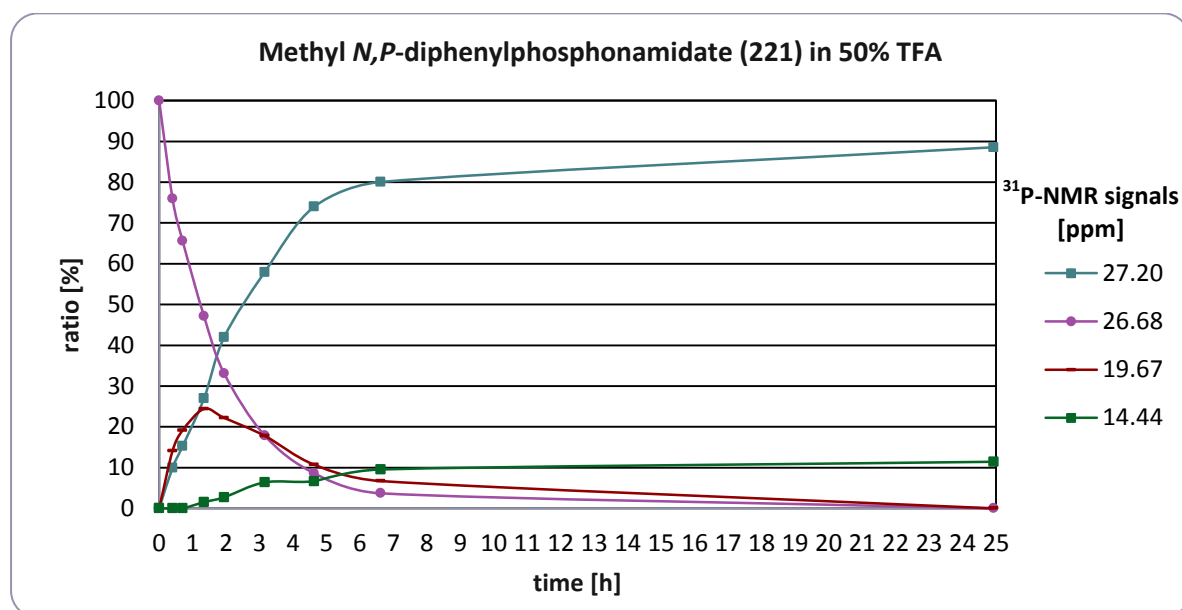
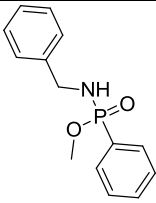
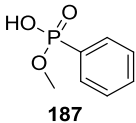


Diagram 6: Decomposition of methyl *N,P*-diphenylphosphoramidate (**221**) in 50% TFA.

Table XVIII: Stability study of methyl *N*-benzyl-*P*-phenylphosphonamidate (**223**) in four different TFA solutions. Compounds detected by ESI-TOF are shown in dependence on the time and TFA concentration.

TFA concentration	time		
		223	187
95% TFA	30 s.	major peak	medium
	2 h 33 min.	no	major peak
50% TFA	30 s	major peak	small
	20 min.	no	major peak
	2 h 30 min.	no	major peak
25% TFA	30 s	major peak	small
	22 min.	no	major peak
	2 h 32 min.	no	major peak
1% TFA	30 s	major peak	no
	2 h 36 min.	major peak	no

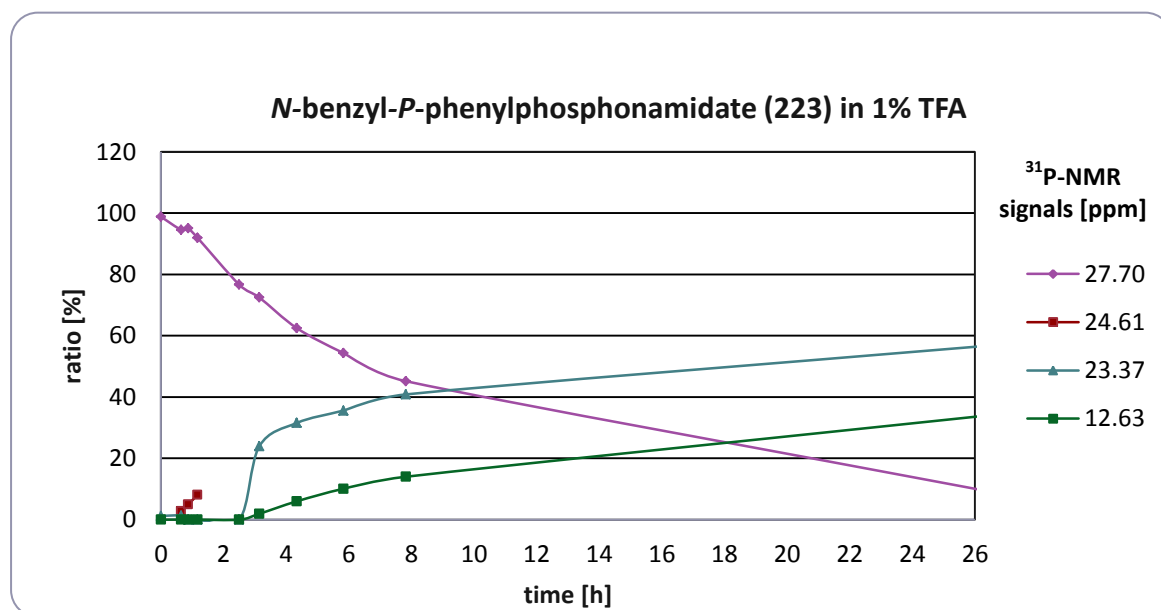


Diagram 8: Decomposition of *N*-benzyl-*P*-phenylphosphonamidate (**223**) in 1% TFA.

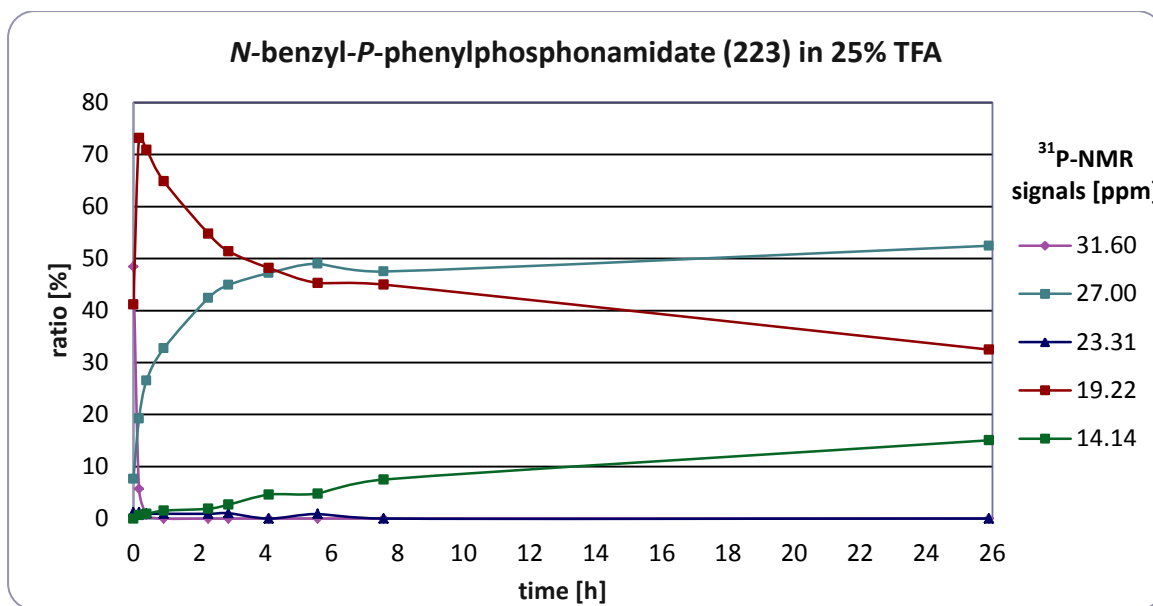


Diagram 9: Decomposition of N-benzyl-P-phenylphosphonamidate (223) in 25% TFA.

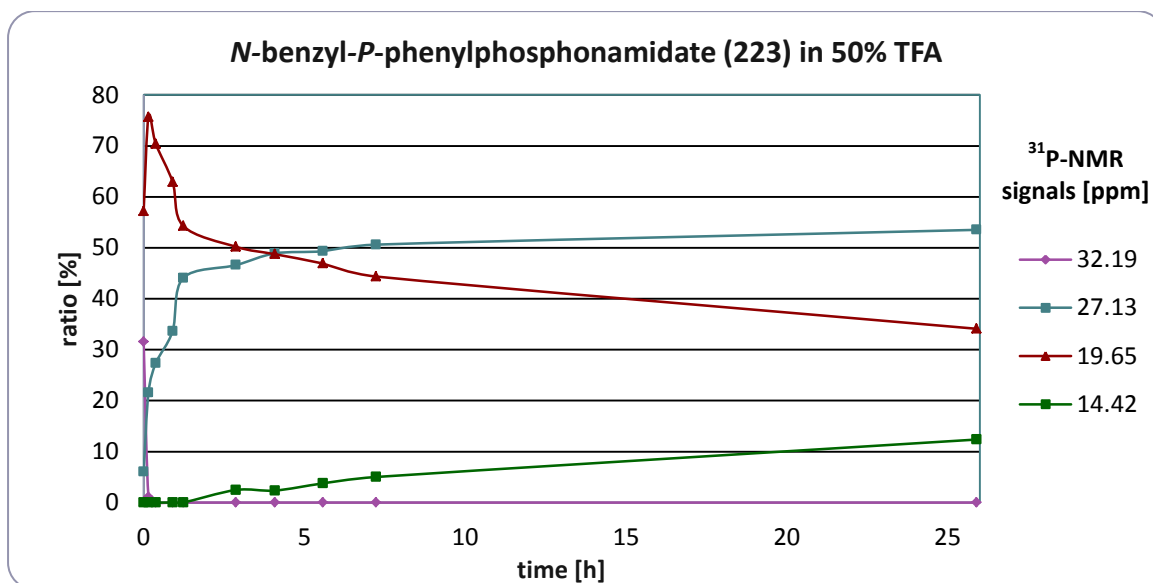


Diagram 10: Decomposition of N-benzyl-P-phenylphosphonamidate (223) in 50% TFA.

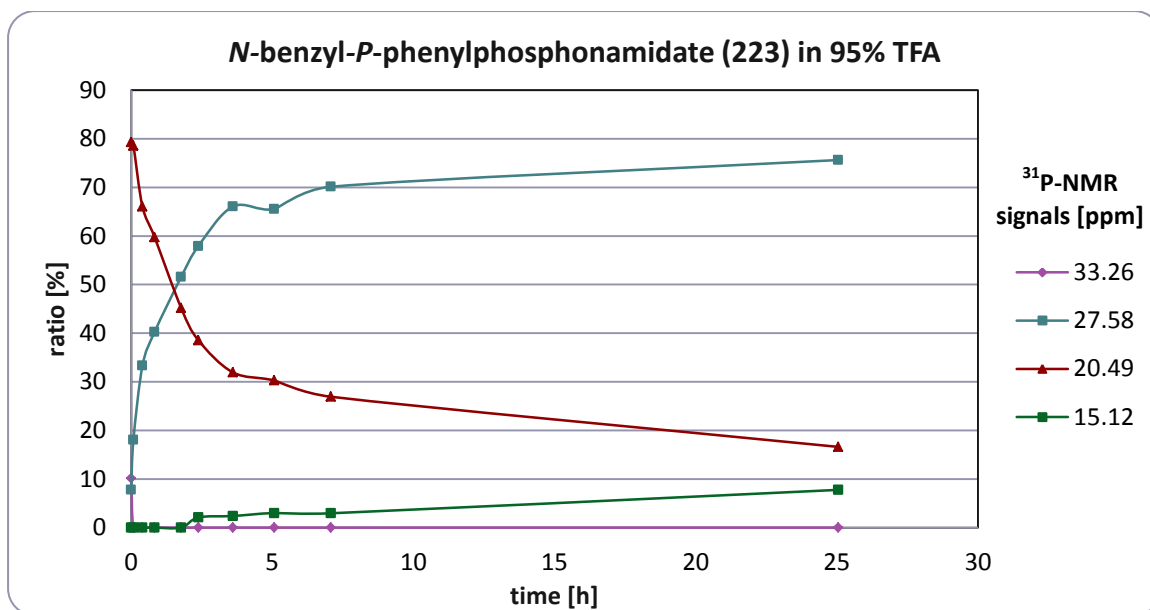


Diagram 11: Decomposition of *N*-benzyl-*P*-phenylphosphoramidate (**223**) in 95% TFA.

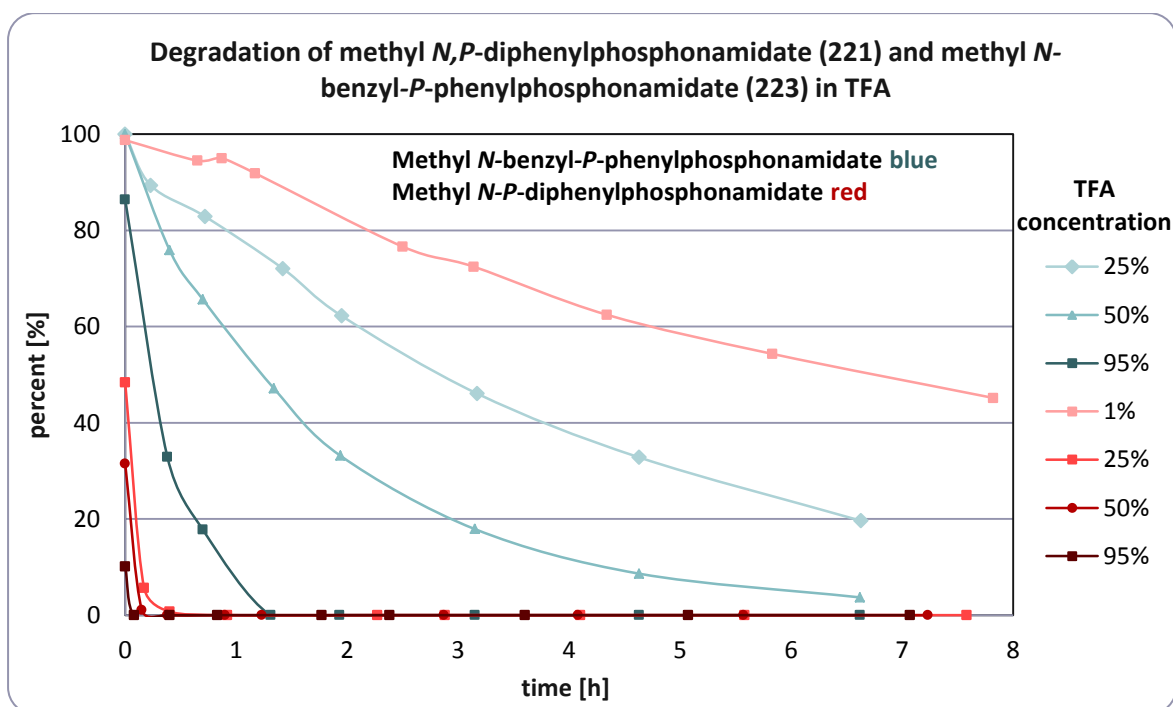


Diagram 12: Degradation of Degradation of methyl *N,P*-diphenylphosphoramidate (**221**) and methyl *N*-benzyl-*P*-phenylphosphoramidate (**223**) in TFA.

As expected, the comparison of the data shows that the phenyl compound **221** is much more stable against acidic cleavage. Nevertheless, neither compounds are stable under conditions that are necessary for the side chain deprotection of common Fmoc-amino acids. This shows that deprotection of the side chains of phosphoramidate peptides under common acidic conditions

would not be possible. Nevertheless, phosphoramidates should be stable under the slightly acidic conditions normally used for HPLC (0.1% TFA or 1% CH₃COOH). Degradation of both compounds in dependence on TFA concentration and time is summarized below (Diagram 12).

4 Conclusion and outlook

Within this thesis, different variants of the Staudinger reaction were investigated for the synthesis of phosphor-, phosphon- and phosphinamidates and their application for peptide and protein modifications. The thesis can be divided into three main projects (chapter 3.1, chapter 3.2, chapter 3.3 and 3.4):

Project I: Lewis acid- and alkyl halide-catalyzed rearrangement of phosphin- and phosphorimidates

Within this first project, an efficient synthetic route to obtain *N,N*-disubstituted phosphoramidates **33a** was developed by optimizing and expanding the scope of the Lewis acid- or alkyl halide-catalyzed rearrangement of phosphorimidates **8a** (Scheme 94). The concept was then transferred to phosphinimidates **8c**, which were not applied in the rearrangement before. The reaction proceeds via a two-step/one-pot process starting from an azide **7** and a phosphite **6a** or phosphinite **6c**. In the first step, the phosphin- or phosphorimidates **8c** and **8a** are formed by the Staudinger reaction. In the second step, the rearrangement is initiated by addition of catalytic amounts of the alkyl halide or the Lewis acid.

In initial studies, the ability of different Lewis acids to induce the rearrangement yielding *N,N*-disubstituted phosphoramidates **33a** was probed by the addition of catalytic amounts of the Lewis acid to the phosphorimidates **8a**. $\text{BF}_3 \cdot \text{Et}_2\text{O}$ and TMSOTf turned out to be the catalysts of choice as nearly quantitative yields of the phosphoramidates **33a** were obtained with 1 mol% of the Lewis acid. Other Lewis acids, like AlCl_3 , TMSCl, TMSBr or TMSI, could not match $\text{BF}_3 \cdot \text{Et}_2\text{O}$ and TMSOTf in reactivity.

To analyze the reaction scope with regard to the azide **7**, different azido compounds were synthesized and employed in the Staudinger reaction. Benzyl, aryl, allyl and alkyl azides could be converted to the desired phosphoramidates **33a** in good to excellent yields (78-98 %). It is important to note that even sterically hindered tertiary azides could be converted successfully. Later on, the reaction scope was extended to azides **7** containing functional groups like a methoxy or a nitro group, and even a peracylated carbohydrate could be employed in the reaction. The corresponding phosphoramidates **33a** were obtained in yields between 65-88%. Not only the azido part could be varied, but also the substituents at the phosphorus could be changed to some extent, and ethyl, allyl and butyl groups could be rearranged delivering the *N,N*-disubstituted phosphoramidates **33a** in yields between 63% and 98%. In contrast, the rearrangement of very long alkyl chains proved to be ineffective. As the reaction was performed

under more diluted conditions compared to previous publications, cross-over experiments were undertaken to attest a partial or complete intermolecular reaction mechanism.

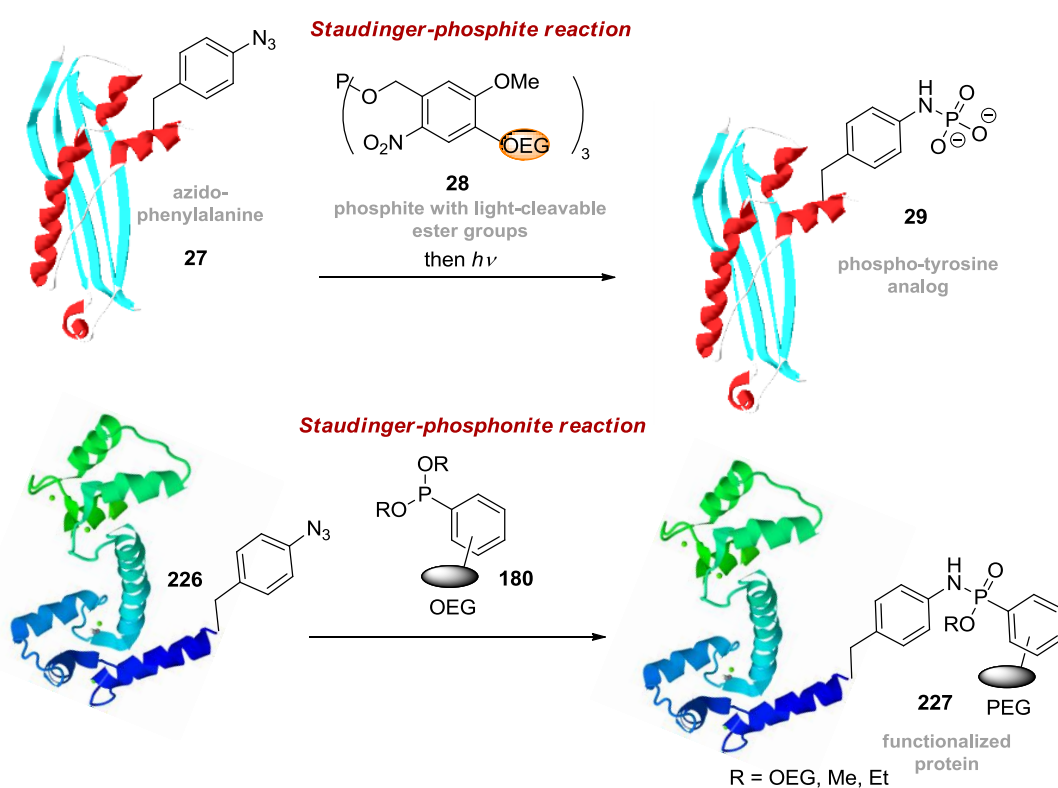
To further facilitate the procedure and avoid isolation of the potentially explosive azides **7**, a one-pot procedure was developed avoiding isolation of the azido compound. The one-pot procedure starts from alkyl bromides, mesylates or tosylates, which are converted to the corresponding azides with sodium azide in acetonitrile at 60°C. Subsequently, the phosphite **6a** is added to the azides **7** followed by the catalyst. It is important to note that complete formation of the phosphorimidate **8a** has to be assured before the catalyst is added. The observed yields were lower compared to the previous results but still good to excellent (52-92%). The limiting factor of the transformation is mainly determined by the substitution of the leaving group by the azide under anhydrous conditions, but also electronic and steric factors turned out to have an influence on the rearrangement like observed for the malonic acid ester.

Next, the rearrangement of phosphinimidates **8c** was studied. First, the alkyl halide-catalyzed variant was used to initiate the rearrangement. Methyl, ethyl and benzyl groups could be effectively rearranged although higher amounts of alkyl halide were needed in comparison to the corresponding phosphorimidates **8a**. The Lewis acid-catalyzed rearrangement could also be applied though yields of the phosphinamidates **33c** were significantly lower. Only the methyl group could be rearranged in comparable high yields.

Project I: Conclusion and outlook

The presented Staudinger reaction and following rearrangement is a valuable method for the synthesis of *N,N*-disubstituted phosphin- and phosphoramidates **33c** and **a** and compliments existing methods. *N,N*-disubstituted phosphin- and phosphoramidates **33c** and **a** are obtained in high yields by a simple and straightforward procedure from easily available starting materials. Future efforts will focus on the application of this methodology for the synthesis of new phosphoramidates and on testing their biological activity. Based on the successful conversion of the azido sugar, the reaction will be probed on more complex molecules or natural products. Moreover, it would be interesting to synthesize phosphites **6a** or phosphinites **6c** with chiral substituents and to employ them in the Staudinger reaction with following rearrangement. In analogy to the work of Denmark *et al.*^[1d, 96c], the resulting *N,N*-disubstituted phosphin- and phosphoramidates would be promising Lewis base catalysts in asymmetric organic reactions.

phosphite **28** was designed that enables the straightforward synthesis of a phospho-tyrosine analogue **29** (Scheme 95). The phosphite was employed for the functionalization of an azido phenylalanine-containing protein **27**, and full conversion of the azide to the phosphoramidate was observed and verified by protein electrophoresis. To test the behavior of the phosphoramidate as a mimic of a phosphorylated protein, the phosphoramidate was saponified under irradiation with a 355 nm laser, and a phospho-tyrosine-specific antibody was applied to the phosphoramidate SecB protein **29** in a Western blot analysis. A strong response to the phosphorylation mimic was evident by luminol-based visualization of the antibody, which proved the success of the concept.



Scheme 95: Staudinger-phosphite and Staudinger-phosphonite reaction for the functionalization of azido proteins.

In the Staudinger-phosphite reaction, hydrolysis of the phosphoramidates **8a** always leads to the loss of one substituent of the phosphite **6a**. Therefore, the functional molecule has to be either incorporated in all three substituents, or the substituents have to be carefully chosen with respect to their leaving group ability. To overcome this problem, phosphonites **6b** were explored as alternatives to phosphites **6a** (general reaction sequence is shown in Scheme 94). Phosphonites **6b** possess one substituent which is connected to the phosphorus by a direct carbon-phosphorus bond that cannot be cleaved during the hydrolysis. Introduction of the

functionalization at this substituent would thereby inhibit the loss of the functional molecule during hydrolysis. Again, the Staudinger-phosphonite reaction was first tested with small molecules, and the reaction of benzyl azide and dimethyl phenylphosphonite delivered the desired phosphoramidates **24b** in high yields between 72% and 83%. Moreover, the reaction could be transferred to unprotected azido peptides in solution as well as on solid support proving the bioorthogonality of the reaction. As methyl phenylphosphonite turned out to be fairly unstable in aqueous solutions and showed a low solubility, aryl-phosphonites **165** functionalized with oligoethyleneglycol chains were synthesized. These compounds reacted rapidly with azido peptides in aqueous systems with high conversions. Subsequently, the impact of different substituents at the phosphonite on the hydrolysis rate as well as the reaction rate was studied, and conversion of azido-calmodulin **226** could prove the applicability for protein functionalization (Scheme 95).

Project II: Conclusion and outlook

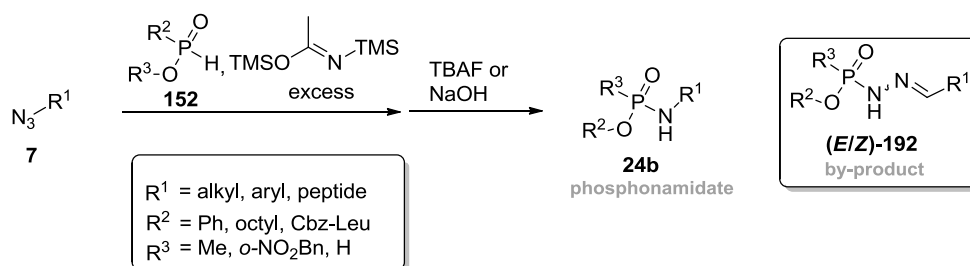
The Staudinger-phosphite and the Staudinger-phosphonite reaction are versatile and metal-free methods for the site-selective functionalization of biomolecules. Both reactions do not interfere with functional groups present in peptides and proteins and proceed smoothly in aqueous systems. Moreover, they stand out due to their clean and high conversions of azido peptides or proteins to the desired phosphoramidates.

The functionalization of peptides and proteins with phosphites or phosphonites offers a wide range of applications including PEGylation, biotinylation, lipidation, phosphorylation or the functionalization with fluorophores, a radioactive label or carbohydrates. Current and future projects are aiming at the direct synthesis of the phosphites and phosphonites and an easy and general entrance for the introduction of a functional molecule. The designed phosphites and phosphonites will thereby allow to study the impact of posttranslational modifications on the behavior, function and structure of proteins more intensively. Moreover, the method can be used for the isolation, purification and visualization of proteins and perhaps even for *in vivo* labeling or bioconjugation.

Project III: Staudinger reaction with silylated phosphinic acid derivatives

In order to develop an easier entrance to phosphoramidates and phosphoramidate peptides **24b** as potential protease inhibitors, the Staudinger reaction between silyl phosphonites and azides **7** was investigated (Scheme 96).

Staudinger reaction with silyl phosphonites



Scheme 96: Staudinger reaction with silyl phosphonites yielding phosphonamidates and phosphonamidate peptides **24b**.

Silylation of the phosphinic acid or ester **152** delivers the silylated trivalent phosphorus species, which can undergo the Staudinger reaction with azides **7** under formation of the phosphonimidate. In this case the phosphinic acid derivatives were favored over phosphonites. Phosphinic acids and their esters are fairly stable whereas phosphonites, especially with an alkyl substituent, are very prone to oxidation and hydrolysis. Moreover, the synthesis of phosphinic acids and aminophosphinic acids is readily established and aminophosphinic acids with different side chains are accessible.^[142]

As silylation reagent, BSA gave the best results and was preferred to TMSCl to avoid salt formation with the yields being nearly the same in both cases when aryl azides were applied. The reaction proceeded well at ambient temperature and acetonitrile as a solvent. Following treatment with TBAF, HF·pyridine or sodium hydroxide solution removed the silyl group and yielded the phosphonamidate **24b**. Phenyl azide and other aryl azides containing different functional groups, like fluoro, carboxy, methoxy or nitro groups, were reacted with methyl phenylphosphinate, benzyl phenylphosphinate or methyl octylphosphinate. The desired phosphonamidates were obtained in moderate to excellent yields between 30% and 95%. Compared to the aryl azides, benzyl azide gave a noticeable lower yield due to the formation of by-products.

Stability tests confirmed the instability of phosphonamidates **24b** under strong acidic conditions, which are commonly applied for the side chain deprotection in Fmoc based solid-phase peptide synthesis. The phosphonamidate derived from phenyl azide thereby showed a significantly higher stability against TFA cleavage than the benzylic derivative.

In order to apply the reaction method for the synthesis of phosphonamidate peptides on solid support, a base-labile TG HMBA resin was used for the synthesis of the azido peptides. This strategy permits complete deprotection of the side chains prior to the Staudinger reaction. The unprotected, solid-supported peptides containing a *para*-azidobenzoic acid at the N-terminus

were subjected to the Staudinger reaction, and the azido peptides underwent clean conversion to the phosphoramidate peptides as confirmed by LC-MS. To our delight, even phosphinic acids yielded the corresponding phosphoramidate with a free OH group at the phosphorus in high conversions and with only small amounts of amino peptides resulting from P-N-bond cleavage. To further simplify the isolation and the storage of the pure product, a *o*-nitrobenzyl phenylphosphinate was synthesized and reacted with an azido peptide. This opens up the possibility to purify and store the compound in its “protected” and more stable form. UV irradiation accomplishes the ester cleavage if needed.

The application of alkyl azides, such as azido glycine, turned out to be more difficult because by-products with very similar retention times during the HPLC measurement were observed, and overall yields were much lower. The structure of the main by-product (***E/Z***-192) could be clarified by HRMS and NMR analysis after isolation (Scheme 96). Furthermore, isotope-labeling experiments with ¹⁵N together with studies on the dependence of the solvent polarity and the silylation reagents supported the exploration of the mechanistic origin of the by-product (***E/Z***-192). Evaluation of the obtained results and comparison with relevant literature led to the proposal of a mechanism which is initiated by decomposition of the phosphazide into methyl *P*-phenylphosphoramidate and a diazo compound. The diazo compound can afterwards react with the silyl phosphonite resulting in the observed by-product.

Similar results were obtained on the peptidic level. In this case, the by-product was formed in larger amounts and additionally the peptidic diazo and hydrazone derivatives could be detected by LC-MS.

Project III: Conclusion and outlook

In conclusion, the Staudinger reaction with silylated phosphinic acid enables the synthesis of phosphoramidates and phosphoramidate peptides with high conversions starting from aryl azides or peptides containing a N-terminal *para*-azidobenzoic acid. The method will be applied to the preparation of potential protease inhibitors, which will have to be tested on different proteases. Furthermore, future efforts will focus on the development of a synthetic strategy that allows the attachment of aminophosphinic acids and esters to the C-terminus of peptides. This would enable the conjugation of two peptidic fragments by the Staudinger reaction resulting in peptides with the phosphoramidate-moiety in the center of the peptide. This would be desirable for the design of inhibitors with a high specificity and binding strength.

In case of alkyl azides, a by-product with a P(O)-NH-N=C-moiety was generated. By probing different reaction conditions it was found that unpolar solvents like *n*-hexane or benzene and an

excess of BSA as silylation reagent gave the best results with respect to the phosphoramidate formation. These conditions will be applied for the synthesis of a variety of phosphoramidates with different substituents at the nitrogen including secondary and tertiary substituents to further broaden the reaction scope. Moreover, the optimized conditions will be used for the synthesis of small inhibitors. Based on the observations on the peptidic level where the phosphoramidate was generated only in small amounts compared to the by-product, it would be interesting to employ single azido amino acids or azido dipeptides to investigate the influence of the acid or amide functionality on the by-product formation at the small molecule level.

The by-product (***E/Z***-192) was preferentially formed in more polar solvents like acetonitrile or DMF, with more than one equivalent of the silyl phosphonite and at low temperatures. These reaction conditions will also be further optimized and applied for the synthesis (***E/Z***-192) derivatives and diazo compounds.

On the peptidic level, MTBSTFA gave the best results with regard to the phosphoramidate peptide formation and will be used for the synthesis of phosphoramidate peptides to test their inhibitory ability. In contrast to the small alkyl azides, the side product (***E/Z***-192) was in all other cases mainly formed. At 4°C in dichloromethane and with MSTFA as silylation reagent it was even the only product. Further studies will show if peptidic derivatives containing P(O)-NH-N=C- moiety also possess an interesting biological activity. Moreover, the reaction enables the access to diazo peptides although yields have to be improved.

5 Experimental part

Materials: All reagents, starting materials and solvents were purchased from commercial suppliers and used without further purification if not further mentioned. Phenyl phosphinic acid, 3-phenylpropyl bromide, dodecyl bromide and anhydrous solvents (CH_3CN , CH_2Cl_2 , DMF, DMSO, THF, benzene, pyridine, *n*-hexane) were purchased from ACROS ORGANICS.

Peptide Synthesis: Peptides were synthesized using standard amide coupling conditions HBTU/HOBt utilizing a NovaSyn® TG HMBA resin or a glycine-preloaded Wang resin (Novabiochem). All amino acids were purchased from Novabiochem.

Methods: LC-UV and LC-MS spectra were recorded on an Agilent 6210 TOF LC/MS system, Agilent Technologies, Santa Clara, CA, USA. Spray voltage was set to 4 kV. Drying gas flow rate was set to 25 psi. Separation of the sample was performed on a Luna 5 μ C18(2) 100 A column (5 μm , 4.6 \times 150 mm) at a flow rate of 0.5 mL/min.

Preparative HPLC purification for peptides was performed on a JASCO LC-2000 Plus system using a Kromasil RP18 column (25 \times 250 mm) at a flow rate of 16 mL/min.

Flash chromatography was performed on silica gel (Acros Silicagel 60 A, 0.035-0.070 mm). TLC was performed on aluminium-backed silica plates (60 mash F254, 0.2 mm, Merck), which were developed using basic potassium permanganate solution as visualizing agent.

^1H -NMR and ^{13}C -NMR spectra were recorded at Jeol ECX/400. H,H-COSY, HMBC and HMQC were recorded at Jeol ECP/500. The residual solvent signal was used as internal standard relative to TMS. ^{15}N -NMRs were recorded at Jeol ECX/400, Bruker AVANCE III 500 and Bruker AVANCE III 700. For ^{15}N -NMRs, CD_3CN was used as internal standard and set to -137.6 ppm relative to CH_3NO_2 .

5.1 Synthesis of azido compounds 7a,b,h,i

5.1.1 Synthesis of dodecyl azide (7a), 3-phenylpropyl azide (7b) and ¹⁵N-labeled 3-phenylpropyl azide (¹⁵N-7b)

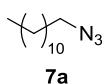


Dodecyl azide (**7a**), 3-phenylpropylazide (**7b**) and ¹⁵N-labeled 3-phenylpropylazide (¹⁵N-**7b**) were synthesized according to a procedure developed by Alvarez and Alvarez.^[145a]

General procedure I:

The alkyl bromide (10.0 mmol) was added to a solution of sodium azide (11.0 mmol, 715 mg) in DMSO (22 mL). The reaction mixture was stirred overnight at room temperature and was afterwards diluted with water (50 mL). The reaction mixture was allowed to cool to room temperature and was subsequently extracted with diethyl ether (3 x 30 mL). The combined organic layers were extracted with water (2 x 50 mL) and brine (50 mL). The organic layer was dried over MgSO₄ and filtrated before the ether was removed under reduced pressure. The azide was obtained as pure compound without further purification.

5.1.2 Dodecyl azide (7a)

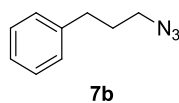


Dodecyl azide (**7a**) was synthesized according to **general procedure I** from dodecyl bromide (**184a**) (10.0 mmol, 2.49 g, 2.40 mL). Dodecyl azide (**7a**) was obtained as a pale oil in a yield of 90% (9.00 mmol, 1.90 g).

¹H-NMR (250 MHz, CDCl₃): δ [ppm] = 3.25 (t, ³J_{H,H} = 6.9 Hz, 2H, CH₂-N), 1.65 – 1.54 (m, 2H, CH₂), 1.43 – 1.13 (m, 18H, CH₂), 0.88 (t, ³J_{H,H} = 6.6 Hz, 3H, CH₃).

NMR data are in accordance with those reported in the literature.^[153]

5.1.3 3-Phenylpropyl azide (7b)

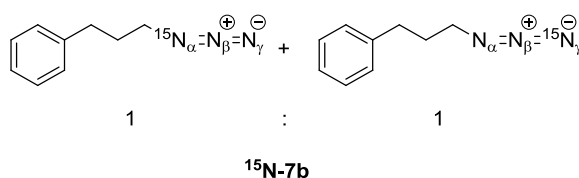


3-Phenylpropyl azide (**7b**) was synthesized according to **general procedure I** from 3-phenylpropyl bromide (**184b**) (10.00 mmol, 1.99 g, 1.52 mL). 3-Phenylpropyl azide (**7b**) was obtained as a pale oil in a yield of 87% (8.70 mmol, 1.40 g).

$^1\text{H-NMR}$ (400 MHz, CDCl_3): δ [ppm] = 7.36 – 7.27 (m, 2H, Ar), 7.25 – 7.17 (m, 3H, Ar), 3.30 (t, $^3J_{\text{H,H}} = 6.8$ Hz, 2H, $\text{CH}_2\text{-N}$), 2.72 (t, $^3J_{\text{H,H}} = 7.6$ Hz, 2H, $\text{CH}_2\text{-Ph}$), 1.97 – 1.85 (m, 2H, CH_2).

NMR data are in accordance with those reported in the literature.^[154]

5.1.4 ^{15}N -3-Phenylpropyl azide (^{15}N -7b)

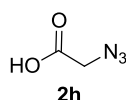


^{15}N -3-Phenylpropyl azide (^{15}N -7b) was synthesized from 3-phenylpropyl bromide (0.50 mmol, 0.10 g, 76 μL) and ^{15}N -sodium azide (terminal) (0.55 mmol, 36 mg) according to **general procedure I**. ^{15}N -3-Phenylpropyl azide was obtained as a pale oil in a yield of 71% (0.36 mmol, 57 mg). Labeling was achieved in a ratio of $\sim 1:1$ in the N_α - and N_γ -position. Spectra can be found in the appendix.

$^1\text{H-NMR}$ (400 MHz, CD_3CN): δ [ppm] = 7.46 – 7.00 (m, 5H, Ar), 3.32-2.29 (m, 2H, $\text{CH}_2\text{-}^{14/15}\text{N}$), 2.67-2.70 (m, 2H, $\text{CH}_2\text{-Ph}$), 1.90 – 1.85 (m, 2H, CH_2); $^{13}\text{C-NMR}$ (176 MHz, CD_3CN): δ [ppm] = 142.5 (Ar), 129.4 (Ar), 129.4 (Ar), 127.0 (Ar), 51.5 ($\text{CH}_2\text{-N}$), 51.5 (d, $^1J_{\text{C-N}} = 3.9$ Hz, $\text{CH}_2\text{-}^{15}\text{N}$), 33.4 ($\text{CH}_2\text{-Ph}$), 31.3 (CH_2); $^{15}\text{N-NMR}$ (41 MHz, CD_3CN): δ [ppm] = -173.67 (s), -312.49- -312.53 (m).

5.1.5 Synthesis of azido acetic acid (7h)

Azido acetic acid (**7h**) was synthesized following a procedure by Lundquist *et al.*^[145b]



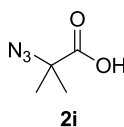
Sodium azide (46.0 mmol, 3.00 g, 2.1 eq.) was suspended in DMSO (120 mL) and stirred at room temperature for 2 h. Afterwards, bromoacetic acid (**184h**) (22.0 mmol, 3.06 g, 1.58 mL) was

added drop wise to the solution. After 12 h, the reaction mixture was diluted with water (100 mL) and acidified with concentrated hydrochloric acid (20 mL). The aqueous solution was extracted with ethyl acetate (3 x 70 mL). The organic layers were combined, washed with brine, dried over MgSO₄, and concentrated to give 85 % (1.81 g, 17.9 mmol) of the desired product (**7h**) as pale oil.

¹H-NMR (400 MHz, CDCl₃): δ [ppm] = 3.75 (s, 2H, CH₂).

NMR data are in accordance with those reported in the literature.^[150b]

5.1.6 2-Azido-2-methylpropionic acid (**7i**)



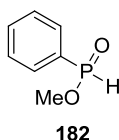
2-Azido-2-methylpropionic acid (**7i**) was synthesized following a procedure by Meldal *et al.*^[145c] Sodium azide (1.44 g, 22.2 mmol, 1.5 eq.) was added to a solution of 2-bromo-2-methylpropionic acid (**184i**) (2.48 g, 14.9 mmol) in dry DMF (25 mL) under argon atmosphere at room temperature and the reaction was stirred for 3 days. Afterwards, the reaction mixture was concentrated under reduced pressure and redissolved in H₂O (15 mL). The aqueous solution was acidified to pH 2 with aqueous hydrochloric acid (3 M) and extracted with CH₂Cl₂ (3 x 15 mL). The organic phase was dried over MgSO₄ and the solvent was removed under reduced pressure. 2-Azido-2-methylpropionic acid (**7i**) was obtained in a yield of 63% (1.21 g, 9.37 mmol) containing 0.5 eq. of DMF judged by ¹H-NMR. The azide was not further purified because a solution of the azide in DMF is needed for the peptide coupling.

¹H-NMR (400 MHz, CDCl₃): δ [ppm] = 1.49 (s, 6H, Me), 11.08 (s, 1H, COOH).

NMR data are in accordance with those reported in the literature.^[145c]

5.2 Synthesis of methyl phenylphosphinate (**182**), monomethyl phenylphosphinate (**187**) and methyl *P*-phenylphosphonamidate (**195**)

5.2.1 Synthesis of methyl phenylphosphinate (**182**)

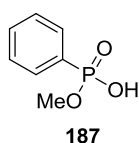


Phenylphosphinic acid (**185**) (710 mg, 5.00 mmol) was dissolved in dichloromethane (80 mL) and one equivalent methyl chloroformate (386 μ L, 473 mg, 5.00 mmol) was added to the solution followed by one equivalent of pyridine (403 μ L, 396 mg, 5.00 mmol). When evanescent had stopped, the reaction mixture was refluxed for 15 min. and was afterwards cooled to room temperature. The reaction mixture was poured into hydrochloric acid (0.1 M, 30 mL) and the organic layer was washed with water (50 mL) and dried over MgSO_4 . The solvent was removed under reduced pressure and the pure ester (**182**) was obtained without further purification as a pale liquid in a yield of 82% (767 mg, 4.91 mmol).^[146a]

$^1\text{H-NMR}$ (400 MHz, CDCl_3): δ [ppm] = 7.68-7.91 (m, 2H, Ar), 7.41-7.69 (m, 3H, Ar), 7.52 (d, $^1J_{\text{H,P}} = 566.1$ Hz, 1H, P-H); 3.81 (d, $^3J_{\text{H,P}} = 12.0$ Hz, CH_3); $^{13}\text{C-NMR}$ (101 MHz, CDCl_3): δ [ppm] = 133.1 (d, $^4J_{\text{C,P}} = 2.6$ Hz, Ar), 130.8 (d, $^2J_{\text{C,P}} = 11.9$ Hz, Ar), 129.2 (d, $^1J_{\text{C,P}} = 131.5$ Hz, Ar), 128.7 (d, $^3J_{\text{C,P}} = 13.8$ Hz, Ar), 52.0 (d, $^2J_{\text{C,P}} = 6.6$ Hz, CH_3); $^{31}\text{P-NMR}$ (162 MHz, CDCl_3): [ppm] = 27.7. HRMS (ESI-TOF): $m/z = 157.0411$ [$\text{M}+\text{H}$] $^+$ (calcd. for $[\text{C}_7\text{H}_{10}\text{O}_2\text{P}]^+$: $m/z = 157.0413$).

Spectroscopic data are in accordance with those reported in the literature.^[146a]

5.2.2 Synthesis of monomethyl phenylphosphinate (**187**)



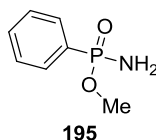
Thionyl chloride (540 μ L, 885 mg, 7.43 mmol, 1.2 eq.) was added to a solution of phenyl phosphonic acid (**186**) (978 mg, 6.00 mmol) in dry DMF (30 mL) at -20 $^\circ\text{C}$. The reaction mixture was allowed to warm up 0 $^\circ\text{C}$ and was kept at that temperature for 20 min. Afterwards methanol (369 μ L, 292 mg, 9.12 mmol, 1.5 eq.) was added and the reaction mixture was stirred overnight

at room temperature. Then, saturated sodium bicarbonate solution (60 mL) was added. The resulting aqueous solution was washed with diethyl ether (2 x 50 mL) and acidified with concentrated hydrochloric acid. The product was extracted with ethyl acetate (3 x 50 mL) and the combined organic phases were dried over MgSO_4 and filtrated. The ethyl acetate was removed under reduced pressure and monomethyl phenylphosphonate (**187**) was obtained in yield of 60% (595 mg, 3.60 mmol) as a pale liquid.^[147]

$^1\text{H-NMR}$ (400 MHz, CDCl_3): δ [ppm] = 7.82-7.73 (m, 2H, Ar), 7.53-7.47 (m, 1H, Ar), 7.44-7.37 (m, 2H, Ar), 3.65 (d, $^3J_{\text{H,P}} = 11.4$ Hz, 3H, CH_3); $^{31}\text{P-NMR}$ (162 MHz, CDCl_3): [ppm] = 21.35.

Spectroscopic data are in accordance with those reported in the literature.^[147]

5.2.3 Synthesis of methyl *P*-phenylphosphonamidate (**195**)



Methyl *P*-phenylphosphonamidate (**195**) was synthesized by the Atherton-Todd reaction according to literature procedure.^[116]

To a mixture of methyl phenylphosphinate (**182**) (156 mg, 1.00 mmol), Et_3N (279 μL , 202 mg, 2.00 mmol), and CCl_4 (1 mL) in acetonitrile (5 mL) was added ammonia solution (28% in water, 1 mL) at 0 °C. The mixture was kept at 0 °C for 30 min. and afterwards stirred at room temperature overnight. The solvent was removed under a reduced pressure, and water was added. The mixture was extracted with EtOAc, and the organic layers were dried over MgSO_4 . After filtration and removal of the solvent, methyl *P*-phenylphosphonamidate (**195**) was obtained in a yield of 97% (166 mg, 0.971 mmol).

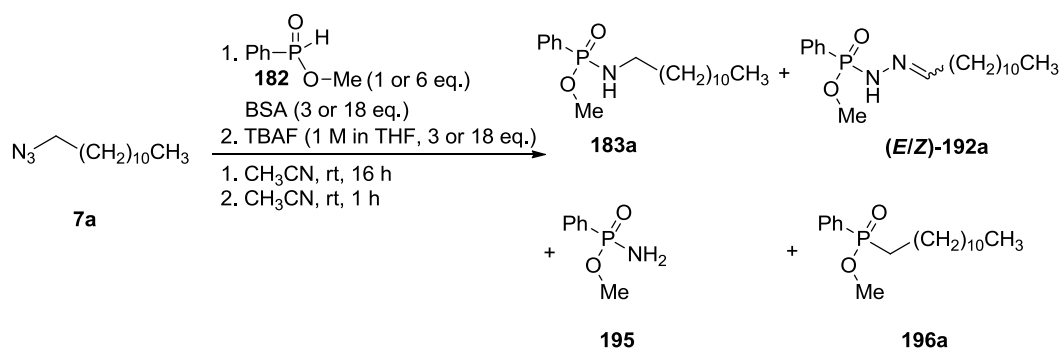
$^1\text{H-NMR}$ (500 MHz, CD_3CN): δ [ppm] = 7.79 – 7.74 (m, 2H), 7.58 – 7.53 (m, 1H), 7.51 – 7.45 (m, 2H), 3.63 (d, $^3J_{\text{H,P}} = 11.4$ Hz, 3H); $^{13}\text{C-NMR}$ (101 MHz, CD_3CN): δ [ppm] = 133.1 (d, $^4J_{\text{C,P}} = 3.1$ Hz), 133.1 (d, $^1J_{\text{C,P}} = 172.9$ Hz), 132.1 (d, $^2J_{\text{C,P}} = 10.0$ Hz), 129.7 (d, $^3J_{\text{C,P}} = 14.4$ Hz), 52.06 (d, $^2J_{\text{C,P}} = 5.8$ Hz); $^{31}\text{P-NMR}$ (202 MHz, CD_3CN): δ [ppm] = 26.00; HRMS (ESI-TOF): $m/z = 171.0487$ [$\text{M}+\text{H}$]⁺ (calcd. for $[\text{C}_7\text{H}_{10}\text{NO}_2\text{P}]^+$: $m/z = 171.0449$).

5.3 Staudinger reaction of silylated phosphinic acids esters with dodecyl and 3-phenylpropyl azide

5.3.1 General procedure for the Staudinger reaction with silylated phosphinic acids esters

General procedure II: The methyl phenylphosphinate (**182**) was added to a solution of the azide **7a** or **b** in the appropriate solvent, followed by the silylation reagent. The reaction mixture was stirred at room temperature overnight before TBAF (1 M in THF) was added. Afterwards, the reaction mixture was stirred for an additional hour. The solvent was removed under reduced pressure and the residue was dissolved in ethyl acetate. The solution was filtered over a pad of silica gel to remove the TBAF and further purified by HPLC or partially purified by column chromatography (ethylacetate : cyclohexane, (1:1 to 3.1)).

5.3.2 Staudinger reaction with dodecyl azide (**7a**)



The reaction was performed according to **general procedure II** with dodecyl azide (**7a**) (0.50 mmol, 0.11 g), methyl phenylphosphinate (**182**) (0.50 mmol, 78 mg) and BSA (1.50 mmol, 305 mg, 367 μL) in acetonitrile (3 mL). The reaction mixture was stirred for 16 h before TBAF (1 M in THF, 1.50 mL, 1.50 mmol) was added. The crude product mixture was analyzed by ^{31}P -NMR.

^{31}P -NMR (162 MHz, CDCl_3): [ppm] = 45.24 (1%, compound **196a**), 25.18 (40%, compound **195**), 23.91 (29%, compound **183a**), 21.39 (5%, compound **(Z)**-**192a**), 20.00 (25%, compound **(E)**-**192a**). The reaction was repeated with 6 eq. of methyl phenylphosphinate (**182**) (3.0 mmol, 468.36 mg) and BSA (9.00 mmol, 1.83 g, 2.20 mL). The reaction mixture was stirred for 16 h before TBAF (1 M in THF, 9.00 mL, 9.00 mmol) was added. The crude product mixture was analyzed by ^{31}P -NMR.

^{31}P -NMR (162 MHz, CDCl_3): [ppm] = 45.56 (2%, compound **196a**), 25.10 (31%, compound **195**), 24.01 (26%, compound **183a**), 20.77 (6%, compound **(Z)**-**192a**), 19.73 (22%, compound **(E)**-**192a**). Separation of the products by column chromatography was not successful, but the partially purified compounds were further analyzed by NMR as discussed in chapter 3.4.5.1. Spectra can be found in the appendix.

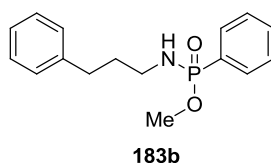
196a: HRMS (ESI-TOF): m/z = 325.2288 $[\text{M}+\text{H}]^+$ (calcd. for $[\text{C}_{19}\text{H}_{34}\text{O}_2\text{P}]^+$: m/z = 325.2291).

195: HRMS (ESI-TOF): m/z = 172.0561 $[\text{M}+\text{H}]^+$ (calcd. for $[\text{C}_7\text{H}_{11}\text{NO}_2\text{P}]^+$: m/z = 172.0522).

183a: HRMS (ESI-TOF): m/z = 340.2397 $[\text{M}+\text{H}]^+$ (calcd. for $[\text{C}_{19}\text{H}_{35}\text{NO}_2\text{P}]^+$: m/z = 340.2400).

(E/Z)-**192a**: HRMS (ESI-TOF): m/z = 353.2351 $[\text{M}+\text{H}]^+$ (calcd. for $[\text{C}_{19}\text{H}_{34}\text{N}_2\text{O}_2\text{P}]^+$: m/z = 353.2352).

5.3.3 Synthesis of methyl *P*-phenyl-(3-phenylpropyl)phosphonamidate (**183b**)



The reaction was performed according to **general procedure II** with 3-phenylpropyl azide (**7b**) (0.50 mmol, 81 mg), methyl phenylphosphinate (**182**) (0.50 mmol, 78 mg) and BSA (1.50 mmol, 305 mg, 1.10 mL) in dichloromethane (3 mL) and stirred for 16 h before TBAF (1 M in THF, 1.50 mL, 1.50 mmol) was added. A ^{31}P -NMR spectrum was measured of the crude mixture.

^{31}P -NMR (162 MHz, CD_3CN): [ppm] = 25.87 (23%, compound **195**), 24.76 (58%, compound **183b**), 22.06 (3%, compound **(Z)**-**192b**), 20.48 (16%, compound **(E)**-**192b**).

The same reaction was performed in acetonitrile and a ^{31}P -NMR spectrum was measured.

^{31}P -NMR (162 MHz, CD_3CN): [ppm] = 25.88 (32%, compound **195**), 24.81 (43%, compound **183b**), 22.14 (5%, compound **(Z)**-**192b**), 20.59 (20%, compound **(E)**-**192b**).

The same reaction in acetonitrile was repeated with 6 eq. of methyl phenylphosphinate (**182**) (3.0 mmol, 468.36 mg) and BSA (9.00 mmol, 1.83 g, 2.20 mL). The reaction mixture was stirred for 16 h before TBAF (1 M in THF, 9.00 mL, 9.00 mmol) was added. A ^{31}P -NMR spectrum was measured.

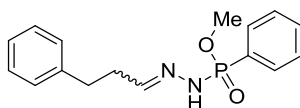
^{31}P -NMR (162 MHz, CD_3CN): [ppm] = 42.65 (9%, compound **196b**), 24.99 (27%, compound **195**), 23.93 (38%, compound **183b**), 20.74 (5%, compound **(Z)**-**192b**), 19.45 (21%, compound **(E)**-**192b**).

The first reaction in dichloromethane and 1 eq. of methyl phenylphosphinate (**182**) was worked up for analysis of the compounds. Dichloromethane was removed under reduced pressure and

The product mixture was further purified by semi-preparative HPLC with the following solvent gradient (A = H₂O, B = CH₃CN): 0-5 min. 0% B, 5-70 min. 0-100% B, 70-80 min., 80-85 min. 100% B, 85-90 min. 100-20% B. The pure product ^{14/15}N-**183b** was obtained in a yield of 31% (22.5 mg, 7.74 μmol) as a 1:1 mixture of the labeled and the unlabeled compound.

¹H-NMR (400 MHz, CD₃CN): [ppm] = 7.76–7.70 (m, 2H, Ar), 7.57–7.52 (m, 1H, Ar), 7.50–7.45 (m, 2H, Ar), 7.27–7.22 (m, 2H, Ar), 7.18–7.11 (m, 3H, Ar), 3.63 (d, ³J_{H,P} = 11.1 Hz, 3H, CH₃-O), 2.92–2.76 (m, 2H, CH₂-N), 2.59–2.55 (m, 2H, CH₂-Ph), 1.74–1.66 (m, 2H, CH₂); ¹³C-NMR (120 MHz, CD₃CN): [ppm] = 143.1 (Ar), 132.8 (d, ¹J_{C,P} = 171.4 Hz, Ar), 132.6 (d, ⁴J_{C,P} = 2.9 Hz, Ar), 132.1 (d, ²J_{C,P} = 9.6 Hz, Ar), 129.4 (d, ³J_{C,P} = 14.0 Hz, Ar), 129.3 (Ar), 129.3 (Ar), 126.7 (Ar), 51.5 (d, ²J_{C,P} = 5.9 Hz, CH₃-O), 41.12 (CH₂-N), 41.11 (d, ¹J_{C,N} = 7.8 Hz, CH₂-N), 34.42 (d, ²J_{C,P} = 5.5 Hz, CH₂-Ph), 34.4 (CH₂-Ph), 33.5–33.5 (m, CH₂); ¹⁵N-NMR (41 MHz, CD₃CN): [ppm] = -334.64 (dd, ¹J_{N,H} = 83.5 Hz, ¹J_{N,P} = 18.2 Hz); ³¹P-NMR (162 MHz, CD₃CN): [ppm] = 24.04; **183b**: HRMS (ESI-TOF): m/z = 290.1307 [M+H]⁺ (calcd. for [C₁₆H₂₁NO₂P]⁺: m/z = 290.1304); ¹⁵N-**183b**: HRMS (ESI-TOF): m/z = 291.1279 [M+H]⁺ (calcd. for [C₁₆H₂₁¹⁵NO₂P]⁺: m/z = 291.1263).

5.3.5 Synthesis of (*E/Z*)-methyl phenyl(2-(3-phenylpropylidene)hydrazinyl)phosphinate ((*E/Z*)-**192b**)



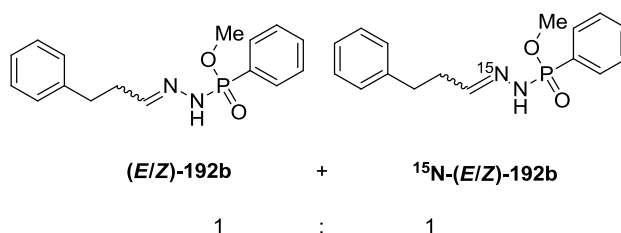
(*E/Z*)-**192b**

The procedure is described for methyl *P*-phenyl-(3-phenylpropyl)phosphonamidate (**183b**). (*E/Z*)-**192b** was formed as a by-product in the described reaction and was obtained after purification by HPLC in a yield of 10% (7.56 mg, 25.0 μmol).

¹H-NMR (400 MHz, CD₃CN): [ppm] = 7.77–7.70 (m, 2H, Ar), 7.60–7.54 (m, 2H, Ar), 7.50–7.44 (m, 3H, Ar), 7.31–7.14 (m, 7H, Ar, =CH-N(*E*)), 6.57 (t, ³J_{H,H} = 5.3 Hz, 1H, =CH-N (*Z*)), 3.67 (d, ³J_{P,H} = 11.2 Hz, 3H, CH₃-O (*Z*)), 3.65 (d, ³J_{P,H} = 11.2 Hz, 3H, CH₃-O (*E*)), 2.82–2.76 (m, 2H, CH₂-N (*Z*)), 2.76–2.70 (m, 2H, CH₂-N (*E*)), 2.50–2.42 (m, 2H, CH₂-Ph (*Z*)), 2.43–2.37 (m, 1H, CH₂-Ph (*E*)); ¹³C-NMR (101 MHz, CD₃CN): [ppm] = 148.5 (d, ¹J_{C,P} = 16.7 Hz, =CH-N (*E*)), 148.0 (d, ¹J_{C,P} = 16.2 Hz, =CH-N(*Z*)), 142.3 (Ar (*Z*)), 142.0 (Ar (*E*)), 132.9 (d, ⁴J_{C,P} = 3.4 Hz, Ar (*Z*)), 132.9 (d, ⁴J_{C,P} = 3.0 Hz, Ar (*E*)), 132.3 (d, ²J_{C,P} = 9.6 Hz, Ar (*Z*)), 132.2 (d, ²J_{C,P} = 9.6 Hz, Ar (*E*)), 131.4 (d, ¹J_{C,P} = 176.7 Hz, Ar), 129.3 (Ar, (*E*)), 129.3 (Ar, (*Z*)), 129.2 (Ar, (*E*)), 129.2 (Ar, (*Z*)), 129.2 (s, ³J_{C,P} = 14.5 Hz, Ar, (*E*)), 129.2 (s,

$^3J_{C,P} = 14.5$ Hz, Ar, (*Z*)), 127.02 (Ar, (*Z*)), 126.8 (Ar, (*E*)), 51.7 (d, $^2J_{C,P} = 6.5$ Hz, CH₃-O (*Z*)), 51.7 (d, $^2J_{C,P} = 6.3$ Hz, CH₃-O (*E*)), 34.6 (CH₂-Ph (*Z*)), 33.2 (CH₂ (*E*)), 32.4 (CH₂-Ph (*Z*)), 28.6 (CH₂ (*Z*)); ^{31}P -NMR (162 MHz, CD₃CN): [ppm] = 20.16 (*Z*), 19.10 (*E*); HRMS (ESI-TOF): $m/z = 303.1252$ [M+H]⁺ (calcd. for [C₁₆H₂₀N₂O₂P]⁺: $m/z = 303.1257$).

5.3.6 Synthesis of $^{14/15}\text{N}$ -(*E/Z*)-methyl phenyl(2-(3-phenylpropylidene)hydrazinyl)phosphinate (^{15}N -(*E/Z*)-192b) (1:1)



The procedure is described for ^{15}N -methyl *P*-phenyl- (3-phenylpropyl)phosphonamidate (^{15}N -183b). (*E/Z*)-192b and ^{15}N -(*E/Z*)-192b is formed as a by-product in the described reaction and was obtained after HPLC in a yield of 13% (9.83 mg, 32.5 μmol).

^1H -NMR (400 MHz, CD₃CN): [ppm] = 7.77–7.70 (m, 2H, Ar), 7.60–7.54 (m, 2H, Ar), 7.50–7.44 (m, 3H, Ar), 7.31–7.15 (m, 4H, Ar, =CH-N (*E/Z*)), 6.60–6.53 (m, 1H, =CH-N (*Z*)), 3.67 (d, $^3J_{P,H} = 11.2$ Hz, 3H, CH₃-O (*Z*)), 3.65 (d, $^3J_{P,H} = 11.2$ Hz, 3H, CH₃-O (*E*)), 2.83–2.75 (m, 2H, CH₂-N (*Z*)), 2.77–2.70 (m, 2H, CH₂-N (*E*)), 2.53–2.46 (m, 2H, CH₂-Ph (*Z*)), 2.46–2.40 (m, 1H, CH₂-Ph (*E*)); ^{13}C -NMR (101 MHz, CD₃CN): [ppm] = 147.7 (d, $^1J_{C,P} = 16.6$ Hz), 147.6 (dd, $^1J_{C,P} = 16.9$ Hz, $^2J_{C,N} = 14.5$ Hz), 141.4 (Ar), 132.1 (d, $^4J_{C,P} = 3.1$ Hz, Ar), 131.4 (d, $^2J_{C,P} = 9.6$ Hz, Ar), 130.4 (d, $^1J_{C,P} = 176.8$ Hz, Ar), 128.6 (Ar), 128.4 (d, $^3J_{C,P} = 14.3$ Hz, Ar), 128.4 (Ar), 126.0 (Ar), 50.9 (d, $^2J_{C,P} = 6.3$ Hz, CH₃-O), 33.6 (CH₂-N), 33.5 (d, $^3J_{C,N} = 5.0$ Hz, CH₂-N), 32.1–32.2 (m, CH₂); ^{31}P -NMR (162 MHz, CD₃CN): [ppm] = 20.22 (d, $^2J_{P,N} = 15.6$ Hz), 19.15, 19.15 (d, $^2J_{P,N} = 13.1$ Hz); ^{15}N -NMR (41 MHz, CD₃CN): [ppm] = -64.22 (d, $^2J_{N,P} = 13.2$ Hz); (Intensity of the signal for the *Z*-isomer was too low for analysis by ^{13}C -NMR and ^{15}N -NMR); (*E/Z*)-192b: HRMS (ESI-TOF): $m/z = 303.1252$ [M+H]⁺ (calcd. for [C₁₆H₂₀N₂O₂P]⁺: $m/z = 303.1257$); ^{15}N -(*E/Z*)-192b: $m/z = 304.1228$ [M+H]⁺ (calcd. for [C₁₆H₂₀¹⁵N₂O₂P]⁺: $m/z = 304.1227$).

5.3.7 Dependence of the Staudinger reaction on the solvent, temperature and silylation reagent

The reaction procedures are described in each chapter. NMR and HRMS methyl *P*-phenyl-(3-phenylpropyl)phosphoramidate **183b** and of (*E/Z*)-methyl phenyl(2-(3-phenylpropylidene)hydrazinyl)phosphinate (***E/Z*-192b**) data were in accordance with the data obtained before (chapter 5.3.3 and 5.3.5). Methyl *P*-phenylphosphoramidate (**195**) was not isolated, but could be identified by HRMS. Based on the HRMS data and the chemical shift the signal at 24.8 ppm was attributed to **195**.

195: HRMS (ESI-TOF): $m/z = 172.0526$ $[M+H]^+$ (calcd. for $[C_7H_{11}NO_2P]^+$: $m/z = 172.0522$).

195+TBDPS: HRMS (ESI-TOF): $m/z = 410.1713$ $[M+H]^+$ (calcd. for $[C_{23}H_{29}NO_2PSi]^+$: $m/z = 410.1700$).

195+TES: HRMS (ESI-TOF): $m/z = 286.1392$ $[M+H]^+$ (calcd. for $[C_{13}H_{25}NO_2PSi]^+$: $m/z = 286.1387$).

5.3.7.1.1 Calibration curve

Ten different amounts between 0.1 nmol and 2.0 nmol of methyl *P*-phenyl-(3-phenylpropyl)phosphoramidate **183b** and of (*E/Z*)-methyl phenyl(2-(3-phenylpropylidene)hydrazinyl)phosphinate (***E/Z*-192b**) were injected to the LC-MS and the signals of the UV-traces at 226 nm were integrated. For the LC-MS-measurement following gradient was applied (A = 1% AcOH in H₂O, B = 1% AcOH in CH₃CN): 0-3 min. 20% B, 3-11 min. 20-90% B, 11-16 min. 90-100% B, 16-21 min. 100% B, 21-26 min. 100-20% B.

All integrals in mAU·min were plotted against the injected quantity in nmol and a line of best fit was adjusted. The resultant linear equations were applied to all subsequent measurements for the determination of the ratio between **183b** and (***E/Z*-192b**) under different reaction conditions. The obtained data and the corresponding linear equation are displayed below (Diagram 13, Table XIX). Two exemplary spectra are shown below (Figure 27):

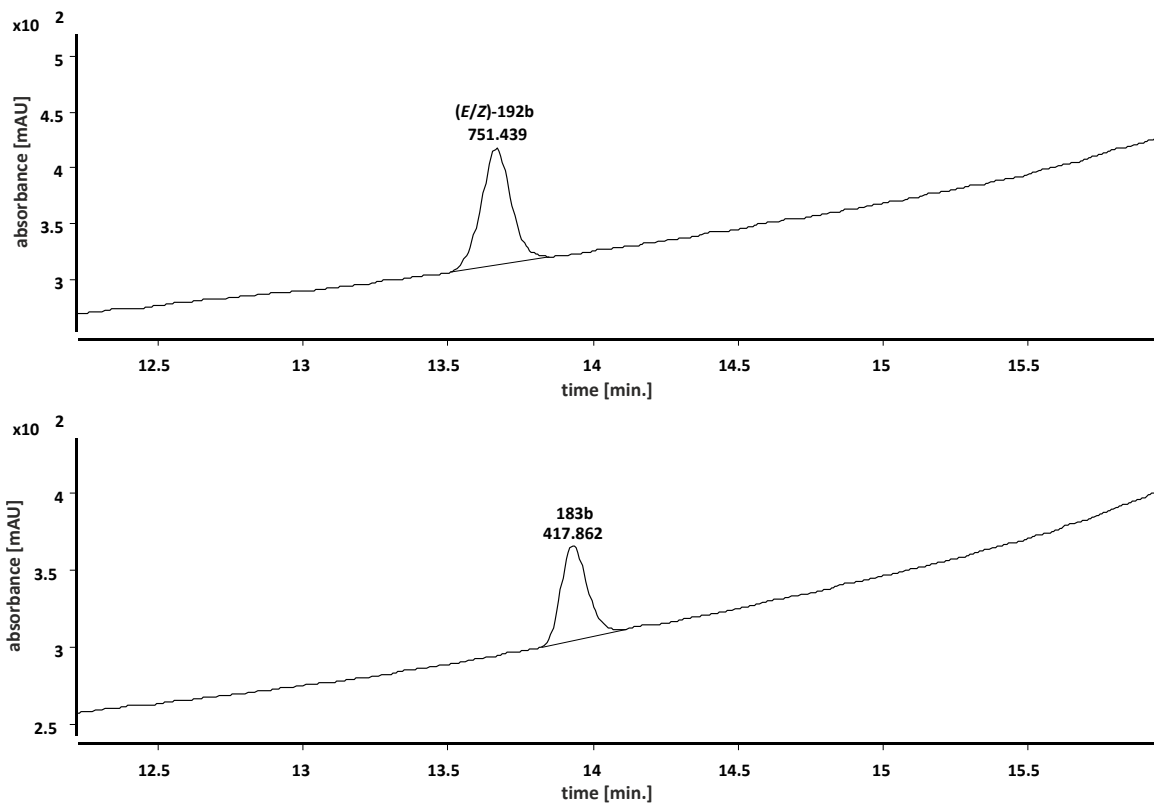


Figure 27: UV-trace of the LC-MS spectrum at 226 nm for **(E/Z)-192b** (1.5 nmol) and for **183b** (2.0 nmol). Integrals are given in mAU·min.

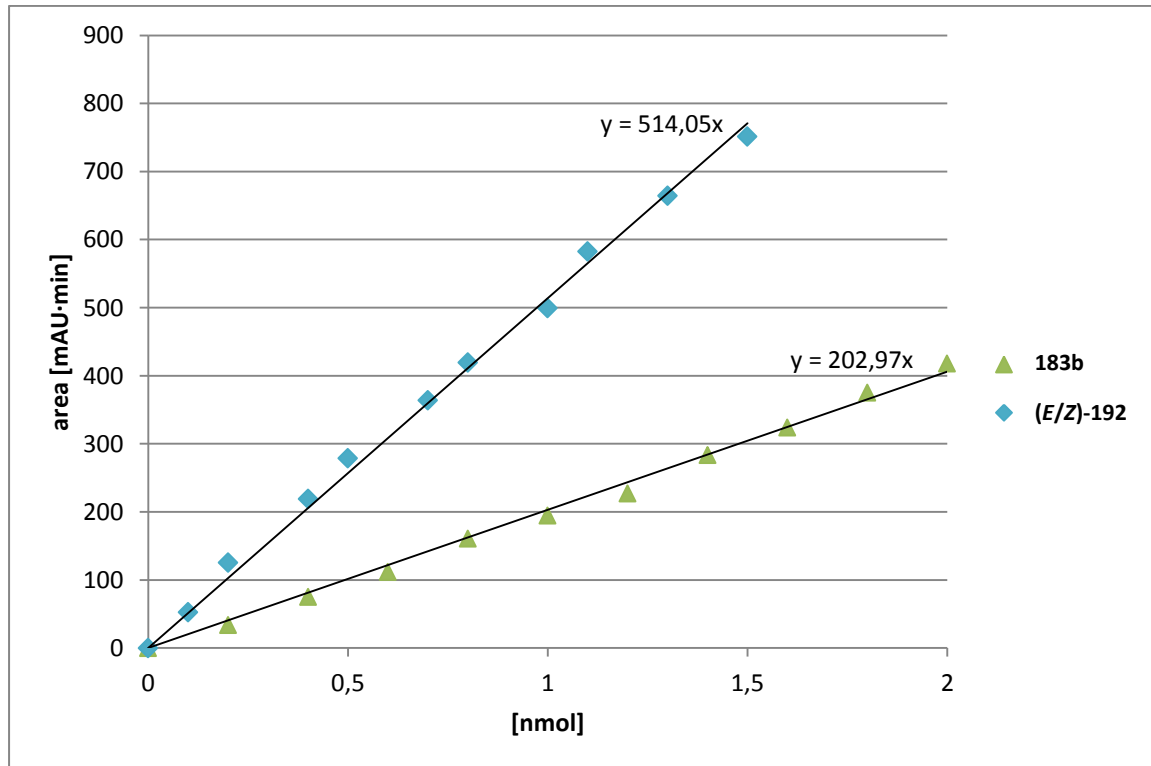
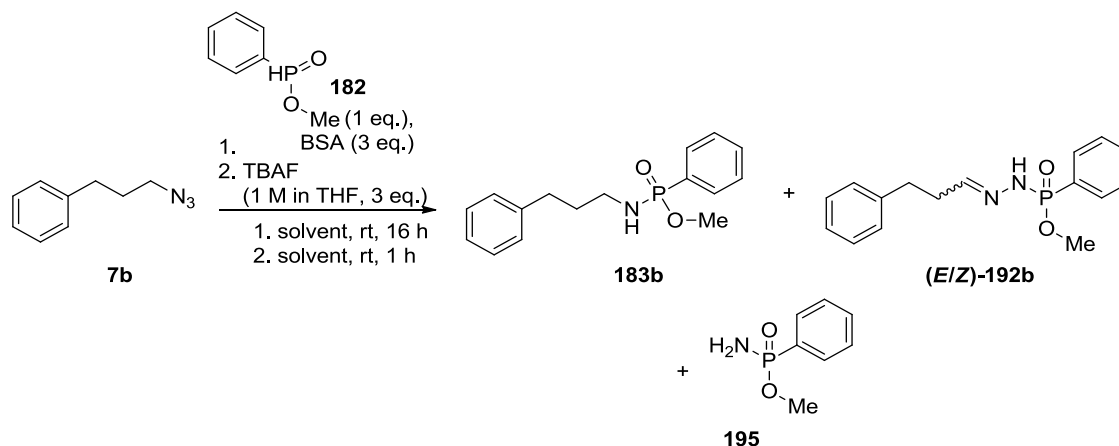


Diagram 13: Area of the signals in mAU·min obtained from the UV-traces at 226 nm plotted against the injected amount of **183b** and **(E/Z)-192b** in nmol. Linear equations of the lines of best fit are given for both compounds.

Table XIX: Area in mAU·min obtained by integration of the signals of the UV-trace from the LC-MS measurements for different amounts of **183b** and (*E/Z*)-**192b**.

(E/Z)-192b		183b	
[nmol]	[mAU·min]	[nmol]	[mAU·min]
0	0	0	0
0.1	52.536	0.2	33.621
0.2	125.643	0.4	74.953
0.4	219.049	0.6	111.967
0.5	278.736	0.8	160.730
0.7	363.924	1.0	194.493
0.8	419.232	1.2	226.976
1.0	499.237	1.4	283.593
1.1	582.750	1.6	324.026
1.3	664.487	1.8	375.083
1.5	751.439	2.0	417.862

5.3.7.2 Solvent effect



All reactions were performed following the **general procedure II**.

The reactions were performed with 3-phenylpropyl azide (**7b**) (0.50 mmol, 80.6 mg), methyl phenylphosphinate (**182**) (0.50 mmol, 78.1 mg) and BSA (1.50 mmol, 229 mg, 279 μ L) in the respective solvent (2.0 mL) and stirred for 16 h. Afterwards TBAF (1 M in THF, 1.5 mL, 1.5 mmol) was added and the reaction mixture was stirred for an additional hour. A ^{31}P -NMR spectrum was measured of the reaction mixture before the solvent was removed under reduced pressure. The ^{31}P -NMR spectra were integrated and analyzed with respect to the generated compounds and their ratios (Table XX). Subsequently, TBAF was removed by filtration over silica using ethyl

acetate as eluent. The pre-purified mixtures were analyzed by LC-MS and the ratio between **183b** and **(E/Z)-192b** was determined by integration of the corresponding signals of the UV-trace at 226 nm based on the linear equation of Diagram 13 (Table XXI). The ratios were compared to the ratios obtained by integration of the ^{31}P -NMR spectra (Table XXI). Furthermore, the amounts of **195** and **(E/Z)-192b** were compared based on the integrals obtained from the ^{31}P -NMR-spectra (Table XXII). All spectra can be found in the appendix.

For the LC-MS-measurements following gradient was applied (A = 1% AcOH in H_2O , B = 1% AcOH in CH_3CN): 0-3 min. 20% B, 3-11 min. 20-90% B, 11-16 min. 90-100% B, 16-21 min. 100% B, 21-26 min. 100-20% B. For the samples in CH_2Cl_2 and DMSO following gradient was applied: (A = 1% AcOH in H_2O , B = 1% AcOH in CH_3CN): 0-2 min. 0% B, 2-32 min. 0-100% B, 32-35 min. 100% B, 35-37 min. 100-0% B, 37-39 min. 0% B.

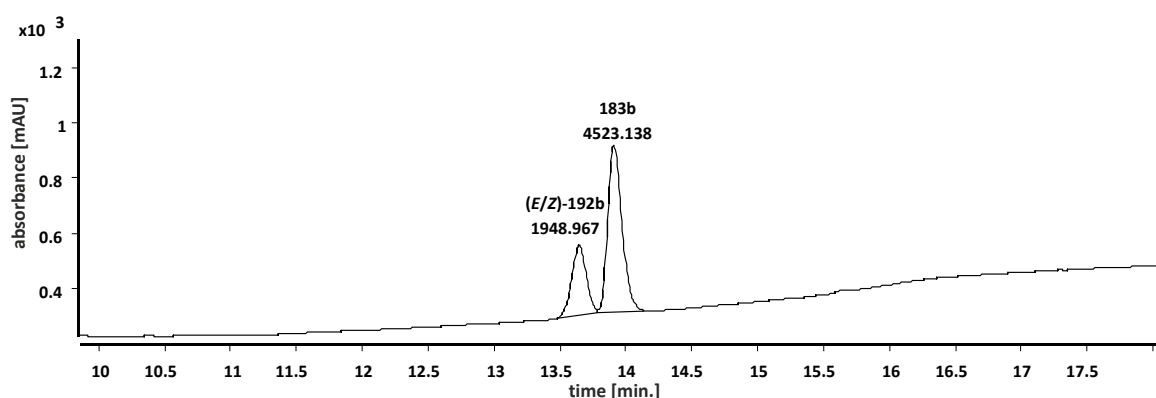


Figure 28: UV-trace of the LC-MS spectrum at 226 nm for the Staudinger reaction in *n*-hexane. Integrals are given in mAU·min.

Table XX: Ratios of all observed compounds determined by integration of ^{31}P -NMR signals.

solvent	compound ratios [%] determined by ^{31}P -NMR				
	195	183b	(Z)-192b	(E)-192b	other
<i>n</i> -hexane	10	75	2	8	6
benzene	11	73	1	8	7
THF	12	72	2	10	4
CH_2Cl_2	22	58	3	16	1
pyridine	19	60	3	15	3
CH_3CN	31	42	4	20	3
DMF	37	32	4	23	4
DMSO	26	11	5	19	39

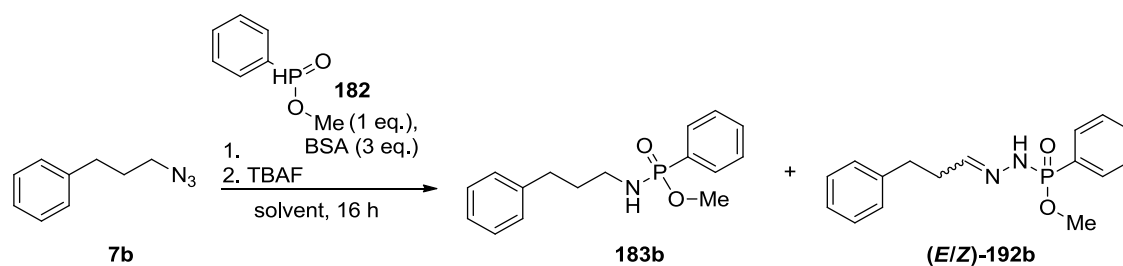
Table XXI: Ratios of **183b** and (*E/Z*)-**192b** determined by LC-MS and ³¹P-NMR.

solvent	(E/Z)-192b				183b			
	UV			NMR	UV			NMR
	[mAU·min]	[nmol]	[%]	[%]	[mAU·min]	[nmol]	[%]	[%]
<i>n</i> -hexane	1948.967	3.7914	15	11	4523.138	22.285	85	89
benzene	779.738	1.5168	14	11	1914.062	9.4303	86	89
THF	2746.398	5.3427	19	14	4770.347	23.503	81	86
CH ₂ Cl ₂	8237.491	16.025	30	25	7480.606	36.856	70	75
pyridine	388.601	0.75596	23	23	503.137	2.4789	77	77
CH ₃ CN	1717.596	3.3413	39	37	1065.452	5.2493	61	63
DMF	1748.072	3.4006	43	45	903.781	4.4528	57	55
DMSO	26010.190	50.599	63	68	5983.570	29.480	37	32

Table XXII: Ratios of **195** and (*E/Z*)-**192b** determined by integration of ³¹P-NMR signals.

solvent	195	(E/Z)-192b	195 : (E/Z)-192b
	[%]	[%]	[%]
<i>n</i> -hexane	10	10	50 : 50
benzene	11	9	55 : 45
THF	12	12	50 : 50
CH ₂ Cl ₂	22	19	54 : 46
pyridine	19	18	51 : 49
DMF	31	24	56 : 44
CH ₃ CN	37	27	58 : 42
DMSO	26	24	52 : 48

5.3.7.3 Temperature effect

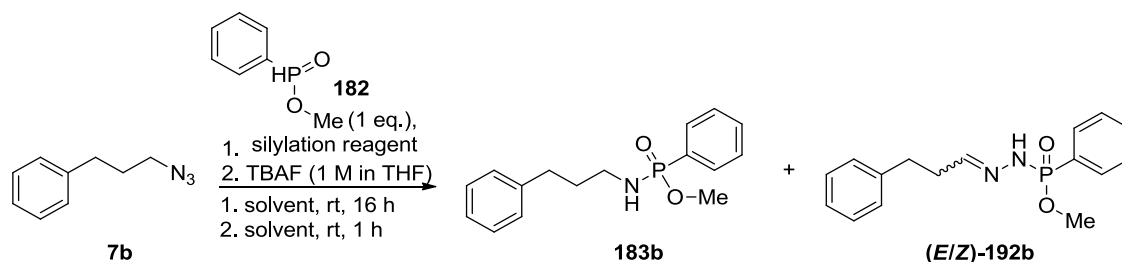


The reaction was performed according to **general procedure II** with 3-phenylpropyl azide (**7b**) (81 mg, 0.50 mmol), methyl phenylphosphinate (**182**) (78 mg, 0.50 mmol) and BSA (1.5 mmol, 0.23 g, 0.28 mL) in acetonitrile (2.0 mL) and stirred for 16 h. Afterwards TBAF (1 M in THF, 1.5 mL, 1.5 mmol) was added and the reaction mixture was stirred for an additional hour. An ^{31}P -NMR was measured of the reaction mixture before the solvent was removed under reduced pressure. Subsequently, TBAF was removed by filtration over a pad of silica gel using ethyl acetate as eluent. The pre-purified mixture was analyzed by LC-MS and the ratios between **183b** and (E/Z)-**192b** were determined by integration of the corresponding signals of the UV-trace at 226 nm based on the linear equation of Diagram 13 (Table XXIII). For the LC-MS-measurements following gradient was applied (A = 1% AcOH in H_2O , B = 1% AcOH in CH_3CN): 0-3 min. 20% B, 3-11 min. 20-90% B, 11-16 min. 90-100% B, 16-21 min. 100% B, 21-26 min. 100-20% B.

Table XXIII: Ratios of **183b** and (E/Z)-**192b** determined by LC-MS and ^{31}P -NMR.

temperature	(E/Z)-192b				183b			
	UV			NMR	UV			NMR
	[mAU·min]	[nmol]	[%]	[%]	[mAU·min]	[nmol]	[%]	[%]
4°C	7001.358	13.627	42	35	3783.714	18.643	58	65
21°C	1839.935	3.5812	32	28	1560.456	7.6885	68	72
80°C	3363.944	6.5476	31	26	2916.187	14.368	69	74

5.3.7.4 Influence of the silylation reagent on the Staudinger reaction



The reaction was performed according to **general procedure II** with 3-phenylpropyl azide (**7b**) (80.6 mg, 0.50 mmol), methyl phenylphosphinate (**182**) (78.1 mg, 0.50 mmol, 1 eq. or 781 mg, 5.00 mmol, 10 eq.) with different silylation reagents and equivalents in dichloromethane (2.0 mL) and stirred for 16 h (Table XXIV).

Table XXIV: Silylation reagents.

silylation reagent	eq.	mmol	mg	mL	base	mmol	mg	mL
BSA	1	0.5	102	0.122	-	-	-	-
BSA	3	1.5	305	0.367	-	-	-	-
BSA	5	2.5	509	0.611	-	-	-	-
BSA	10	5.0	1.02	1.22	-	-	-	-
MSTFA	1	0.5	99.6	0.0927	-	-	-	-
MSTFA	10	5.0	996	0.927	-	-	-	-
TMSCI	1	0.5	54.3	0.0635	Et ₃ N	0.5	0.0506	0.0418
TMSCI	5	2.5	272	0.317	Et ₃ N	2.5	0.253	0.209
MTBSTFA	10	5.0	1.207	1.165	-	-	-	-
TBDMSCI	5	2.5	377	0.433	imidazole	2.5	170	-
TESCI	1	0.5	75.4	0.0839	Et ₃ N	0.5	0.0506	0.0418
TESCI	3	1.5	226	0.252	Et ₃ N	1.5	0.152	0.209
TIPSCI	3	1.5	289	0.321	imidazole	1.5	102	-
TBDPCI	1	0.5	137	0.130	imidazole	0.5	34.0	-
TBDPCI	3	1.5	412	0.390	imidazole	1.5	102	-
TBDPCI	5	2.5	687	0.650	imidazole	2.5	170	-
TPSCI	1	0.5	147	-	imidazole	0.5	34.0	-

Afterwards TBAF (1 M in THF, 1-10 eq. according to the silylation reagent) was added and the reaction mixture was stirred for an additional hour. A ³¹P-NMR spectrum was measured of the

reaction mixture before the solvent was removed under reduced pressure. The ^{31}P -NMR spectra were integrated and analyzed with respect to the generated compounds and their ratios (Table XXVII). Subsequently, TBAF was removed by filtration over a pad of silica gel with ethyl acetate. The pre-purified mixture was analyzed by LC-MS and the ratio between **183b** and (**E/Z**)-**192b** was determined by integration of the corresponding signals of the UV-trace at 226 nm based on the linear equation in Diagram 13 (Table XXV). Ratios of **183b** and (**E/Z**)-**192b** obtained from the LC-MS measurement were compared to those from the ^{31}P -NMR (Table XXVI).

Table XXV: Ratios of **183b** and (**E/Z**)-**192b** determined by integration of the UV-trace at 226 nm of the measured LC-MS spectra after the Staudinger reaction with different silylation reagents and equivalents after removal of TBAF.

silylation reagent	eq.	(E/Z)-192b			183b		
		[mAU ²]	[nmol]	[%]	[mAU·min]	[nmol]	[%]
BSA	1	57.984	0.11280	10	200.893	0.98977	90
BSA	3	77.365	0.15050	25	93.092	0.45865	75
BSA	5	117.343	0.22827	12	324.672	1.2996	88
BSA	10	55.851	0.10865	3	631.55	3.1115	97
MSTFA	1	2170.84	4.2230	39	1321.8	6.5123	61
MSTFA	10	187.823	0.36538	63	42.988	0.21179	37
MSTFA	10 ^a	623.015	1.2120	74	87.82	0.43267	26
TMSCI	1	46.534	0.09052	12	130.514	0.64302	88
TMSCI	5	65.935	0.12827	12	187.178	0.92220	88
MTBSTFA	10	115.515	0.22471	4	1101.192	5.4254	96
TBDMSCI	5	0	0	0	0	0	0
TESCI	1	58.957	0.11469	46	26.997	0.13301	54
TESCI	3	0	0	0	0	0	0
TIPSCI	3	0	0	0	0	0	0
TBDPCI	1	0	0	0	0	0	0
TBDPCI	3	0	0	0	22.658	0.11163	100
TBDPCI	5	0	0	0	0	0	0
TPSCI	1	0	0	0	0	0	0

^a reaction was performed with 10 eq. of methyl *P*-phenyl phosphinate **182**.

Table XXVI: Ratios of (E/Z)-192b and 183b after the Staudinger reaction with different silylation reagents and different equivalents. Ratios were determined by integration of the corresponding signals of the ³¹P-NMR and by integration of the UV-trace of the LC-MS spectra.

silylation reagent	eq.	183b		(E/Z)-192b	
		UV [%]	NMR [%]	UV [%]	NMR [%]
BSA	1	90	89	10	11
	3	75	75	25	25
	5	88	88	12	12
	10	97	97	3	3
MSTFA	1	61	56	39	44
	10	37	41	63	59
TMSCI	1	88	94	12	6
	5	88	92	12	8
TESCI	1	54	64	46	36
TBDMSCI	5	0	100	0	0
MTBSTFA	10	96	94	4	6
TBDPCI	1	0	0	0	0
	5	0	100	0	0
TPSCI	1	0	0	0	0

Table XXVII: Ratios of all compounds observed after the Staudinger reaction with different silylation reagents and equivalents determined by ³¹P-NMR.

silylation reagent	equivalents	183b [%]	(E/Z)-192b [%]	195 [%]	other [%]
BSA	1	33	4	9	54
	3	58	19	23	0
	5	63	9	15	13
	10	70	5	0	25
MSTFA	1	35	27	35	3
	10	16	23	59	2
TMSCI	1	30	2	53	15
	5	12	1	70	17

TESCI	1	9	5	65	21
TBDMSCI	5	2	0	32	66
MTBSTFA	10	17	1	27	55
TBDPCI	1	0	0	27	73
	5	1	0	21	79
TPSCI	1	0	0	0	100

5.3.8 Staudinger reaction with 1,3-dichloro-1,1,3,3-tetramethyldisiloxane

The reaction was performed according to **general procedure II** with 3-phenylpropyl azide (**7b**) (80.6 mg, 0.50 mmol), phenylphosphinic acid (**185**) (71.0 mg, 0.50 mmol, 1 eq.), 1,3-dichloro-1,1,3,3-tetramethyldisiloxane (102 mg, 97.8 μ L, 0.50 mmol) and Et₃N (101 mg, 139 μ L, 1.0 mmol) in dichloromethane (5.0 mL) and stirred for 3 d at room temperature. No product formation was observed.

5.4 Peptides synthesis

5.4.1 Peptide synthesis on NovaSyn® TG HMBA resin – azido peptides 7c, d, f

Attachment of the first amino acid:

Fmoc-Gly-OH was attached to NovaSyn® TG HMBA resin using MSNT/Melm activation as described by Novabiochem:

For 0.1 mmol peptide, NovaSyn® TG HMBA resin (400 mg, 0.25 mmol/g) was swollen and afterwards washed with dichloromethane. Subsequently, the resin was covered with sufficient dichloromethane and the reaction vessel was flushed with argon. Fmoc-Gly-OH (149 mg, 0.500 mmol eq.) was dissolved in dichloromethane (1.5 mL) under argon atmosphere and Melm (30.8 mg, 29.9 μ L, 0.375 mmol, 3.75 eq.) followed by MSNT (148 mg, 0.500 mmol, 5 eq.) was added. The reaction mixture was stirred until a clear solution was obtained. The solution was added to the resin and the coupling was allowed to proceed for 1 h at ambient temperature under gentle agitation. The reaction solution was removed and the resin was washed with dichloromethane. The procedure was repeated once to ensure high loading.

Standard Fmoc-based coupling protocol:

Coupling of further amino acids was achieved by standard Fmoc-based coupling conditions using the Fmoc-amino acid (10 eq.), HOBt (10 eq.), HBTU (10 eq.) and DIEA (10 eq.) in DMF and NMP as reaction solvent with an ABI 433A Peptide Synthesizer from Applied Biosystems (Fast-moc protocol with HOBt/HBTU conditions). Alternatively, peptides were synthesized manually using following procedure (Table XXVIII):

Table XXVIII: Standard protocol for manual Fmoc solid-phase peptide synthesis.

process step	reagent	time
amino acid coupling	5 eq. Fmoc-X-OH	2 h
	5 eq. HOBt (68mg, 0.50 mmol)	
	5 eq. HBTU (0.19 g, 0.50 mmol)	
	5 eq. DIEA (65 mg, 85 μ L, 0.50 mmol)	
washing	5 mL DMF	5 x 1 min
Fmoc deprotection	2 mL 20% piperidine in DMF	30 min
washing	2 mL DMF	5 x 1 min

For peptide synthesis, the following Fmoc-protected amino acids were purchased from Novabiochem:

Fmoc-Ala-OH, Fmoc-Glu(tBu)-OH, Fmoc-Gly-OH, Fmoc-His(Trt)-OH, Fmoc-Phe-OH, Fmoc-Tyr(tBu)-OH, Fmoc-Trp(Boc)-OH, Fmoc-Lys(Boc)-OH

Coupling of azido glycine (2h) and 2-azido-2-methylpropionic acid (2i):

The described manual procedure was used for the coupling of azido glycine **2h** and 2-azido-2-methylpropionic acid **2i** (Table XXVIII). In case of incomplete coupling, the protocol was repeated.

Deprotection of the peptide:

The peptide-loaded resin was treated with a standard TFA-cleavage cocktail (95% TFA, 2.5% TIS, 2.5% H₂O, 1 mL) and the reaction was allowed to proceed for 3 h at ambient temperature under gentle agitation. Afterwards the resin was washed several times with DMF and CH₂Cl₂ and dried under reduced pressure. The on-resin azido peptide was stored in the fridge for further use.

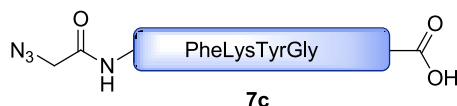
Resin cleavage:

Cleavage of the peptide from resin was achieved by treatment with an ice-cold basic cleavage cocktail (NaOH-solution (1 M in H₂O): 1,4-dioxane, 1:3) for ten minutes. The strong basic solution

with the azido peptide or peptidic reaction products was neutralized with diluted hydrochloric acid (0.2 M) and/or addition of TRIS-buffer (1 M).

Success of the synthesis was verified by a test cleavage and analysis by ESI-TOF HRMS.

5.4.1.1 Synthesis of azido glycine peptide 7c



The azido peptide **7c** was synthesized on a NovaSyn® TG HMBA resin following the procedure described above (5.4.1) with the peptide synthesizer. A test cleavage and a LC-MS measurement proved the success of the synthesis (Figure 29).

Solvent gradient (A = H₂O (1% AcOH), B = CH₃CN (1% AcOH)): 0-5 min. 0% B, 5-25 min. 0-100% B, 25-28 min. 100% B, 28-30 min. 100%-20%.

HRMS (ESI-TOF): m/z = 597.2750 [M+H]⁺ (calcd. for [C₂₈H₃₇N₈O₇]⁺: m/z = 597.2780).

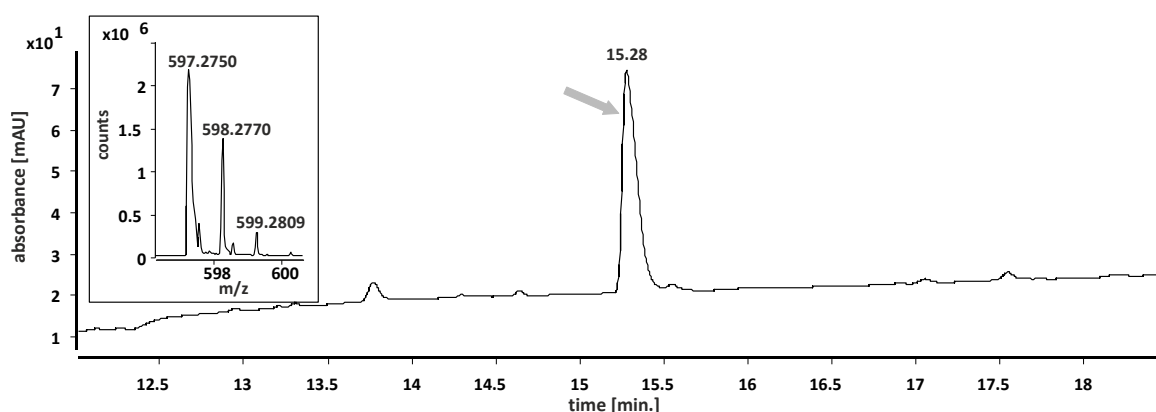
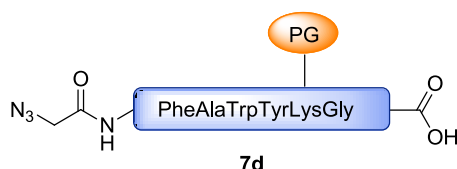


Figure 29: LC-MS spectrum (UV trace at 280 nm) and HRMS of azido peptide **7c**.

5.4.1.2 Synthesis of azido glycine peptide 7d



The azido peptide **7d** was synthesized on a NovaSyn® TG HMBA resin following the procedure described above (5.4.1). A test cleavage without deprotection of the side chains and a LC-MS measurement proved the success of the synthesis (Figure 30).

Solvent gradient (A = H₂O (1% AcOH), B = CH₃CN (1% AcOH)): 0-3 min. 0% B, 3-14 min. 0-100% B, 14-18 min. 100% B, 18-20 min. 100%-20%.

HRMS (ESI-TOF): $m/z = 1110.5621$ $[M+H]^+$ (calcd. for $[C_{56}H_{76}N_{11}O_{13}]^+$: $m/z = 1110.5619$).

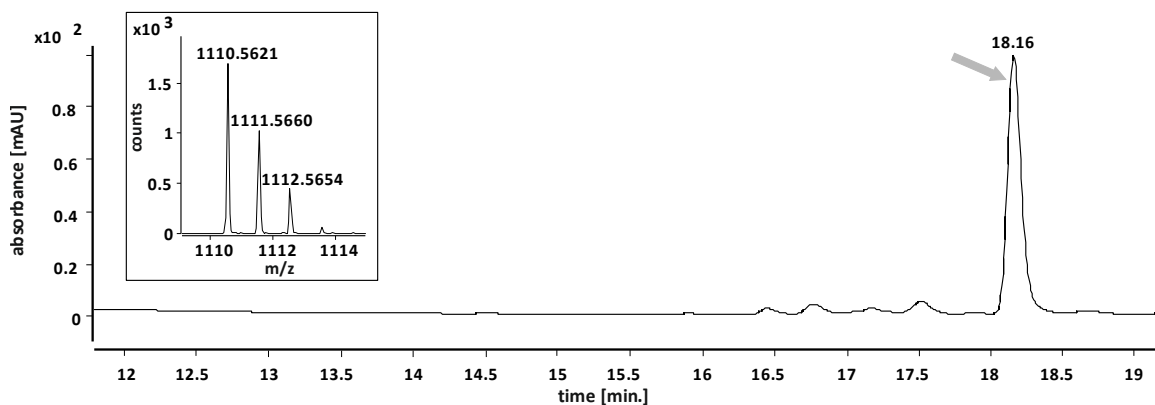
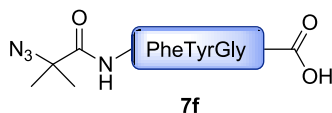


Figure 30: LC-MS (UV trace at 280 nm) and HRMS spectrum of azido peptide **7d**.

5.4.1.3 Synthesis of 2-azido-2-methyl alanine peptide **7f**



The azido peptide **7f** was synthesized on a NovaSyn® TG HMBA resin following the procedure described above (5.4.1). A test cleavage and a LC-MS measurement proved the success of the synthesis (Figure 31).

Solvent gradient (A = H₂O (1% AcOH), B = CH₃CN (1% AcOH)): 0-3 min. 0% B, 3-14 min. 0-100% B, 14-18 min. 100% B, 18-20 min. 100%-20%.

HRMS (ESI-TOF): $m/z = 497.2121$ $[M+H]^+$ (calcd. for $[C_{24}H_{29}N_6O_6]^+$: $m/z = 497.2143$).

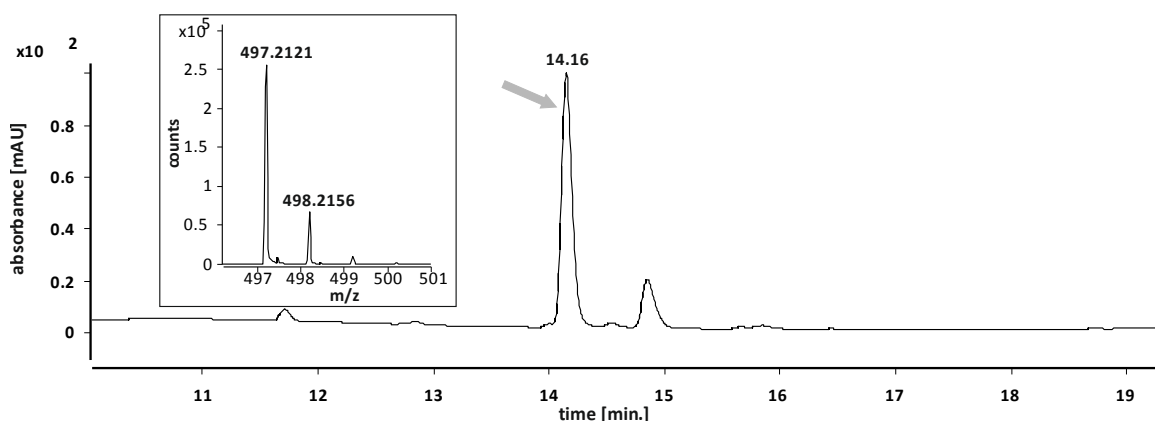


Figure 31: LC-MS spectrum (UV trace at 280 nm) of azido peptide **7f**.

5.4.2 Peptide synthesis on a Gly-preloaded Wang resin – azido peptides **7e** and **g**

Standard Fmoc-based coupling protocol and coupling of azido glycine (**2h**) and 2-azido-2-methylpropionic acid (**2i**):

Peptide synthesis was achieved following the procedures described for the NovaSyn® TG HMBA resin (0.1 mmol) (chapter 5.4.1).

Deprotection of the peptide and resin cleavage:

Deprotection of the peptide and cleavage from the resin was achieved simultaneously by treatment with standard TFA-cleavage cocktail (95% TFA, 2.5% TIS, 2.5% H₂O, 1 mL). The deprotection was allowed to proceed for 3 h at ambient temperature under gentle agitation. The TFA-solution containing all peptidic products was collected and treated with ice-cold ether to precipitate the peptides. After centrifugation for 2 min. at 4000 rpm, the ether-TFA mixture was decanted to yield the crude peptides. The azido peptides **7e** and **7g** were purified by semi-preparative HPLC with the following solvent gradient (A = H₂O, B = CH₃CN): 0-5 min. 0% B, 5-40 min. 0-100% B, 40-45 min. 100% B, 45-52 min. 100%-20%.

5.4.2.1 Synthesis of azido glycine peptide **7e**



The peptide was synthesized by standard Fmoc solid-phase peptide synthesis using 0.1 mmol glycine preloaded Wang resin on the peptide synthesizer as described above (5.4.2). The peptide was cleaved from the resin and deprotected by using 1 mL of cleavage cocktail (95% TFA, 2.5% TIS, 2.5% H₂O). Afterwards the peptide was purified by preparative HPLC (solvent gradient (A = H₂O (0.1% TFA), B = CH₃CN (0.1% TFA)): 0 % B 0-3 min.; 0-100 % B 3-40 min.; 100% B 40-45 min.; 100-20% B 45-50 min.; retention time 19 min.). The peptide was obtained in a yield of 15% (12.1 mg). A HRMS spectrum was measured (Figure 32).

HRMS (ESI-TOF): $m/z = 806.3207$ [M+H]⁺ (calcd. for [C₃₆H₄₄N₁₁O₁₁]⁺: $m/z = 806.3216$), $m/z = 828.3018$ [M+Na]⁺ (calcd. for [C₃₆H₄₃N₁₁NaO₁₁]⁺: $m/z = 828.3036$).

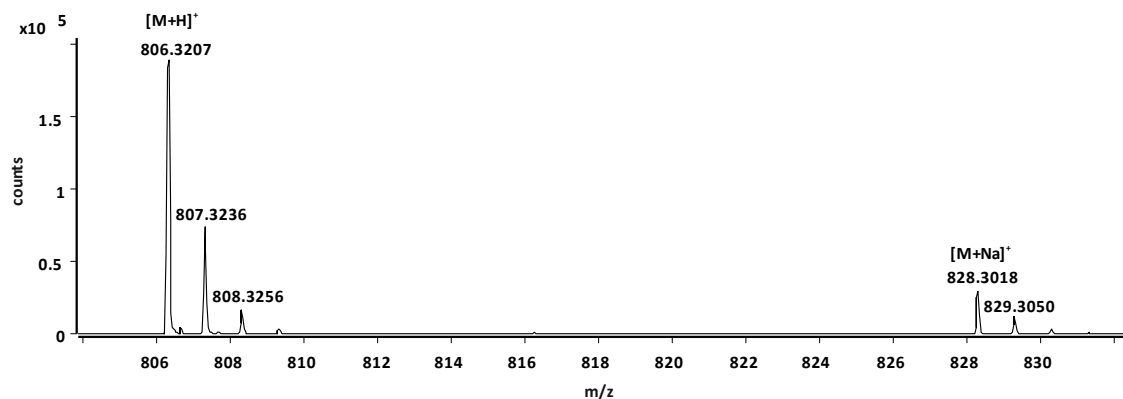


Figure 32: HRMS spectrum of azido peptide 7e.

5.4.2.2 Synthesis of 2-azido-2-methyl alanine peptide 7g



The peptide was synthesized by standard Fmoc-solid-phase peptide synthesis using 0.10 mmol glycine preloaded Wang resin on the peptide synthesizer as described above (5.4.2). The peptide was cleaved from the resin and deprotected by using 1 mL of cleavage cocktail (95% TFA, 2.5% TIS, 2.5% H₂O). Afterwards the peptide was purified by preparative HPLC (solvent gradient (A = H₂O (0.1% TFA), B = CH₃CN (0.1% TFA)): 0 % B 0-3 min.; 0-100 % B 3-40 min.; 100% B 40-45 min.; 100-20% B 45-50 min.; retention time 20 min.). The peptide was obtained in a yield of 12% (9.8 mg). A HRMS spectrum was measured (Figure 33).

HRMS (ESI-TOF): m/z = 834.3528 [M+H]⁺ (calcd. for [C₃₈H₄₈N₁₁O₁₁]⁺: m/z = 834.3529), m/z = 856.3349 [M+Na]⁺ (calcd. for [C₃₈H₄₇N₁₁NaO₁₁]⁺: m/z = 856.3349).

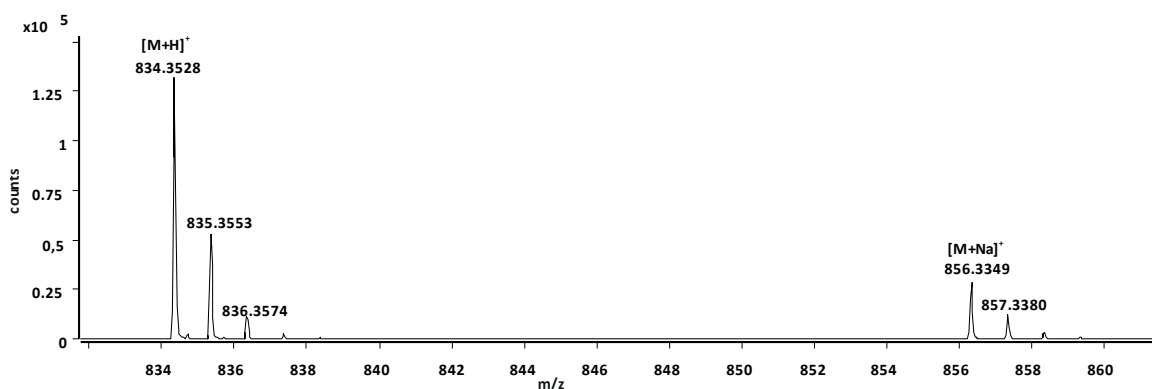


Figure 33: HRMS spectrum of azido peptide 7g.

5.5 Staudinger reaction with azido peptides

5.5.1 Staudinger reaction on solid support – General procedure

General procedure III: Anhydrous dichloromethane was added to the unprotected azido peptide on resin under argon atmosphere followed by either dimethyl phenylphosphonite (**188**) or methyl phenylphosphinate **182** and the silylation reagent. The reaction was allowed to proceed under gentle agitation at ambient temperature 19 h. The solvent and the reagents were removed and the resin was washed five times with dichloromethane (2 mL). The products were cleaved from the resin with aqueous NaOH-solution (1 M) and 1,4-dioxane (1:3) as described before (5.4.1). The solution was brought to neutral pH and a LC-MS spectrum was measured. The conversion and product ratios were determined by integration of the signals of the UV trace at 280 nm.

5.5.2 Staudinger reaction in solution – General procedure

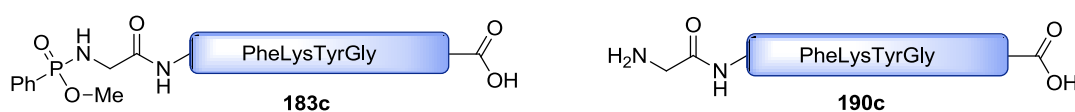
General procedure IV: Methyl phenylphosphinate (**182**) and BSA were added to a suspension of the unprotected azido peptide in anhydrous CH₂Cl₂ at room temperature under argon atmosphere. The reaction mixture was allowed to stir for additional 24 h at ambient temperature. The reaction mixture was analyzed by LC-MS and the ratio of both products was determined by integration of the UV-trace at 280 nm.

5.5.3 Staudinger reaction between azido glycine peptide **7c** and dimethyl phenylphosphonite (**188**)

The Staudinger reaction was performed with azido peptide **7c** on resin (51.6 mg, 10.0 μmol) and dimethyl phenylphosphonite (**188**) (80 μL, 85 mg, 0.5 mmol, 50 eq.) according to **general procedure III**. The LC-MS spectrum is shown below (Figure 34).

183c: HRMS (ESI-TOF): $m/z = 725.3090$ [M+H]⁺ (calcd. for [C₃₅H₄₆N₆O₉P]⁺: $m/z = 725.3058$).

190c: HRMS (ESI-TOF): $m/z = 571.2901$ [M+H]⁺ (calcd. for [C₂₈H₃₉N₆O₇]⁺: $m/z = 571.2875$).



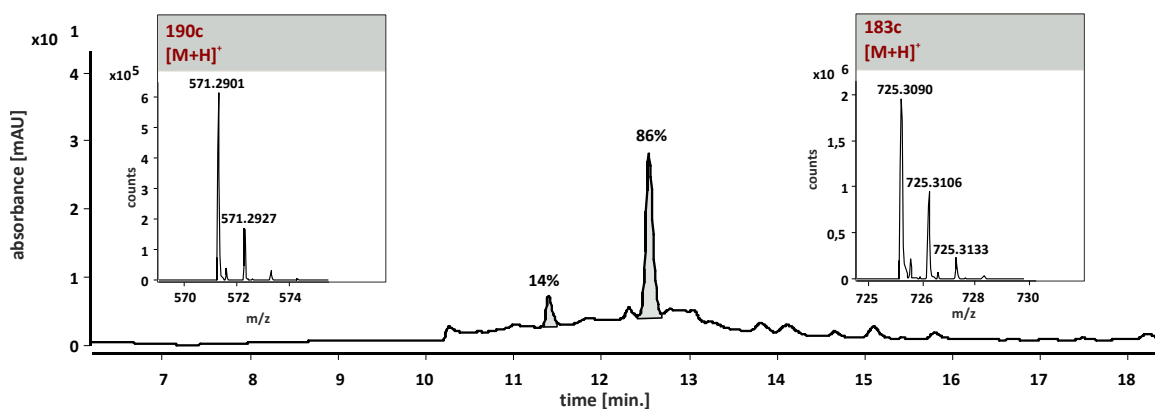


Figure 34: LC-MS spectrum (UV trace at 280 nm) of the Staudinger reaction between azido peptide **7c** and dimethyl phenylphosphonite **188**.

5.5.4 Staudinger reaction between azido glycine peptide **7c** and methyl phenylphosphinate (**182**) with BSA

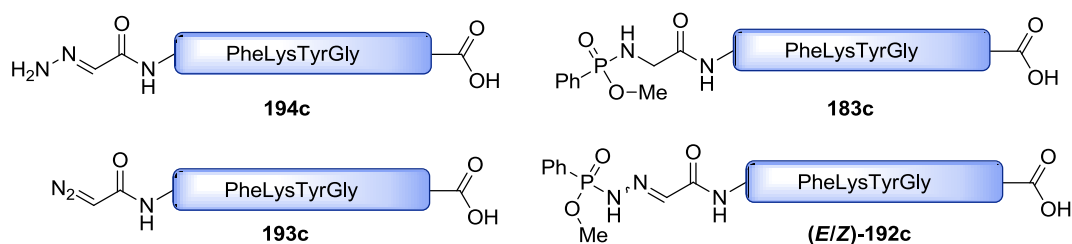
The Staudinger reaction was performed with azido peptide **7c** (51.6 mg, 10.0 μmol) and methyl phenylphosphinate (**182**) (77.0 mg, 0.500 mmol, 50 eq.) and BSA (305 mg, 367 μL , 1.50 mmol) on resin according to **general procedure III**. The LC-MS spectrum is shown below (Figure 35).

183c: HRMS (ESI-TOF): $m/z = 725.3004$ $[\text{M}+\text{H}]^+$ (calcd. for $[\text{C}_{35}\text{H}_{46}\text{N}_6\text{O}_9\text{P}]^+$: $m/z = 725.3058$).

193c: HRMS (ESI-TOF): $m/z = 582.2663$ $[\text{M}+\text{H}]^+$ (calcd. for $[\text{C}_{28}\text{H}_{36}\text{N}_7\text{O}_7]^+$: $m/z = 582.2671$).

194c: HRMS (ESI-TOF): $m/z = 584.2814$ $[\text{M}+\text{H}]^+$ (calcd. for $[\text{C}_{28}\text{H}_{38}\text{N}_7\text{O}_7]^+$: $m/z = 584.2827$).

(E/Z)-192c: HRMS (ESI-TOF): $m/z = 738.3008$ $[\text{M}+\text{H}]^+$ (calcd. for $[\text{C}_{35}\text{H}_{45}\text{N}_7\text{O}_9\text{P}]^+$: $m/z = 738.3011$).



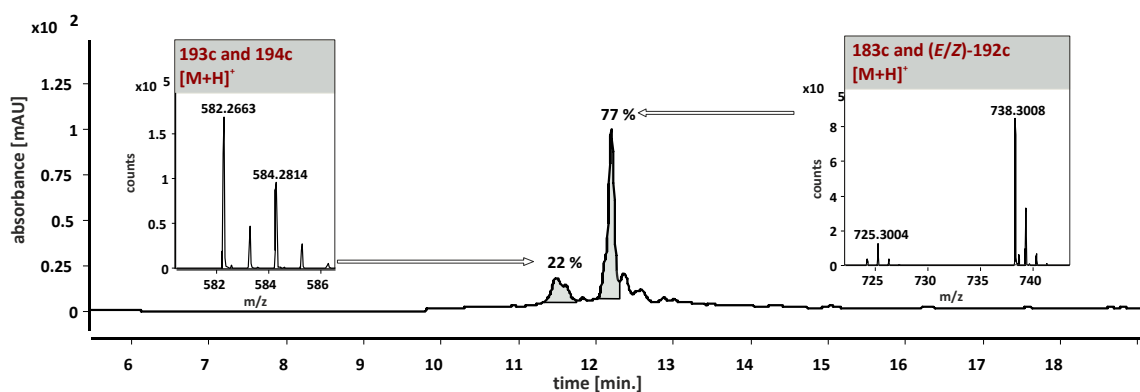


Figure 35: LC-MS spectrum (UV trace at 280 nm) of the Staudinger reaction between azido peptide **7c** and methyl phenylphosphinate (**182**) with BSA.

5.5.5 Staudinger reaction at 4 °C, rt and 30 °C

The reaction was performed according to **general procedure III** with azido peptide **7c** (12.2 mg, 24.9 μ mol), methyl phenylphosphinate (**182**) (39.0 mg, 0.250 mmol, 100 eq.) and BSA (203 mg, 245 μ L, 1.00 mmol, 400 eq.) at 4 °C, rt and 30 °C for 19 h on resin (TG HMBA). All product mixtures were analyzed by LC-MS (Figure 36 - 38). HRMS spectra of the reactions at rt and 30 °C are displayed below (Figure 39).

4 °C: HRMS spectra only show products **(E/Z)-192c** and **(E/Z)-192c-Me** resulting from ester cleavage.

(E/Z)-192c: HRMS (ESI-TOF): $m/z = 738.3039$ $[M+H]^+$ (calcd. for $[C_{35}H_{45}N_7O_9P]^+$: $m/z = 738.3011$).

(E/Z)-192c-CH₂: HRMS (ESI-TOF): $m/z = 724.2875$ $[M-CH_2+H]^+$ (calcd. for $[C_{34}H_{43}N_7O_9P]^+$: $m/z = 724.2854$).

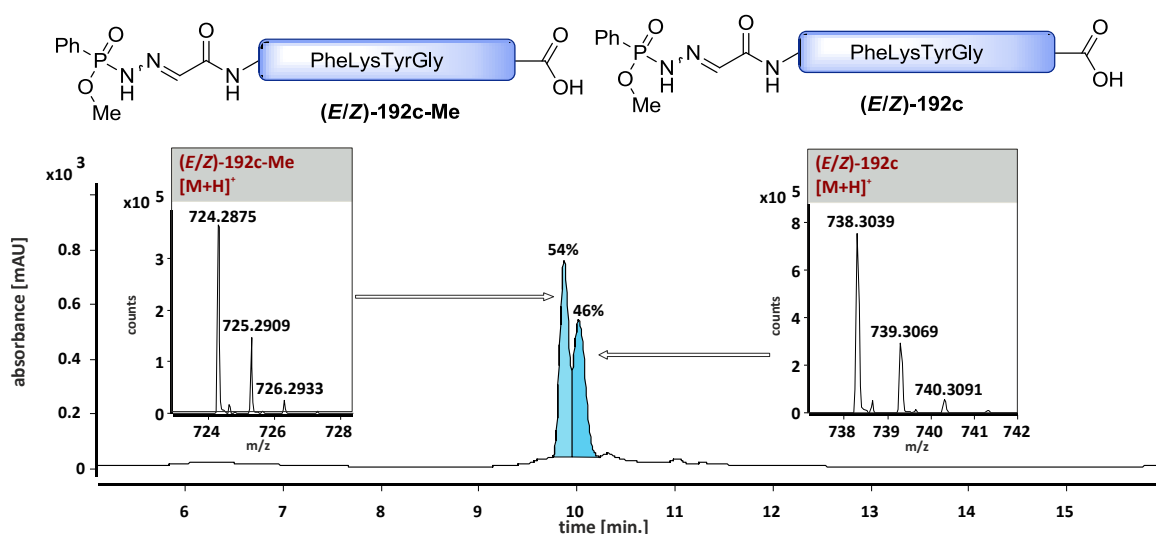


Figure 36: LC-MS (UV trace at 280 nm) and corresponding HRMS spectra of the Staudinger reaction at 4 °C.

rt and 30 °C: Both LC-MS spectra show following products: **190c**, **193c**, **194c**, **183c**, **(E/Z)-192c** and **(E/Z)-192c-Me** resulting from the ester cleavage.

190c: HRMS (ESI-TOF): $m/z = 571.2899$ $[M+H]^+$ (calcd. for $[C_{28}H_{39}N_6O_7]^+$: $m/z = 571.2875$).

193c: HRMS (ESI-TOF): $m/z = 582.2698$ $[M+H]^+$ (calcd. for $[C_{28}H_{36}N_7O_7]^+$: $m/z = 582.2671$).

194c: HRMS (ESI-TOF): $m/z = 584.2839$ $[M+H]^+$ (calcd. for $[C_{28}H_{38}N_7O_7]^+$: $m/z = 584.2827$).

183c: HRMS (ESI-TOF): $m/z = 725.3103$ $[M+H]^+$ (calcd. for $[C_{35}H_{46}N_6O_9P]^+$: $m/z = 725.3058$).

(E/Z)-192c: HRMS (ESI-TOF): $m/z = 738.3075$ $[M+H]^+$ (calcd. for $[C_{35}H_{45}N_7O_9P]^+$: $m/z = 738.3011$).

(E/Z)-192c-Me: HRMS (ESI-TOF): $m/z = 724.2888$ $[M+H]^+$ (calcd. for $[C_{34}H_{43}N_7O_9P]^+$: $m/z = 724.2854$).

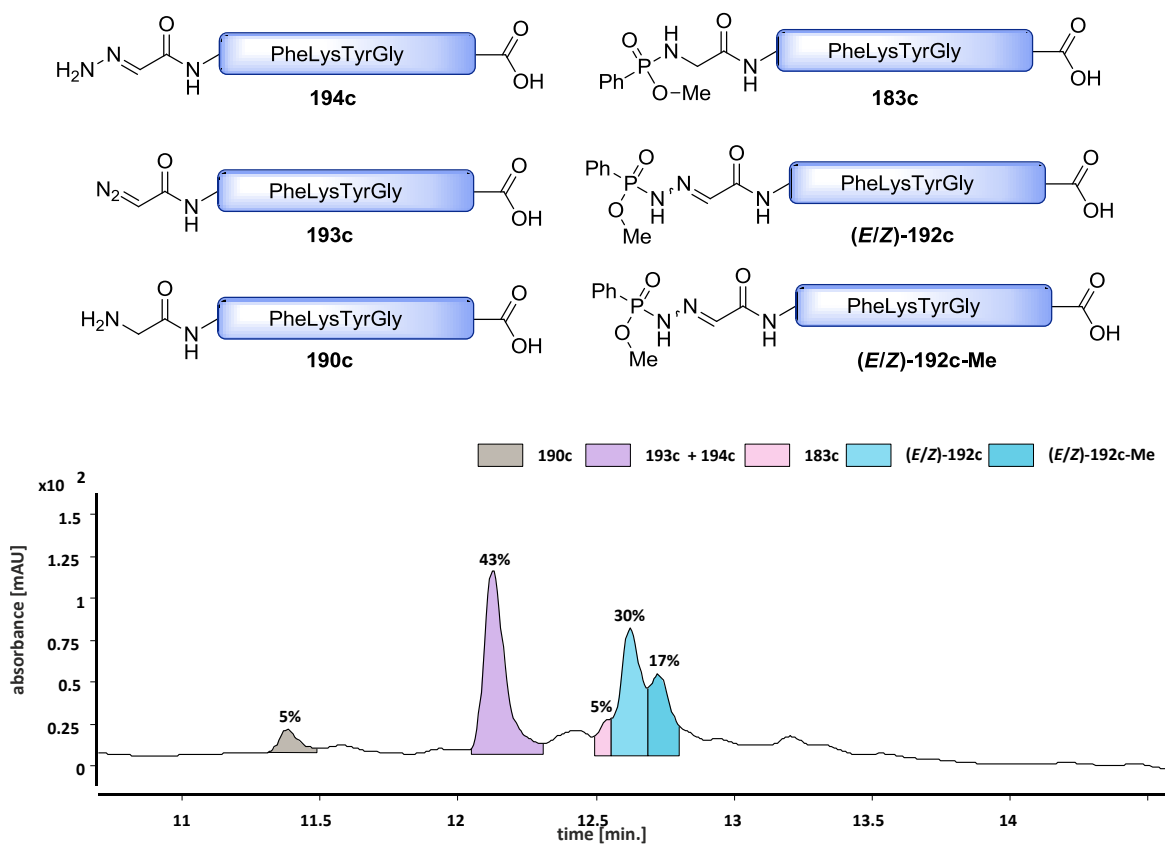


Figure 37: LC-MS spectrum (UV trace at 280 nm) of the Staudinger reaction at rt.

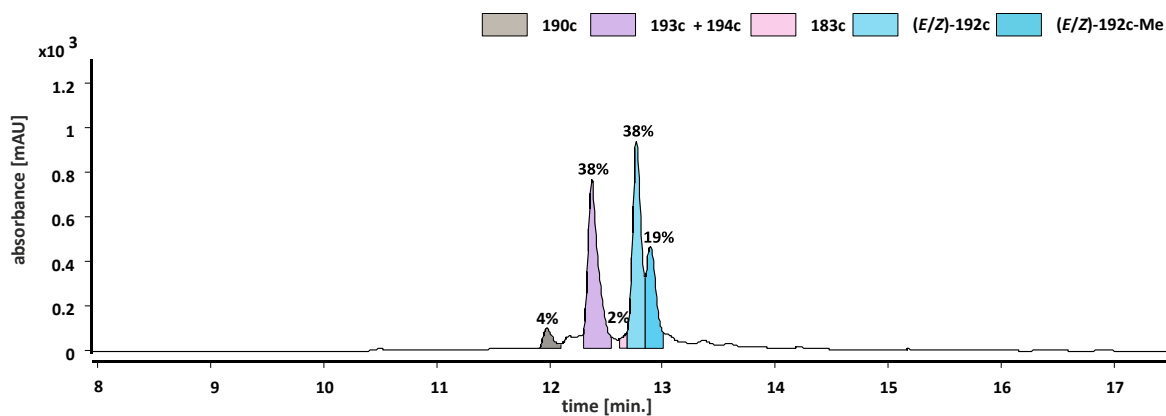


Figure 38: LC-MS spectrum (UV trace at 280 nm) of the Staudinger reaction at 30 °C.

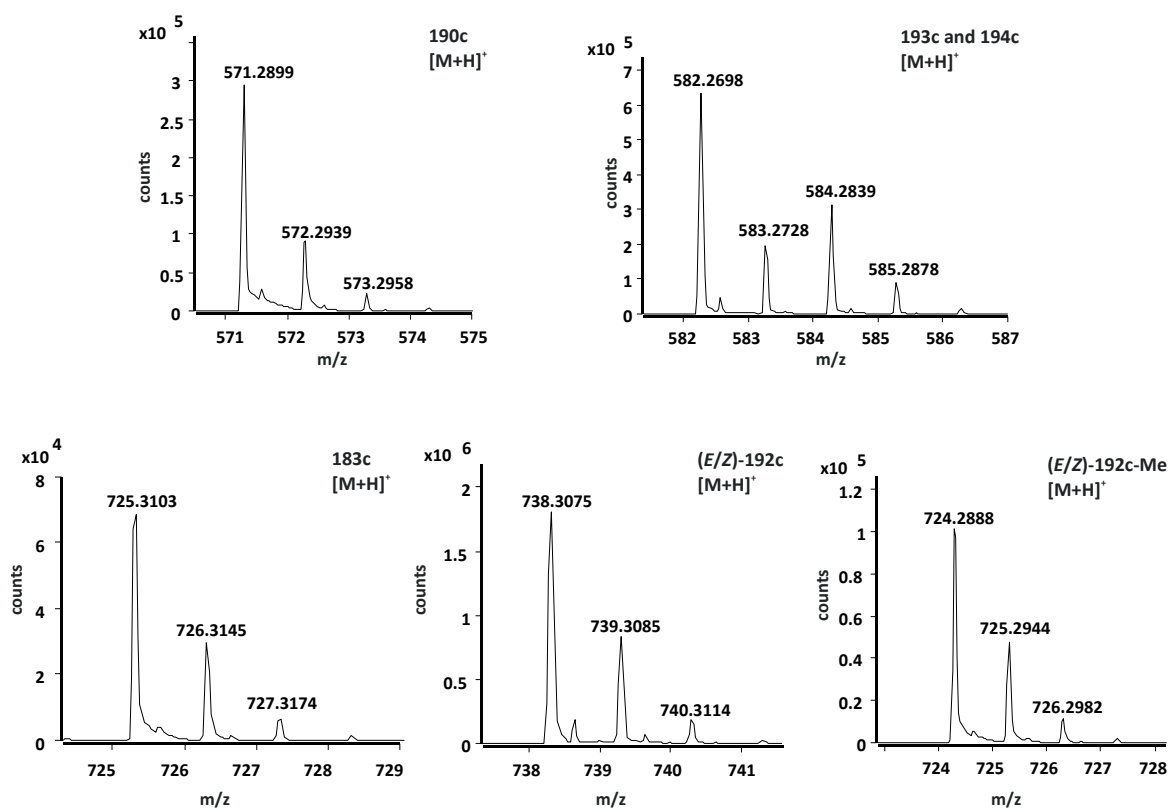


Figure 39: Corresponding HRMS spectra of all detected compounds for the Staudinger reaction at 30 °C **190c**, **193c**, **194c**, **183c**, **(E/Z)-192c** and **(E/Z)-192c-Me**. HRMS spectra for the reaction at rt are not shown but gave identical results.

5.5.6 Staudinger reaction with different silylation reagents

5.5.6.1 Staudinger reaction with TBDPCL and methyl phenylphosphinate (**182**)

The reaction was performed according to the **general procedure III** starting from resin-bound azido peptide **7c** (1.2 μmol , 5.4 mg), methyl phenylphosphinate (**182**) (19 mg, 0.12 mmol, 100 eq.), TBDPCL (99 mg, 94 μL , 0.36 mmol, 300 eq.) and imidazole (25 mg, 0.36 mmol, 300 eq.).

The reaction was allowed to proceed at room temperature for 19 h. LC-MS spectrum and HRMS spectra are displayed below (Figure 40 and Figure 41).

7c+TBDPS: HRMS (ESI-TOF): $m/z = 835.3997 [M+H]^+$ (calcd. for $[C_{44}H_{55}N_8O_7Si]^+$: $m/z = 835.3958$).

193c+TBDPS: HRMS (ESI-TOF): $m/z = 820.3906 [M+H]^+$ (calcd. for $[C_{44}H_{54}N_7O_7Si]^+$: $m/z = 820.3849$).

(E/Z)-192c+TBDPS: HRMS (ESI-TOF): $m/z = 976.4235 [M+H]^+$ (calcd.: $m/z = 976.4189$).

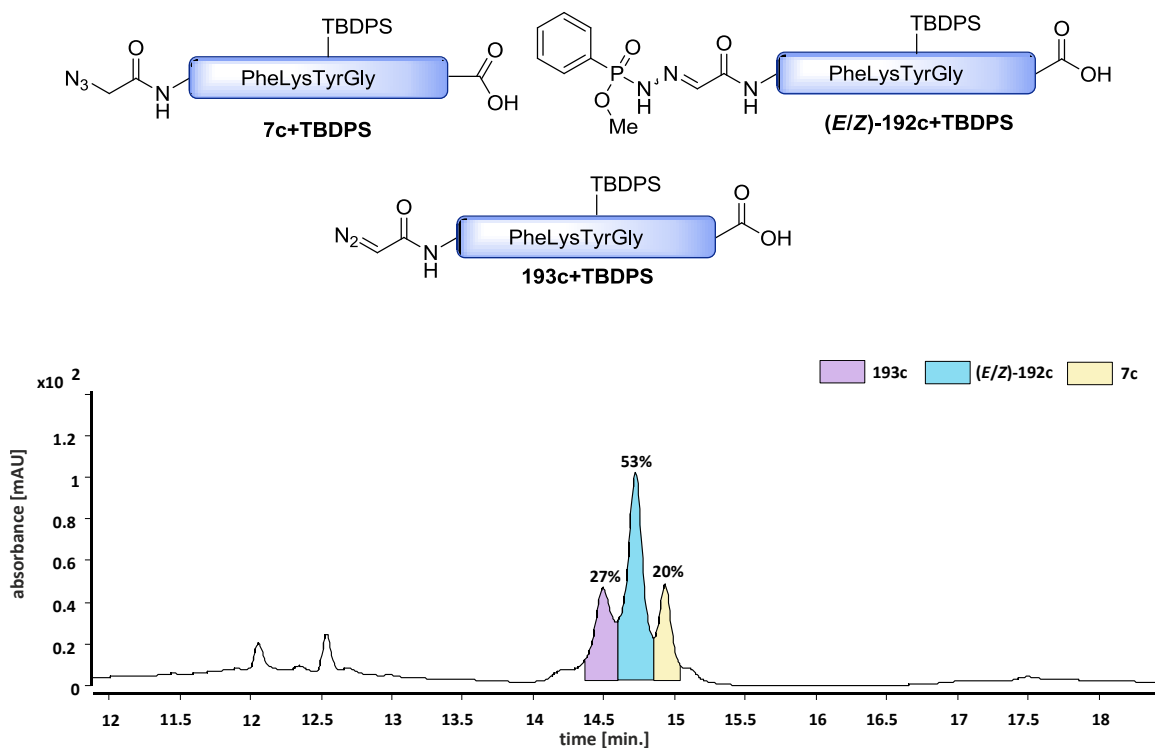


Figure 40: LC-MS spectrum (UV trace at 280 nm) of the Staudinger reaction with TBDPSCI.

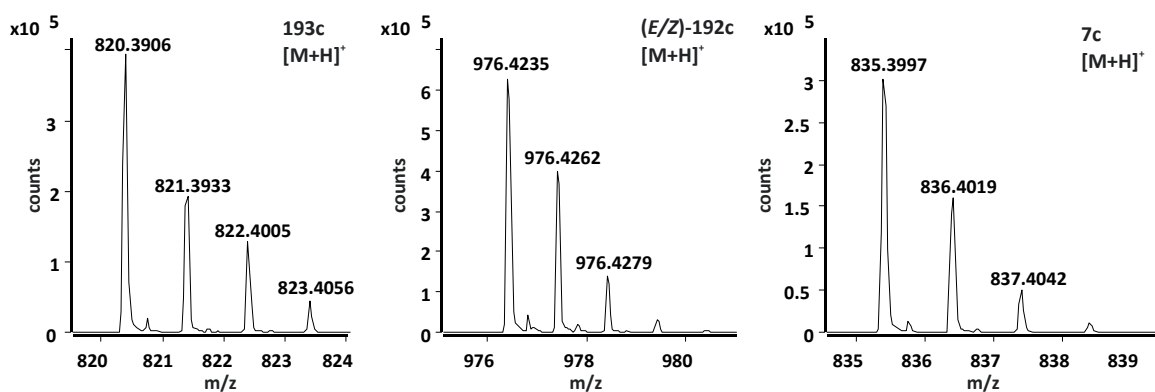


Figure 41: HRMS spectra of the UV-signals of 7c, (E/Z)-192c and 193c.

5.5.6.2 Staudinger reaction with TMSCl and methyl phenylphosphinate (182)

The reaction was performed according to the **general procedure III** starting from resin-bound azido peptide **7c** (2.4 μmol , 11 mg), methyl phenylphosphinate (**182**) (38 mg, 0.24 mmol, 100 eq.), TMSCl (78 mg, 91 μL , 0.72 mmol, 300 eq.) and Et_3N (73 mg, 0.10 mL, 0.36 mmol, 300 eq.). The reaction was allowed to proceed at room temperature for 19 h. LC-MS spectrum and HRMS spectra are displayed below (Figure 42 and Figure 43).

193c: HRMS (ESI-TOF): $m/z = 582.2635$ $[\text{M}+\text{H}]^+$ (calcd. for $[\text{C}_{28}\text{H}_{36}\text{N}_7\text{O}_7]^+$: $m/z = 582.2671$).

(E/Z)-192c: HRMS (ESI-TOF): $m/z = 738.3008$ $[\text{M}+\text{H}]^+$ (calcd. for $[\text{C}_{35}\text{H}_{45}\text{N}_7\text{O}_9\text{P}]^+$: $m/z = 738.3011$).

(E/Z)-192c-Me: HRMS (ESI-TOF): $m/z = 724.2749$ $[\text{M}+\text{H}]^+$ (calcd. for $[\text{C}_{34}\text{H}_{43}\text{N}_7\text{O}_9\text{P}]^+$: $m/z = 724.2854$).

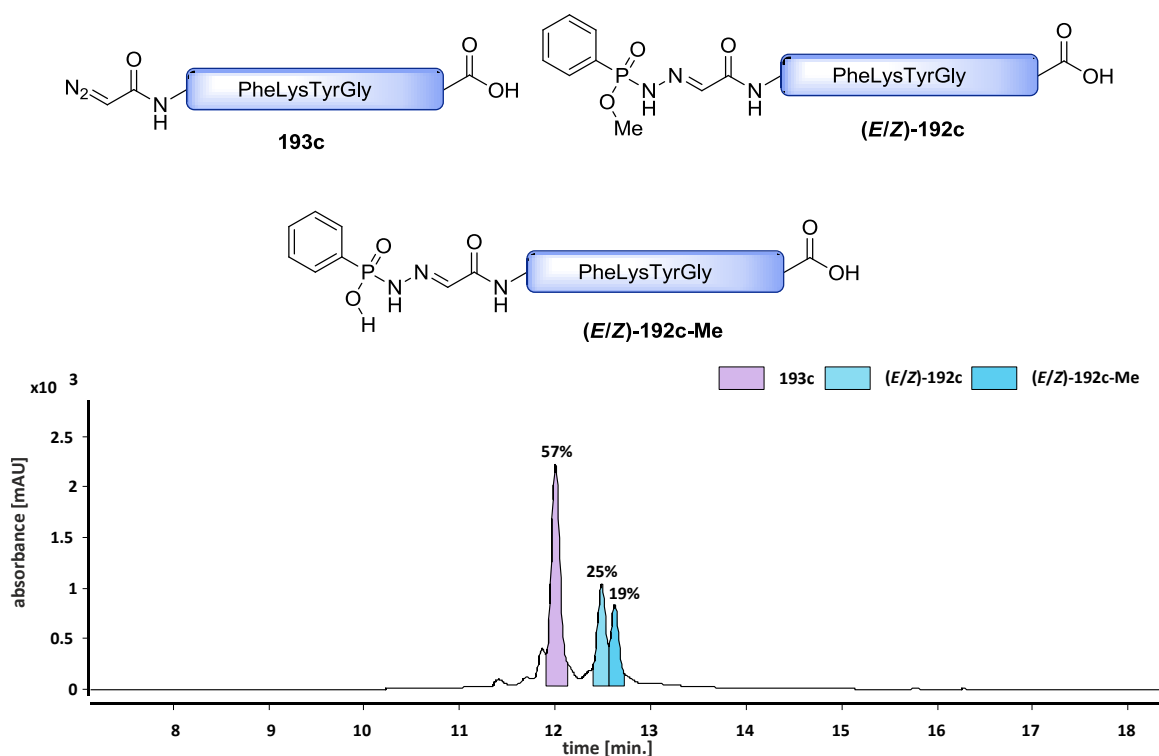


Figure 42: LC-MS spectrum (UV trace at 280 nm) of the Staudinger reaction with TMSCl.

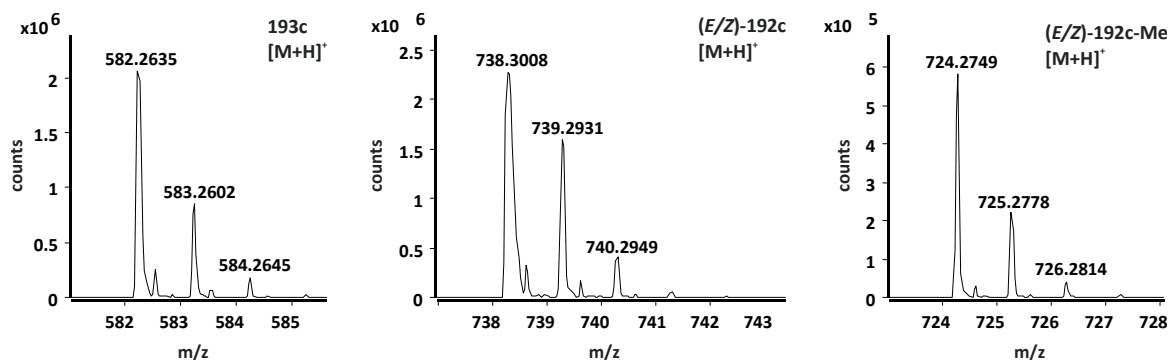


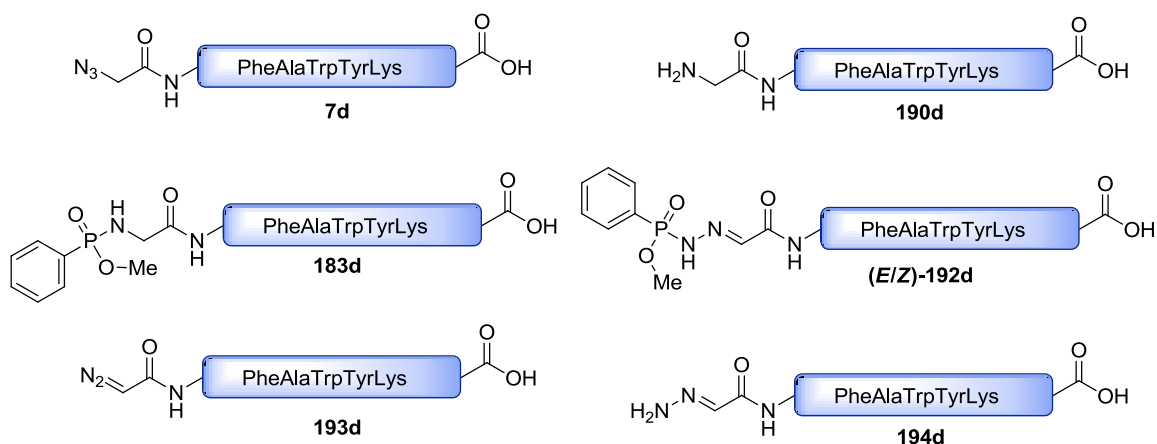
Figure 43: HRMS spectra of the UV-signals of **193c**, **(E/Z)-192c** and **(E/Z)-192c-Me**.

5.5.6.3 Staudinger reaction with MSTFA or TBDMSTFA and methyl phenylphosphinate (182)

The reaction was performed according to the **general procedure III** with resin-bound azido peptide **7d** (2.30 μmol , 10.0 mg), methyl phenylphosphinate **182** (17.9 mg, 0.115 mmol, 50 eq.) and MSTFA (50 eq. or 500eq.) or TBDMSTFA (50 eq. or 500eq.) (Table XXIX). The reaction was allowed to proceed at room temperature for 19 h. LC-MS spectrum and HRMS spectra are displayed below (Figure 44-Figure 49).

Table XXIX Table XXIX: Silylation reagents and equivalents.

silylation reagent	equivalents	mmol	mg	μL
MSTFA	50	0.115	22.9	21.3
MSTFA	500	1.15	229	213
MTBSTFA	50	0.115	27.8	27.2
MTBSTFA	100	0.575	55.6	54.3
MTBSTFA	500	1.15	278	272



7d: HRMS (ESI-TOF): $m/z = 854.3885$ $[\text{M}+\text{H}]^+$ (calcd. for $[\text{C}_{42}\text{H}_{52}\text{N}_{11}\text{O}_9]^+$: $m/z = 854.3944$).

190d: HRMS (ESI-TOF): $m/z = 828.3991$ $[\text{M}+\text{H}]^+$ (calcd. for $[\text{C}_{42}\text{H}_{54}\text{N}_9\text{O}_9]^+$: $m/z = 828.4039$).

193d: HRMS (ESI-TOF): $m/z = 839.3781$ $[\text{M}+\text{H}]^+$ (calcd. for $[\text{C}_{42}\text{H}_{51}\text{N}_{10}\text{O}_9]^+$: $m/z = 839.3835$).

194d: HRMS (ESI-TOF): $m/z = 841.3931$ $[\text{M}+\text{H}]^+$ (calcd. for $[\text{C}_{42}\text{H}_{53}\text{N}_{10}\text{O}_9]^+$: $m/z = 841.3992$).

183d: HRMS (ESI-TOF): $m/z = 982.4157$ $[\text{M}+\text{H}]^+$ (calcd. for $[\text{C}_{49}\text{H}_{61}\text{N}_9\text{O}_{11}\text{P}]^+$: $m/z = 982.4223$).

(E/Z)-192d: HRMS (ESI-TOF): $m/z = 995.4134$ $[\text{M}+\text{H}]^+$ (calcd. for $[\text{C}_{49}\text{H}_{60}\text{N}_{10}\text{O}_{11}\text{P}]^+$: $m/z = 995.4175$).

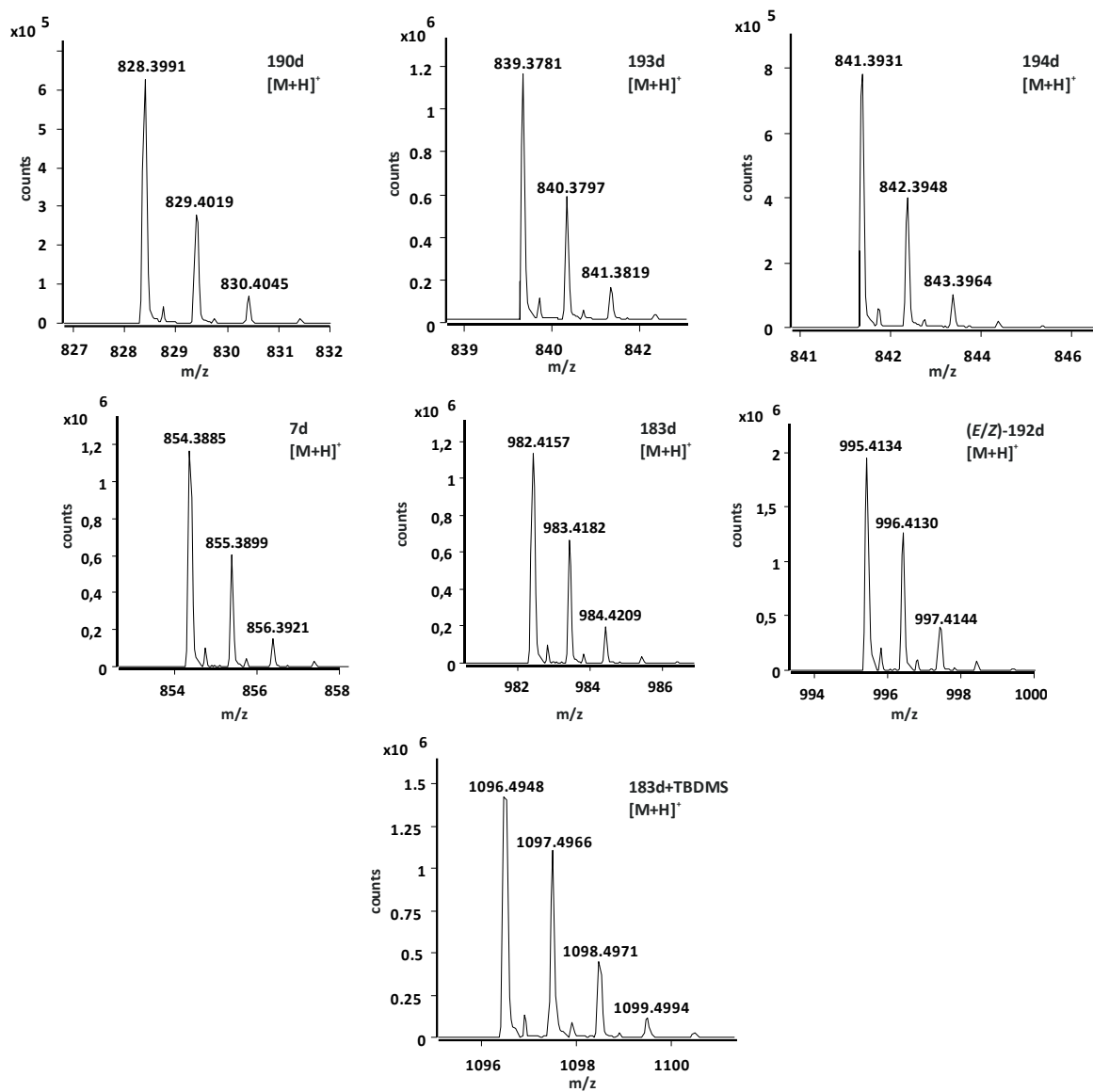


Figure 44: HRMS spectra of the UV-signals of **7d**, **190d**, **193d**, **194d**, **183d**, **183d+TBDMS** and **(E/Z)-192d**.

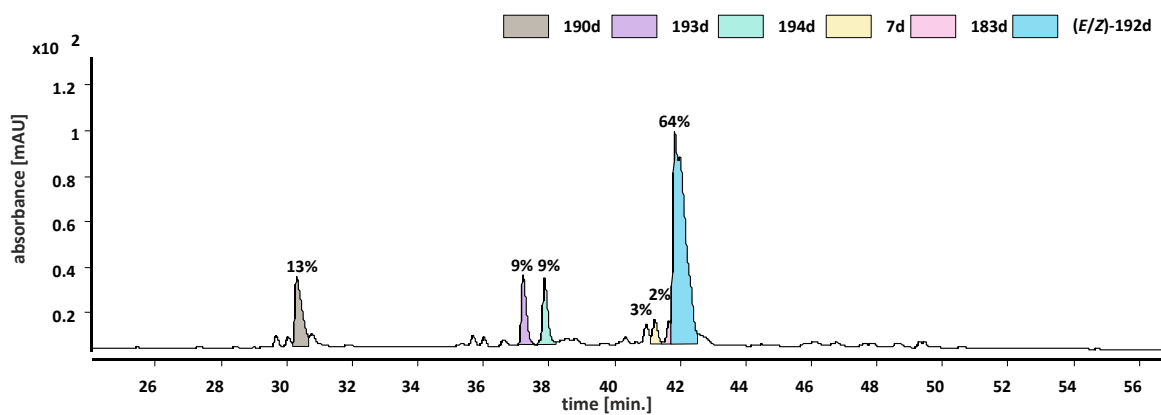


Figure 45: LC-MS spectrum (UV trace at 280 nm) of the Staudinger reaction with 50 equivalents MSTFA.

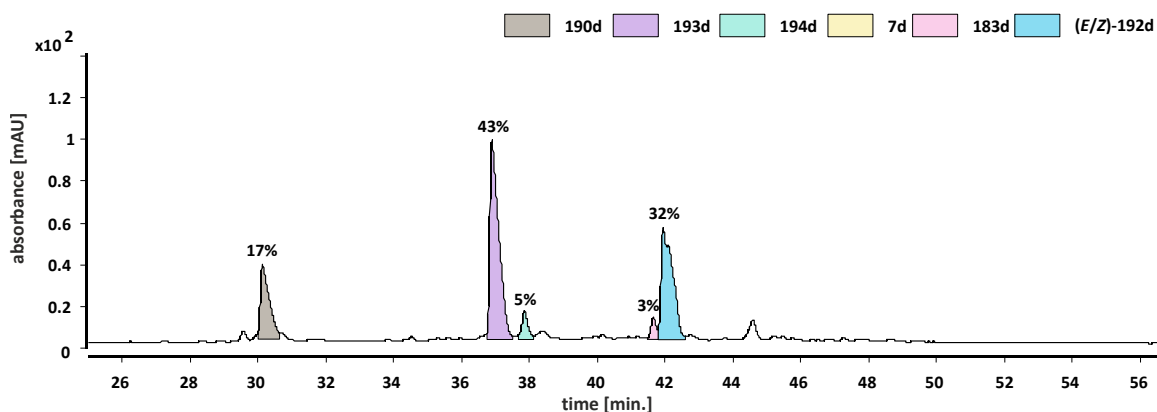


Figure 46: LC-MS spectrum of the Staudinger reaction with 500 equivalents MSTFA.

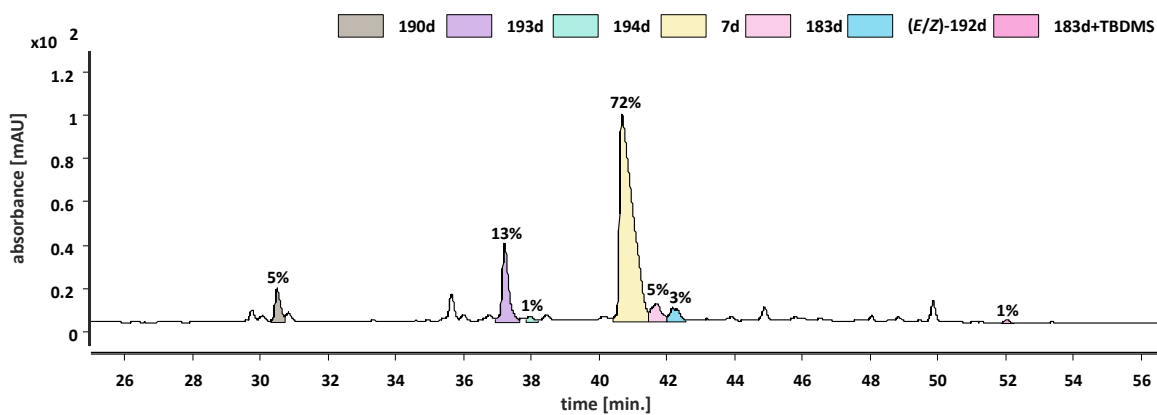


Figure 47: Reaction with 50 equivalents MTBSTFA.

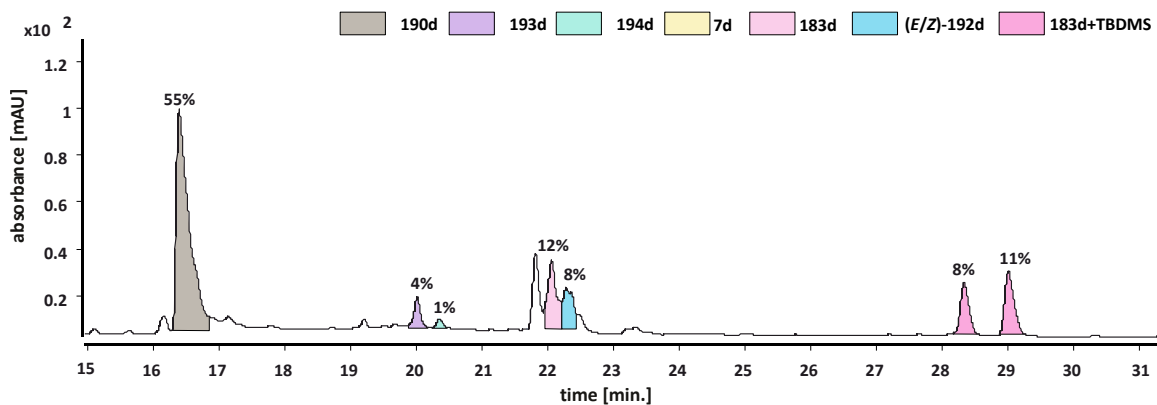


Figure 48: Reaction with 100 equivalents MTBSTFA.

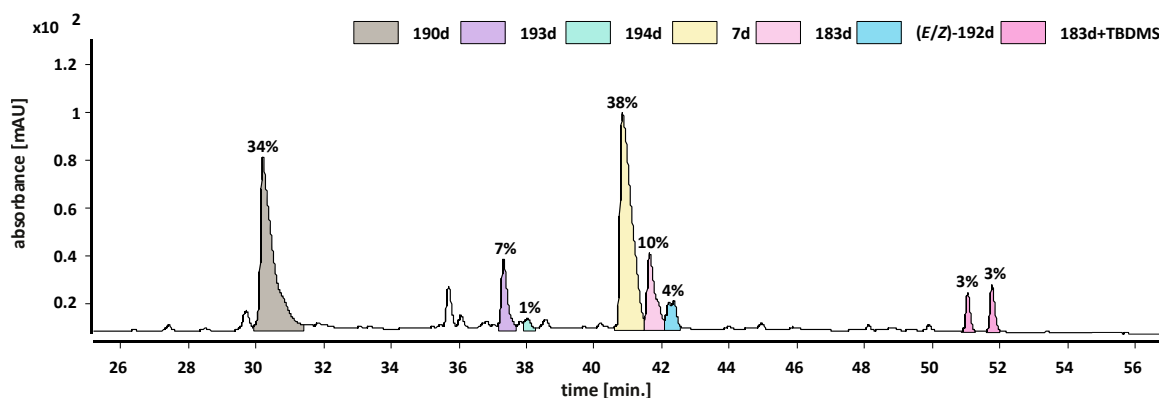


Figure 49: Reaction with 500 equivalents MTBSTFA.

5.5.7 Staudinger reaction in solution

The reaction was performed according to **general procedure IV** with methyl phenylphosphinate (**182**) (67 μmol , 11 mg), BSA (0.20 mmol, 40.9 mg, 49.1 μL) or MTBSTFA (0.20 mmol, 48.5 mg, 43.3 μL) and azido peptide **7e** (0.54 mg, 0.67 μmol) in anhydrous CH_2Cl_2 (500 μL). The reaction was allowed to proceed at room temperature for 24 h. The reaction mixture was analyzed by LC-MS and the ratio of both products was determined by integration of the UV-trace at 280 nm. LC-MS spectra and HRMS spectra are displayed below (Figure 50 and Figure 51).

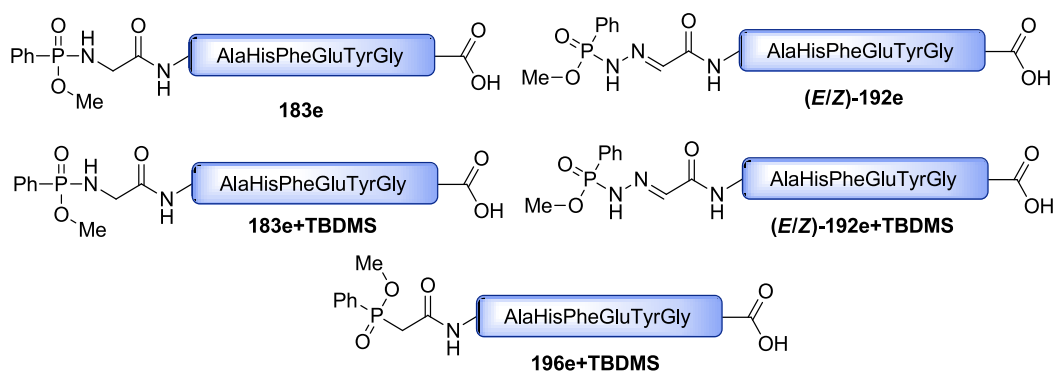
183e: HRMS (ESI-TOF): $m/z = 934.3430$ $[\text{M}+\text{H}]^+$ (calcd. for $[\text{C}_{43}\text{H}_{53}\text{N}_9\text{O}_{13}\text{P}]^+$: $m/z = 934.3495$).

(E/Z)-192e: HRMS (ESI-TOF): $m/z = 947.3382$ $[\text{M}+\text{H}]^+$ (calcd. for $[\text{C}_{43}\text{H}_{52}\text{N}_{10}\text{O}_{13}\text{P}]^+$: $m/z = 947.3447$).

183e+TBDMS: HRMS (ESI-TOF): $m/z = 1048.4349$ $[\text{M}+\text{H}]^+$ (calcd. for $[\text{C}_{49}\text{H}_{67}\text{N}_9\text{O}_{13}\text{PSi}]^+$: $m/z = 1048.4360$).

(E/Z)-192e+TBDMS: HRMS (ESI-TOF): $m/z = 1061.4291$ $[\text{M}+\text{H}]^+$ (calcd. for $[\text{C}_{49}\text{H}_{66}\text{N}_{10}\text{O}_{13}\text{PSi}]^+$: $m/z = 1061.4312$).

196e+TBDMS: HRMS (ESI-TOF): $m/z = 1033.4231$ $[\text{M}+\text{H}]^+$ (calcd. for $[\text{C}_{49}\text{H}_{66}\text{N}_8\text{O}_{13}\text{PSi}]^+$: $m/z = 1033.4251$).



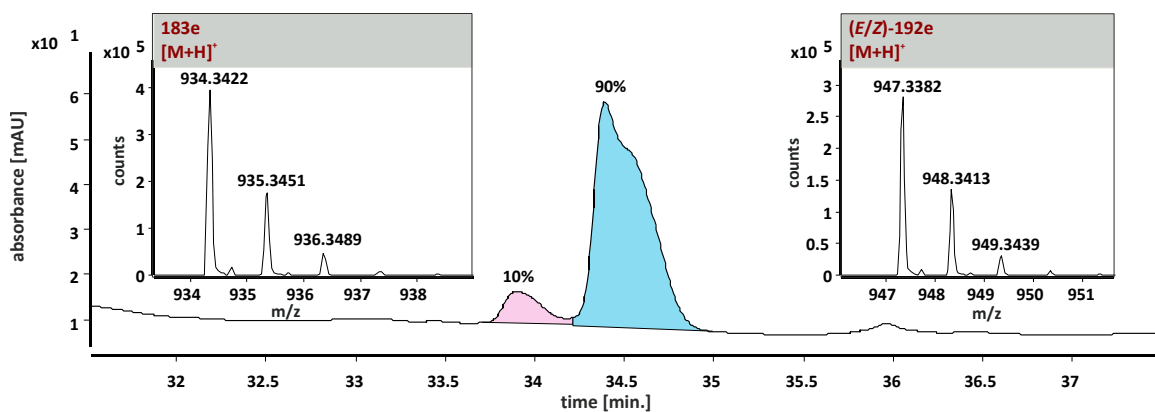


Figure 50: LC-MS spectrum of the Staudinger reaction with BSA in solution.

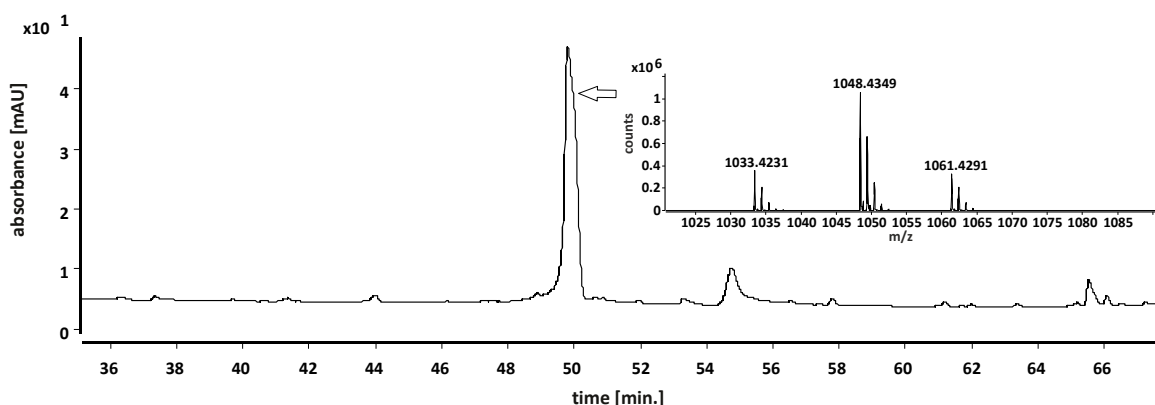
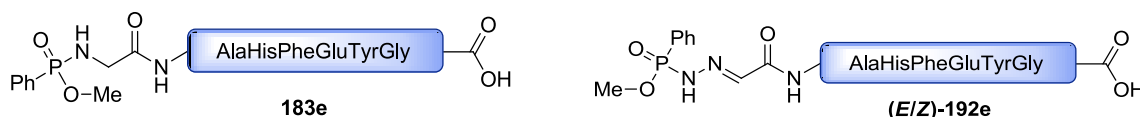


Figure 51: LC-MS spectrum of the Staudinger reaction with MTBSTFA in solution.

5.5.8 Purification of 183e and (E/Z)-192e for MS/MS analysis

The reaction was performed according to **general procedure IV** with methyl phenylphosphinate (**182**) (77.6 μmol , 12.1 mg), BSA (233 μmol , 47.3 mg, 56.9 μL) and azido peptide **7e** (6.25 mg, 7.76 μmol) in anhydrous CH_2Cl_2 (500 μL) for 24 h. The peptides **183e** and (**E/Z**)-**192e** were purified by semi-preparative HPLC with the following solvent gradient (A = H_2O , B = CH_3CN): 0-5 min. 0% B, 5-80 min. 0-100% B, 80-85 min. 100% B, 85-90 min. 100%-20%. The products were separated by HPLC and the isolated compounds were analyzed by HRMS (**Figure 52**) and MS/MS (Table XV).



183e: HRMS (ESI-TOF): $m/z = 934.3471$ $[\text{M}+\text{H}]^+$ (calcd. for $[\text{C}_{43}\text{H}_{53}\text{N}_9\text{O}_{13}\text{P}]^+$: $m/z = 934.3495$).

(**E/Z**)-**192e**: HRMS (ESI-TOF): $m/z = 947.3414$ $[\text{M}+\text{H}]^+$ (calcd. for $[\text{C}_{43}\text{H}_{52}\text{N}_{10}\text{O}_{13}\text{P}]^+$: $m/z = 947.3447$).

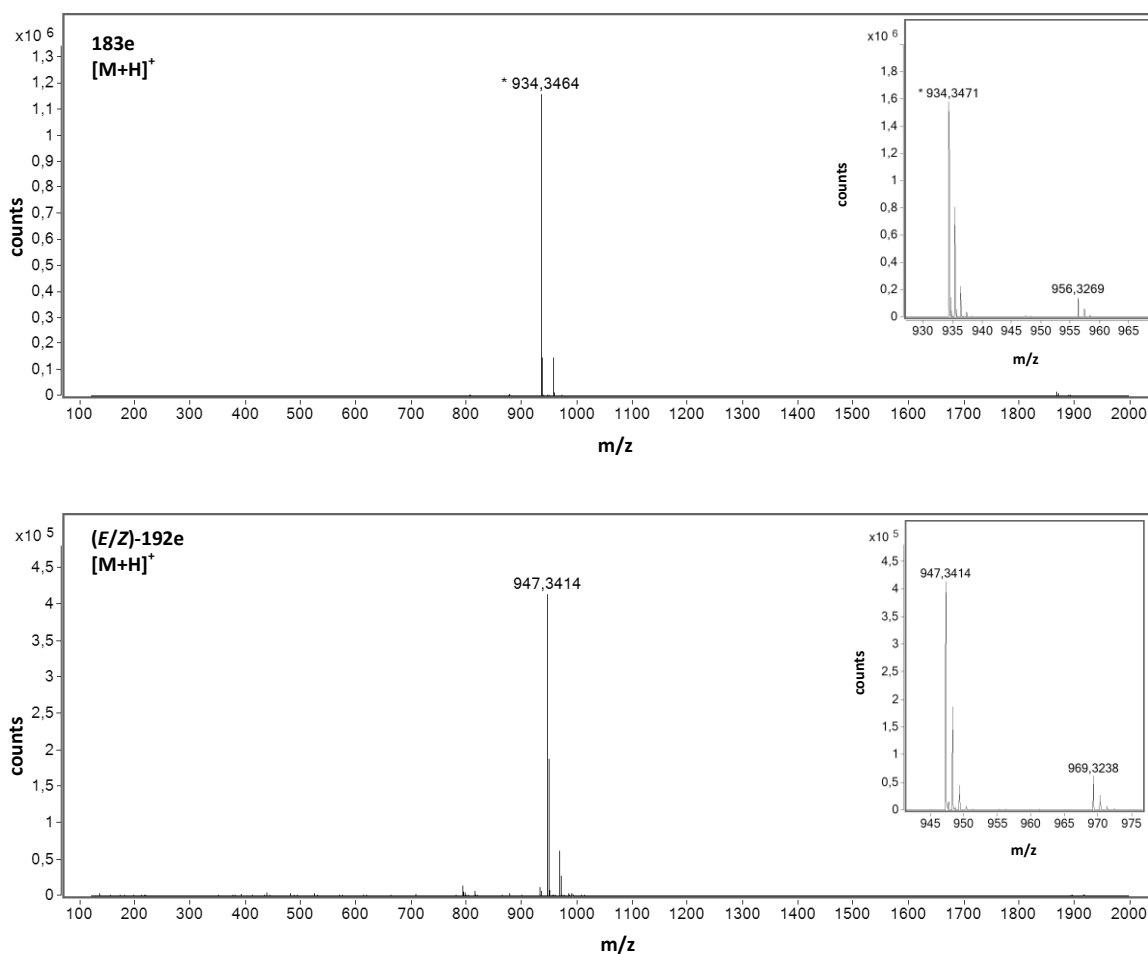


Figure 52: HRMS spectra of **183e** and **(E/Z)-192e** after HPLC purification.

5.5.9 Studies on the Staudinger reaction with 2-azido-2-methyl alanine peptides

On solid support:



The reaction was performed according to **general procedure III** with resin-bound peptide **7f** (19.6 mg, 5.05 μ mol), methyl phenylphosphinate (**182**) (40.0 mg, 0.253 mmol) and BSA (186 μ L, 154 mg, 0.759 mmol) and stirred for 19 h. After cleavage from the resin an LC-MS spectrum was measured (Figure 53).

219f: HRMS (ESI-TOF): m/z = 454.1923 [M+H]⁺ (calcd.: m/z = 454.1973).

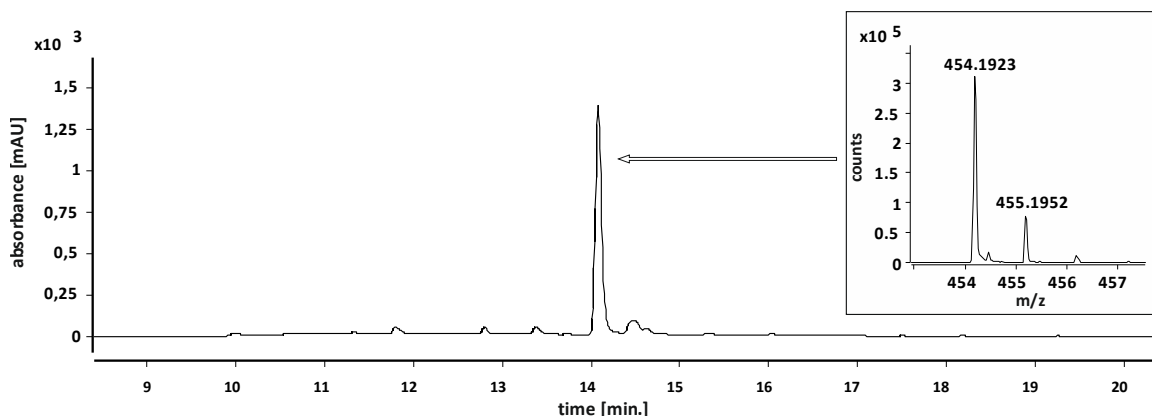
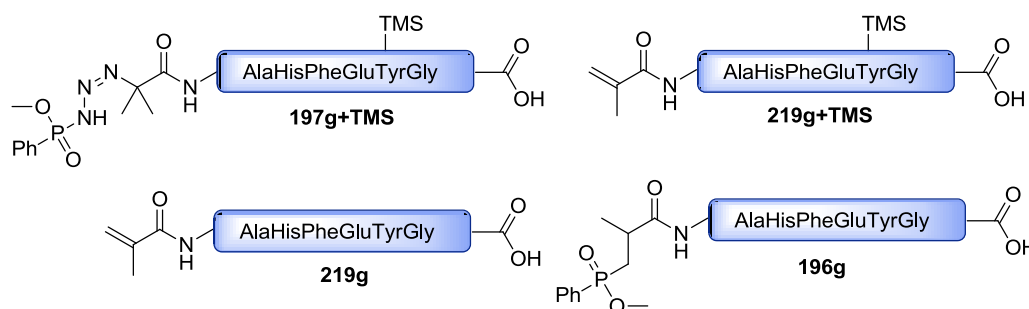


Figure 53: UV-trace (280 nm) and HRMS of the LC-MS spectrum of the Staudinger reaction with azido peptide **7f**.

Reaction in solution:

The reaction was performed according to **general procedure IV** with methyl phenylphosphinate (**182**) (72 μmol , 11 mg), BSA (216 μmol , 43.9 mg, 52.8 μL) and azido peptide **7f** (0.60 mg, 0.72 μmol) in anhydrous CH_3CN (500 μL). The reaction mixture was afterwards analyzed by HRMS and LC-MS (Figure 54) after stirring for 1 h and 25 h at room temperature.



197g+TMS: HRMS (ESI-TOF): $m/z = 1062.4297$ $[\text{M}+\text{H}]^+$ (calcd. for $[\text{C}_{48}\text{H}_{65}\text{N}_{11}\text{O}_{13}\text{PSi}]^+$: $m/z = 1062.4265$).

219g+TMS: HRMS (ESI-TOF): $m/z = 863.3779$ $[\text{M}+\text{H}]^+$ (calcd. for $[\text{C}_{41}\text{H}_{55}\text{N}_8\text{O}_{11}\text{Si}]^+$: $m/z = 863.3754$).

197g: HRMS (ESI-TOF): $m/z = 990.3832$ $[\text{M}+\text{H}]^+$ (calcd. for $[\text{C}_{45}\text{H}_{57}\text{N}_{11}\text{O}_{13}\text{P}]^+$: $m/z = 990.3869$).

219g: HRMS (ESI-TOF): $m/z = 791.3303$ $[\text{M}+\text{H}]^+$ (calcd. for $[\text{C}_{38}\text{H}_{47}\text{N}_8\text{O}_{11}]^+$: $m/z = 791.3359$).

196g: HRMS (ESI-TOF): $m/z = 791.3303$ $[\text{M}+\text{H}]^+$ (calcd. for $[\text{C}_{45}\text{H}_{56}\text{N}_8\text{O}_{13}\text{P}]^+$: $m/z = 947.3699$).

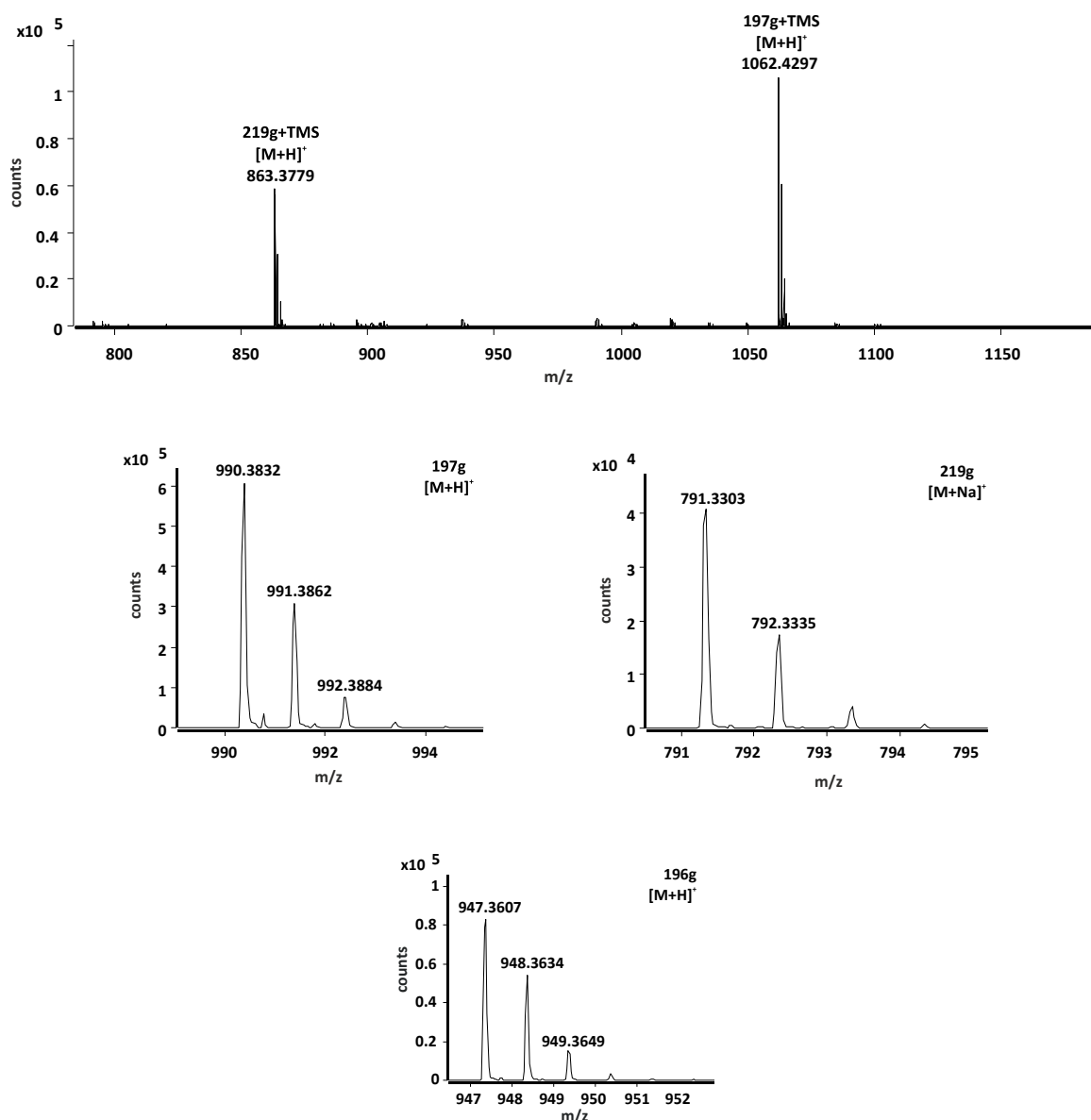


Figure 54: HRMS spectrum of the Staudinger reaction with azido peptide **7g** (1. HRMS spectrum after 1 h, 2. HRMS spectra of compounds **197g**, **219g** and **196g** after 25 h.

5.5.10 Stability studies

Methyl *N,P*-phenylphosphonamidate (**223**) (10 mg, 48 μ mol) or *N,P*-diphenylphosphonamidate (**221**) (10 mg, 40 μ mol) were dissolved in for different TFA-solutions in wet CH_2Cl_2 (0.6 ml) and ^{31}P -NMR spectra were measured over 26 h. Integrals (total 100%) of the different signals are displayed below (*N,P*-diphenylphosphonamidate (**223**) was stable in 1% TFA) (Table XXX-Table XXXVI):

Table XXX: *N,P*-diphenylphosphonamidate (**221**) in TFA (25%). Ratios of observed signals determined by integration of the ³¹P-NMR spectra.

time	31.64 ppm	26.96 ppm	25.87 ppm	19.17 ppm	13.93 ppm
0	0.0%	0.0%	100.0%	0.0%	0.0%
14 min.	0.0%	5.2%	89.4%	5.4%	0.0%
43 min.	0.0%	9.7%	82.9%	7.4%	0.0%
1 h 25 min.	0.0%	16.9%	72.1%	11.1%	0.0%
1 h 57 min.	0.0%	25.2%	62.2%	9.7%	2.9%
3 h 10 min.	0.5%	38.7%	46.1%	10.8%	4.5%
4 h 38 min.	0.5%	51.6%	32.8%	7.2%	8.4%
6 h 38 min.	0.3%	65.3%	19.6%	4.2%	10.6%
24 h 57 min.	0.0%	82.9%	0.0%	0.0%	17.1%

Table XXXI: *N,P*-diphenylphosphonamidate (**221**) in TFA (50%). Ratios of observed signals determined by integration of the ³¹P-NMR spectra.

time	27.2 ppm	26.68 ppm	19.67 ppm	14.44 ppm
0	0.0%	100.0%	0.0%	0.0%
2 min.	10.0%	75.9%	14.1%	0.0%
4 min.	15.2%	65.6%	19.1%	0.0%
1 h 20 min.	27.0%	47.1%	24.4%	1.5%
1 h 56 min.	41.9%	33.1%	22.2%	2.7%
3 h 9 min.	57.9%	17.9%	17.8%	6.4%
4 h 38 min.	74.0%	8.6%	10.7%	6.7%
6 h 37 min.	80.1%	3.7%	6.7%	9.5%
24 h 56 min.	88.6%	0.0%	0.0%	11.4%

Table XXXII: *N,P*-diphenylphosphonamidate (**221**) in TFA (95%). Ratios of observed signals determined by integration of the ³¹P-NMR spectra.

time	31.62 ppm	27.86 ppm	27.56 ppm	20.48 ppm	15.11 ppm
0	0.0%	86.4%	0.0%	13.6%	0.0%
23 min.	0.0%	32.9%	20.4%	46.7%	0.0%
1 h 6 min.	0.0%	17.8%	26.5%	53.2%	2.5%
1 h 19 min.	0.4%	0.0%	54.0%	42.3%	3.4%
1 h 56 min.	0.0%	0.0%	64.0%	31.7%	4.3%
3 h 9 min.	0.0%	0.0%	75.5%	20.8%	6.1%
4 h 38 min.	0.0%	0.0%	82.1%	11.9%	4.2%
6 h 37 min.	1.2%	0.0%	86.1%	6.6%	6.1%
24 h 55 min.	0.0%	0.0%	94.5%	0.0%	5.5%

Table XXXIII: Methyl *N,P*-phenylphosphonamidate (**223**) in TFA (1%). Ratios of observed signals determined by integration of the ³¹P-NMR spectra.

time	27.7 ppm	24.61 ppm	23.37 ppm	12.63 ppm
0 min.	98.8%	0.0%	1.2	0.0%
39 min.	94.5%	2.7%	1.3	0.0%
52 min.	95.0%	5.0%	0.0%	0.0%
1 h 10 min.	91.9%	8.1%	0.0%	0.0%
2 h 3 min.	76.6v	0.0%	0.0%	0.0%
3 h 8 min.	72.5%	0.0%	23.9%	1.9%
4 h 20 min.	62.5%	0.0%	31.6%	6.0%
5 h 50 min.	54.3%	0.0%	35.6%	10.1%
7 h 50 min.	45.2%	0.0%	40.9%	14.0%
26 h 8 min.	9.8%	0.0%	56.5%	33.7%

Table XXXIV: Methyl *N,P*-phenylphosphonamidate (**223**) in TFA (25%). Ratios of observed signals determined by integration of the ³¹P-NMR spectra.

time	31.6 ppm	27.0 ppm	23.3 ppm	19.2 ppm	14.23 ppm
0 min.	48.4%	7.7%	1.2%	41.2%	0.0%
10 min.	5.7%	19.2%	1.2%	73.2%	0.7%
24 min.	0.7%	26.5%	0.9%	70.9%	0.9%
55 min.	0.0%	32.7%	0.9%	64.8%	1.5%
2 h 16 min.	0.0%	42.4%	0.9%	54.8%	1.9%
2 h 53 min.	0.0%	44.9%	1.0%	51.4%	2.7%
4 h 0 min.	0.0%	47.2%	0.0%	48.2%	4.6%
5 h 35 min.	0.0%	49.0%	0.9%	45.3%	4.8%
7 h 35 min.	0.0%	47.5%	0.0%	45.0%	7.5%
25 h 5 min.	0.0%	52.5%	0.0%	32.5%	15.1%

Table XXXV: Methyl *N,P*-phenylphosphonamidate (**223**) in TFA (50%). Ratios of observed signals determined by integration of the ³¹P-NMR spectra.

time	32.19 ppm	27.13 ppm	19.65 ppm	14.42 ppm
0 min.	31.5%	6.1%	57.2%	0.0%
9 min.	1.1%	21.6%	75.6%	0.0%
23 min.	0.0%	27.4%	70.4%	0.0%
54 min.	0.0%	33.6%	62.9%	0.0%
1 h 14 min.	0.0%	44.1%	54.3%	0.0%
2 h 52 min.	0.0%	46.6%	50.2%	2.5%
4 h 5 min.	0.0%	48.9%	48.7%	2.4%
5 h 34 min.	0.0%	49.3%	46.9%	3.8%
7 h 14 min.	0.0%	50.6%	44.4%	5.0%
25 h 5 min.	0.0%	53.5%	34.1%	12.4%

Table XXXVI: Methyl *N,P*-phenylphosphonamidate (**223**) in TFA (95%). Ratios of observed signals determined by integration of the ^{31}P -NMR spectra.

time	33.26 ppm	27.58 ppm	20.49 ppm	15.12 ppm
0 min.	10.1%	7.8%	79.3%	0.0%
5 min.	0.0%	18.1%	78.6%	0.0%
24 min.	0.0%	33.3%	66.0%	0.0%
50 min.	0.0%	40.2%	59.8%	0.0%
1 h 46 min.	0.0%	51.5%	45.2%	0.0%
2 h 23 min.	0.0%	57.9%	38.6%	2.1%
3 h 4 min.	0.0%	66.1%	32.0%	2.4%
5 h 4 min.	0.0%	65.5%	30.3%	3.0%
7 h 4 min.	0.0%	70.1%	26.9%	3.0%
25 h 3 min.	0.0%	75.6%	16.6%	7.8%

223: HRMS (ESI-TOF): $m/z = 262.0994$ $[\text{M}+\text{H}]^+$ (calcd. for $[\text{C}_{14}\text{H}_{17}\text{NO}_2\text{P}]^+$: $m/z = 262.0991$).

221: HRMS (ESI-TOF): $m/z = 248.0835$ $[\text{M}+\text{H}]^+$ (calcd. for $[\text{C}_{13}\text{H}_{15}\text{NO}_2\text{P}]^+$: $m/z = 248.0835$).

187: HRMS (ESI-TOF): $m/z = 173.0365$ $[\text{M}+\text{H}]^+$ (calcd. for $[\text{C}_7\text{H}_{10}\text{O}_3\text{P}]^+$: $m/z = 173.0362$).

6 Literature

- [1] a) S. E. Denmark, D. M. Coe, N. E. Pratt, B. D. Griedel, *J. Org. Chem.* **1994**, *59*, 6161-6163; b) S. E. Denmark, S. B. D. Winter, X. Su, K.-T. Wong, *J. Am. Chem. Soc.* **1996**, *118*, 7404-7405; c) S. E. Denmark, K.-T. Wong, R. A. Stavenger, *J. Am. Chem. Soc.* **1997**, *119*, 2333-2334; d) S. E. Denmark, R. A. Stavenger, K. T. Wong, X. P. Su, *J. Am. Chem. Soc.* **1999**, *121*, 4982-4991; e) S. E. Denmark, R. A. Stavenger, K.-T. Wong, X. Su, *J. Am. Chem. Soc.* **1999**, *121*, 4982-4991; f) S. E. Denmark, R. A. Stavenger, *J. Am. Chem. Soc.* **2000**, *122*, 8837-8847; g) S. E. Denmark, S. K. Ghosh, *Angew. Chem. Int. Ed.* **2001**, *40*, 4759-4762; h) S. E. Denmark, J. P. Fu, *J. Am. Chem. Soc.* **2003**, *125*, 2208-2216; i) S. E. Denmark, G. L. Beutner, T. Wynn, M. D. Eastgate, *J. Am. Chem. Soc.* **2005**, *127*, 3774-3789; j) S. E. Denmark, B. M. Eklov, P. J. Yao, M. D. Eastgate, *J. Am. Chem. Soc.* **2009**, *131*, 11770-11787; k) S. E. Denmark, S. Fujimori, S. M. Pham, *J. Org. Chem.* **2005**, *70*, 10823-10840; l) A. Hasegawa, Y. Naganawa, M. Fushimi, K. Ishihara, H. Yamamoto, *Org. Lett.* **2006**, *8*, 3175-3178; m) D. Nakashima, H. Yamamoto, *J. Am. Chem. Soc.* **2006**, *128*, 9626-9627; n) C. H. Cheon, H. Yamamoto, *J. Am. Chem. Soc.* **2008**, *130*, 9246-9247; o) P. Jiao, D. Nakashima, H. Yamamoto, *Angew. Chem. Int. Ed.* **2008**, *47*, 2411-2413; p) M. Rueping, W. leawsuwan, A. P. Antonchick, B. J. Nachtsheim, *Angew. Chem.* **2007**, *119*, 2143-2146; q) M. Rueping, W. leawsuwan, *Chem. Commun.* **2011**, *47*, 11450-11452; r) M. Rueping, B. J. Nachtsheim, W. leawsuwan, I. Atodiresei, *Angew. Chem. Int. Ed.* **2011**, *50*, 6706-6720; s) S. Vellalath, I. Čorić, B. List, *Angew. Chem. Int. Ed.* **2010**, *49*, 9749-9752; t) V. N. Wakchaure, B. List, *Angew. Chem. Int. Ed.* **2010**, *49*, 4136-4139; u) B. Burns, J. R. Studley, M. Wills, *Tetrahedron Lett.* **1993**, *34*, 7105-7106.
- [2] a) J. Ruprecht, O. E. Ukponmwan, P. V. Admiraal, M. R. Dzoljic, *Neurosci. Lett.* **1983**, *41*, 331-335; b) T. Komiyama, H. Suda, T. Aoyagi, T. Takeuchi, H. Umezawa, K. Fujimoto, S. Umezawa, *Arch. Biochem. Biophys.* **1975**, *171*, 727-731; c) H. Suda, T. Aoyagi, T. Takeuchi, H. Umezawa, *J. Antibiot.* **1973**, *26*, 621-623; d) R. J. Cox, J. S. Gibson, M. B. Mayo Martín, *ChemBioChem* **2002**, *3*, 874-886; e) L. Y. Wu, M. O. Anderson, Y. Toriyabe, J. Maung, T. Y. Campbell, C. Tajon, M. Kazak, J. Moser, C. E. Berkman, *Biorg. Med. Chem.* **2007**, *15*, 7434-7443; f) N. E. Jacobsen, P. A. Bartlett, *J. Am. Chem. Soc.* **1981**, *103*, 654-657; g) P. A. Bartlett, C. K. Marlowe, *Biochemistry* **1983**, *22*, 4618-4624; h) K. A. Mookhtiar, C. K. Marlowe, P. A. Bartlett, H. E. Van Wart, *Biochemistry* **1987**, *26*, 1962-1965; i) R. L. Elliott, N. Marks, M. J. Berg, P. S. Portoghese, *J. Med. Chem.* **1985**, *28*, 1208-1216; j) D. A. McLeod, R. I. Brinkworth, J. A. Ashley, K. D. Janda, P. Wirsching, *Bioorg. Med. Chem. Lett.* **1991**, *1*, 653-658; k) N. P. Camp, D. A. Perrey, D. Kinchington, P. C. D. Hawkins, D. Gani, *Bioorg. Med. Chem.* **1995**, *3*, 297-312; l) A. Mucha, A. Kunert, J. Grembecka, M. Pawelczak, P. Kafarski, *Eur. J. Med. Chem.* **2006**, *41*, 768-772.
- [3] H. Staudinger, J. Meyer, *Helv. Chim. Acta* **1919**, *2*, 635-646.
- [4] a) I. Wilkening, G. del Signore, C. P. R. Hackenberger, *Chem. Commun.* **2008**, 2932-2934; b) I. Wilkening, G. del Signore, W. Ahlbrecht, C. P. R. Hackenberger, *Synthesis* **2011**, 2709-2720.
- [5] a) G. K. Genkina, V. A. Gilyarov, E. I. Matrosov, M. I. Kabachnik, *Zh. Obshch. Khim.* **1970**, *40*, 1496-1501; b) B. C. Challis, J. A. Challis, J. N. Iley, *J. Chem. Soc., Perkin Trans. 2* **1978**, 813-818; c) V. A. Gilyarov, B. A. Kvasov, T. M. Shcherbina, M. I. Kabachnik, *Bull. Acad. Sci. USSR Div. Chem. Sci. (Engl. Transl.)* **1980**, *29*, 136-139; d) V. A. Gilyarov, T. M. Shcherbina, A. P. Laretina, M. I. Kabachnik, *Bull. Russ. Acad. Sci.: Chem. Science* **1992**, *41*, 1931-1934; e) T. A. Mastryukova, N. V. Mashchenko, I. L. Odinets, P. V. Petrovskii, M. I. Kabachnik, *Zh. Obshch. Khim.* **1988**, *58*, 1967-1973; f) T. M. Shcherbina, A. P. Laretina, V. A. Gilyarov, M. I. Kabachnik, *Russ. Chem. Bull.* **1994**, *43*, 641-644; g) T. M. Shcherbina, A. P. Laretina, V. A. Gilyarov, A. A. Korokin, M. I. Kabachnik, *Bull. Acad. Sci. USSR Div. Chem. Sci. (Engl. Transl.)* **1991**, *40*, 239-239.
- [6] a) R. Serwa, I. Wilkening, G. Del Signore, M. Mühlberg, I. Claussnitzer, C. Weise, M. Gerrits, C. P. R. Hackenberger, *Angew. Chem. Int. Ed.* **2009**, *48*, 8234-8239; b) M. R. J. Vallée, P. Majkut, I. Wilkening, C. Weise, G. Müller, C. P. R. Hackenberger, *Org. Lett.* **2011**, *13*, 5440-5443.
- [7] I. Wilkening, G. del Signore, C. P. R. Hackenberger, *Chem. Commun.* **2011**, *47*, 349-351.
- [8] a) S. Gryaznov, T. Skorski, C. Cucco, M. Nieborowska-Skorska, C. Ying Chiu, D. Lloyd, J.-K. Chen, M. Koziolkiewicz, B. Calabretta, *Nucleic Acids Res.* **1996**, *24*, 1508-1514; b) S. M. Gryaznov, H. Winter, *Nucleic Acids Res.* **1998**, *26*, 4160-4167; c) V. Tereshko, S. Gryaznov, M. Egli, *J. Am. Chem. Soc.* **1998**, *120*, 269-283.

- [9] a) M. Kohn, R. Breinbauer, *Angew. Chem. Int. Ed. Engl.* **2004**, *43*, 3106-3116; b) C. I. Schilling, N. Jung, M. Biskup, U. Schepers, S. Bräse, *Chem Soc Rev* **2011**, *40*, 4840-4871; c) S. S. van Berkel, M. B. van Eldijk, J. C. van Hest, *Angew. Chem. Int. Ed. Engl.* **2011**, *50*, 8806-8827; d) E. Saxon, J. I. Armstrong, C. R. Bertozzi, *Org Lett* **2000**, *2*, 2141-2143; e) E. Saxon, C. R. Bertozzi, *Science* **2000**, *287*, 2007-2010; f) M. J. Hangauer, C. R. Bertozzi, *Angew. Chem. Int. Ed. Engl.* **2008**, *47*, 2394-2397; g) F. L. Lin, H. M. Hoyt, H. van Halbeek, R. G. Bergman, C. R. Bertozzi, *J. Am. Chem. Soc.* **2005**, *127*, 2686-2695; h) J. A. Prescher, D. H. Dube, C. R. Bertozzi, *Nature* **2004**, *430*, 873-877; i) H. C. Hang, C. Yu, M. R. Pratt, C. R. Bertozzi, *J. Am. Chem. Soc.* **2004**, *126*, 6-7; j) G. A. Lemieux, C. L. De Graffenried, C. R. Bertozzi, *J. Am. Chem. Soc.* **2003**, *125*, 4708-4709; k) E. Saxon, S. J. Luchansky, H. C. Hang, C. Yu, S. C. Lee, C. R. Bertozzi, *J. Am. Chem. Soc.* **2002**, *124*, 14893-14902; l) K. L. Kiick, E. Saxon, D. A. Tirrell, C. R. Bertozzi, *Proc Natl Acad Sci U S A* **2002**, *99*, 19-24.
- [10] a) P. Cuatrecasas, *Annu. Rev. Biochem* **1974**, *43*, 169-214; b) A. G. Gilman, *Annu. Rev. Biochem* **1987**, *56*, 615-649; c) A. Gutteridge, J. M. Thornton, *Trends Biochem. Sci* **2005**, *30*, 622-629; d) L. N. Kinch, N. V. Grishin, *Curr. Opin. Struct. Biol.* **2002**, *12*, 400-408; e) C. T. Walsh, S. Garneau-Tsodikova, G. J. Gatto, *Angew. Chem. Int. Ed.* **2005**, *44*, 7342-7372; f) N. Wettschureck, S. Offermanns, *Physiol. Rev.* **2005**, *85*, 1159-1204; g) Donald Voet, Judith G. Voet, C. W. Pratt, *Lehrbuch der Biochemie, 2., aktualis. u. erw. Aufl.*, Wiley-Vch, Weinheim, **2010**; h) Jeremy M. Berg, John L. Tymoczko, L. Stryer, *Stryer Biochemie*, Spektrum Akademischer Verlag **2006**.
- [11] H. Staudinger, J. Meyer, *Helv. Chim. Acta* **1919**, *2*, 619-635.
- [12] Y. G. Gololobov, I. N. Zhmurova, L. F. Kasukhin, *Tetrahedron* **1981**, *37*, 437-472.
- [13] I. Kabachnik, V. A. Gilyarov., *Izv. Akad. Nauk SSSR. Otd. Khim. Nauk* **1956**, 790.
- [14] a) Y. G. Gololobov, L. F. Kasukhin, V. S. Petrenko, *Phosphorus, Sulfur Silicon Relat. Elem.* **1987**, *30*, 393-396; b) Y. G. Gololobov, L. F. Kasukhin, *Tetrahedron* **1992**, *48*, 1353-1406.
- [15] Y. Gololobov, L. Kasukhin, M. Ponomarchuk, T. Klepa, R. Yurchenko, *Phosphorus, Sulfur Silicon Relat. Elem.* **1981**, *10*, 339-342.
- [16] a) M. Desamparados Velasco, P. Molina, P. M. Fresneda, M. A. Sanz, *Tetrahedron* **2000**, *56*, 4079-4084; b) G. C. Fortman, B. Captain, C. D. Hoff, *Inorg. Chem.* **2009**, *48*, 1808-1810; c) P. M. Fresneda, M. Castañeda, M. A. Sanz, P. Molina, *Tetrahedron Lett.* **2004**, *45*, 1655-1657; d) J. R. Goerlich, M. Farkens, A. Fischer, P. G. Jones, R. Schmutzler, *Z. Anorg. Allg. Chem.* **1994**, *620*, 707-715; e) V. P. Kukhar, L. F. Kasukhin, M. P. Ponomarchuk, A. N. Chernega, M. Y. Antipin, Y. T. Struchkov, *Phosphorus, Sulfur Silicon Relat. Elem.* **1989**, *44*, 149-153.
- [17] a) M. Alajarin, C. Conesa, H. S. Rzepa, *J. Chem. Soc., Perkin Trans. 2* **1999**, 1811-1814; b) W. Q. Tian, Y. A. Wang, *J. Org. Chem.* **2004**, *69*, 4299-4308.
- [18] a) C. Widauer, H. Grützmacher, I. Shevchenko, V. Gramlich, *Eur. J. Inorg. Chem.* **1999**, 1999, 1659-1664; b) M. W. P. Bebbington, D. Bourissou, *Coord. Chem. Rev.* **2009**, *253*, 1248-1261.
- [19] P. M. Wehn, J. Du Bois, *Angew. Chem. Int. Ed.* **2009**, *48*, 3802-3805.
- [20] T. Graening, H. G. Schmalz, *Angew. Chem. Int. Ed.* **2004**, *43*, 3230-3256.
- [21] S. Nagarajan, B. Ganem, *J. Org. Chem.* **1987**, *52*, 5044-5046.
- [22] J. Rebek, S. H. Shaber, Y. K. Shue, J. C. Gehret, S. Zimmerman, *J. Org. Chem.* **1984**, *49*, 5164-5174.
- [23] a) X. Ariza, F. Urpi, C. Viladomat, J. Vilarrasa, *Tetrahedron Lett.* **1998**, *39*, 9101-9102; b) X. Ariza, F. Urpi, J. Vilarrasa, *Tetrahedron Lett.* **1999**, *40*, 7515-7517.
- [24] a) A. Koziara, K. Osowskapacewiczka, S. Zawadzki, A. Zwierzak, *Synthesis* **1985**, 202-204; b) A. Koziara, K. Osowskapacewiczka, S. Zawadzki, A. Zwierzak, *Synthesis* **1987**, 487-489; c) A. Zwierzak, A. Koziara, *Phosphorus, Sulfur Silicon Relat. Elem.* **1987**, *30*, 331-334.
- [25] a) E. Fabiano, B. T. Golding, M. M. Sadeghi, *Synthesis* **1987**, 190-192; b) A. Koziara, A. Zwierzak, *Tetrahedron Lett.* **1987**, *28*, 6513-6516; c) A. Koziara, *J. Chem. Res., Synop.* **1989**, 296-297.
- [26] S. I. Murahashi, Y. Taniguchi, Y. Imada, Y. Tanigawa, *J. Org. Chem.* **1989**, *54*, 3292-3303.
- [27] S. Kusumoto, K. Sakai, T. Shiba, *Bull. Chem. Soc. Jpn.* **1986**, *59*, 1296-1298.
- [28] a) A. R. Katritzky, J. L. Jiang, L. Urogdi, *Tetrahedron Lett.* **1989**, *30*, 3303-3306; b) A. R. Katritzky, J. L. Jiang, L. Urogdi, *Synthesis* **1990**, 565-567.
- [29] E. Årstad, A. G. M. Barrett, B. T. Hopkins, J. Köbberling, *Org. Lett.* **2002**, *4*, 1975-1977.
- [30] a) K. Furukawa, H. Abe, K. Hibino, Y. Sako, S. Tsuneda, Y. Ito, *Bioconjugate Chem.* **2009**, *20*, 1026-1036; b) R. M. Franzini, E. T. Kool, *ChemBioChem* **2008**, *9*, 2981-2988; c) K. Gorska, A. Manicardi, S. Barluenga, N. Winssinger, *Chem. Commun.* **2011**, *47*, 4364-4366; d) R. M. Franzini, E. T. Kool, *Bioconjugate Chem.* **2011**, *22*, 1869-1877; e) K. Gorska, I. Keklikoglou, U. Tschulena, N. Winssinger, *Chemical Science* **2011**, *2*, 1969-1975; f) R. M. Franzini, E. T. Kool, *J. Am. Chem. Soc.*

- 2009, 131, 16021-16023; g) R. M. Franzini, E. T. Kool, *Chem. Eur. J.* **2011**, 17, 2168-2175; h) K. Furukawa, H. Abe, J. Wang, M. Uda, H. Koshino, S. Tsuneda, Y. Ito, *Org. Biomol. Chem.* **2009**, 7, 671-677; i) Z. Pianowski, K. Gorska, L. Oswald, C. A. Merten, N. Winssinger, *J. Am. Chem. Soc.* **2009**, 131, 6492-6497; j) A. Shibata, H. Abe, K. Furukawa, S. Tsuneda, Y. Ito, *Chem. Pharm. Bull.* **2009**, 57, 1223-1226; k) M. Stoop, C. J. Leumann, *Chem. Commun.* **2011**, 47, 7494-7496.
- [31] J. Zaloom, M. Calandra, D. C. Roberts, *J. Org. Chem.* **1985**, 50, 2601-2603.
- [32] M. Jie, W. L. K. Lam, H. B. Lao, *J. Chem. Soc., Perkin Trans.1* **1989**, 1-11.
- [33] S. Friedrichbochnitschek, H. Waldmann, H. Kunz, *J. Org. Chem.* **1989**, 54, 751-756.
- [34] a) J. Garcia, J. Vilarrasa, X. Bordas, A. Banaszek, *Tetrahedron Lett.* **1986**, 27, 639-640; b) J. Barluenga, M. Ferrero, F. Palacios, *J. Chem. Soc., Perkin Trans.1* **1990**, 2193-2197.
- [35] a) M. D. Bachi, J. Vaya, *J. Org. Chem.* **1979**, 44, 4393-4396; b) M. D. Bachi, J. Klein, *J. Chem. Soc., Perkin Trans.1* **1983**, 1925-1928.
- [36] A. Koziara, *J. Prakt. Chem.* **1988**, 330, 473-475.
- [37] a) V. Böhrsch, R. Serwa, P. Majkut, E. Krause, C. P. R. Hackenberger, *Chem. Commun.* **2010**, 46, 3176-3178; b) R. Serwa, P. Majkut, B. Horstmann, J.-M. Swiecicki, M. Gerrits, E. Krause, C. P. R. Hackenberger, *Chemical Science* **2010**, 1, 596-602; c) R. A. Serwa, J.-M. Swiecicki, D. Homann, C. P. R. Hackenberger, *J. Pept. Sci.* **2010**, 16, 563-567.
- [38] a) E. E. Lee, R. A. Batey, *Angew. Chem. Int. Ed. Engl.* **2004**, 43, 1865-1868; b) B. Chen, A. K. Mapp, *J. Am. Chem. Soc.* **2004**, 126, 5364-5365.
- [39] M. Karpf, R. Trussardi, *Angew. Chem. Int. Ed.* **2009**, 48, 5760-5762.
- [40] S. Ayesa, B. Samuelsson, B. Classon, *Synlett* **2008**, 2008, 97,99.
- [41] a) F. Palacios, C. Alonso, D. Aparicio, G. Rubiales, J. M. de los Santos, *Tetrahedron* **2007**, 63, 523-575; b) P. M. Fresneda, P. Molina, *Synlett* **2004**, 2004, 1,17; c) H. Wamhoff, G. Richardt, S. Stöben, in *Adv. Heterocycl. Chem., Vol. Volume 64* (Ed.: R. K. Alan), Academic Press, **1995**, pp. 159-249; d) P. Molina, M. J. Vilaplana, *Synthesis* **1994**, 1994, 1197,1218.
- [42] a) T. Kawashima, T. Soda, R. Okazaki, *Angew. Chem. Int. Ed.* **1996**, 35, 1096-1098; b) N. Kano, X. J. Hua, S. Kawa, T. Kawashima, *Tetrahedron Lett.* **2000**, 41, 5237-5241.
- [43] a) J. Koketsu, Y. Ninomiya, Y. Suzuki, N. Koga, *Inorg. Chem.* **1997**, 36, 694-702; b) W. C. Lu, C. B. Liu, C. C. Sun, *J. Phys. Chem. A* **1999**, 103, 1078-1083; c) W. C. Lu, C. C. Sun, Q. J. Zang, C. B. Liu, *Chem. Phys. Lett.* **1999**, 311, 491-498.
- [44] a) A. B. Charette, A. A. Boezio, M. K. Janes, *Org. Lett.* **2000**, 2, 3777-3779; b) K. Hemming, M. J. Bevan, C. Loukou, S. D. Patel, D. Renaudeau, *Synlett* **2000**, 1565-1568.
- [45] P. Molina, F. Murcia, P. M. Fresneda, *Tetrahedron Lett.* **1994**, 35, 1453-1456.
- [46] F. Palacios, E. Herran, G. Rubiales, J. M. Ezpeleta, *J. Org. Chem.* **2002**, 67, 2131-2135.
- [47] T. Bohn, W. Kramer, R. Neidlein, H. Suschitzky, *J. Chem. Soc., Perkin Trans.1* **1994**, 947-951.
- [48] F. Palacios, A. M. a. O. de Retana, E. M. n. de Marigorta, M. Rodriguez, J. Pagalday, *Tetrahedron* **2003**, 59, 2617-2623.
- [49] a) J. García Fernández, C. Ortiz Mellet, V. M. Díaz Pérez, J. Fuentes, J. Kovács, I. Pintér, *Tetrahedron Lett.* **1997**, 38, 4161-4164; b) J. García Fernández, C. Ortiz Mellet, V. M. Díaz Pérez, J. Fuentes, J. Kovács, I. Pintér, *Carbohydr. Res.* **1997**, 304, 261-270.
- [50] D. R. Williams, M. G. Fromhold, J. D. Earley, *Org. Lett.* **2001**, 3, 2721-2724.
- [51] C. K. Sha, R. T. Chiu, C. F. Yang, N. T. Yao, W. H. Tseng, F. L. Liao, S. L. Wang, *J. Am. Chem. Soc.* **1997**, 119, 4130-4135.
- [52] T. Sugimori, T. Okawa, S. Eguchi, E. Yashima, Y. Okamoto, *Chem. Lett.* **1997**, 869-870.
- [53] a) W. Kurosawa, T. Kan, T. Fukuyama, *J. Am. Chem. Soc.* **2003**, 125, 8112-8113; b) W. Kurosawa, H. Kobayashi, T. Kan, T. Fukuyama, *Tetrahedron* **2004**, 60, 9615-9628.
- [54] a) J. F. Bower, R. Jumnah, A. C. Williams, J. M. J. Williams, *J. Chem. Soc., Perkin Trans.1* **1997**, 1411-1420; b) K. Burgess, L. T. Liu, B. Pal, *J. Org. Chem.* **1993**, 58, 4758-4763; c) C. Cativiela, M. D. Diaz-de-Villegas, *Tetrahedron: Asymmetry* **1998**, 9, 3517-3599; d) T. Hayashi, A. Yamamoto, Y. Ito, E. Nishioka, H. Miura, K. Yanagi, *J. Am. Chem. Soc.* **1989**, 111, 6301-6311; e) R. Jumnah, J. M. J. Williams, A. C. Williams, *Tetrahedron Lett.* **1993**, 34, 6619-6622.
- [55] B. M. Trost, D. L. Vanvranken, *J. Am. Chem. Soc.* **1993**, 115, 444-458.
- [56] a) E. Airiau, N. Girard, M. Pizzeti, J. Salvadori, M. Taddei, A. Mann, *J. Org. Chem.* **2010**, 75, 8670-8673; b) S. A. Kozmin, T. Iwama, Y. Huang, V. H. Rawal, *J. Am. Chem. Soc.* **2002**, 124, 4628-4641; c) P. Magnus, J. Lacour, I. Coldham, B. Mugrage, W. B. Bauta, *Tetrahedron* **1995**, 51, 11087-11110; d) B. M. Trost, *Angew. Chem. Int. Ed.* **1989**, 28, 1173-1192.

- [57] a) T. A. Johnson, M. D. Curtis, P. Beak, *J. Am. Chem. Soc.* **2001**, *123*, 1004-1005; b) E. Vedejs, M. Gingras, *J. Am. Chem. Soc.* **1994**, *116*, 579-588; c) K. Burgess, M. J. Ohlmeyer, *J. Org. Chem.* **1991**, *56*, 1027-1036; d) G. Petranyi, N. S. Ryder, A. Stutz, *Science* **1984**, *224*, 1239-1241.
- [58] B. Chen, A. K. Mapp, *J. Am. Chem. Soc.* **2005**, *127*, 6712-6718.
- [59] a) C. E. Anderson, L. E. Overman, *J. Am. Chem. Soc.* **2003**, *125*, 12412-12413; b) Y. K. Chen, A. E. Lurain, P. J. Walsh, *J. Am. Chem. Soc.* **2002**, *124*, 12225-12231; c) L. E. Overman, *J. Am. Chem. Soc.* **1974**, *96*, 597-599; d) L. E. Overman, *Acc. Chem. Res.* **1980**, *13*, 218-224; e) L. E. Overman, *J. Am. Chem. Soc.* **1976**, *98*, 2901-2910; f) M. Calter, T. K. Hollis, L. E. Overman, J. Ziller, G. G. Zipp, *J. Org. Chem.* **1997**, *62*, 1449-1456; g) L. E. Overman, G. G. Zipp, *J. Org. Chem.* **1997**, *62*, 2288-2291; h) Y. Donde, L. E. Overman, *J. Am. Chem. Soc.* **1999**, *121*, 2933-2934; i) T. K. Hollis, L. E. Overman, *J. Organomet. Chem.* **1999**, *576*, 290-299; j) L. E. Overman, C. E. Owen, M. M. Pavan, C. J. Richards, *Org. Lett.* **2003**, *5*, 1809-1812; k) S. F. Kirsch, L. E. Overman, *J. Am. Chem. Soc.* **2005**, *127*, 2866-2867.
- [60] E. J. Cabrita, C. A. M. Afonso, A. G. D. Santos, *Chem. Eur. J.* **2001**, *7*, 1455-1467.
- [61] S. Hanessian, Y. L. Bennani, Y. Leblanc, *Heterocycles* **1993**, *35*, 1411-1424.
- [62] A. Alexakis, S. Mutti, P. Mangeney, *J. Org. Chem.* **1992**, *57*, 1224-1237.
- [63] a) C. E. Anderson, Y. Donde, C. J. Douglas, L. E. Overman, *J. Org. Chem.* **2005**, *70*, 648-657; b) J. Kang, K. H. Yew, T. H. Kim, D. H. Choi, *Tetrahedron Lett.* **2002**, *43*, 9509-9512; c) E. E. Lee, R. A. Batey, *J. Am. Chem. Soc.* **2005**, *127*, 14887-14893.
- [64] S. F. Kirsch, L. E. Overman, M. P. Watson, *J. Org. Chem.* **2004**, *69*, 8101-8104.
- [65] A. M. Danowitz, C. E. Taylor, T. M. Shrikian, A. K. Mapp, *Org Lett* **2010**, *12*, 2574-2577.
- [66] E. Skucas, J. R. Zbieg, M. J. Krische, *J. Am. Chem. Soc.* **2009**, *131*, 5054-5055.
- [67] M. Kimura, Y. Horino, Y. Wakamiya, T. Okajima, Y. Tamaru, *J. Am. Chem. Soc.* **1997**, *119*, 10869-10870.
- [68] a) C. J. T. Hyland, L. S. Hegedus, *J. Org. Chem.* **2006**, *71*, 8658-8660; b) C. R. Berry, R. P. Hsung, J. E. Antoline, M. E. Petersen, R. Challeppan, J. A. Nielson, *J. Org. Chem.* **2005**, *70*, 4038-4042.
- [69] L. L. Wei, R. P. Hsung, H. Xiong, J. A. Mulder, N. T. Nkansah, *Org. Lett.* **1999**, *1*, 2145-2148.
- [70] a) R. Hayashi, R. P. Hsung, J. B. Feltenberger, A. G. Lohse, *Org. Lett.* **2009**, *11*, 2125-2128; b) T. Lu, R. Hayashi, R. P. Hsung, K. A. DeKorver, A. G. Lohse, Z. Song, Y. Tang, *Org. Biomol. Chem.* **2009**, *7*, 3331-3337.
- [71] a) A. Armstrong, D. P. G. Emmerson, *Org. Lett.* **2009**, *11*, 1547-1550; b) C. J. T. Hyland, L. S. Hegedus, *J. Org. Chem.* **2005**, *70*, 8628-8630; c) L. C. Shen, R. P. Hsung, Y. S. Zhang, J. E. Antoline, X. J. Zhang, *Org. Lett.* **2005**, *7*, 3081-3084; d) A. Armstrong, R. S. Cooke, S. E. Shanahan, *Org. Biomol. Chem.* **2003**, *1*, 3142-3143; e) J. P. Bacci, K. L. Greenman, D. L. Van Vranken, *J. Org. Chem.* **2003**, *68*, 4955-4958; f) K. Banert, S. Groth, *Angew. Chem. Int. Ed.* **1992**, *31*, 866-868; g) P. B. D. Ranslow, L. S. Hegedus, C. D. L. Rios, *J. Org. Chem.* **2004**, *69*, 105-111; h) B. M. Trost, D. T. Stiles, *Org. Lett.* **2005**, *7*, 2117-2120; i) L. L. Wei, H. Xiong, R. P. Hsung, *Acc. Chem. Res.* **2003**, *36*, 773-782.
- [72] a) H. C. Brown, P. V. Ramachandran, *Acc. Chem. Res.* **1992**, *25*, 16-24; b) C. J. Helal, P. A. Magriotis, E. J. Corey, *J. Am. Chem. Soc.* **1996**, *118*, 10938-10939; c) D. E. Frantz, R. Fassler, E. M. Carreira, *J. Am. Chem. Soc.* **2000**, *122*, 1806-1807.
- [73] a) R. A. Fairhurst, S. P. Collingwood, D. Lambert, *Synlett* **2001**, 473-476; b) R. A. Fairhurst, S. P. Collingwood, D. Lambert, R. J. Taylor, *Synlett* **2001**, *2001*, 0467,0472; c) R. A. Fairhurst, S. P. Collingwood, D. Lambert, E. Wissler, *Synlett* **2002**, 763-766.
- [74] a) A. Dondoni, *Angew. Chem. Int. Ed.* **2008**, *47*, 8995-8997; b) A. N. Glazer, *Annu. Rev. Biochem.* **1970**, *39*, 101-130; c) P. Jonkheijm, D. Weinrich, M. Köhn, H. Engelkamp, P. C. M. Christianen, J. Kuhlmann, J. C. Maan, D. Nüsse, H. Schroeder, R. Wacker, R. Breinbauer, C. M. Niemeyer, H. Waldmann, *Angew. Chem. Int. Ed.* **2008**, *47*, 4421-4424; d) S. Nampalli, M. G. McDougall, K. Lavrenov, H. Xiao, S. Kumar, *Bioconjugate Chem.* **2002**, *13*, 468-473; e) S. Park, M.-R. Lee, I. Shin, *Chem. Commun.* **2008**, 4389-4399; f) J. C. Schlatterer, A. Jäschke, *Biochem. Biophys. Res. Commun.* **2006**, *344*, 887-892; g) I. Shin, S. Park, M.-r. Lee, *Chem. Eur. J.* **2005**, *11*, 2894-2901; h) G. T. Hermanson, *Bioconjugate Techniques*, Second Edition ed., Elsevier Inc., **2008**.
- [75] a) R. Huisgen, *Angew. Chem.* **1963**, *75*, 604-637; b) J. E. Moses, A. D. Moorhouse, *Chem. Soc. Rev.* **2007**, *36*; c) V. V. Rostovtsev, L. G. Green, V. V. Fokin, K. B. Sharpless, *Angew. Chem.* **2002**, *114*, 2708-2711; d) C. W. Tornøe, C. Christensen, M. Meldal, *J. Org. Chem.* **2002**, *67*, 3057-3064.

- [76] a) N. J. Agard, J. A. Prescher, C. R. Bertozzi, *J. Am. Chem. Soc.* **2004**, *126*, 15046-15047; b) J. M. Baskin, C. R. Bertozzi, *Aldrichim. Acta* **2010**, *43*, 15-23; c) J. M. Baskin, J. A. Prescher, S. T. Laughlin, N. J. Agard, P. V. Chang, I. A. Miller, A. Lo, J. A. Codelli, C. R. Bertozzi, *Proc. Natl. Acad. Sci.* **2007**, *104*, 16793-16797; d) P. V. Chang, J. A. Prescher, E. M. Sletten, J. M. Baskin, I. A. Miller, N. J. Agard, A. Lo, C. R. Bertozzi, *Proc. Natl. Acad. Sci.* **2010**, *107*, 1821-1826; e) X. Ning, J. Guo, M. A. Wolfert, G.-J. Boons, *Angew. Chem.* **2008**, *120*, 2285-2287; f) S. S. van Berkel, A. J. Dirks, M. F. Debets, F. L. van Delft, J. J. L. M. Cornelissen, R. J. M. Nolte, F. P. J. T. Rutjes, *ChemBioChem* **2007**, *8*, 1504-1508; g) G. Wittig, A. Krebs, *Chem. Ber.* **1961**, *94*, 3260-3275.
- [77] S. Bräse, C. Gil, K. Knepper, V. Zimmermann, *Angew. Chem. Int. Ed.* **2005**, *44*, 5188-5240.
- [78] a) J. A. Johnson, Y. Y. Lu, J. A. Van Deventer, D. A. Tirrell, *Curr. Opin. Chem. Biol.* **2010**, *14*, 774-780; b) R. K. V. Lim, Q. Lin, *Chem. Commun.* **2010**, *46*, 1589-1600; c) X. Wu, P. G. Schultz, *J. Am. Chem. Soc.* **2009**, *131*, 12497-12515; d) E. M. Sletten, C. R. Bertozzi, *Angew. Chem. Int. Ed.* **2009**, *48*, 6974-6998.
- [79] A. K. Bhattacharya, G. Thyagarajan, *Chem. Rev.* **1981**, *81*, 415-430.
- [80] R. Kleineweischede, C. P. R. Hackenberger, *Angew. Chem. Int. Ed.* **2008**, *47*, 5984-5988.
- [81] B. L. Nilsson, L. L. Kiessling, R. T. Raines, *Org. Lett.* **2000**, *2*, 1939-1941.
- [82] a) A. Tam, M. B. Soellner, R. T. Raines, *Org. Biomol. Chem.* **2008**, *6*, 1173-1175; b) B. L. Nilsson, L. L. Kiessling, R. T. Raines, *Org. Lett.* **2000**, *3*, 9-12; c) M. B. Soellner, B. L. Nilsson, R. T. Raines, *J. Am. Chem. Soc.* **2006**, *128*, 8820-8828; d) A. Tam, M. B. Soellner, R. T. Raines, *J. Am. Chem. Soc.* **2007**, *129*, 11421-11430.
- [83] M. B. Soellner, A. Tam, R. T. Raines, *J. Org. Chem.* **2006**, *71*, 9824-9830.
- [84] R. B. Merrifield, *J. Am. Chem. Soc.* **1963**, *85*, 2149-2154.
- [85] P. Dawson, T. Muir, I. Clark-Lewis, S. Kent, *Science* **1994**, *266*, 776-779.
- [86] T. Wieland, E. Bokelmann, L. Bauer, H. U. Lang, H. Lau, *Justus Liebigs Ann. Chem.* **1953**, *583*, 129-149.
- [87] B. L. Nilsson, R. J. Hondal, M. B. Soellner, R. T. Raines, *J. Am. Chem. Soc.* **2003**, *125*, 5268-5269.
- [88] R. Merckx, D. T. S. Rijkers, J. Kemmink, R. M. J. Liskamp, *Tetrahedron Lett.* **2003**, *44*, 4515-4518.
- [89] O. David, W. J. N. Meester, H. Bieräugel, H. E. Schoemaker, H. Hiemstra, J. H. van Maarseveen, *Angew. Chem. Int. Ed.* **2003**, *42*, 4373-4375.
- [90] E. M. Sletten, C. R. Bertozzi, *Angew. Chem. Int. Ed. Engl.* **2009**, *48*, 6974-6998.
- [91] a) A. S. Cohen, E. A. Dubikovskaya, J. S. Rush, C. R. Bertozzi, *J. Am. Chem. Soc.* **2010**, *132*, 8563-8565; b) H. C. Hang, J. Loureiro, E. Spooner, A. W. M. van der Velden, Y.-M. Kim, A. M. Pollington, R. Maehr, M. N. Starnbach, H. L. Ploegh, *ACS Chem. Biol.* **2006**, *1*, 713-723; c) M. J. Hangauer, C. R. Bertozzi, *Angew. Chem. Int. Ed.* **2008**, *47*, 2394-2397; d) M. Kohn, R. Wacker, C. Peters, H. Schroder, L. Soulere, R. Breinbauer, C. M. Niemeyer, H. Waldmann, *Angew. Chem. Int. Ed. Engl.* **2003**, *42*, 5830-5834; e) I. Kosiova, A. Janicova, P. Kois, *Beilstein J. Org. Chem.* **2006**, *2*, 23; f) G. A. Lemieux, C. L. de Graffenried, C. R. Bertozzi, *J. Am. Chem. Soc.* **2003**, *125*, 4708-4709; g) J. A. Prescher, D. H. Dube, C. R. Bertozzi, *Nature* **2004**, *430*, 873-877; h) K. A. Stubbs, A. Scaffidi, A. W. Debowski, B. L. Mark, R. V. Stick, D. J. Vocadlo, *J. Am. Chem. Soc.* **2007**, *130*, 327-335; i) A. Vila, K. A. Tallman, A. T. Jacobs, D. C. Liebler, N. A. Porter, L. J. Marnett, *Chem. Res. Toxicol.* **2008**, *21*, 432-444; j) A. Watzke, M. Gutierrez-Rodriguez, M. Kohn, R. Wacker, H. Schroeder, R. Breinbauer, J. Kuhlmann, K. Alexandrov, C. M. Niemeyer, R. S. Goody, H. Waldmann, *Bioorg. Med. Chem.* **2006**, *14*, 6288-6306; k) A. Watzke, M. Kohn, M. Gutierrez-Rodriguez, R. Wacker, H. Schroeder, R. Breinbauer, J. Kuhlmann, K. Alexandrov, C. M. Niemeyer, R. S. Goody, H. Waldmann, *Angew. Chem. Int. Ed. Engl.* **2006**, *45*, 1408-1412.
- [92] A. Baccaro, S. H. Weisbrod, A. Marx, *Synthesis* **2007**, *2007*, 1949,1954.
- [93] D. H. Dube, J. A. Prescher, C. N. Quang, C. R. Bertozzi, *Proc. Natl. Acad. Sci. U. S. A.* **2006**, *103*, 4819-4824.
- [94] a) H. J. Reich, A. W. Sanders, A. T. Fiedler, M. J. Bevan, *J. Am. Chem. Soc.* **2002**, *124*, 13386-13387; b) C. Elschenbroich, *Organometallics, Vol. 5*, Vieweg and Teubner Verlag, **2005**.
- [95] S. E. Denmark, T. Bui, *J. Org. Chem.* **2005**, *70*, 10393-10399.
- [96] a) S. E. Denmark, S. B. D. Winter, *Synlett* **1997**, 1087-1089; b) S. E. Denmark, J. P. Fu, D. M. Coe, X. P. Su, N. E. Pratt, B. D. Griedel, *J. Org. Chem.* **2006**, *71*, 1513-1522; c) S. E. Denmark, J. P. Fu, M. J. Lawler, *J. Org. Chem.* **2006**, *71*, 1523-1536; d) S. E. Denmark, S. M. Pham, R. A. Stavenger, X. P. Su, K. T. Wong, Y. Nishigaichi, *J. Org. Chem.* **2006**, *71*, 3904-3922; e) S. E. Denmark, R. A. Stavenger, X. P. Su, K. T. Wong, Y. Nishigaichi, *Pure Appl. Chem.* **1998**, *70*, 1469-1476; f) S. E. Denmark, R. A.

- Stavenger, K.-T. Wong, *J. Org. Chem.* **1998**, *63*, 918-919; g) S. E. Denmark, S. M. Pham, *J. Org. Chem.* **2003**, *68*, 5045-5055.
- [97] S. E. Denmark, G. L. Beutner, *Angew. Chem. Int. Ed.* **2008**, *47*, 1560-1638.
- [98] S. E. Denmark, P. A. Barsanti, G. L. Beutner, T. W. Wilson, *Adv. Synth. Catal.* **2007**, *349*, 567-582.
- [99] a) M. Wills, M. Gamble, M. Palmer, A. Smith, J. Studley, J. Kenny, *J. Mol. Catal. A: Chem.* **1999**, *146*, 139-148; b) R. Hulst, H. Heres, N. C. M. W. Peper, R. M. Kellogg, *Tetrahedron: Asymmetry* **1996**, *7*, 1373-1384; c) B. Burns, N. P. King, J. R. Studley, H. Tye, M. Wills, *Tetrahedron: Asymmetry* **1994**, *5*, 801-804.
- [100] a) O. Chiodi, F. Fotiadu, M. Sylvestre, G. Buono, *Tetrahedron Lett.* **1996**, *37*, 39-42; b) V. Peper, J. Martens, *Tetrahedron Lett.* **1996**, *37*, 8351-8354; c) B. Burns, N. Paul King, H. Tye, J. R. Studley, M. Gamble, M. Wills, *J. Chem. Soc., Perkin Trans. 1* **1998**, 1027-1038; d) M. P. Gamble, A. R. C. Smith, M. Wills, *J. Org. Chem.* **1998**, *63*, 6068-6071.
- [101] a) T. Akiyama, J. Itoh, K. Yokota, K. Fuchibe, *Angew. Chem. Int. Ed.* **2004**, *43*, 1566-1568; b) D. Uraguchi, M. Terada, *J. Am. Chem. Soc.* **2004**, *126*, 5356-5357.
- [102] a) I. A. Natchev, *Bull. Chem. Soc. Jpn.* **1988**, *61*, 4491-4493; b) R. L. Mackman, A. S. Ray, H. C. Hui, L. Zhang, G. Birkus, C. G. Booramra, M. C. Desai, J. L. Douglas, Y. Gao, D. Grant, G. Laflamme, K.-Y. Lin, D. Y. Markevitch, R. Mishra, M. McDermott, R. Pakdaman, O. V. Petrakovsky, J. E. Vela, T. Cihlar, *Bioorg. Med. Chem.* **2010**, *18*, 3606-3617; c) G. V. Kapustin, G. Fejer, J. L. Gronlund, D. G. McCafferty, E. Seto, F. A. Etzkorn, *Org. Lett.* **2003**, *5*, 3053-3056; d) Y. Ishibashi, K. Miyata, M. Kitamura, *Eur. J. Org. Chem.* **2010**, 4201-4204; e) Y. Ishibashi, M. Kitamura, *Chem. Commun.* **2009**, 6985-6987; f) J.-M. Campagne, J. Coste, P. Jouin, *J. Org. Chem.* **1995**, *60*, 5214-5223.
- [103] a) L. Demange, M. Moutiez, C. Dugave, *J. Med. Chem.* **2002**, *45*, 3928-3933; b) M. Hariharan, S. Chaberek, A. E. Martell, *Syn. Commun.* **1973**, *3*, 375-379; c) W. P. Malachowski, J. K. Coward, *J. Org. Chem.* **1994**, *59*, 7616-7624; d) V. A. Shokol, B. N. Kozhushko, Y. A. Paliichuk, Y. P. Egorov, *Zh. Obshch. Khim.* **1979**, *49*, 1474-1491; e) K. Yamauchi, M. Kinoshita, M. Imoto, *Bull. Chem. Soc. Jap.* **1972**, *45*, 2531-2534; f) K. Yamauchi, S. Ohtsuki, M. Kinoshita, *J. Org. Chem.* **1984**, *49*, 1158-1163.
- [104] a) S. A. Biller, C. Forster, E. M. Gordon, T. Harrity, W. A. Scott, C. P. Ciosek, Jr., *J. Med. Chem.* **1988**, *31*, 1869-1871; b) M. Delomenede, F. Bedos-Belval, H. Duran, C. Vindis, M. Baltas, A. Negre-Salvayre, *J. Med. Chem.* **2008**, *51*, 3171-3181; c) M. MacDonald, M. Lanier, J. Cashman, *Synlett* **2010**, 1951-1954; d) W. P. Malachowski, J. K. Coward, *J. Org. Chem.* **1994**, *59*, 7625-7634; e) W. P. Malachowski, J. K. Coward, *J. Org. Chem.* **1994**, *59*, 7616-7624; f) M. Saady, L. Lebeau, C. Mioskowski, *Tetrahedron Lett.* **1995**, *36*, 4785-4786; g) A. B. Smith, III, C. M. Taylor, S. J. Benkovic, R. Hirschmann, *Tetrahedron Lett.* **1994**, *35*, 6853-6856.
- [105] L. Ylagan, A. Benjamin, A. Gupta, R. Engel, *Synth. Commun.* **1988**, *18*, 285-289.
- [106] a) J. Gao, X. Chu, Y. Qiu, L. Wu, Y. Qiao, J. Wu, D. Li, *Chem. Commun.* **2010**, *46*, 5340-5342; b) R. Hirschmann, K. M. Yager, C. M. Taylor, J. Witherington, P. A. Sprengeler, B. W. Phillips, W. Moore, A. B. Smith, III, *J. Am. Chem. Soc.* **1997**, *119*, 8177-8190; c) T. Kawashima, Y. Miki, T. Tomita, N. Inamoto, *Chem. Lett.* **1986**, 501-504; d) Q. Y. Vo, A. M. Gravey, R. Simonneau, Q. L. Vo, A. M. Lacoste, G. F. Le, *Tetrahedron Lett.* **1987**, *28*, 6167-6170; e) W. Yuan, M. H. Gelb, *J. Am. Chem. Soc.* **1988**, *110*, 2665-2666.
- [107] a) L. Briseno-Roa, J. Hill, S. Notman, D. Sellers, A. P. Smith, C. M. Timperley, J. Wetherell, N. H. Williams, G. R. Williams, A. R. Fersht, A. D. Griffiths, *J. Med. Chem.* **2006**, *49*, 246-255; b) P. J. R. Bryant, A. H. Ford-Moore, B. J. Perry, A. W. H. Wardrop, T. F. Watkins, *J. Chem. Soc.* **1960**, 1553-1555.
- [108] a) A. C. Gaumont, X. Morise, J. M. Denis, *J. Org. Chem.* **1992**, *57*, 4292-4295; b) X. Morise, P. Savignac, J. C. Guillemin, J. M. Denis, *Synth. Commun.* **1991**, *21*, 793-798.
- [109] a) C. Yuan, G. Wang, *Phosphorus, Sulfur Silicon Relat. Elem.* **1992**, *71*, 207-212; b) H.-J. Musiol, F. Grams, S. Rudolph-Boehner, L. Moroder, *J. Org. Chem.* **1994**, *59*, 6144-6146; c) A. Mucha, P. Kafarski, F. Plenat, H.-J. Cristau, *Tetrahedron* **1994**, *50*, 12743-12754; d) A. Mucha, P. Kafarski, *Tetrahedron* **2002**, *58*, 5855-5863; e) A. Mucha, J. Grembecka, T. Cierpicki, P. Kafarski, *Eur. J. Org. Chem.* **2003**, 4797-4803; f) R. Hirschmann, K. M. Yager, C. M. Taylor, W. Moore, P. A. Sprengeler, J. Witherington, B. W. Phillips, A. B. Smith, III, *J. Am. Chem. Soc.* **1995**, *117*, 6370-6371; g) M. P. de, L. S. Ingrassia, M. E. Mulliez, *J. Org. Chem.* **2003**, *68*, 8424-8430; h) A. P. Kaplan, P. A. Bartlett, *Biochemistry* **1991**, *30*, 8165-8170.
- [110] J. Oleksyszyn, L. Subotkowska, P. Mastalerz, *Synthesis* **1979**, 985-986.

- [111] a) J. Picha, M. Budesinsky, I. Hanclova, M. Sanda, P. Fiedler, V. Vanek, J. Jiracek, *Tetrahedron* **2009**, *65*, 6090-6103; b) J. Grembecka, A. Mucha, T. Cierpicki, P. Kafarski, *J. Med. Chem.* **2003**, *46*, 2641-2655; c) P. P. Giannousis, P. A. Bartlett, *J. Med. Chem.* **1987**, *30*, 1603-1609; d) J. T. Whitteck, W. Ni, B. M. Griffin, A. C. Eliot, P. M. Thomas, N. L. Kelleher, W. W. Metcalf, d. D. W. A. van, *Angew. Chem. Int. Ed.* **2007**, *46*, 9089-9092; e) A. M. Lacoste, A. M. Chollet-Gravey, Q. L. Vo, Q. Y. Vo, G. F. Le, *Eur. J. Med. Chem.* **1991**, *26*, 255-260; f) M. Hoffmann, *Phosphorus, Sulfur Silicon Relat. Elem.* **1998**, *134/135*, 109-118; g) F. Fini, G. Micheletti, L. Bernardi, D. Pettersen, M. Fochi, A. Ricci, *Chem. Commun.* **2008**, 4345-4347; h) B. Boduszek, A. Halama, R. Latajka, *Phosphorus, Sulfur Silicon Relat. Elem.* **2000**, *158*, 141-149; i) P. A. Bartlett, J. E. Hanson, P. P. Giannousis, *J. Org. Chem.* **1990**, *55*, 6268-6274; j) B. Lejczak, P. Kafarski, H. Sztajer, P. Mastalerz, *J. Med. Chem.* **1986**, *29*, 2212-2217; k) B. Lejczak, P. Kafarski, J. Szewczyk, *Synthesis* **1982**, 412-414.
- [112] S. D. Rushing, R. P. Hammer, *J. Am. Chem. Soc.* **2001**, *123*, 4861-4862.
- [113] F. R. Atherton, H. T. Openshaw, A. R. Todd, *J. Chem. Soc.* **1945**, 660-663.
- [114] F. R. Atherton, A. R. Todd, *J. Chem. Soc.* **1947**, 674-678.
- [115] E. M. Georgiev, J. Kaneti, K. Troev, D. M. Roundhill, *J. Am. Chem. Soc.* **1993**, *115*, 10964-10973.
- [116] G. Wang, R. W. Shen, Q. Xu, M. Goto, Y. F. Zhao, L. B. Han, *J. Org. Chem.* **2010**, *75*, 3890-3892.
- [117] Y. B. Zhou, G. Wang, Y. Saga, R. W. Shen, M. Goto, Y. F. Zhao, L. B. Han, *J. Org. Chem.* **2010**, *75*, 7924-7927.
- [118] T. D. Smith, *J. Chem. Soc.* **1962**, 1122-1123.
- [119] a) C. Seife, *Science* **1997**, *277*, 1602-1603; b) H. C. Castro, P. A. Abreu, R. B. Geraldo, R. C. A. Martins, R. dos Santos, N. I. V. Loureiro, L. M. Cabral, C. R. Rodrigues, *J. Mol. Recognit.* **2011**, *24*, 165-181; c) H.-N. Woo, S.-H. Baik, J.-S. Park, A. R. Gwon, S. Yang, Y.-K. Yun, D.-G. Jo, *Biochem. Biophys. Res. Commun.* **2011**, *404*, 10-15; d) A. K. Ghosh, S. Gemma, J. Tang, *Neurotherapeutics* **2008**, *5*, 399-408; e) R. Vassar, B. D. Bennett, S. Babu-Khan, S. Kahn, E. A. Mendiaz, P. Denis, D. B. Teplow, S. Ross, P. Amarante, R. Loeloff, Y. Luo, S. Fisher, J. Fuller, S. Edenson, J. Lile, M. A. Jarosinski, A. L. Biere, E. Curran, T. Burgess, J.-C. Louis, F. Collins, J. Treanor, G. Rogers, M. Citron, *Science* **1999**, *286*, 735-741; f) H. Gabriel, *Int. J. Biochem.* **1992**, *24*, 1365-1375; g) D. Beher, S. L. Graham, *Expert Opin. Invest. Drugs* **2005**, *14*, 1385-1409.
- [120] a) J. Tang, R. N. S. Wong, *J. Cell. Biochem.* **1987**, *33*, 53-63; b) H. A. Chapman, R. J. Riese, G.-P. Shi, *Annu. Rev. Physiol.* **1997**, *59*, 63-88; c) L. Hedstrom, *Chem. Rev.* **2002**, *102*, 4501-4524.
- [121] E. Erez, D. Fass, E. Bibi, *Nature* **2009**, *459*, 371-378.
- [122] a) A. Brik, C.-H. Wong, *Org. Biomol. Chem.* **2003**, *1*, 5-14; b) J.-T. Nguyen, Y. Hamada, T. Kimura, Y. Kiso, *Arch. Pharm.* **2008**, *341*, 523-535; c) S. Roggo, *Curr. Top. Med. Chem.* **2002**, *2*, 359-370; d) C. Boss, O. Corminboeuf, C. Grisostomi, T. Weller, *Expert Opin. Ther. Pat.* **2006**, *16*, 295-317; e) T. D. Meek, *J. Enzyme Inhib.* **1992**, *6*, 65-98; f) A. Mastrolorenzo, S. Rusconi, A. Scozzafava, G. Barbaro, C. T. Supuran, *Curr. Med. Chem.* **2007**, *14*, 2734-2748; g) A. Jedinak, T. Maliar, *Neoplasma* **2005**, *52*, 185-192; h) I. Hussain, *IDrugs* **2004**, *7*, 653-658; i) V. Frecer, T. Maliar, S. Miertus, *Int. J. Med., Biol. Environ.* **2000**, *28*, 161-173; j) G. Abbenante, D. P. Fairlie, *Med. Chem.* **2005**, *1*, 71-104; k) D. Leung, G. Abbenante, D. P. Fairlie, *J. Med. Chem.* **2000**, *43*, 305-341; l) S. Scharpe, M. I. De, D. Hendriks, G. Vanhoff, S. M. Van, G. Vriend, *Biochimie* **1991**, *73*, 121-126; m) A. K. Ghosh, L. Hong, J. Tang, *Curr. Med. Chem.* **2002**, *9*, 1135-1144; n) *Expert Opin. Ther. Pat.* **2003**, *13*, 547-550; o) T. D. Meek, *J. Enzyme Inhib. Med. Chem.* **1992**, *6*, 65-98; p) E. Haber, *Clin. Exp. Hypertens.* **1983**, *a5*, 1193-1205; q) M. Whittaker, C. D. Floyd, P. Brown, A. J. H. Gearing, *Chem. Rev.* **1999**, *99*, 2735-2776.
- [123] B. Turk, *Nat. Rev. Drug Discov.* **2006**, *5*, 785-799.
- [124] a) R. A. Wiley, D. H. Rich, *Med. Chem. Res.* **1993**, *13*, 327-384; b) A. Giannis, T. Kolter, *Angew. Chem. Int. Ed.* **1993**, *32*, 1244-1267; c) J. Gante, *Angew. Chem. Int. Ed.* **1994**, *33*, 1699-1720; d) A. S. Ripka, D. H. Rich, *Curr. Opin. Chem. Biol.* **1998**, *2*, 441-452; e) J. Vagner, H. Qu, V. J. Hruby, *Curr. Opin. Chem. Biol.* **2008**, *12*, 292-296.
- [125] a) L. H. Weaver, W. R. Kester, B. W. Matthews, *J. Mol. Biol.* **1977**, *114*, 119-132; b) J. E. Hanson, A. P. Kaplan, P. A. Bartlett, *Biochemistry* **1989**, *28*, 6294-6305; c) Y. Kiso, *Biopolymers* **1996**, *40*, 235-244; d) J. L. Radkiewicz, M. A. McAllister, E. Goldstein, K. N. Houk, *J. Org. Chem.* **1998**, *63*, 1419-1428; e) Y. Kiso, H. Matsumoto, S. Mizumoto, T. Kimura, Y. Fujiwara, K. Akaji, *Biopolymers* **1999**, *51*, 59-68; f) C.-A. Chen, S. M. Sieburth, A. Glekas, G. W. Hewitt, G. L. Trainor, S. Erickson-Viitanen, S. S. Garber, B. Cordova, S. Jeffry, R. M. Klabe, *Chemistry & Biology* **2001**, *8*, 1161-1166.

- [126] a) W. P. Jencks, *Adv. Enzymol. Relat. Areas Mol. Biol.* **1975**, *43*, 219-410; b) W. P. Jencks, *Proc. Natl. Acad. Sci. U. S. A.-Biol. Science* **1981**, *78*, 4046-4050.
- [127] D. Leung, G. Abbenante, D. P. Fairlie, *J. Med. Chem.* **2000**, *43*, 305-341.
- [128] a) J. A. Martin, *Antiviral Res.* **1992**, *17*, 265-278; b) D. Grobelny, E. M. Wondrak, R. E. Galardy, S. Oroszlan, *Biochem. Biophys. Res. Commun.* **1990**, *169*, 1111-1116; c) W. J. Moree, G. A. van der Marel, R. M. J. Liskamp, *Tetrahedron Lett.* **1991**, *32*, 409-412; d) T. Komiyama, T. Aoyagi, T. Takeuchi, H. Umezawa, *Biochem. Biophys. Res. Commun.* **1975**, *65*, 352-357.
- [129] a) P. A. Bartlett, C. K. Marlowe, *Biochemistry* **1987**, *26*, 8553-8561; b) P. A. Bartlett, C. K. Marlowe, *Phosphorus, Sulfur Silicon Relat. Elem.* **1987**, *30*, 537-543; c) V. Copie, A. Kolbert, D. Drewry, P. Bartlett, T. Oas, R. Griffin, *Biophys. J.* **1990**, *57*, A40-A40; d) V. Copie, A. C. Kolbert, D. H. Drewry, P. A. Bartlett, T. G. Oas, R. G. Griffin, *Biochemistry* **1990**, *29*, 9176-9184; e) B. P. Morgan, J. M. Scholtz, M. D. Ballinger, I. D. Zipkin, P. A. Bartlett, *J. Am. Chem. Soc.* **1991**, *113*, 297-307; f) D. Grobelny, U. B. Goli, R. E. Galardy, *Biochemistry* **1989**, *28*, 4948-4951.
- [130] a) M. Hariharan, R. J. Motekaitis, A. E. Martell, *J. Org. Chem.* **1975**, *40*, 470-473; b) K. Yamauchi, Y. Mitsuda, M. Kinoshita, *Bull. Chem. Soc. Jpn.* **1975**, *48*, 3285-3286.
- [131] a) N. P. Camp, P. C. D. Hawkins, P. B. Hitchcock, D. Gani, *Bioorg. Med. Chem. Lett.* **1992**, *2*, 1047-1052; b) J. H. Bateson, B. C. Gasson, T. Khushi, J. E. Neale, D. J. Payne, D. A. Tolson, G. Walker, *Bioorg. Med. Chem. Lett.* **1994**, *4*, 1667-1672; c) J. Grembecka, A. Mucha, T. Cierpicki, P. Kafarski, *Phosphorus, Sulfur Silicon Relat. Elem.* **2002**, *177*, 1739-1743; d) P. de Medina, L. S. Ingrassia, M. E. Mulliez, *J. Org. Chem.* **2003**, *68*, 8424-8430.
- [132] K. A. Mookhtiar, C. K. Marlowe, P. A. Bartlett, H. E. Vanwart, *Biochemistry* **1987**, *26*, 1962-1965.
- [133] a) M. J. Slater, A. P. Laws, M. I. Page, *Bioorg. Chem.* **2001**, *29*, 77-95; b) M. I. Page, A. P. Laws, *Chem. Commun.* **1998**, 1609-1617; c) D. J. Payne, J. H. Bateson, D. Tolson, B. Gasson, T. Khushi, P. Ledent, J. M. Frere, *Biochem. J.* **1996**, *314* (Pt 2), 457-461; d) J. Rahil, R. F. Pratt, *Biochemistry* **1993**, *32*, 10763-10772.
- [134] a) D. S. Karanewsky, M. C. Badia, *Tetrahedron Lett.* **1993**, *34*, 39-42; b) J. A. Robl, L. A. Duncan, J. Pluscec, D. S. Karanewsky, E. M. Gordon, C. P. Ciosek, Jr., L. C. Rich, V. C. Dehmel, D. A. Slusarchyk, a. et, *J. Med. Chem.* **1991**, *34*, 2804-2815; c) D. S. Karanewsky, M. C. Badia, C. P. Ciosek, Jr., J. A. Robl, M. J. Sofia, L. M. Simpkins, B. DeLange, T. W. Harrity, S. A. Biller, E. M. Gordon, *J. Med. Chem.* **1990**, *33*, 2952-2956.
- [135] A. M. Lacoste, M. Poulsen, A. Cassaigne, E. Neuzil, *Curr. Microbiol.* **1979**, *2*, 113-117.
- [136] D. Hilvert, *Annu. Rev. Biochem.* **2000**, *69*, 751-793.
- [137] a) F. R. Atherton, C. H. Hassall, R. W. Lambert, *J. Med. Chem.* **1986**, *29*, 29-40; b) F. R. Atherton, M. J. Hall, C. H. Hassall, R. W. Lambert, P. S. Ringrose, *Antimicrob. Agents Chemother.* **1979**, *15*, 677-683.
- [138] R. N. Salvatore, C. H. Yoon, K. W. Jung, *Tetrahedron* **2001**, *57*, 7785-7811.
- [139] P. A. Bartlett, L. A. Lamden, *Bioorg. Chem.* **1986**, *14*, 356-377.
- [140] a) B. P. Morgan, D. R. Holland, B. W. Matthews, P. A. Bartlett, *J. Am. Chem. Soc.* **1994**, *116*, 3251-3260; b) S. D. Rushing, R. P. Hammer, *J. Am. Chem. Soc.* **2001**, *123*, 4861-4862.
- [141] a) E. Andrew Boyd, M. E. K. Boyd, V. M. Loh Jr, *Tetrahedron Lett.* **1996**, *37*, 1651-1654; b) E. Andrew Boyd, M. Corless, K. James, A. C. Regan, *Tetrahedron Lett.* **1990**, *31*, 2933-2936; c) M. N. Dimukhametov, I. A. Nuretdinov, *Izv. Akad. Nauk SSSR, Ser. Khim.* **1983**, 1214-1215; d) D. E. Gibbs, *Tetrahedron Lett.* **1977**, 679-682.
- [142] a) E. K. Baylis, C. D. Campbell, J. G. Dingwall, *J. Chem. Soc., Perkin Trans. 1* **1984**, 2845-2853; b) R. Hamilton, B. J. Walker, B. Walker, *Tetrahedron Lett.* **1993**, *34*, 2847-2850; c) R. Liboska, J. Pícha, I. Hančlová, M. Buděšínský, M. Šanda, J. Jiráček, *Tetrahedron Lett.* **2008**, *49*, 5629-5631; d) J. Pícha, M. Buděšínský, P. Fiedler, M. Šanda, J. Jiráček, *Amino Acids* **2010**, *39*, 1265-1280.
- [143] a) C. P. R. Hackenberger, D. Schwarzer, *Angew. Chem. Int. Ed.* **2008**, *47*, 10030-10074; b) D. P. Gamblin, E. M. Scanlan, B. G. Davis, *Chem. Rev.* **2008**, *109*, 131-163; c) N. Jessani, B. F. Cravatt, *Curr. Opin. Chem. Biol.* **2004**, *8*, 54-59; d) J. A. Prescher, C. R. Bertozzi, *Nat. Chem. Biol.* **2005**, *1*, 13-21; e) P. F. van Swieten, M. A. Leeuwenburgh, B. M. Kessler, H. S. Overkleeft, *Org. Biomol. Chem.* **2005**, *3*, 20-27; f) H. C. Hang, C. R. Bertozzi, *Acc. Chem. Res.* **2001**, *34*, 727-736; g) R. W. Hoffmann, *Synthesis* **2006**, *2006*, 3531,3541; h) I. S. Young, P. S. Baran, *Nat. Chem.* **2009**, *1*, 193-205.
- [144] a) L. D. Lavis, R. T. Raines, *ACS Chem. Biol.* **2008**, *3*, 142-155; b) B. G. Davis, *Pure Appl. Chem.* **2009**, *81*, 285-298.

-
- [145] a) S. G. Alvarez, M. T. Alvarez, *Synthesis* **1997**, 413-414; b) Lundquist, J. C. Pelletier, *Org. Lett.* **2001**, *3*, 781-783; c) C. W. Tornøe, P. Davis, F. Porreca, M. Meldal, *J. Pept. Sci.* **2000**, *6*, 594-602.
- [146] a) K. Afarinkia, H.-w. Yu, *Tetrahedron Lett.* **2003**, *44*, 781-783; b) D. Hewitt, *Aust. J. Chem.* **1979**, *32*, 463-464.
- [147] Y.-C. Oh, Y. Bao, W. S. Jenks, *J. Photochem. Photobiol., A* **2003**, *161*, 69-77.
- [148] I. Abrunhosa-Thomas, C. E. Sellers, J.-L. Montchamp, *J. Org. Chem.* **2007**, *72*, 2851-2856.
- [149] P. Molina, C. LopezLeonardo, J. LlamasBotia, C. FocesFoces, C. FernandezCastano, *Tetrahedron* **1996**, *52*, 9629-9642.
- [150] E. L. Myers, R. T. Raines, *Angew. Chem. Int. Ed.* **2009**, *48*, 2359-2363.
- [151] C. Reichardt, T. Welton, in *Solvents and Solvent Effects in Organic Chemistry*, Wiley-VCH Verlag GmbH & Co. KGaA, **2010**, pp. 549-586.
- [152] J. G. Dingwall, J. Ehrenfreund, R. G. Hall, *Tetrahedron* **1989**, *45*, 3787-3808.
- [153] M. Juríček, P. H. J. Kouwer, J. Reháč, J. Sly, A. E. Rowan, *J. Org. Chem.* **2008**, *74*, 21-25.
- [154] T. Suzuki, Y. Ota, Y. Kasuya, M. Mutsuga, Y. Kawamura, H. Tsumoto, H. Nakagawa, M. G. Finn, N. Miyata, *Angew. Chem. Int. Ed.* **2010**, *49*, 6817-6820.

7 Curriculum Vitae

Der Lebenslauf ist in der Online-Version aus Gründen des Datenschutzes nicht
enthalten.

8 Appendix

8.1 NMR spectra

8.1.1 NMR spectra of ^{15}N -3-phenylpropyl azide (^{15}N -7b)

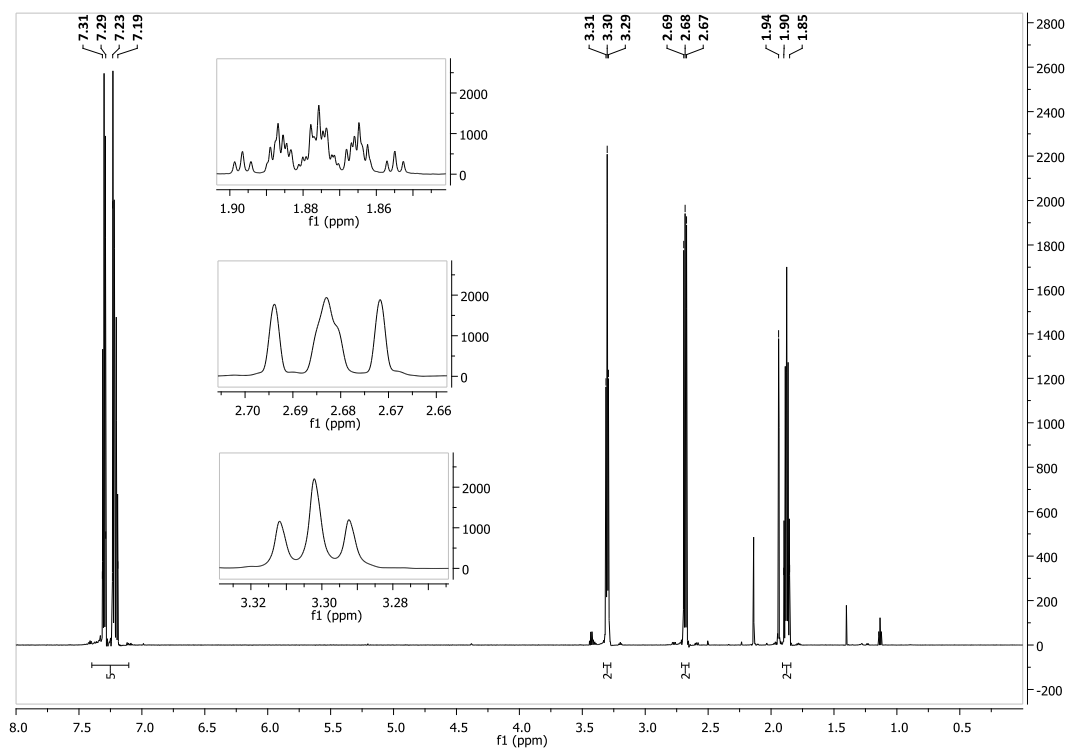


Figure 55: ^1H -NMR spectrum of ^{15}N -3-phenylpropyl azide (^{15}N -7b) (400 MHz, CD_3CN).

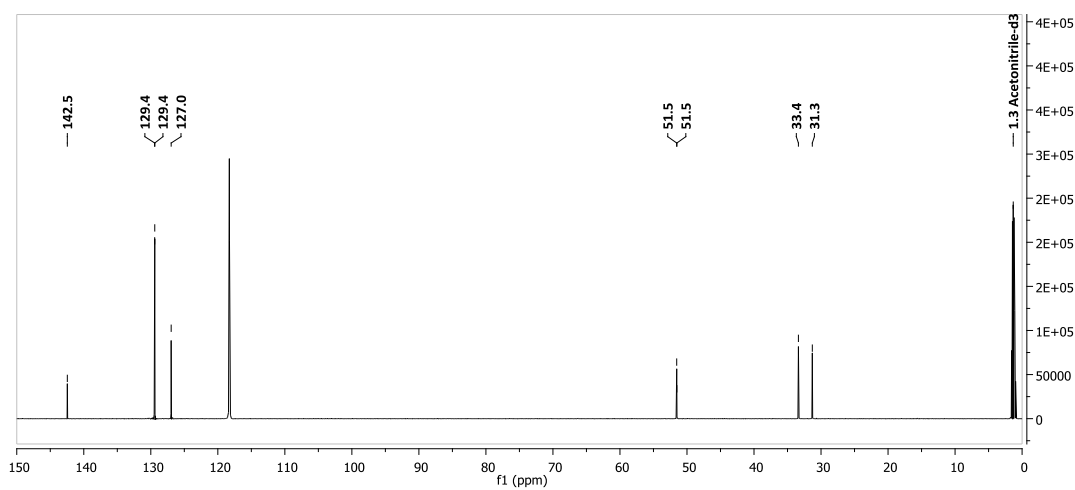


Figure 56: ^{13}C -NMR spectrum of ^{15}N -3-phenylpropyl azide (^{15}N -7b) (176 MHz, CD_3CN).

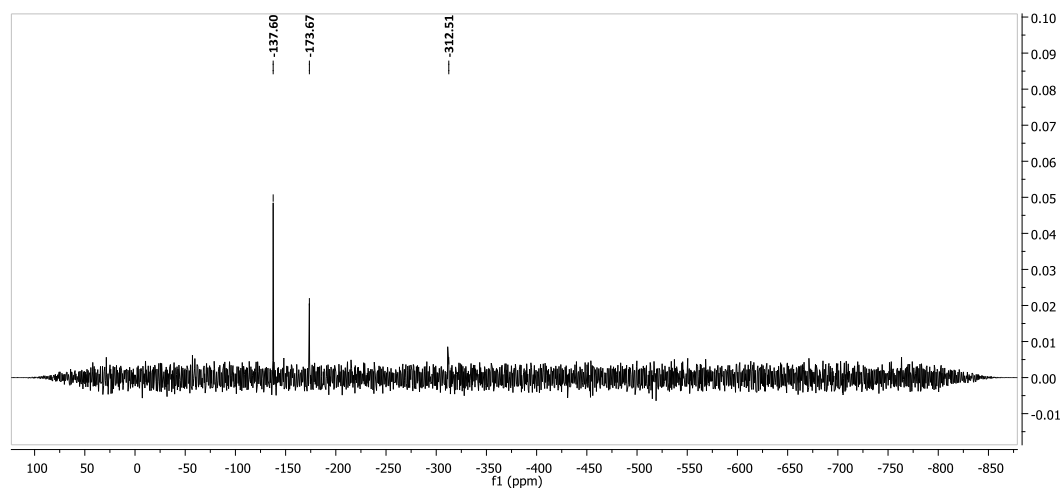


Figure 57: ^{15}N -NMR spectrum of ^{15}N -3-Phenylpropyl azide (^{15}N -7b) (41 MHz, CD_3CN). CD_3CN was used as internal standard and set to -137.60 ppm ($\text{CH}_3\text{NO}_2 = 0$ ppm).

8.1.2 NMR spectra to the Staudinger reaction between dodecyl azide (7a) and methyl phenylphosphinate (182) (6 eq.) with BSA (18 eq.)

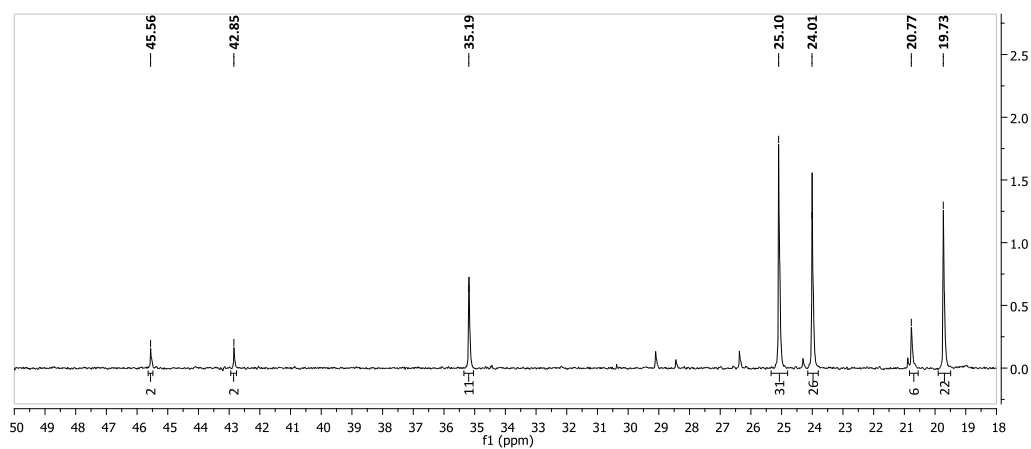


Figure 58: ^{31}P -NMR spectrum of the crude reaction mixture of the Staudinger reaction between dodecyl azide (7a) and methyl phenylphosphinate (182) (6 eq.) with BSA (18 eq.) after addition of TBAF (162 MHz, CDCl_3).

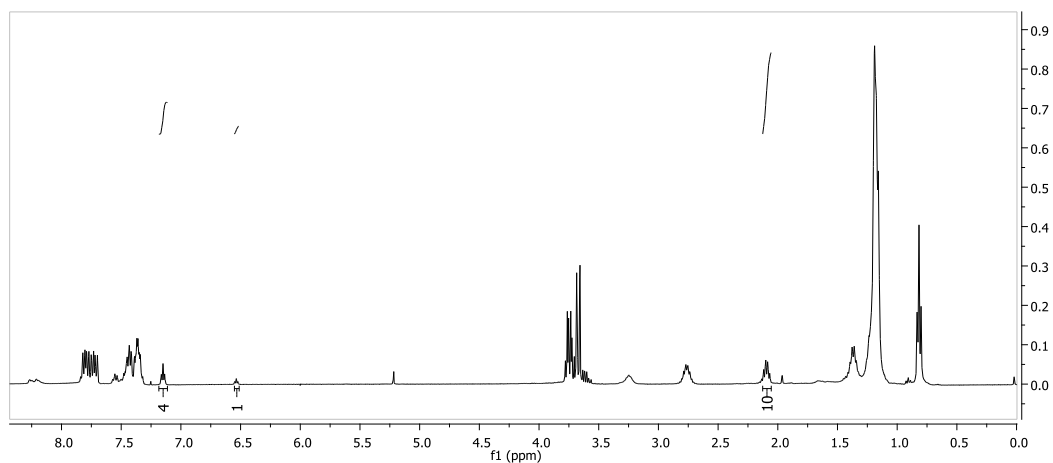


Figure 59: ^1H -NMR spectrum of the crude reaction mixture of the Staudinger reaction between dodecyl azide (**7a**) and methyl phenylphosphinate (**182**) (6 eq.) with BSA (18 eq.) after addition of TBAF (400 MHz, CDCl_3).

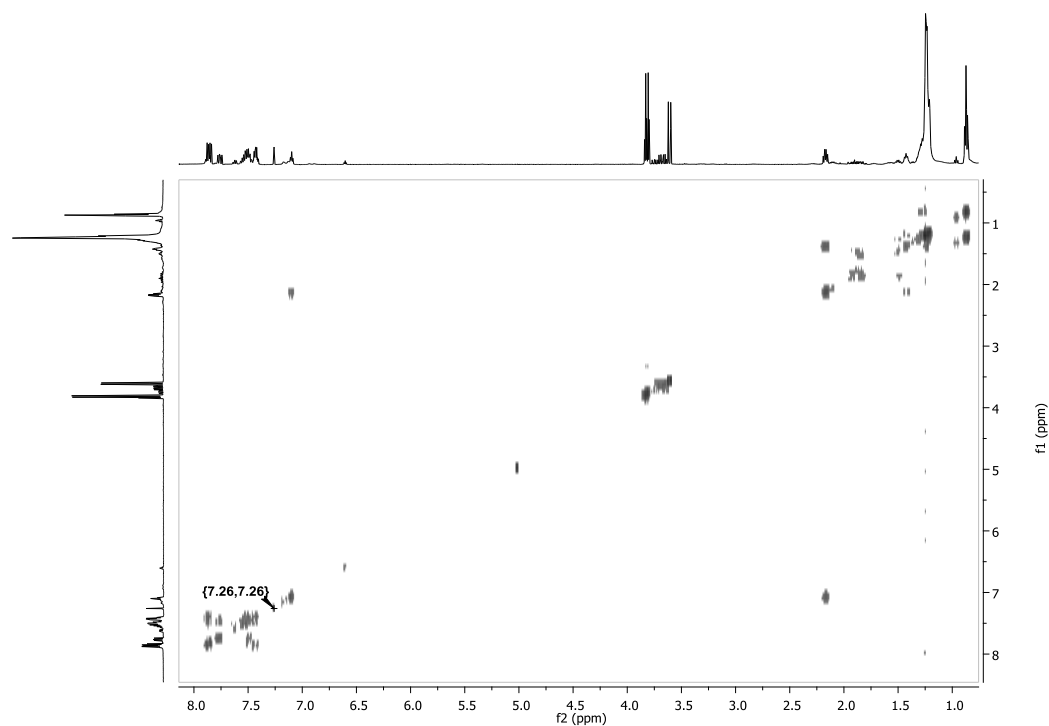


Figure 60: ^1H , ^1H -COSY spectrum of the crude reaction mixture of the Staudinger reaction between dodecyl azide (**7a**) and methyl phenylphosphinate (**182**) (6 eq.) with BSA (18 eq.) after addition of TBAF in CDCl_3 .

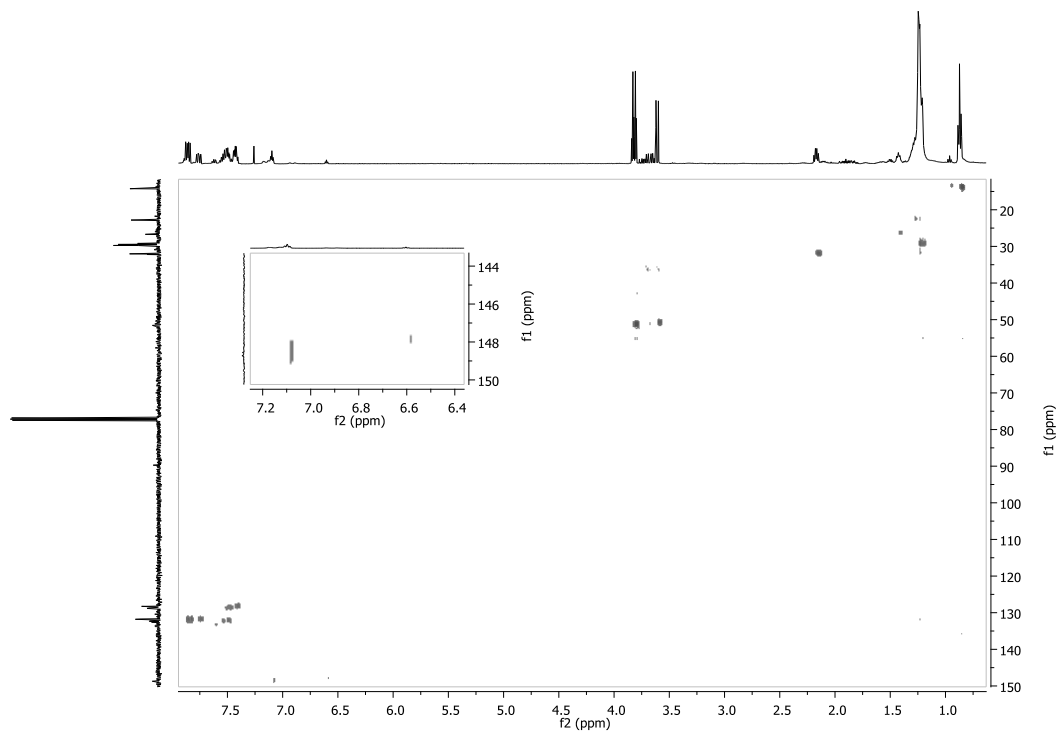


Figure 61: HMOC spectrum of the crude reaction mixture of the Staudinger reaction between dodecyl azide (**7a**) and methyl phenylphosphinate (**182**) (6 eq.) with BSA (18 eq.) after addition of TBAF in CDCl_3 .

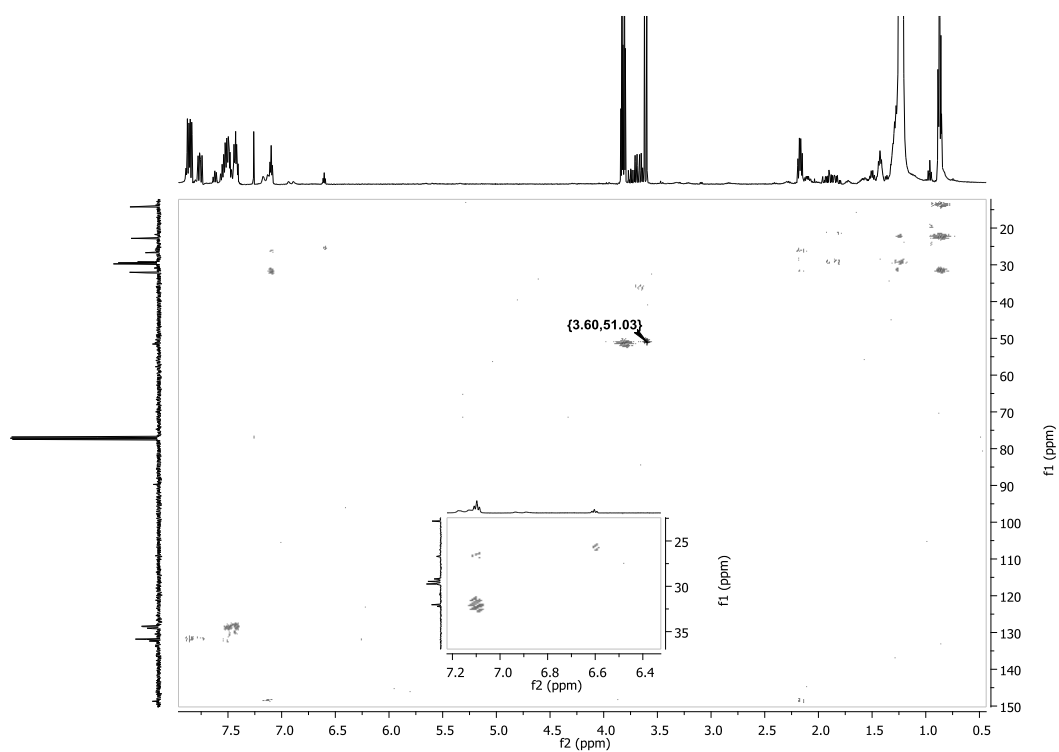


Figure 62: HMBC spectrum of the crude reaction mixture of the Staudinger reaction between dodecyl azide (**7a**) and methyl phenylphosphinate (**182**) (6 eq.) with BSA (18 eq.) after addition of TBAF in CDCl_3 .

8.1.3 NMR spectra of methyl *P*-phenyl-(3-phenylpropyl)phosphonamidate (**183b**)

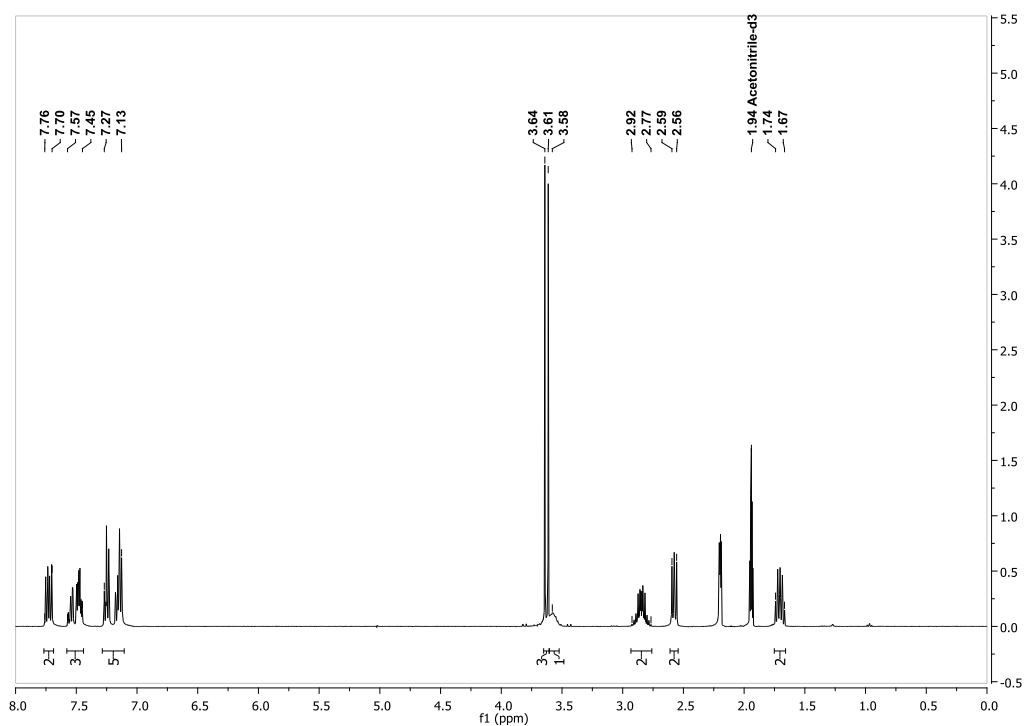


Figure 63: ¹H-NMR spectrum of methyl *P*-phenyl-(3-phenylpropyl)phosphonamidate (**183b**) (400 MHz, CD₃CN).

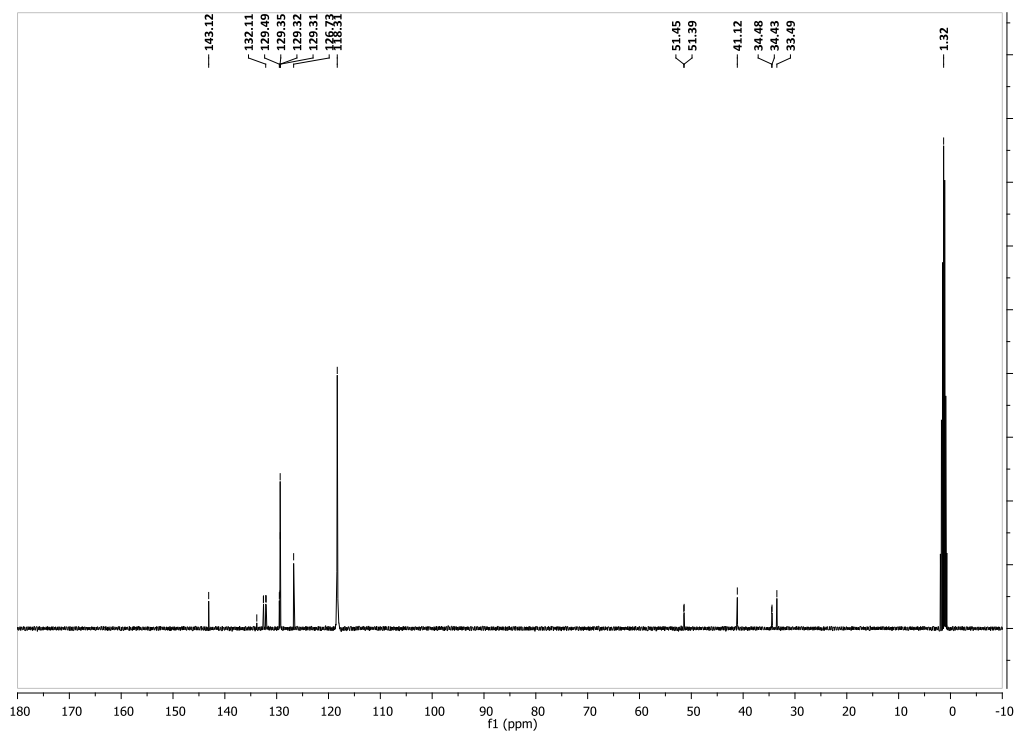


Figure 64: ¹³C-NMR spectrum of methyl *P*-phenyl-(3-phenylpropyl)phosphonamidate (**183b**) (101 MHz, CD₃CN).

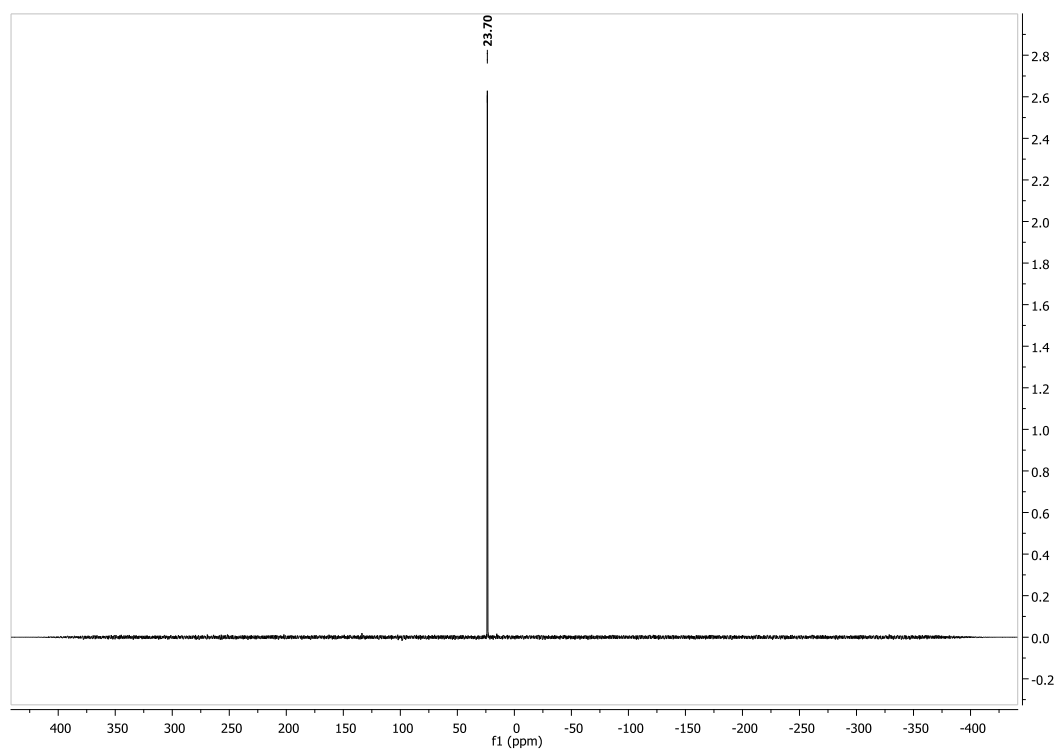


Figure 65: ^{31}P -NMR spectrum of methyl *P*-phenyl-(3-phenylpropyl)phosphonamidate (**183b**) (162 MHz, CD_3CN).

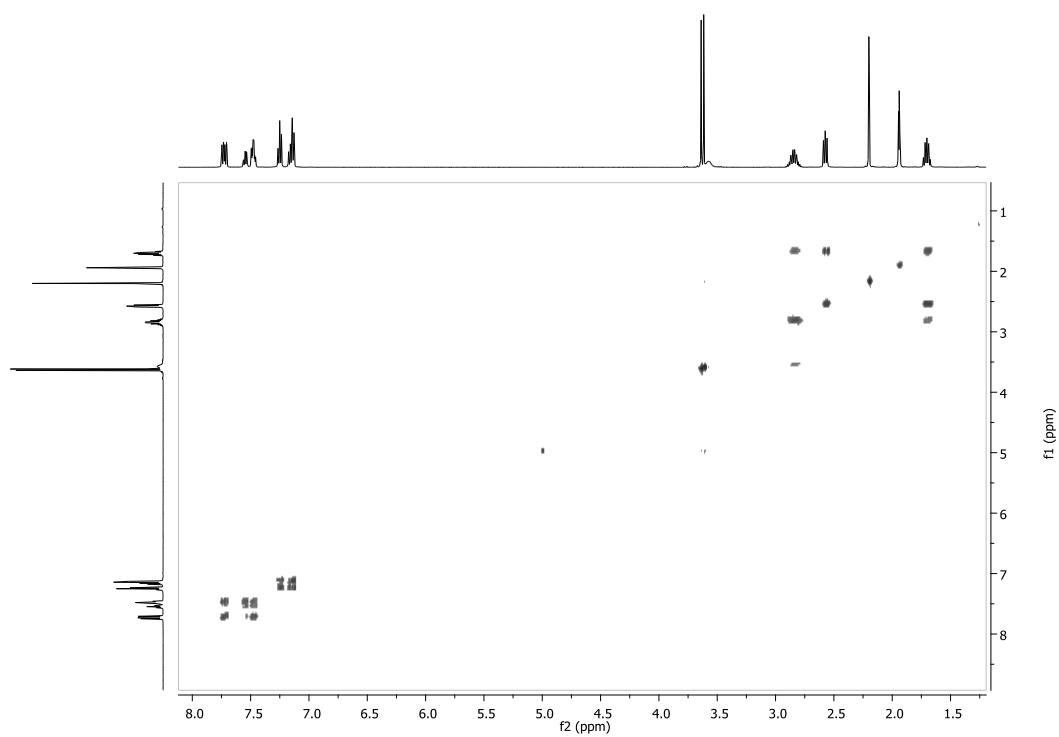


Figure 66: H,H-COSY spectrum of methyl *P*-phenyl-(3-phenylpropyl)phosphonamidate (**183b**) (CD_3CN).

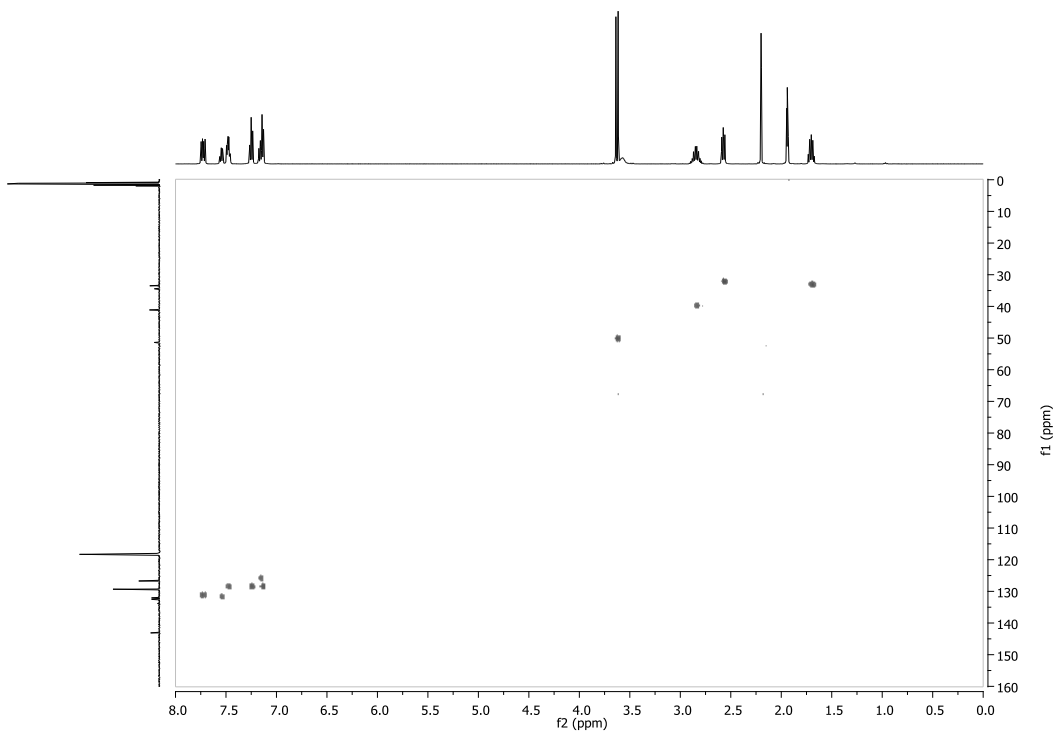


Figure 67: HMQC spectrum of methyl *P*-phenyl-(3-phenylpropyl)phosphonamidate (**183b**) (CD_3CN).

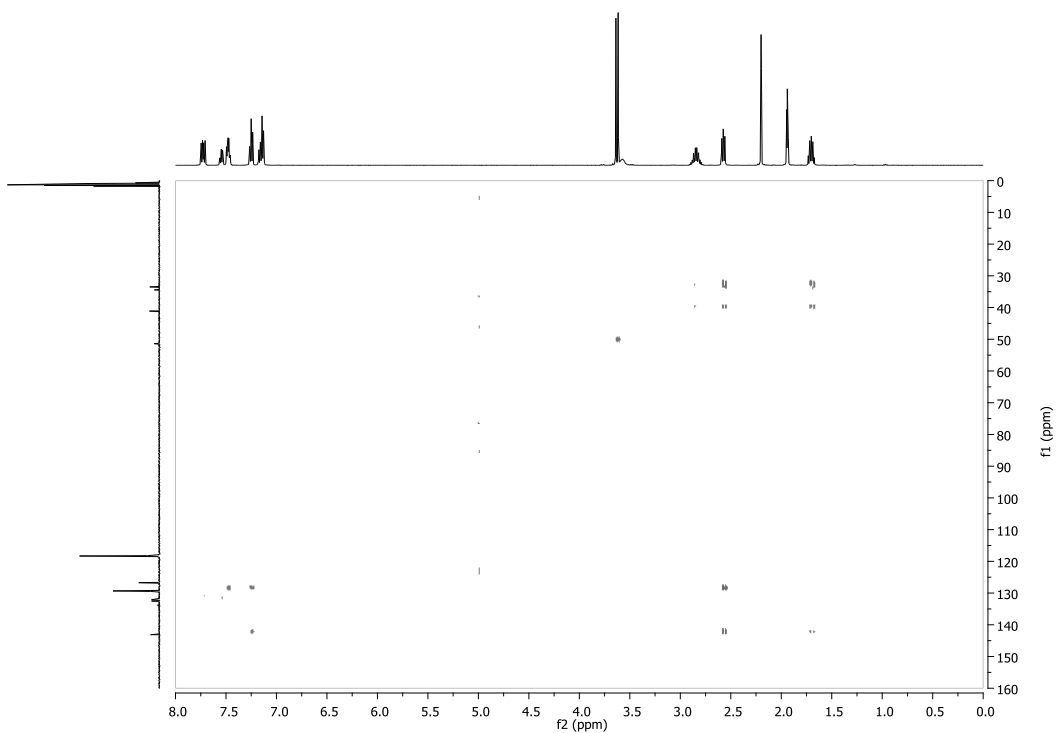


Figure 68: HMBC spectrum of methyl *P*-phenyl-(3-phenylpropyl)phosphonamidate (**183b**) (CD_3CN).

8.1.4 NMR spectra of methyl *P*-phenyl-^{14/15}N-(3-phenylpropyl) phosphoramidate (¹⁵N-183b)

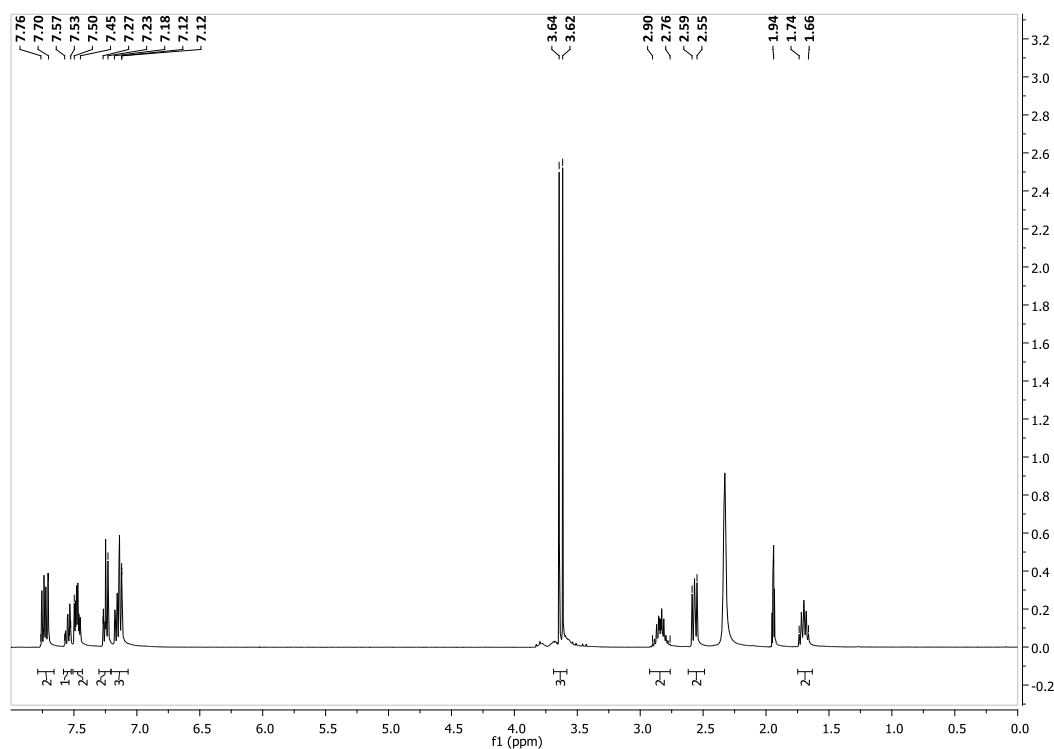


Figure 69: ¹H-NMR spectrum of a mixture of ¹⁵N-183b and 183b (1:1) (400 MHz, CD₃CN).

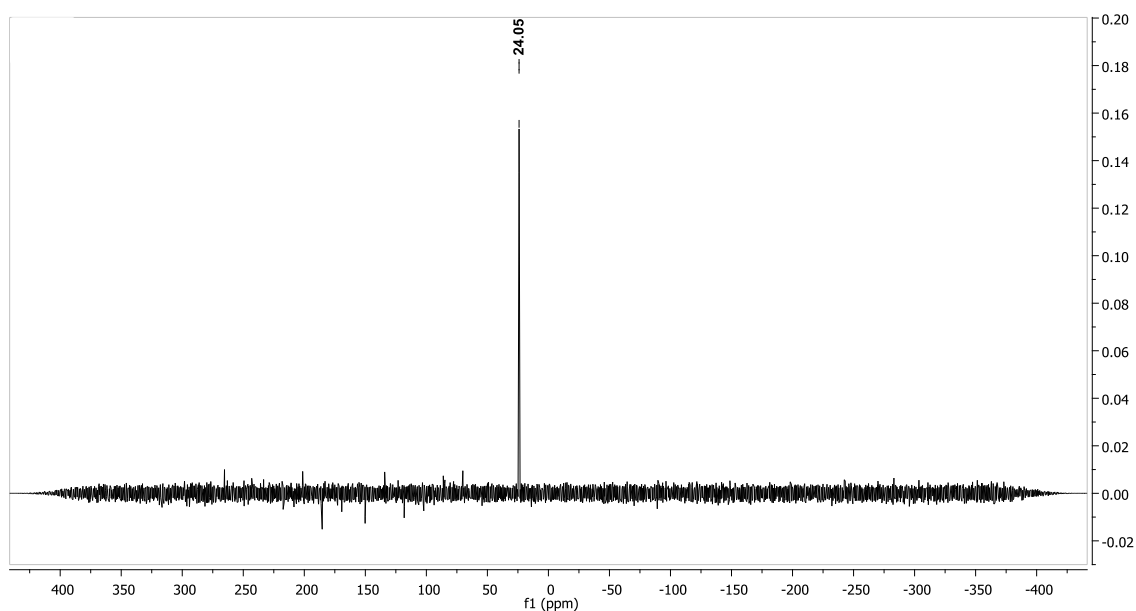


Figure 70: ³¹P-NMR spectrum of a mixture of ¹⁵N-183b and 183b (1:1) (162 MHz, CD₃CN, H-decoupled).

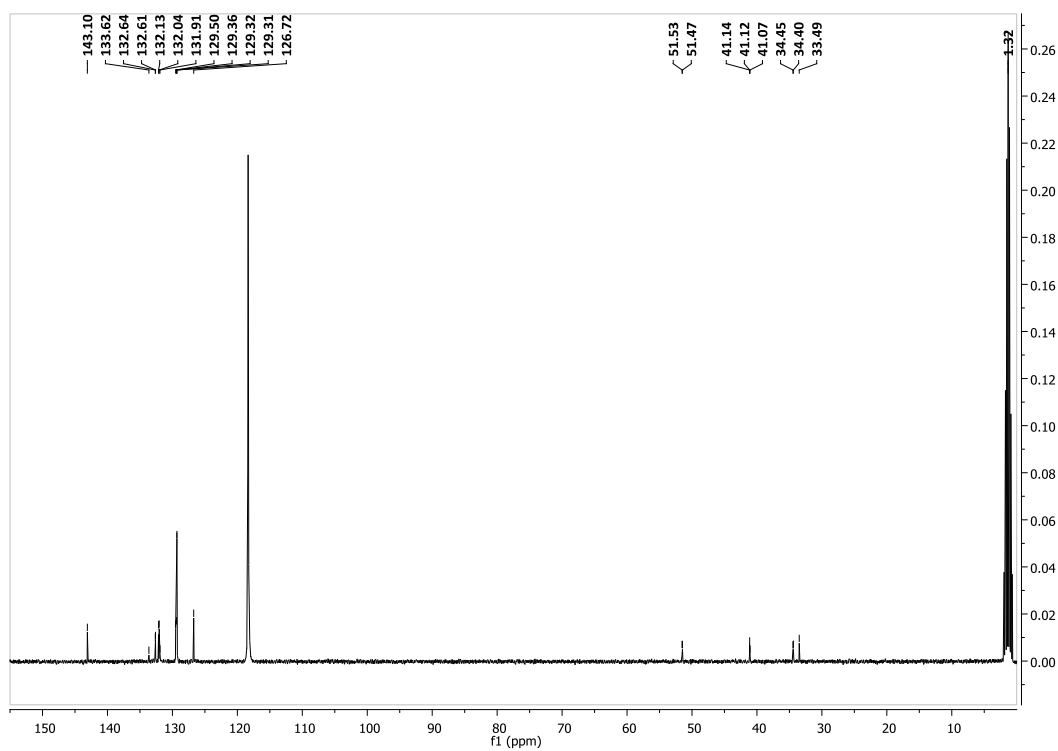


Figure 71: ^{13}C -NMR spectrum of a mixture of ^{15}N -183b and 183b (1:1) (120 MHz, CD_3CN).

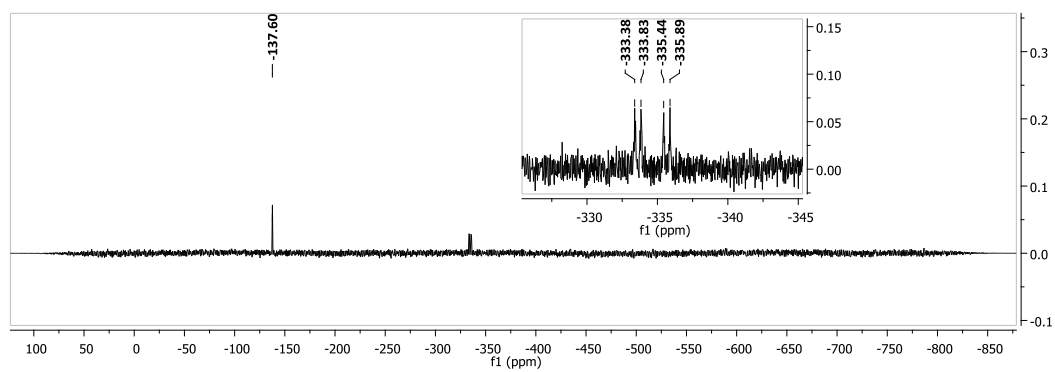


Figure 72: ^{15}N -NMR spectrum of a mixture of ^{15}N -183b and 183b (1:1) (41 MHz, CD_3CN).

8.1.5 NMR spectra of (*E/Z*)-methyl phenyl(2-(3-phenylpropylidene)hydrazinyl)phosphinate (*E/Z*-192b)

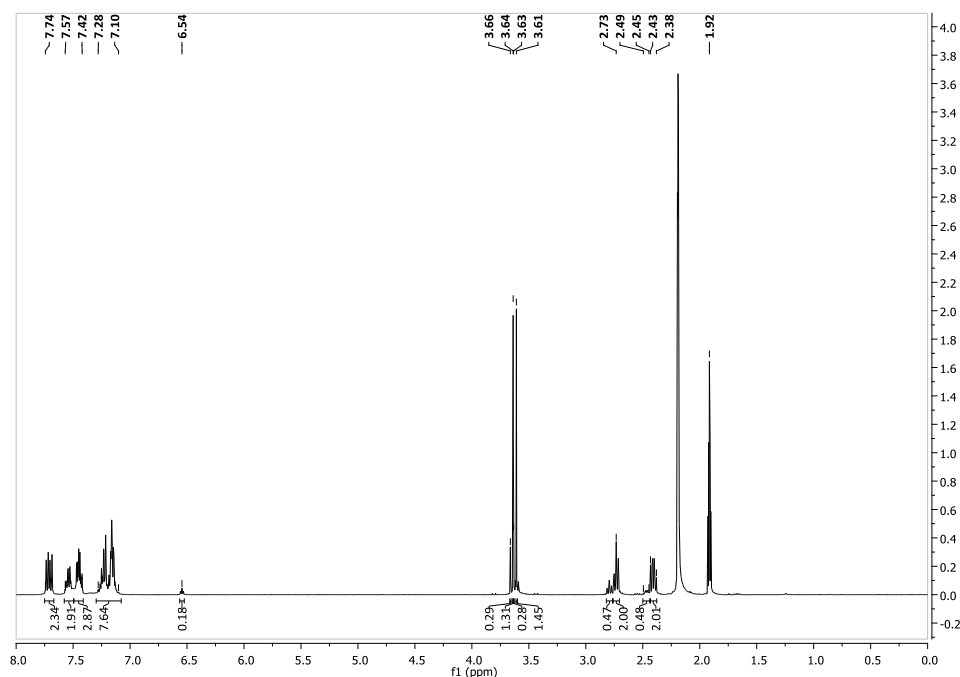


Figure 73: ^1H -NMR spectrum of (*E/Z*)-methyl phenyl(2-(3-phenylpropylidene)hydrazinyl)phosphinate (*E/Z*-192b) (400 MHz, CD_3CN).

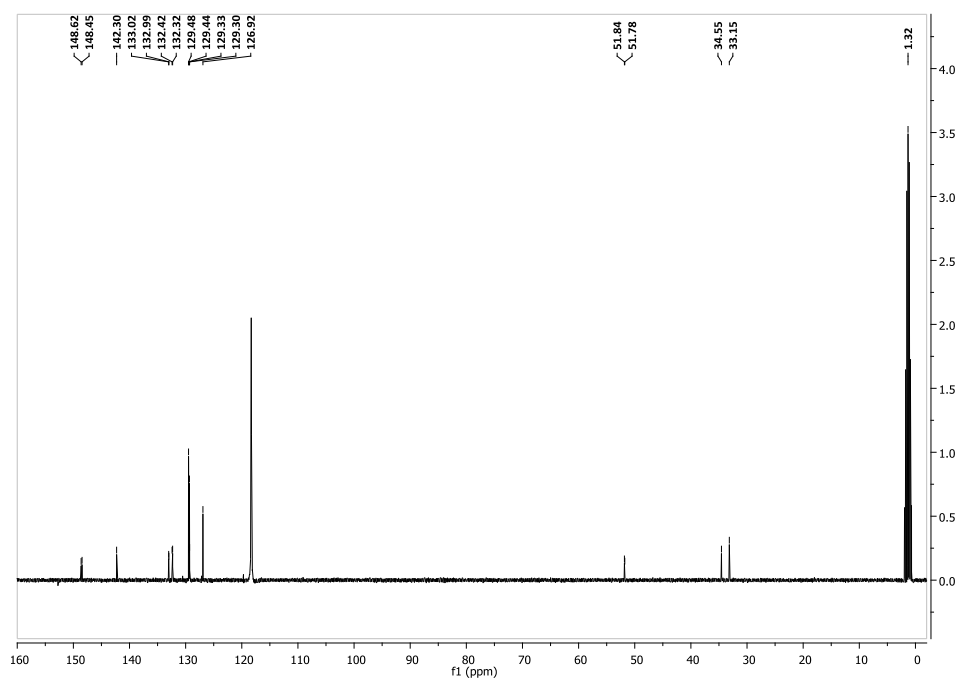


Figure 74: ^{13}C -NMR spectrum of (*E/Z*)-methyl phenyl(2-(3-phenylpropylidene)hydrazinyl)phosphinate (*E/Z*-192b) (101 MHz, CD_3CN).

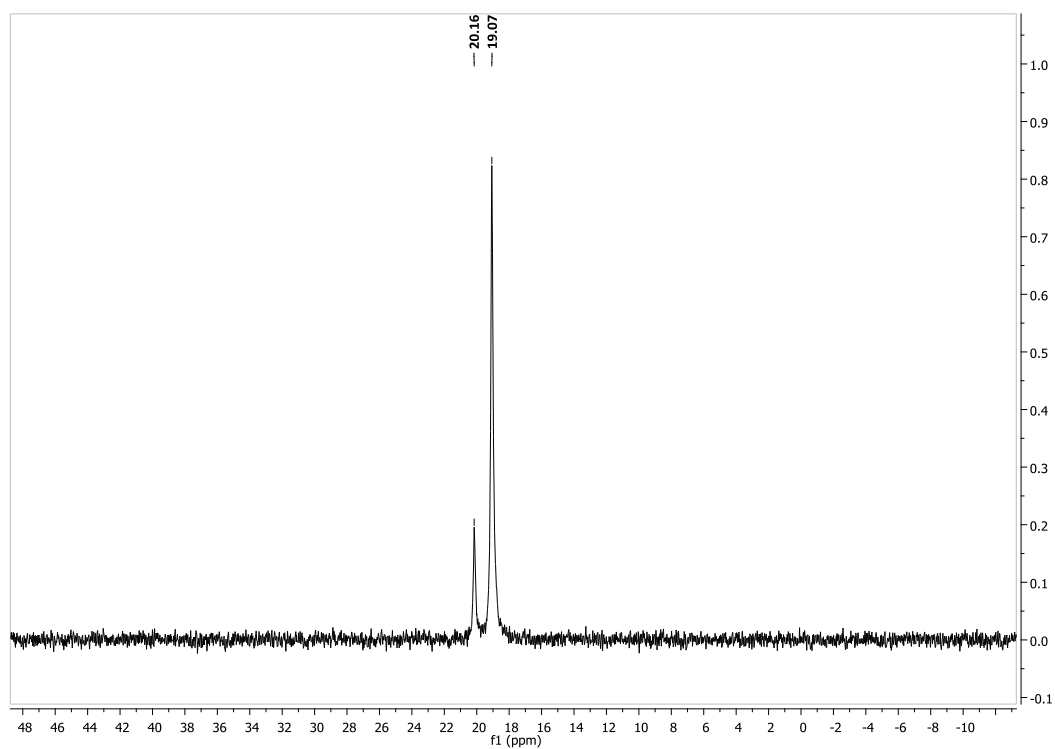


Figure 75: ^{31}P -NMR spectrum of *(E/Z)*-methyl phenyl(2-(3-phenylpropylidene)hydrazinyl)phosphinate (*(E/Z)*-192b (162 MHz, CD_3CN).

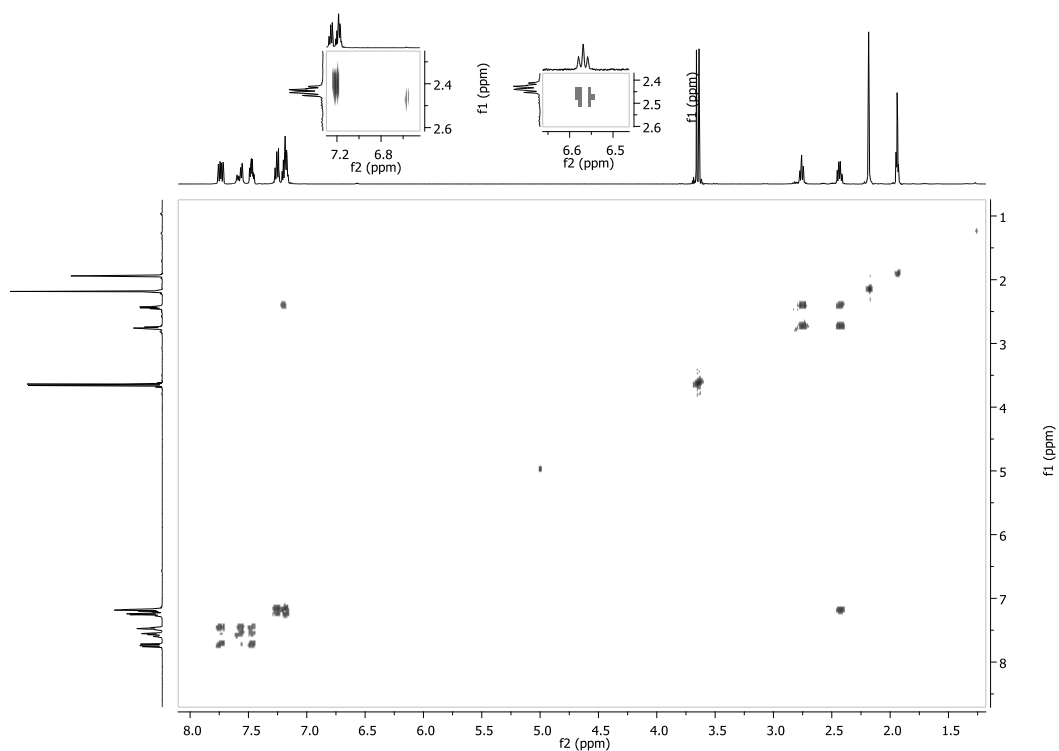


Figure 76: ^1H , ^1H -COSY spectrum of *(E/Z)*-methyl phenyl(2-(3-phenylpropylidene)hydrazinyl)phosphinate (*(E/Z)*-192b (CD_3CN).

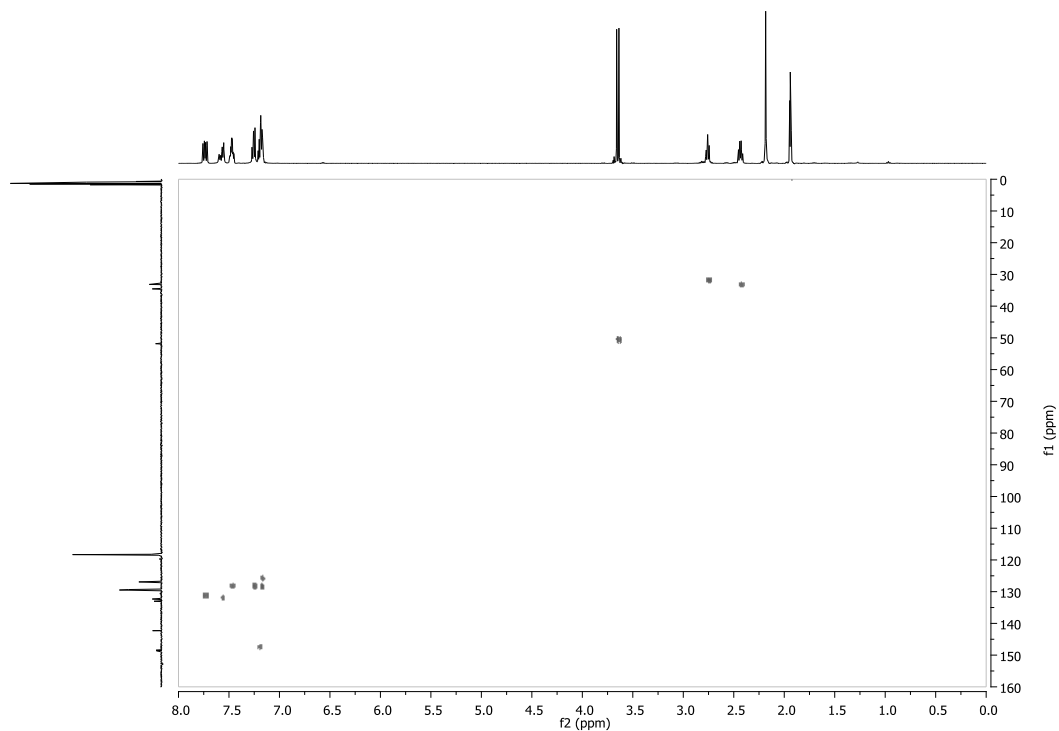


Figure 77: HMQC spectrum of *(E/Z)*-methyl phenyl(2-(3-phenylpropylidene)hydrazinyl)phosphinate **(E/Z)-192b** (CD_3CN).

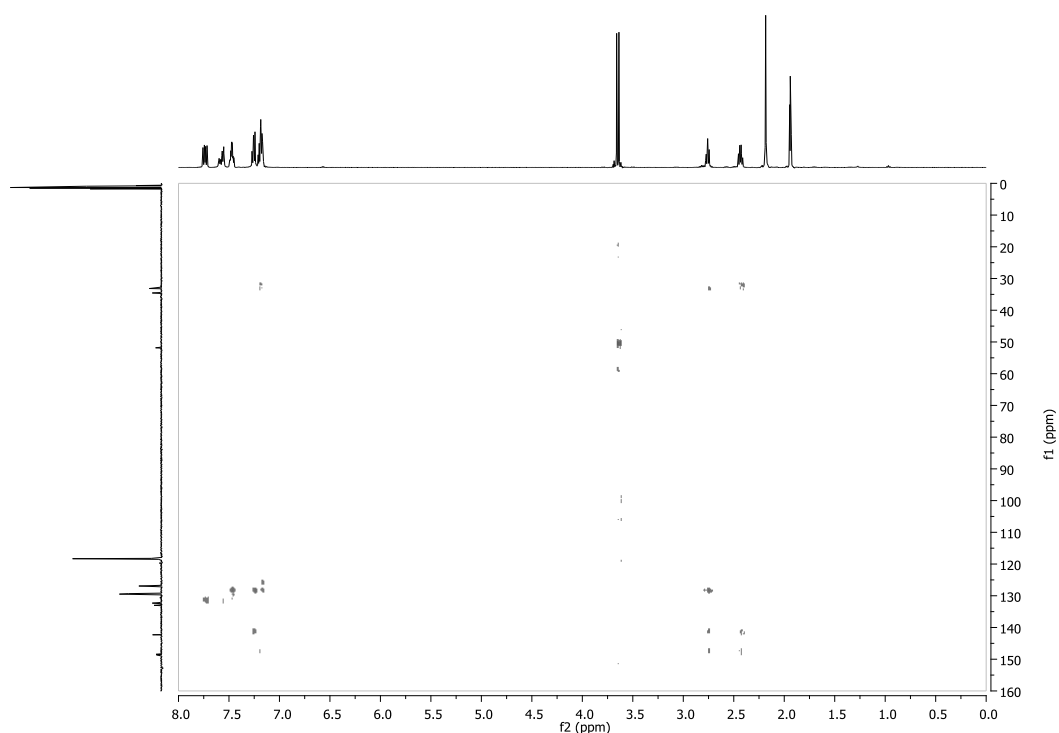


Figure 78: HMBC spectrum of *(E/Z)*-methyl phenyl(2-(3-phenylpropylidene)hydrazinyl)phosphinate **(E/Z)-192** (CD_3CN).

8.1.6 NMR spectra of $^{14/15}\text{N}$ -(*E/Z*)-methyl phenyl(2-(3-phenylpropylidene)hydrazinyl)phosphinate (^{15}N -(*E/Z*)-192b)

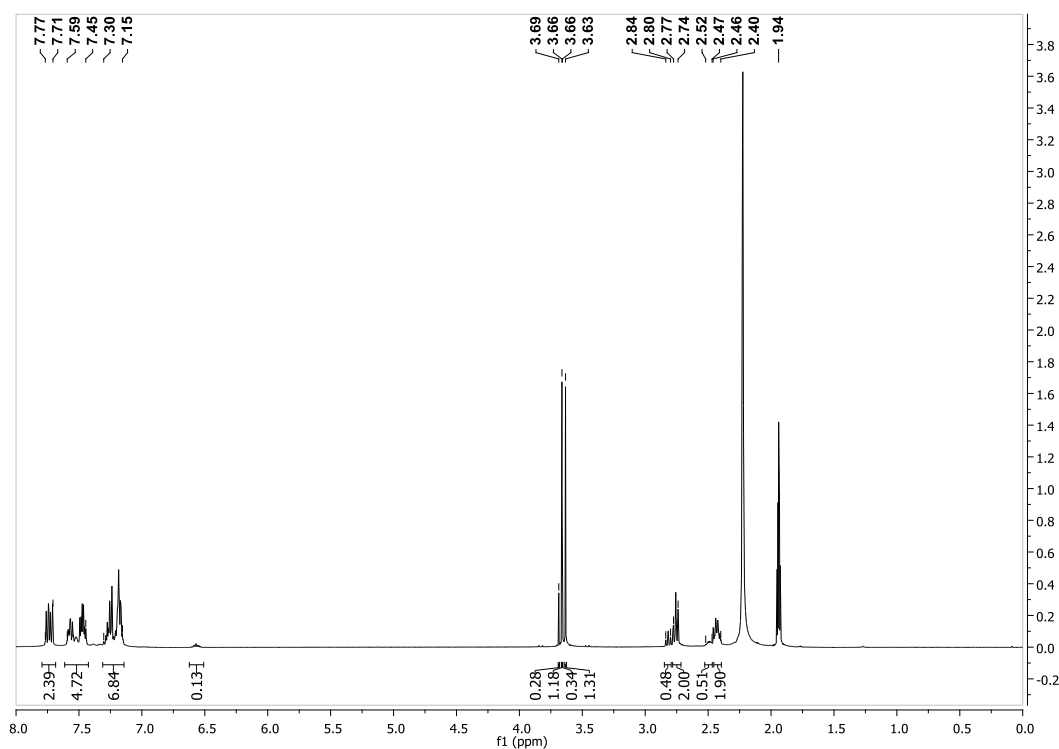


Figure 79: ^1H -NMR spectrum of a mixture of ^{15}N -(*E/Z*)-192b and (*E/Z*)-192b (1:1) (400 MHz, CD_3CN).

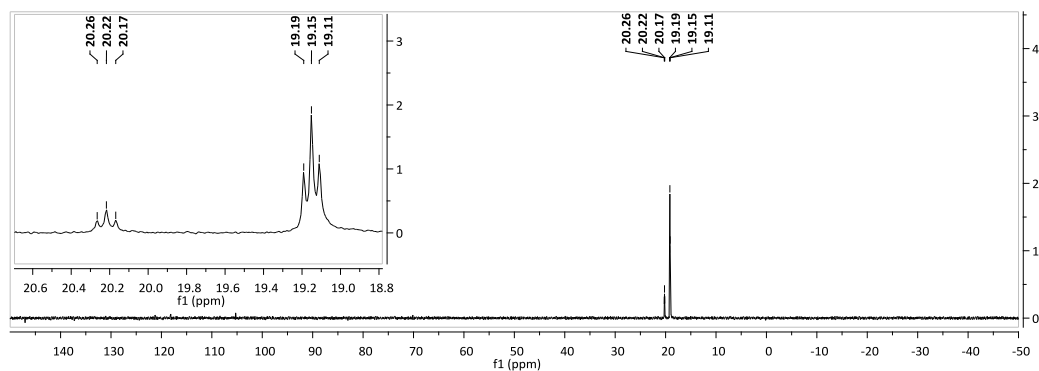


Figure 80: ^{31}P -NMR spectrum of a mixture of ^{15}N -(*E/Z*)-192b and (*E/Z*)-192b (1:1) (162 MHz, CD_3CN).

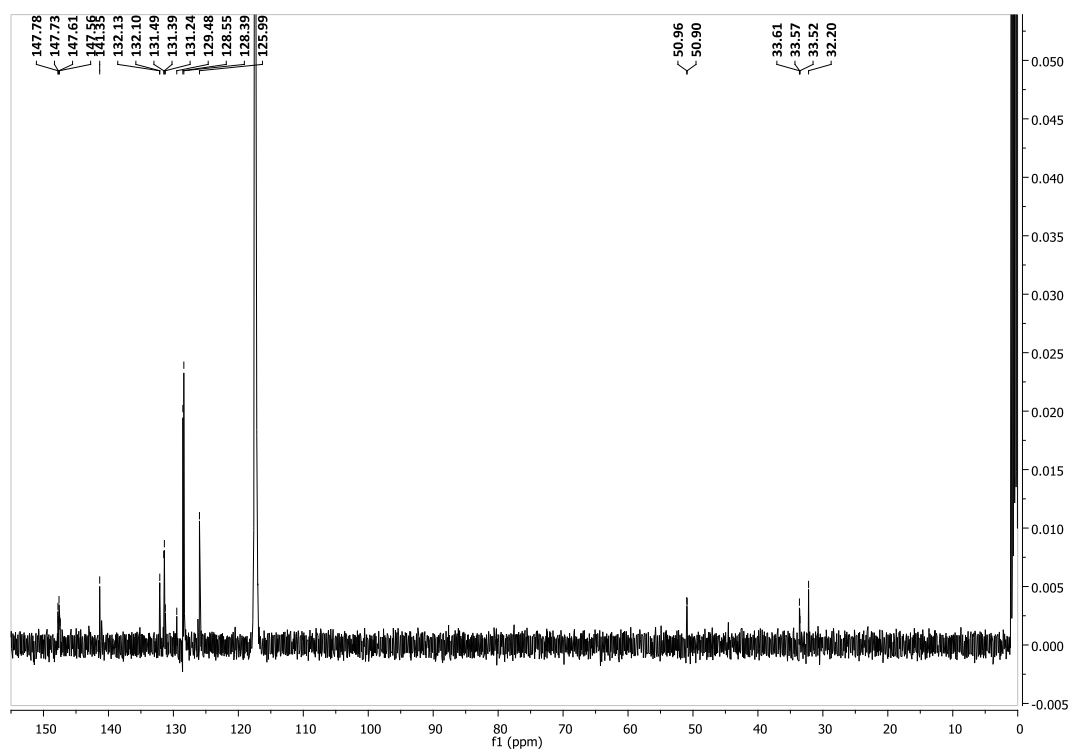


Figure 81: ^{13}C -NMR spectrum of a mixture of ^{15}N -(E/Z)-192b and (E/Z)-192b (1:1) (101 MHz, CD_3CN).

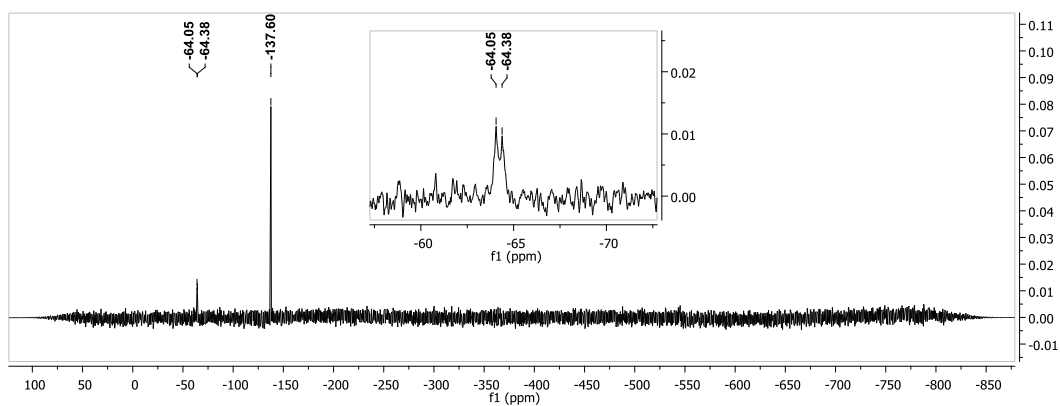


Figure 82: ^{15}N -NMR spectrum of a mixture of ^{15}N -(E/Z)-192b and (E/Z)-192b (1:1) (41 MHz, CD_3CN). NMR spectrum only shows the E-isomer.

8.2 Solvent effect – ^{31}P -NMR and LC spectra (UV-trace)

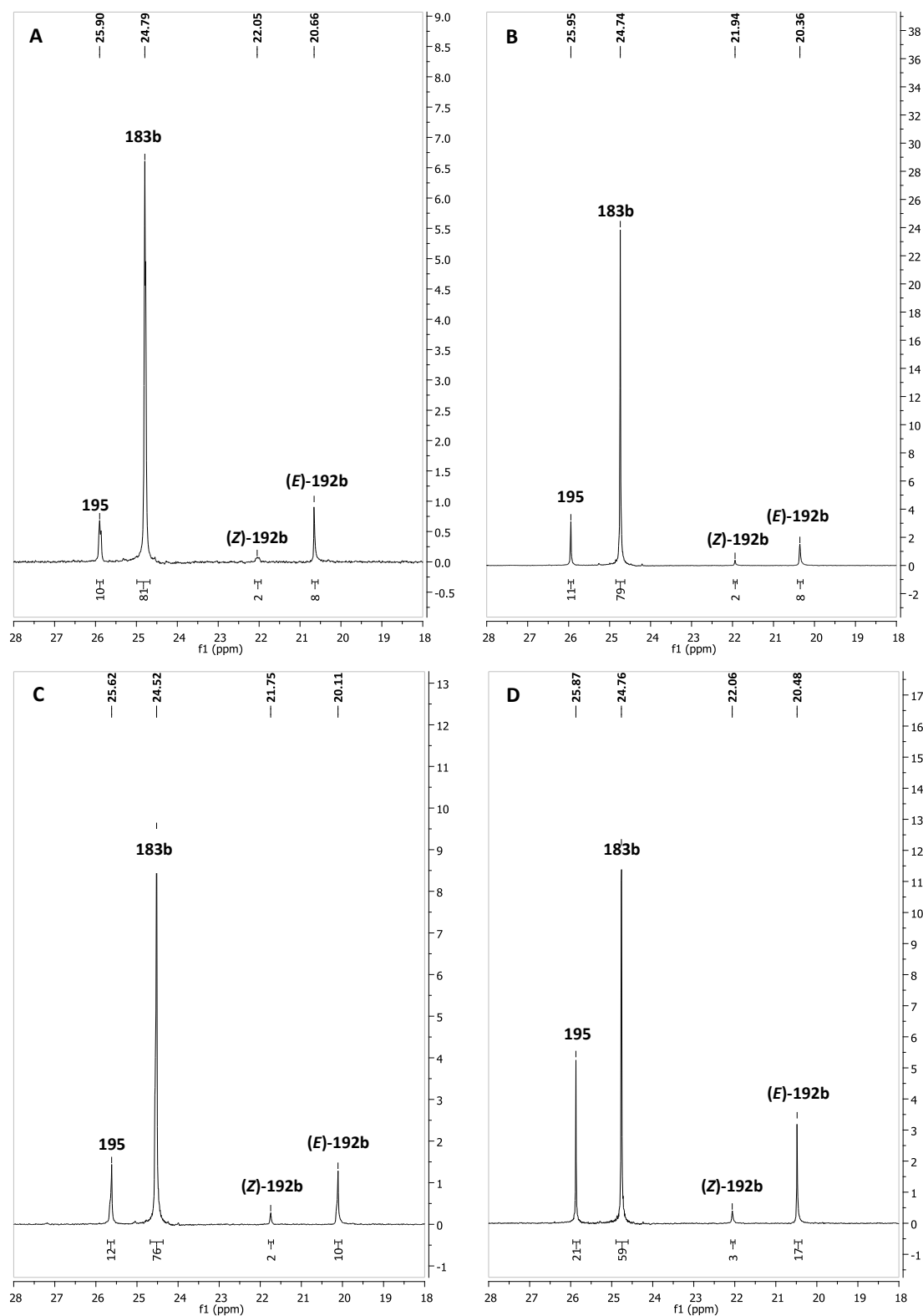


Figure 83: ^{31}P -NMR spectra of the crude reaction mixture after the Staudinger reaction between 3-phenylpropyl azide (**7b**) and methyl phenylphosphinate (**182**) with BSA (3 eq.) and treatment with TBAF in different solvents: A) n-hexane, B) benzene, C) THF and D) CH_2Cl_2 .

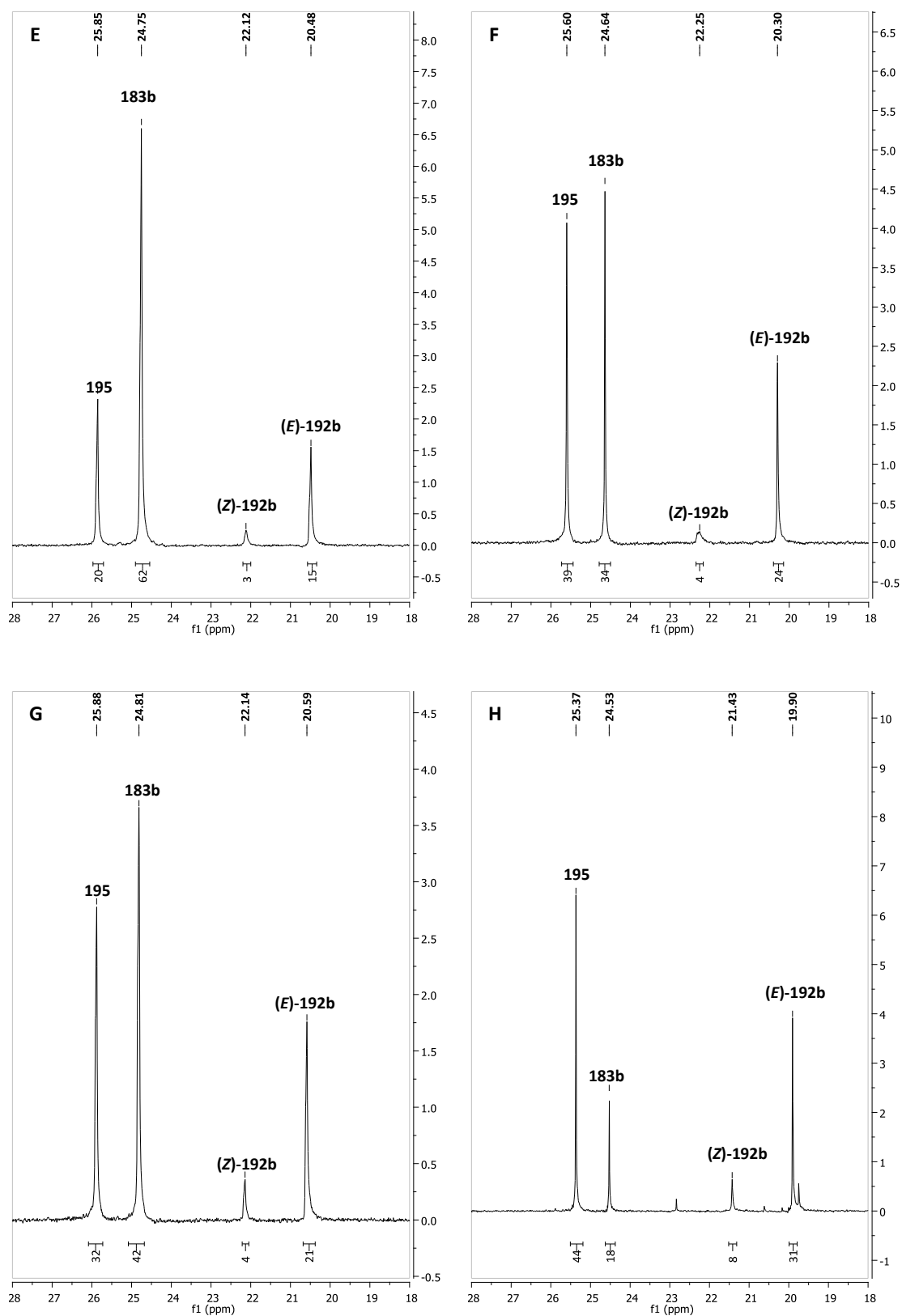


Figure 84: ^{31}P -NMR spectra of the crude reaction mixture after the Staudinger reaction between 3-phenylpropyl azide (**7b**) and methyl phenylphosphinate (**182**) with BSA (3 eq.) and treatment with TBAF in different solvents: E) pyridine, F) DMF, G) CH_3CN and H) DMSO.

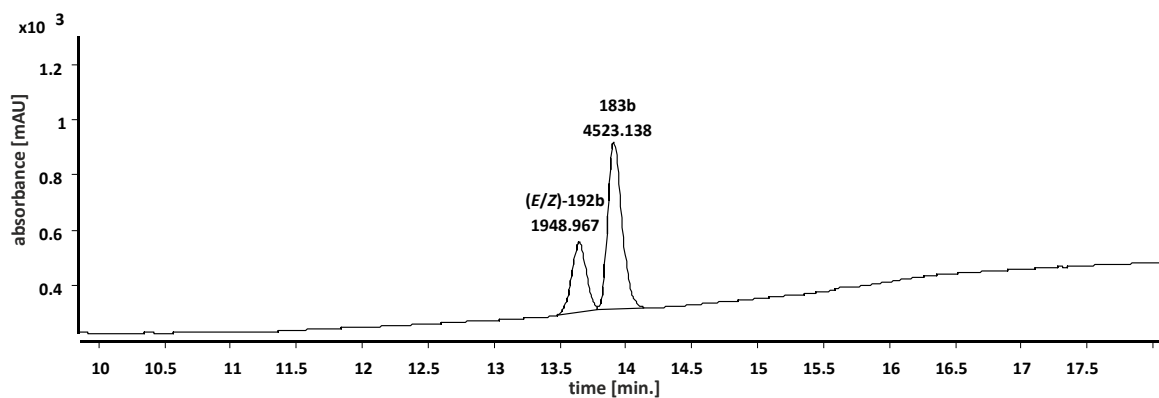


Figure 85: UV-trace (226 nm) of the LC-MS spectra of the crude reaction mixture after the Staudinger reaction between 3-phenylpropyl azide (**7b**) and methyl phenylphosphinate (**182**) with BSA (3 eq.) in *n*-hexane after removal of TBAF.

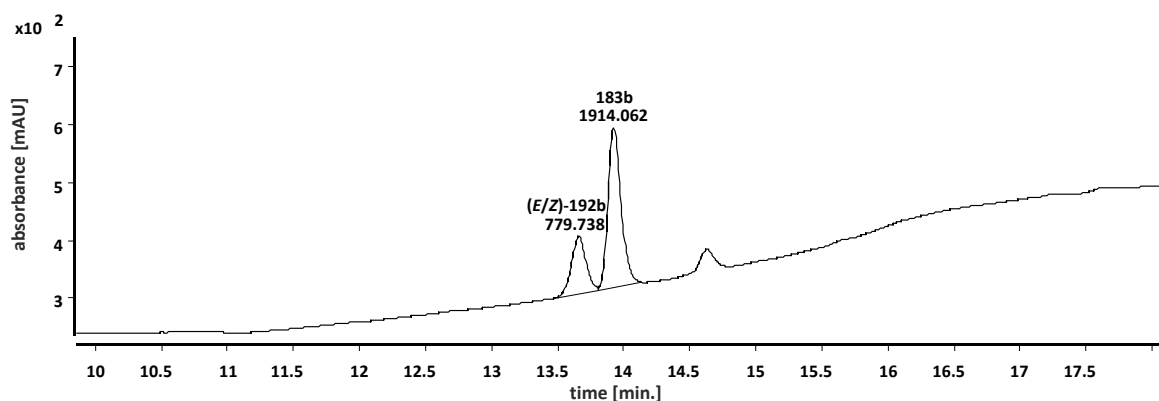


Figure 86: UV-trace (226 nm) of the LC-MS spectra of the crude reaction mixture after the Staudinger reaction between 3-phenylpropyl azide (**7b**) and methyl phenylphosphinate (**182**) with BSA (3 eq.) in benzene after removal of TBAF.

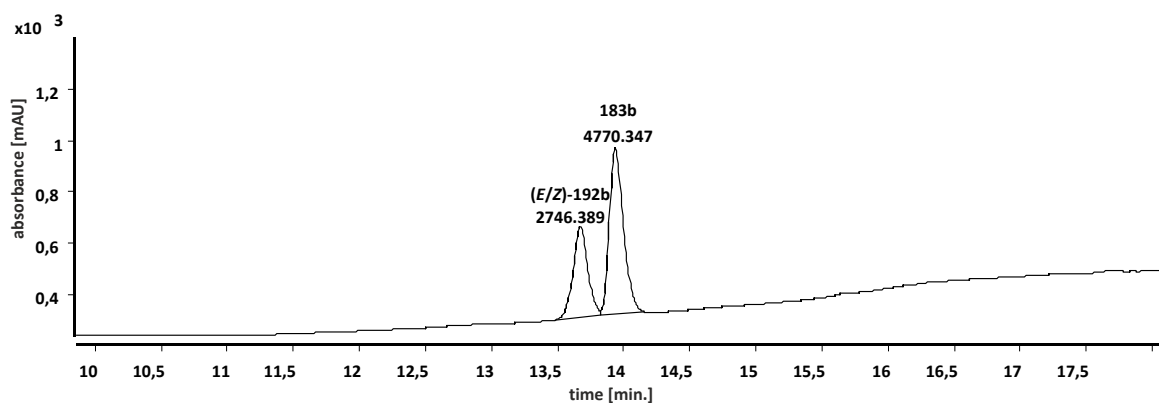


Figure 87: UV-trace (226 nm) of the LC-MS spectra of the crude reaction mixture after the Staudinger reaction between 3-phenylpropyl azide (**7b**) and methyl phenylphosphinate (**182**) with BSA (3 eq.) in THF after removal of TBAF.

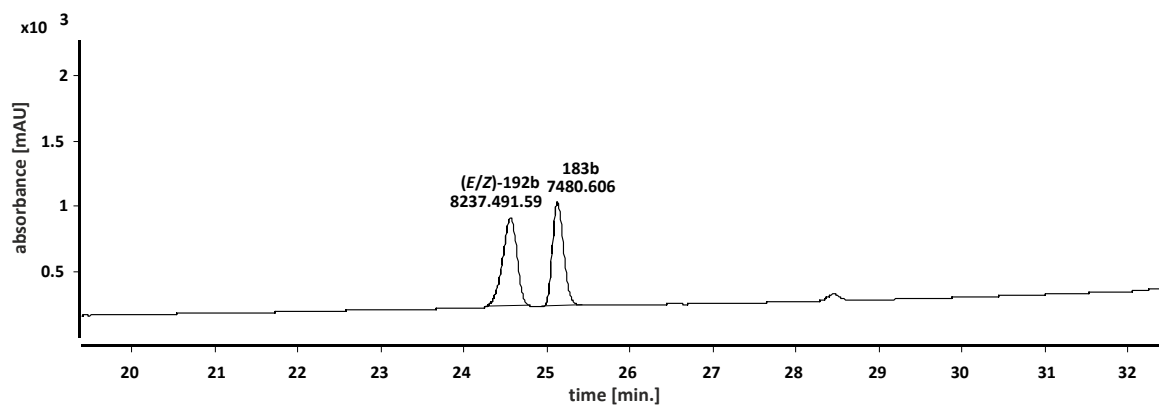


Figure 88: UV-trace (226 nm) of the LC-MS spectra of the crude reaction mixture after the Staudinger reaction between 3-phenylpropyl azide (**7b**) and methyl phenylphosphinate (**182**) with BSA (3 eq.) in CH_2Cl_2 after removal of TBAF.

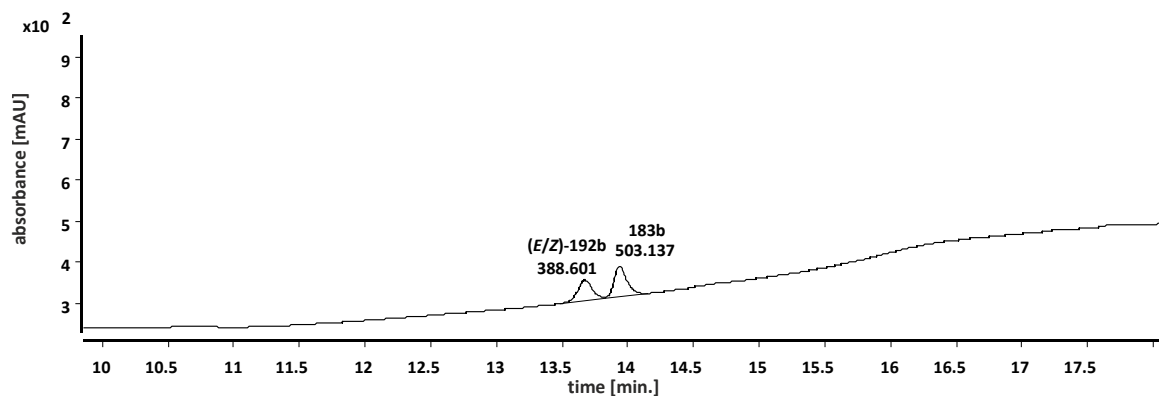


Figure 89: UV-trace (226 nm) of the LC-MS spectra of the crude reaction mixture after the Staudinger reaction between 3-phenylpropyl azide (**7b**) and methyl phenylphosphinate (**182**) with BSA (3 eq.) in *pyridine* after removal of TBAF.

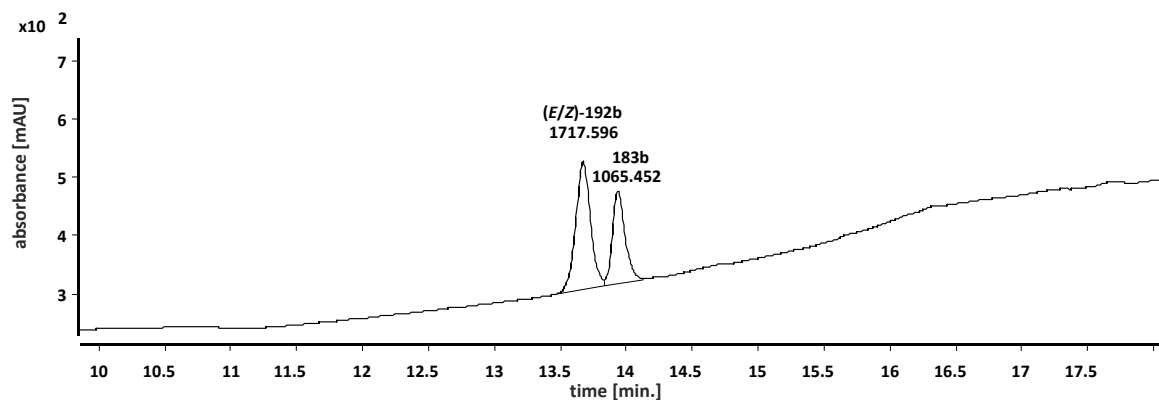


Figure 90: UV-trace (226 nm) of the LC-MS spectra of the crude reaction mixture after the Staudinger reaction between 3-phenylpropyl azide (**7b**) and methyl phenylphosphinate (**182**) with BSA (3 eq.) in *acetonitrile* after removal of TBAF.

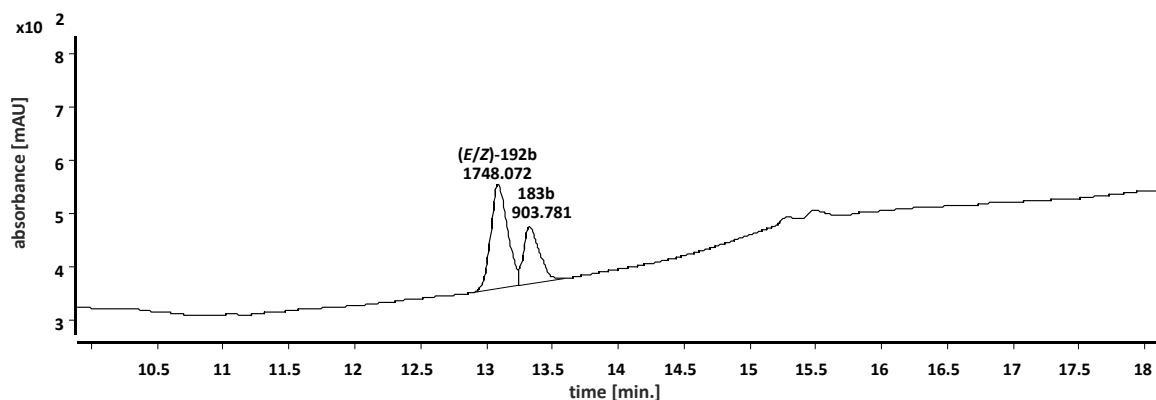


Figure 91: UV-trace (226 nm) of the LC-MS spectra of the crude reaction mixture after the Staudinger reaction between 3-phenylpropyl azide (**7b**) and methyl phenylphosphinate (**182**) with BSA (3 eq.) in **DMF** after removal of TBAF.

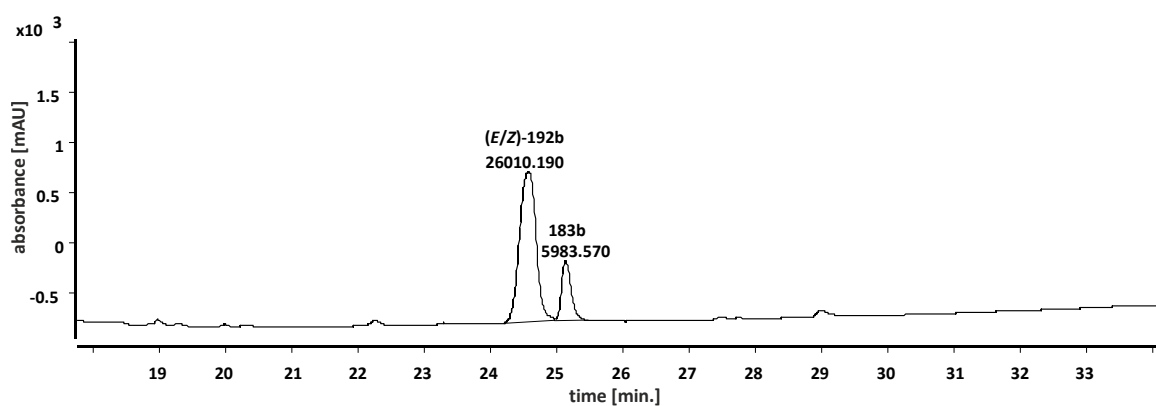


Figure 92: UV-trace (226 nm) of the LC-MS spectra of the crude reaction mixture after the Staudinger reaction between 3-phenylpropyl azide (**7b**) and methyl phenylphosphinate (**182**) with BSA (3 eq.) in **DMSO** after removal of TBAF.

8.3 Temperature effect – ³¹P-NMR and LC spectra (UV-trace)

³¹P-NMRs after the Staudinger reaction at 4 °C, 21 °C, 80 °C and corresponding UV-trace of the LC-MS spectra at 226 nm after removal of TBAF:

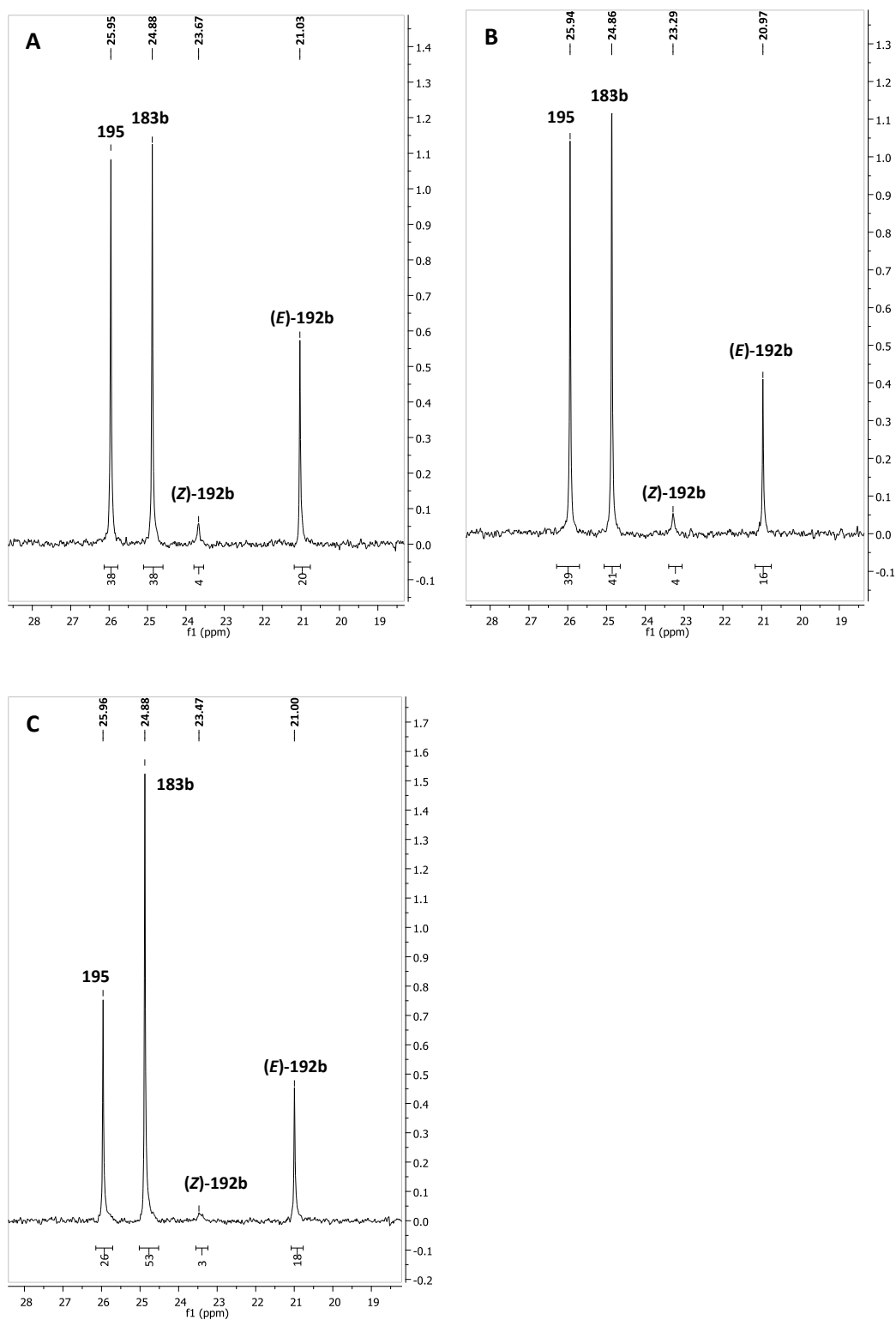


Figure 93: ^{31}P -NMR spectra of the crude reaction mixture after the Staudinger reaction between 3-phenylpropyl azide (**7b**) and methyl phenylphosphinate (**182**) with BSA (3 eq.) and treatment with TBAF in CH_3CN at three different temperatures: A) 4 °C, B) 21 °C and 80 °C.

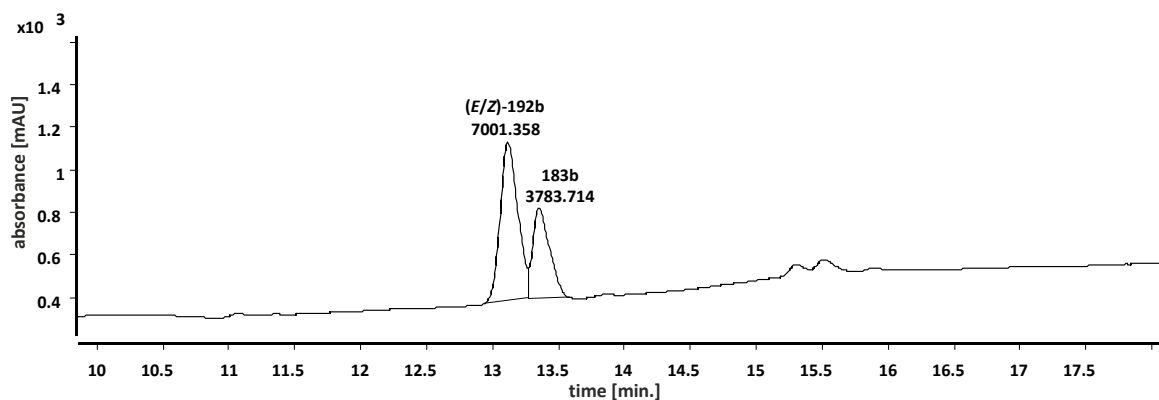


Figure 94: UV-trace (226 nm) of the LC-MS spectra of the crude reaction mixture after the Staudinger reaction between 3-phenylpropyl azide (**7b**) and methyl phenylphosphinate (**182**) with BSA (3 eq.) in CH₃CN at 4 °C after removal of TBAF.

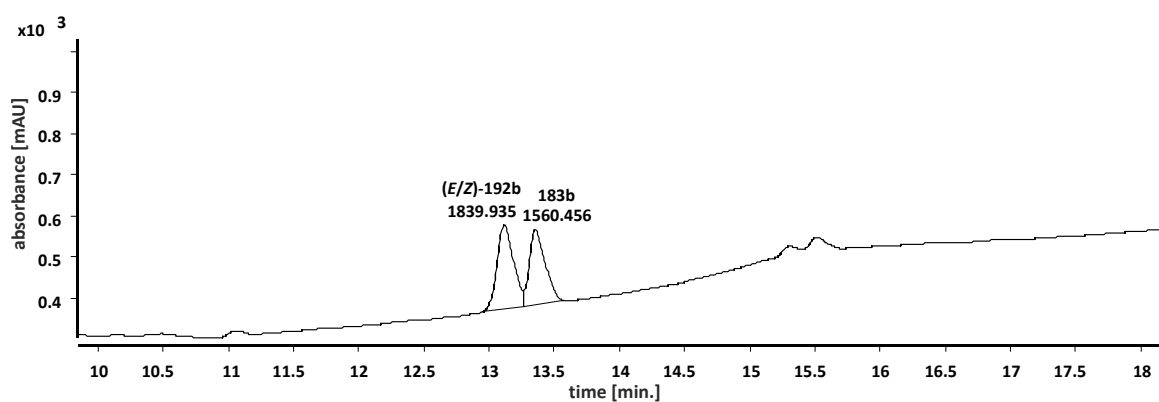


Figure 95: UV-trace (226 nm) of the LC-MS spectra of the crude reaction mixture after the Staudinger reaction between 3-phenylpropyl azide (**7b**) and methyl phenylphosphinate (**182**) with BSA (3 eq.) in CH₃CN at 21 °C after removal of TBAF.

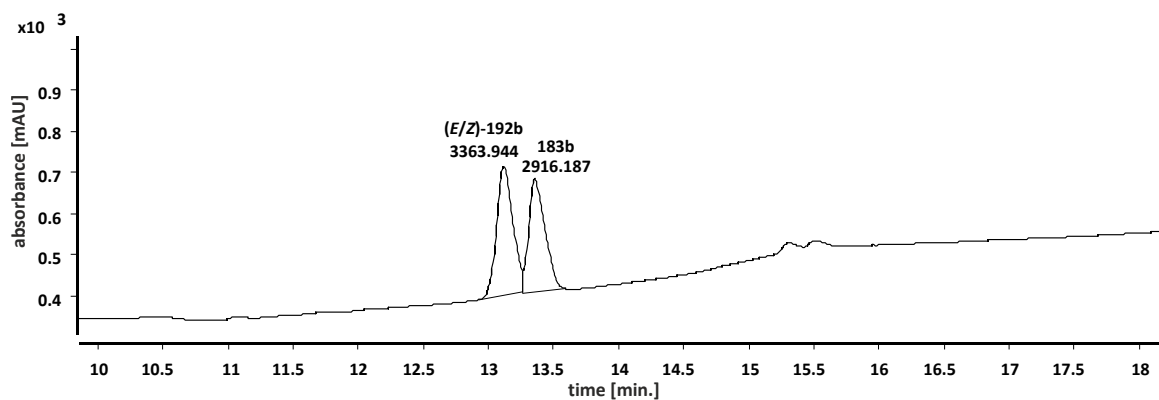


Figure 96: UV-trace (226 nm) of the LC-MS spectra of the crude reaction mixture after the Staudinger reaction between 3-phenylpropyl azide (**7b**) and methyl phenylphosphinate (**182**) with BSA (3 eq.) in CH₃CN at 80 °C after removal of TBAF.

8.4 Influence of the silylation reagent on the Staudinger reaction – ^{31}P -NMR and LC spectra (UV-trace)

^{31}P -NMRs after the Staudinger reaction between 3-phenylpropyl azide (**7b**) and methyl phenylphosphinate (**182**) (1 eq. unless otherwise noted) in CH_2Cl_2 with different silylation reagents after addition of TBAF and corresponding UV-trace of the LC-MS spectra at 226 nm after removal of TBAF were measured.

8.4.1 Silylation with BSA

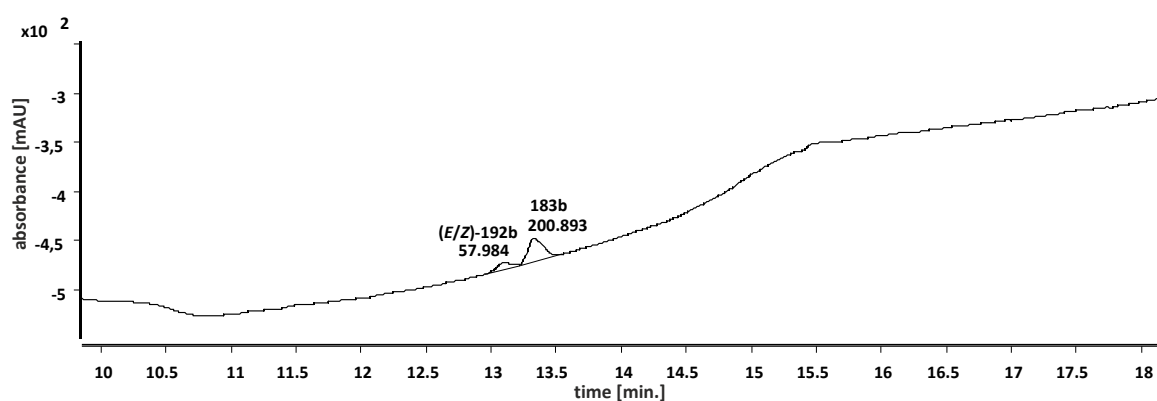


Figure 97: UV-trace (226 nm) of the LC-MS spectra of the crude reaction mixture after the Staudinger reaction between 3-phenylpropyl azide (**7b**) and methyl phenylphosphinate (**182**) with **BSA** (1 eq.) in CH_2Cl_2 at room temperature after removal of TBAF.

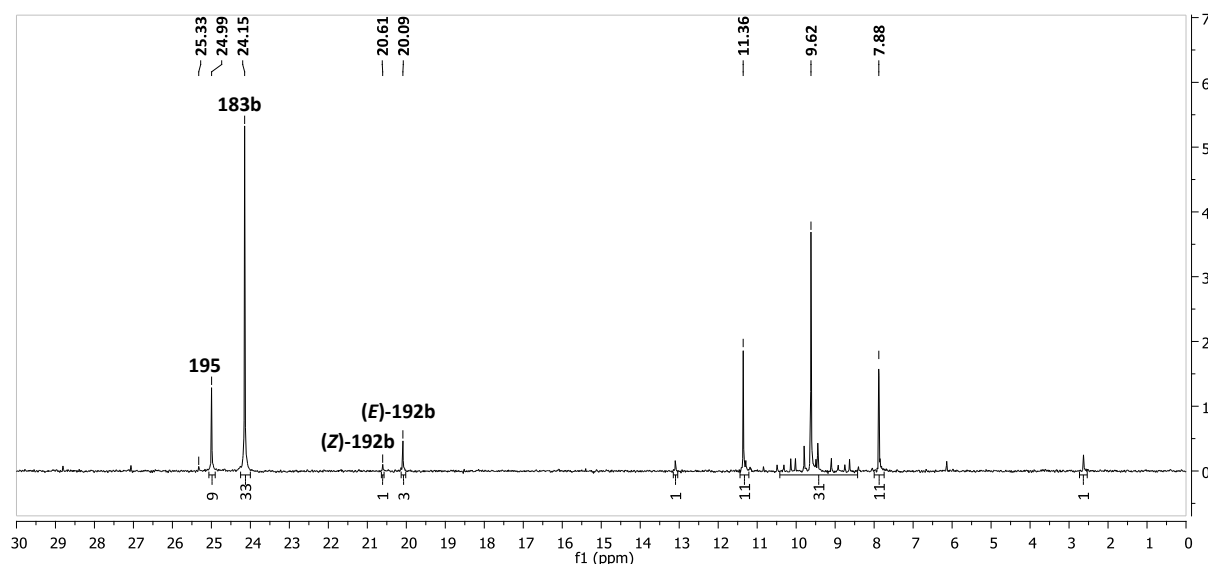


Figure 98: ^{31}P -NMR spectra of the crude reaction mixture after the Staudinger reaction between 3-phenylpropyl azide (**7b**) and methyl phenylphosphinate (**182**) with **BSA** (1 eq.) and treatment with TBAF in CH_2Cl_2 at room temperature.

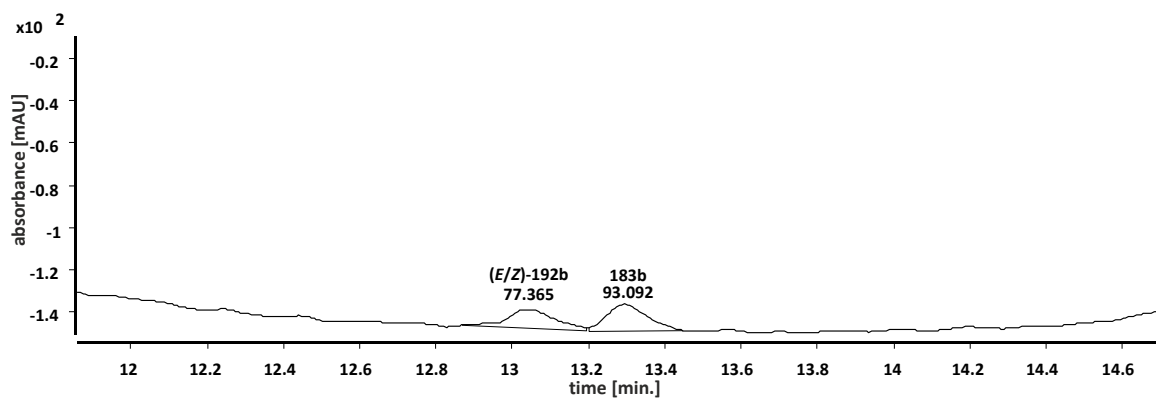


Figure 99: UV-trace (226 nm) of the LC-MS spectra of the crude reaction mixture after the Staudinger reaction between 3-phenylpropyl azide (**7b**) and methyl phenylphosphinate (**182**) with BSA (**3 eq.**) in CH_2Cl_2 at room temperature after removal of TBAF.

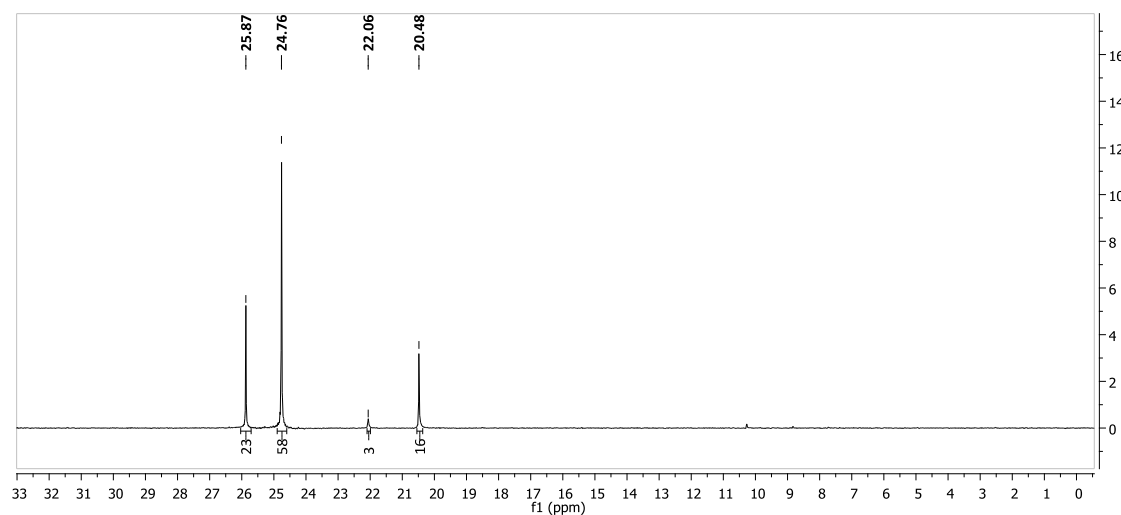


Figure 100: ^{31}P -NMR spectra of the crude reaction mixture after the Staudinger reaction between 3-phenylpropyl azide (**7b**) and methyl phenylphosphinate (**182**) with BSA (**3 eq.**) and treatment with TBAF in CH_2Cl_2 at room temperature.

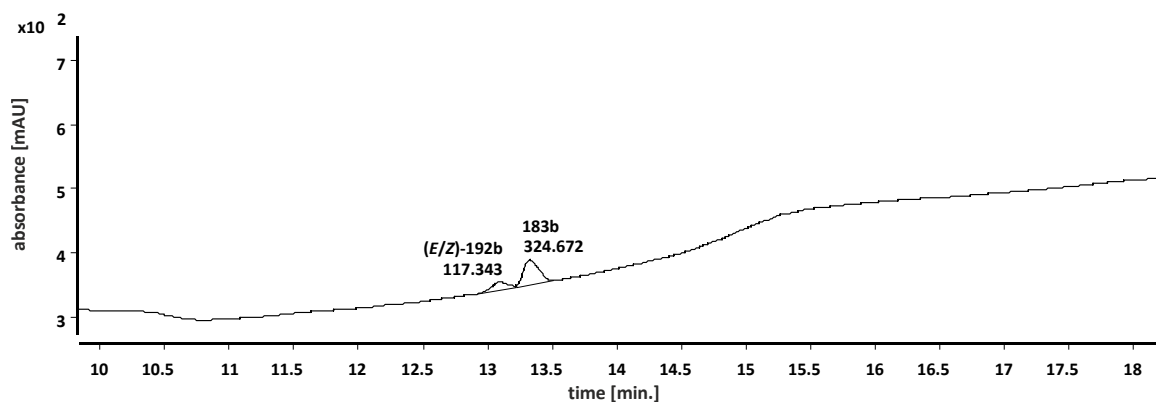


Figure 101: UV-trace (226 nm) of the LC-MS spectra of the crude reaction mixture after the Staudinger reaction between 3-phenylpropyl azide (**7b**) and methyl phenylphosphinate (**182**) with BSA (**5 eq.**) in CH_2Cl_2 at room temperature after removal of TBAF.

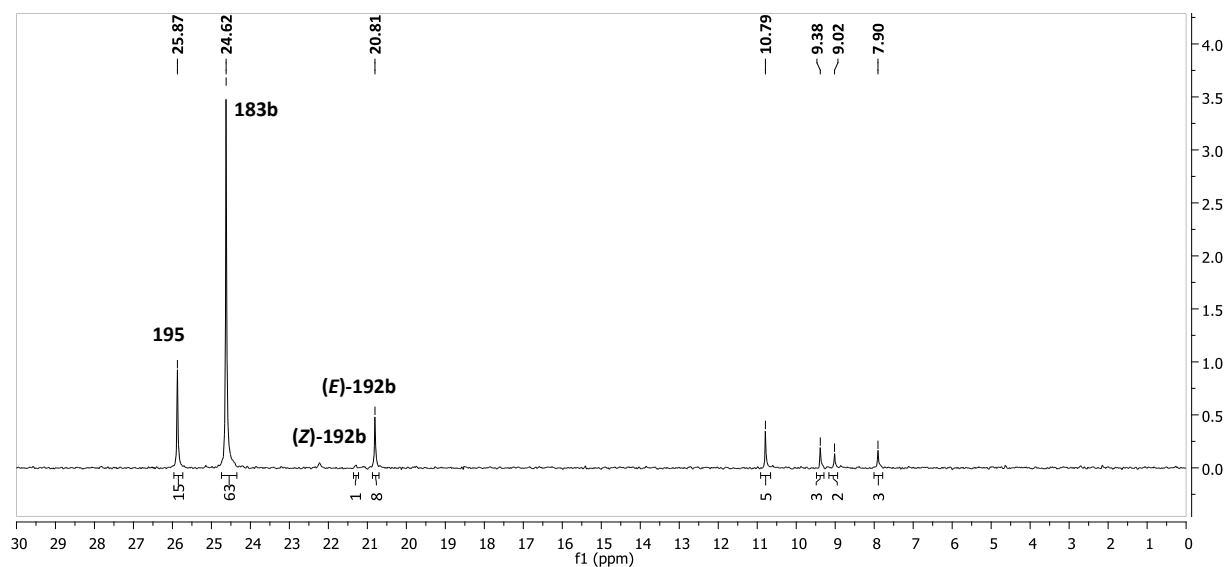


Figure 102: ^{31}P -NMR spectra of the crude reaction mixture after the Staudinger reaction between 3-phenylpropyl azide (**7b**) and methyl phenylphosphinate (**182**) with BSA (**5 eq.**) and treatment with TBAF in CH_2Cl_2 at room temperature.

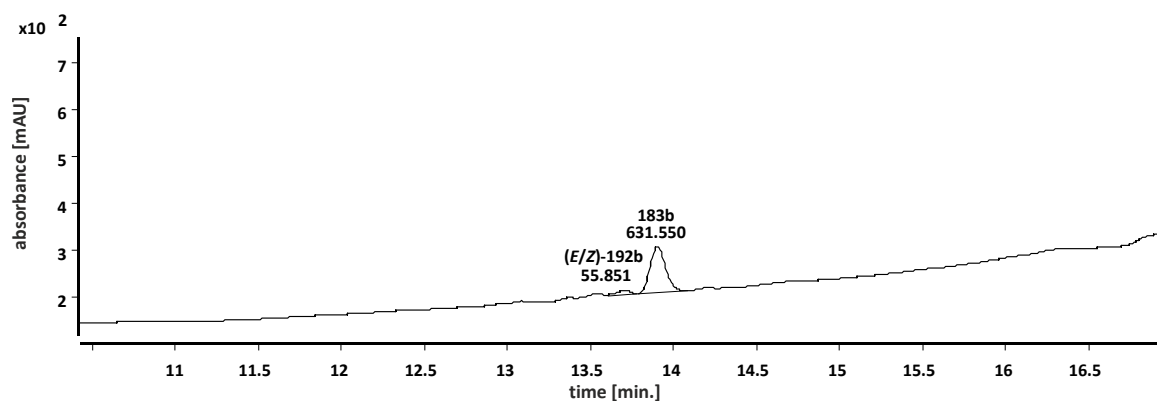


Figure 103: UV-trace (226 nm) of the LC-MS spectra of the crude reaction mixture after the Staudinger reaction between 3-phenylpropyl azide (**7b**) and methyl phenylphosphinate (**182**) with BSA (**10 eq.**) in CH_2Cl_2 at room temperature after removal of TBAF.

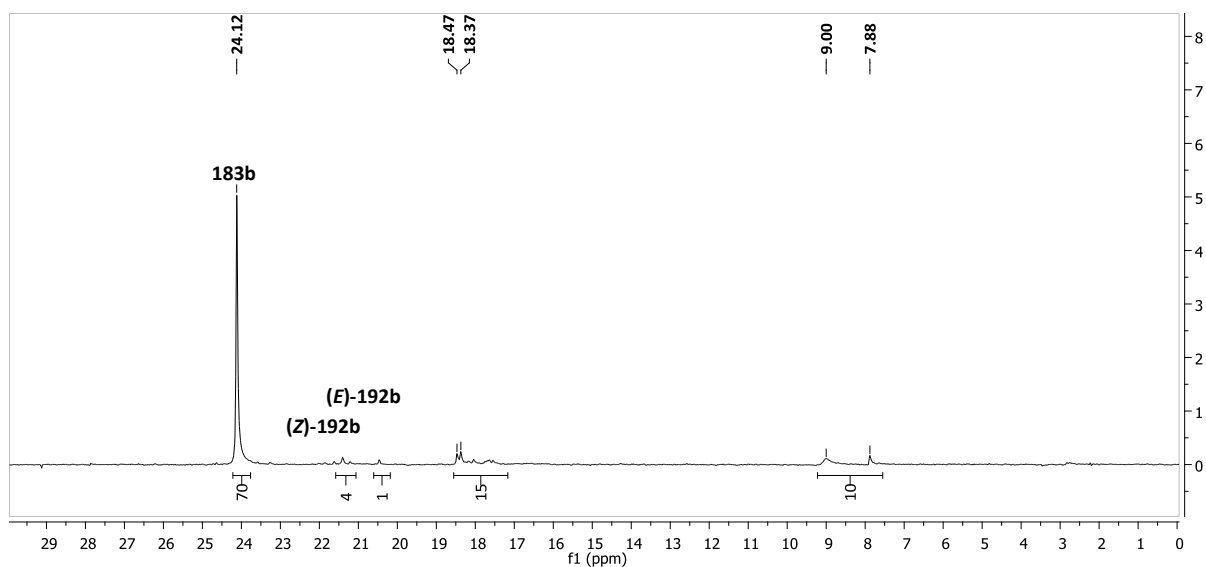


Figure 104: ^{31}P -NMR spectra of the crude reaction mixture after the Staudinger reaction between 3-phenylpropyl azide (**7b**) and methyl phenylphosphinate (**182**) with **BSA (10 eq.)** and treatment with TBAF in CH_2Cl_2 at room temperature.

8.4.2 Silylation with MSTFA

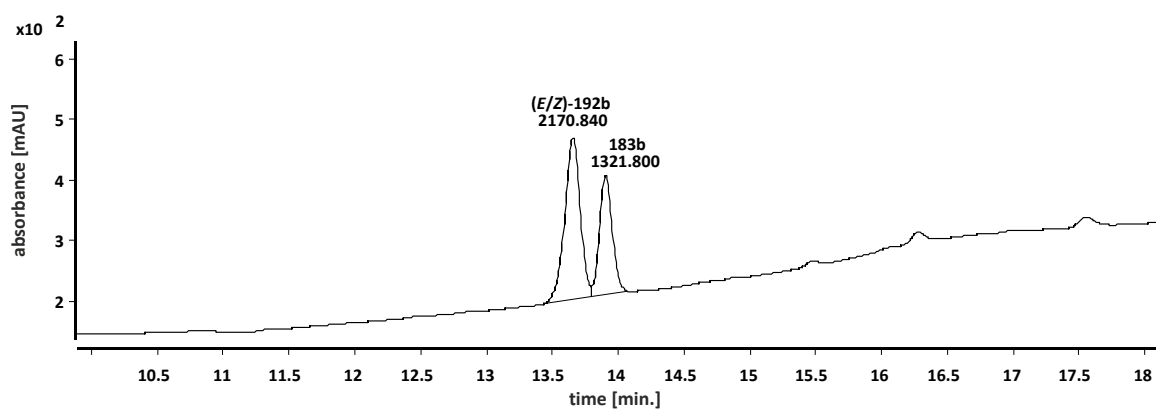


Figure 105: UV-trace (226 nm) of the LC-MS spectra of the crude reaction mixture after the Staudinger reaction between 3-phenylpropyl azide (**7b**) and methyl phenylphosphinate (**182**) with **MSTFA (1 eq.)** in CH_2Cl_2 at room temperature after removal of TBAF.

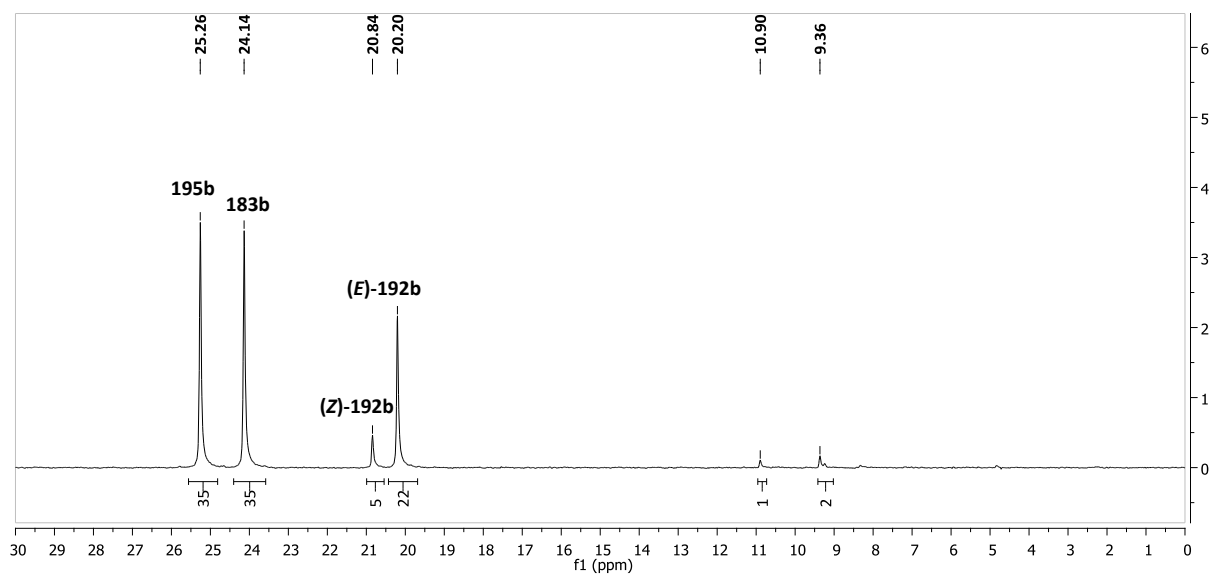


Figure 106: ^{31}P -NMR spectra of the crude reaction mixture after the Staudinger reaction between 3-phenylpropyl azide (**7b**) and methyl phenylphosphinate (**182**) with MSTFA (1 eq.) and treatment with TBAF in CH_2Cl_2 at room temperature.

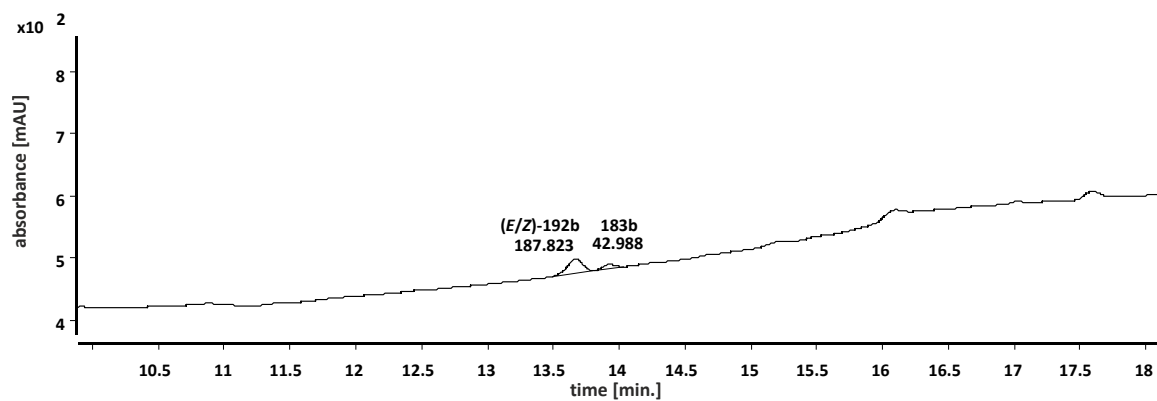


Figure 107: UV-trace (226 nm) of the LC-MS spectra of the crude reaction mixture after the Staudinger reaction between 3-phenylpropyl azide (**7b**) and methyl phenylphosphinate (**182**) with MSTFA (10 eq.) in CH_2Cl_2 at room temperature after removal of TBAF.

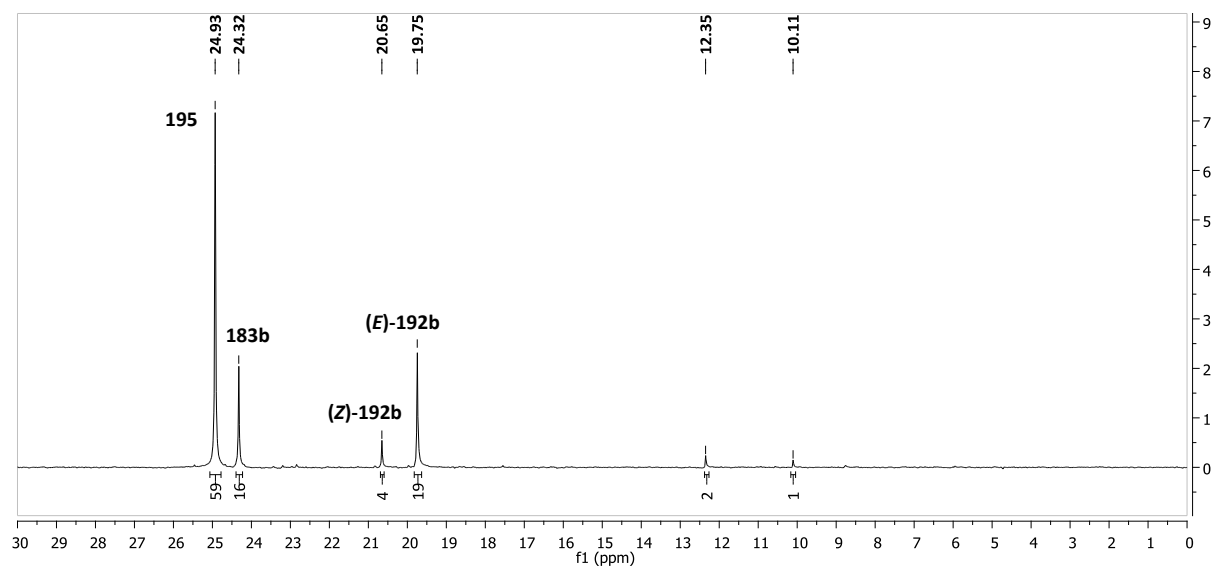


Figure 108: ^{31}P -NMR spectra of the crude reaction mixture after the Staudinger reaction between 3-phenylpropyl azide (**7b**) and methyl phenylphosphinate (**182**) with MSTFA (10 eq.) and treatment with TBAF in CH_2Cl_2 at room temperature.

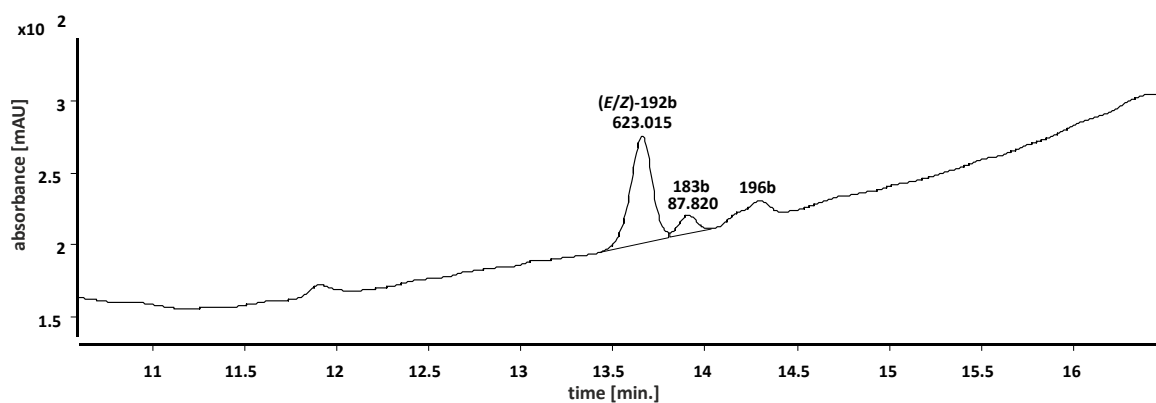


Figure 109: UV-trace (226 nm) of the LC-MS spectra of the crude reaction mixture after the Staudinger reaction between 3-phenylpropyl azide (**7b**) and methyl phenylphosphinate (**182**) (10 eq.) with MSTFA (10 eq.) in CH_2Cl_2 at room temperature after removal of TBAF.

8.4.3 Silylation with TMSCl

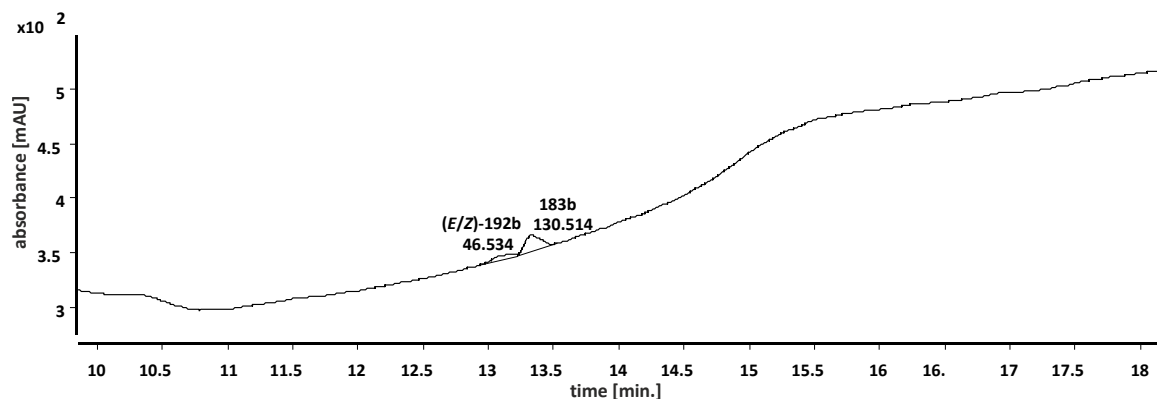


Figure 110: UV-trace (226 nm) of the LC-MS spectra of the crude reaction mixture after the Staudinger reaction between 3-phenylpropyl azide (**7b**) and methyl phenylphosphinate (**182**) with **TMSCl** (1 eq.) in CH_2Cl_2 at room temperature after removal of TBAF.

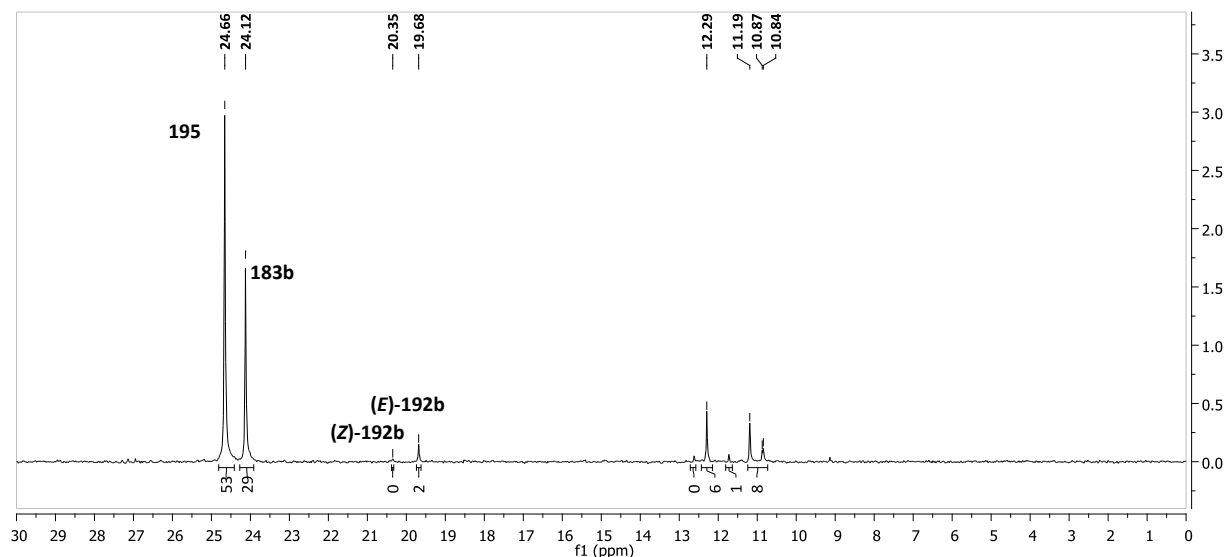


Figure 111: ^{31}P -NMR spectra of the crude reaction mixture after the Staudinger reaction between 3-phenylpropyl azide (**7b**) and methyl phenylphosphinate (**182**) with **TMSCl** (1 eq.) and treatment with TBAF in CH_2Cl_2 at room temperature.

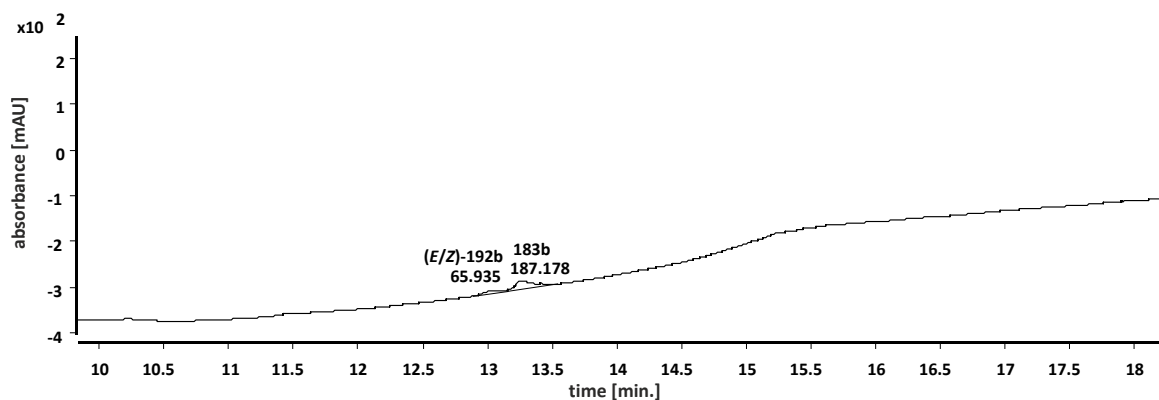


Figure 112: UV-trace (226 nm) of the LC-MS spectra of the crude reaction mixture after the Staudinger reaction between 3-phenylpropyl azide (**7b**) and methyl phenylphosphinate (**182**) with **TMSCI** (5 eq.) in CH_2Cl_2 at room temperature after removal of TBAF.

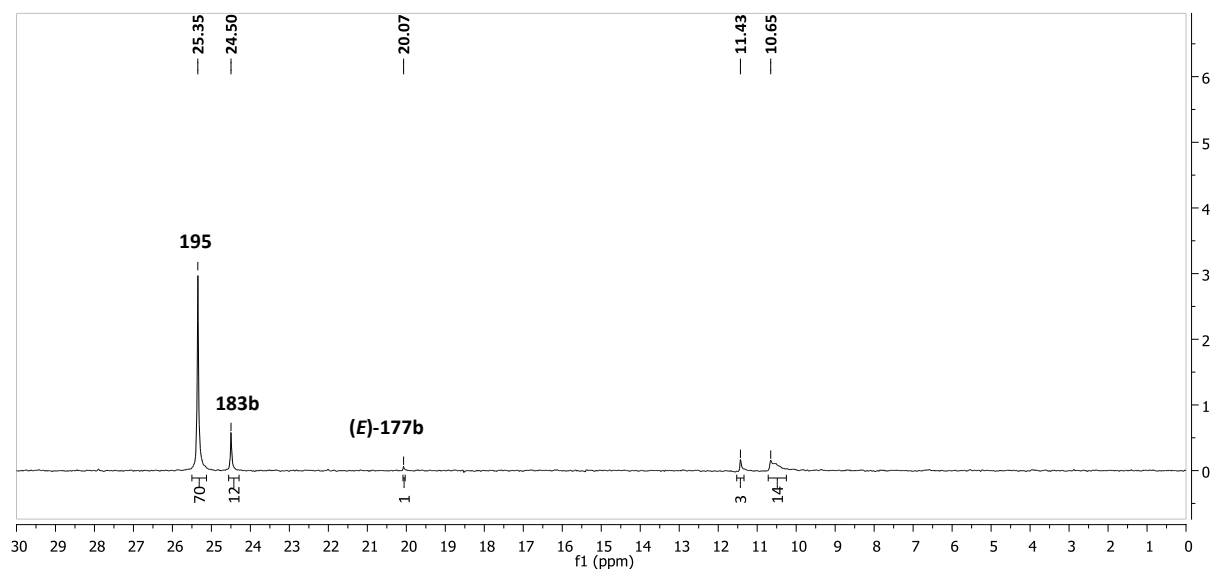


Figure 113: ³¹P-NMR spectra of the crude reaction mixture after the Staudinger reaction between 3-phenylpropyl azide (**7b**) and methyl phenylphosphinate (**182**) with **TMSCI** (5 eq.) and treatment with TBAF in CH_2Cl_2 at room temperature.

8.4.4 Silylation with TESCI

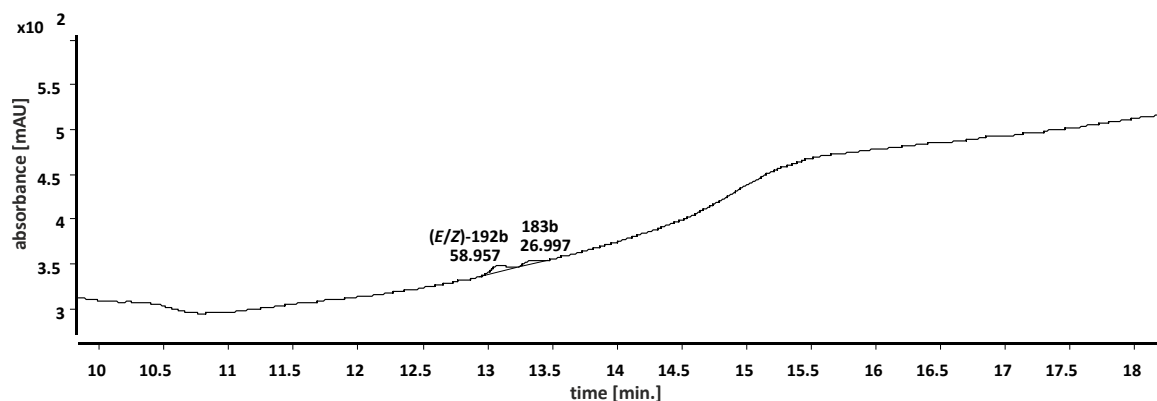


Figure 114: UV-trace (226 nm) of the LC-MS spectra of the crude reaction mixture after the Staudinger reaction between 3-phenylpropyl azide (**7b**) and methyl phenylphosphinate (**182**) with TESCI (1 eq.) in CH_2Cl_2 at room temperature after removal of TBAF.

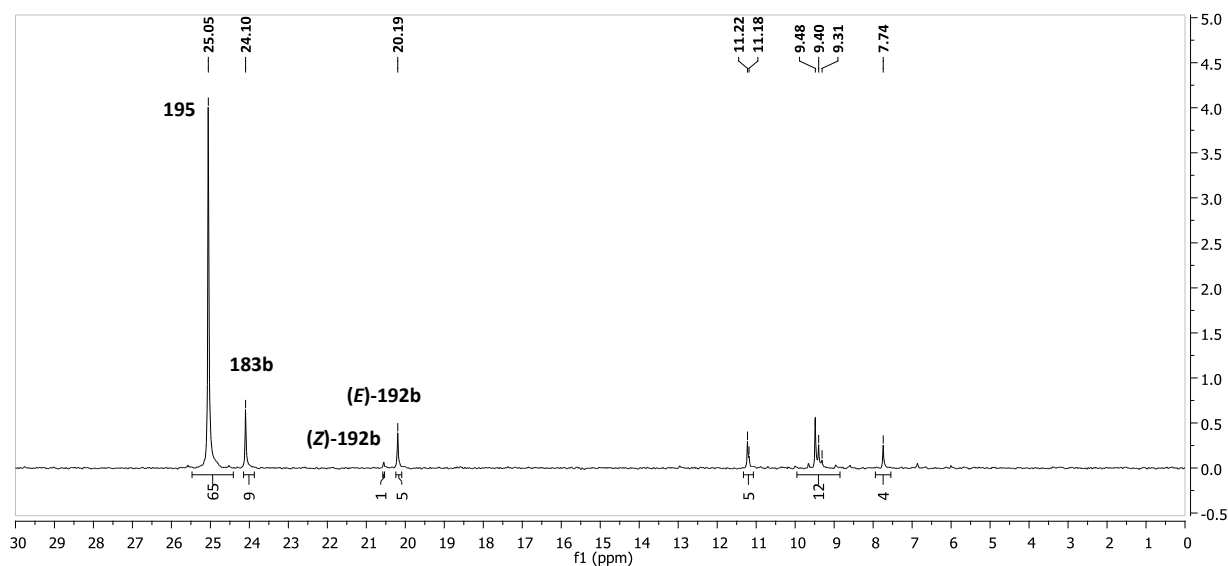


Figure 115: ^{31}P -NMR spectra of the crude reaction mixture after the Staudinger reaction between 3-phenylpropyl azide (**7b**) and methyl phenylphosphinate (**182**) with TESCI (1 eq.) and treatment with TBAF in CH_2Cl_2 at room temperature.

8.4.5 Silylation with TBDMSCl

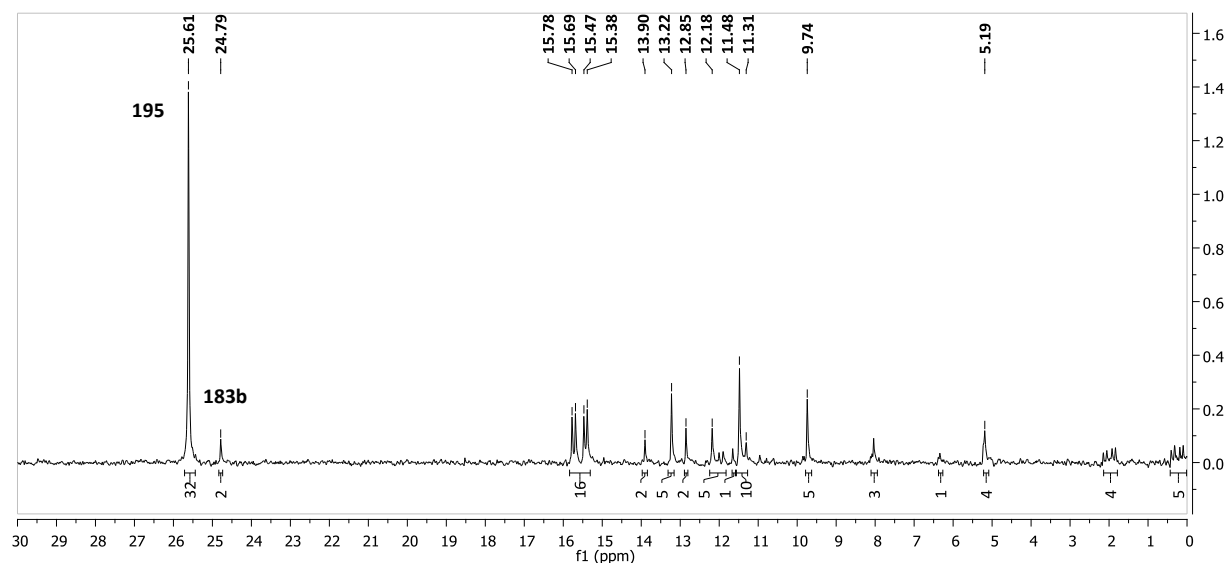


Figure 116: ^{31}P -NMR spectra of the crude reaction mixture after the Staudinger reaction between 3-phenylpropyl azide (**7b**) and methyl phenylphosphinate (**182**) with **TBDMSCl** (**5 eq.**) and treatment with **TBAF** in CH_2Cl_2 at room temperature.

8.4.6 Silylation with MTBSTFA

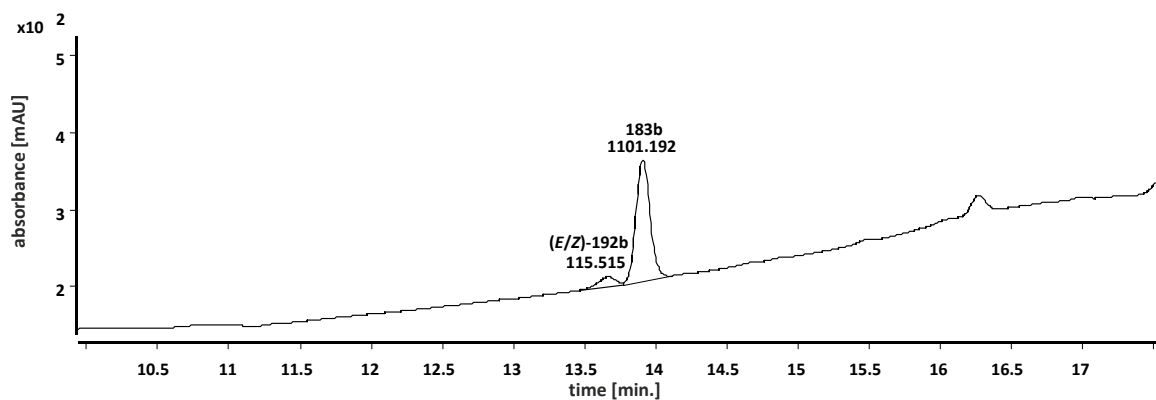


Figure 117: UV-trace (226 nm) of the LC-MS spectra of the crude reaction mixture after the Staudinger reaction between 3-phenylpropyl azide (**7b**) and methyl phenylphosphinate (**182**) with **MTBSTFA** (**10 eq.**) in CH_2Cl_2 at room temperature after removal of **TBAF**.

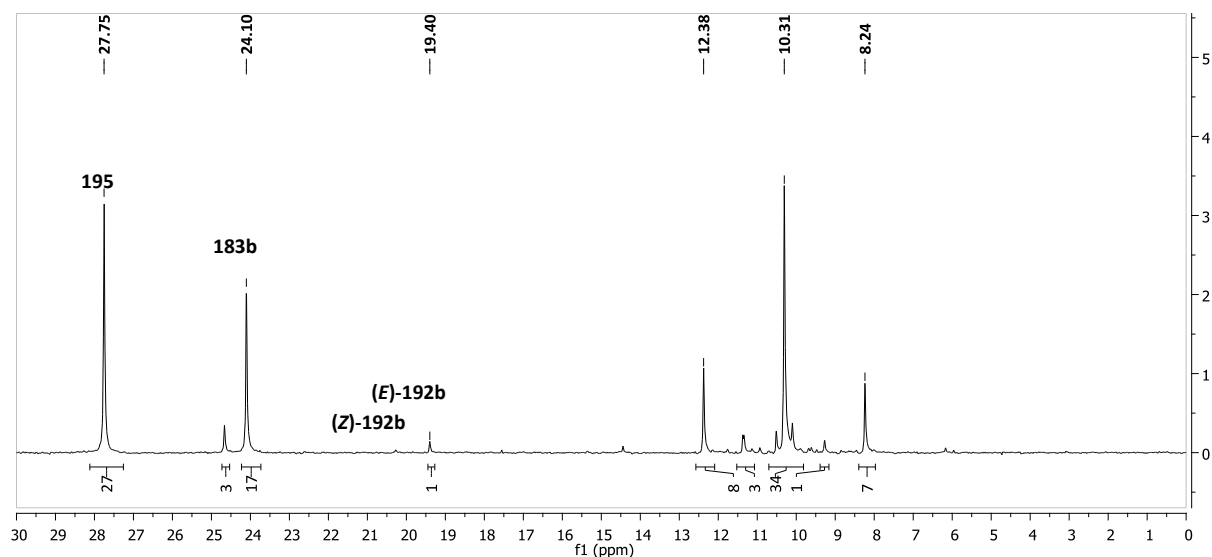


Figure 118: ^{31}P -NMR spectra of the crude reaction mixture after the Staudinger reaction between 3-phenylpropyl azide (**7b**) and methyl phenylphosphinate (**182**) with **MTBSTFA** (10 eq.) and treatment with TBAF in CH_2Cl_2 at room temperature.

8.4.7 Silylation with TBDSPCI

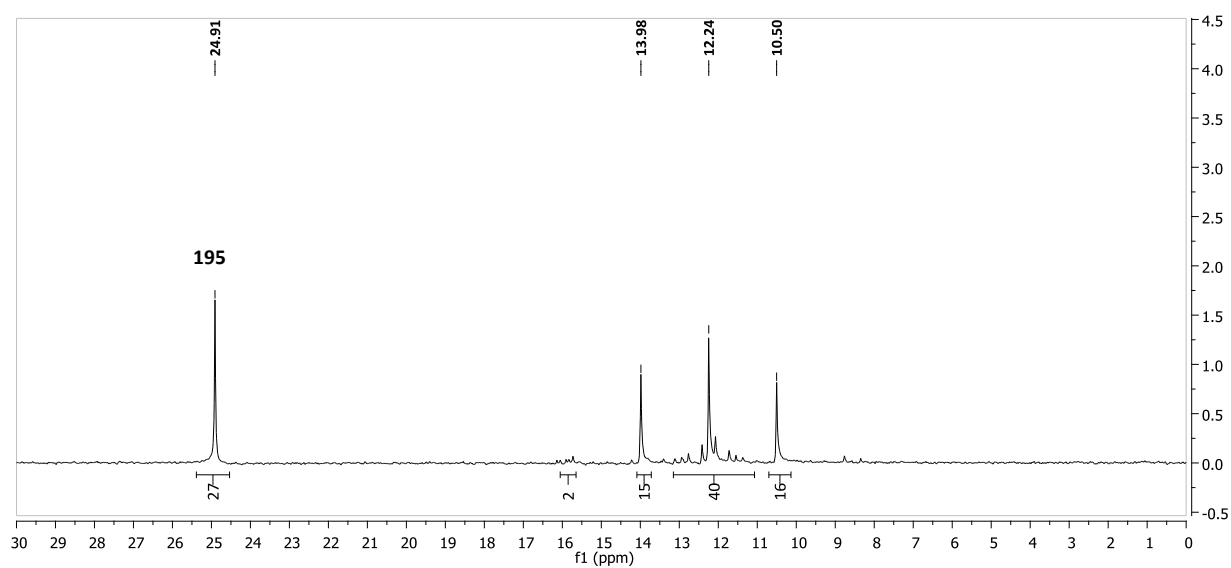


Figure 119: ^{31}P -NMR spectra of the crude reaction mixture after the Staudinger reaction between 3-phenylpropyl azide (**7b**) and methyl phenylphosphinate (**182**) with **TBDSPCI** (1 eq.) and treatment with TBAF in CH_2Cl_2 at room temperature.

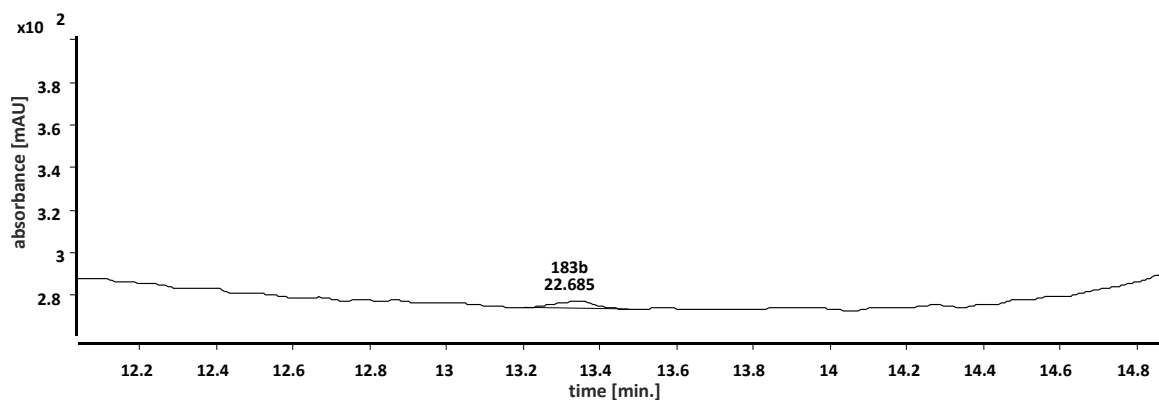


Figure 120: UV-trace (226 nm) of the LC-MS spectra of the crude reaction mixture after the Staudinger reaction between 3-phenylpropyl azide (**7b**) and methyl phenylphosphinate (**182**) with **TBDPCI** (3 eq.) in CH_2Cl_2 at room temperature after removal of TBAF.

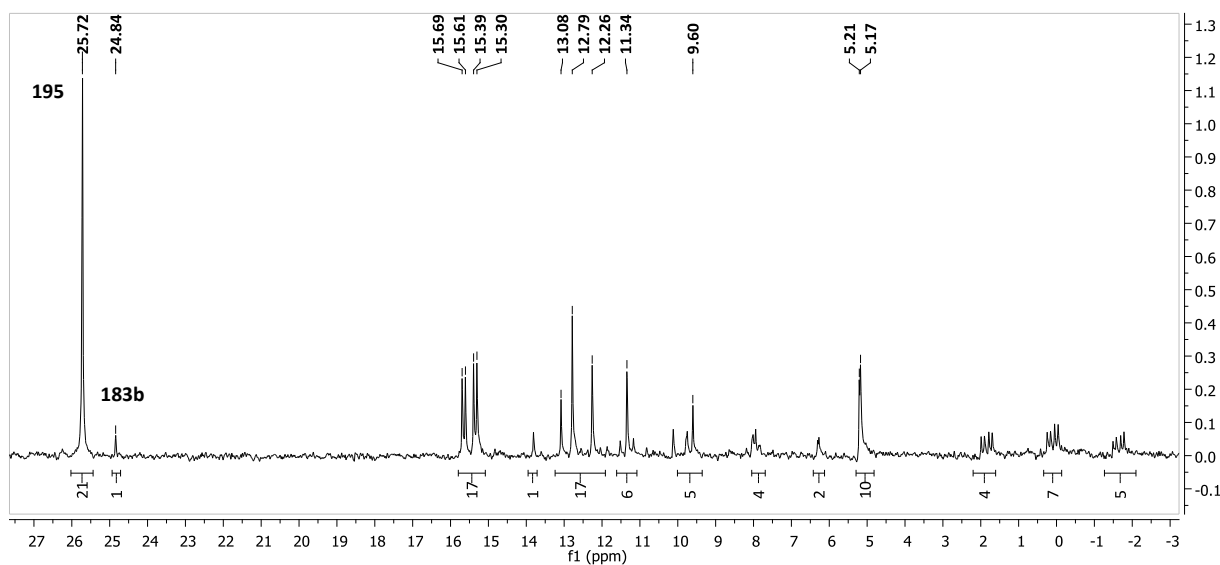


Figure 121: ^{31}P -NMR spectra of the crude reaction mixture after the Staudinger reaction between 3-phenylpropyl azide (**7b**) and methyl phenylphosphinate (**182**) with **TBDPCI** (5 eq.) and treatment with TBAF in CH_2Cl_2 at room temperature.

8.4.8 Silylation with TPSCI

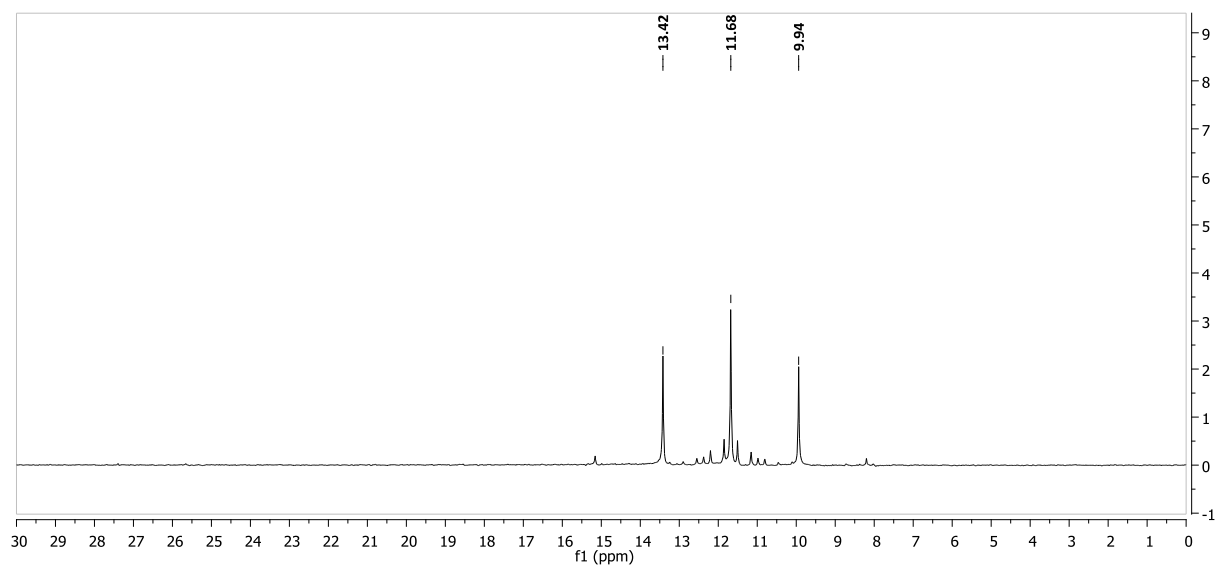


Figure 122: ^{31}P -NMR spectra of the crude reaction mixture after the Staudinger reaction between 3-phenylpropyl azide (**7b**) and methyl phenylphosphinate (**182**) with TPSCI (1 eq.) and treatment with TBAF in CH_2Cl_2 at room temperature.